



Fisheries and Oceans
Canada

Pêches et Océans
Canada

Ecosystems and
Oceans Science

Sciences des écosystèmes
et des océans

Canadian Science Advisory Secretariat (CSAS)

Research Document 2024/071

Pacific Region

Arrowtooth Flounder (*Atheresthes stomias*) Stock Assessment for the West Coast of British Columbia in 2021

Chris J. Grandin¹, Sean C. Anderson¹ and Philina A. English¹

¹Pacific Biological Station
Fisheries and Oceans Canada, 3190 Hammond Bay Road
Nanaimo, British Columbia, V9T 6N7, Canada

Foreword

This series documents the scientific basis for the evaluation of aquatic resources and ecosystems in Canada. As such, it addresses the issues of the day in the time frames required and the documents it contains are not intended as definitive statements on the subjects addressed but rather as progress reports on ongoing investigations.

Published by:

Fisheries and Oceans Canada
Canadian Science Advisory Secretariat
200 Kent Street
Ottawa ON K1A 0E6

<http://www.dfo-mpo.gc.ca/csas-sccs/>
csas-sccs@dfo-mpo.gc.ca



© His Majesty the King in Right of Canada, as represented by the Minister of the Department of Fisheries and Oceans, 2026

This report is published under the [Open Government Licence – Canada](#)

ISSN 1919-5044

ISBN 978-0-660-73774-4 Cat. No. Fs70-5/2024-071E-PDF

Correct citation for this publication:

Grandin, C.J., Anderson, S.C. and English, P.A. 2026. Arrowtooth Flounder (*Atheresthes stomias*) Stock Assessment for the West Coast of British Columbia in 2021. DFO Can. Sci. Advis. Sec. Res. Doc. 2024/071. v + 142 p.

Aussi disponible en français :

Grandin, C.J., Anderson, S.C. et English, P.A. 2026. Évaluation du stock de la plie à dents de flèche (Atheresthes stomias) sur la côte ouest de la Colombie-Britannique en 2021. Secr. can. de consult. sci. du MPO. Doc. de rech 2024/071. v + 147 p.

TABLE OF CONTENTS

ABSTRACT	iv
1 INTRODUCTION	1
1.1 PURPOSE OF DOCUMENT	1
1.2 BIOLOGICAL BACKGROUND	1
1.3 FISHERY AND MANAGEMENT HISTORY	2
2 STOCK ASSESSMENT MODELLING	3
2.1 DATA INPUTS	3
2.2 STATISTICAL CATCH-AT-AGE MODEL	7
2.3 FISHERY REFERENCE POINTS	8
2.4 RESULTS	11
2.5 SENSITIVITY ANALYSES	16
2.6 RETROSPECTIVE ANALYSES	20
3 RECOMMENDATIONS AND YIELD OPTIONS	21
3.1 REFERENCE REMOVAL RATE	21
3.2 PROJECTIONS AND DECISION TABLE	21
3.3 SOURCES OF UNCERTAINTY AND FUTURE RESEARCH	22
4 ACKNOWLEDGEMENTS	24
5 FIGURES	24
5.1 BRIDGE MODEL FIGURES	40
5.2 MCMC DIAGNOSTIC FIGURES FOR THE BASE MODEL	45
5.3 SENSITIVITY MODEL FIGURES	52
5.4 PROJECTION FIGURES FOR THE BASE MODEL	69
6 TABLES	72
REFERENCES CITED	83
APPENDIX A. BIOLOGICAL DATA	88
APPENDIX B. PROPORTION FEMALE ANALYSIS	96
APPENDIX C. DISCARD CPUE INDEX STANDARDIZATION	102
APPENDIX D. GEOSTATISTICAL STANDARDIZATION OF SURVEY INDICES	114
APPENDIX E. TRENDS IN BODY CONDITION	123
APPENDIX F. ECOSYSTEM CONSIDERATIONS	127
APPENDIX G. MODEL DESCRIPTION	129
APPENDIX H. COMPUTATIONAL ENVIRONMENT	140

ABSTRACT

Arrowtooth Flounder (*Atheresthes stomias*, Turbot) are an important component of the bottom trawl fishery in British Columbia. They are managed as a coastwide stock, with a current Total Allowable Catch (TAC) of 5 kilotonnes (kt) and catch of 3.051 kt in 2021. Prior to the introduction of freezer trawlers in the mid-2000s, most of the historical catch of Arrowtooth Flounder is understood to have been discarded at sea. This was largely due to proteolysis, which occurs in the muscle tissue of this species a short time after it is caught, making the flesh unpalatable. In the past decade, markets have been established for fillets that have been frozen at sea.

This assessment fits a two-sex two-fleet Bayesian age-structured model to catch, survey, and age-composition data from the years 1996–2021 for management areas 3CD (West Coast Vancouver Island), 5AB (Queen Charlotte Sound), 5CD (Hecate Strait), and 5E (West Coast Haida Gwaii) combined. Catch data prior to the introduction of at-sea observers in 1996 were considered too unreliable for inclusion in the assessment due to unknown quantities of discarding at sea.

The base model presented in this assessment estimates the 2022 median spawning biomass to be 67.77 kt and to have been on a decreasing trajectory since 2011, with a flattening trend from 2020–2022. Reference points based on maximum sustainable yield (MSY) were strongly impacted by the relationship between estimated maturity ogives and commercial age selectivity in the trawl fisheries. Reference points based on fractions of B_0 (unfished spawning biomass) were chosen instead, as was done in the last assessment. The median 2022 spawning biomass was projected to be below the USR (Upper Stock Reference) $0.4B_0$ and above the LRP (Limit Reference Point) $0.2B_0$. There was zero probability that the spawning biomass was below the LRP of $0.2B_0$ in 2022 in the base model, although one sensitivity model with the selectivity set to be time-varying for the Queen Charlotte Sound Synoptic Survey, the relative biomass reached $0.31B_0$. Other sensitivity analyses were done to test the effects of fixed parameters, prior probability distributions, and input data treatment on model outcomes. In several sensitivity models, there were poor MCMC (Markov chain Monte Carlo) diagnostics or unreasonable estimates of selectivity and/or catchability. A series of retrospective model runs back eight years indicated a distinct change in the biomass estimates for the model. Prior to 2019, retrospective models had a more optimistic view of the stock, with a terminal year relative biomass of approximately 0.5 or greater. After 2019, models estimated a terminal year relative biomass of approximately 0.4 or less.

Management advice is provided in the form of a harvest decision table that forecast the impacts of a range of 2022 catch levels on Arrowtooth Flounder stock status relative to the reference points. The base-model decision table suggests that a 2022 catch equal to 5 kt (the 2022 TAC), would result in a 2023 biomass being below the USR of $0.4B_0$ with a probability of 0.68. The same catch would give a near zero probability of the 2023 biomass falling below the LRP of $0.2B_0$. A constant catch equal to 15 kt would result in a 2026 biomass with an approximate 0.5 probability of being below the $0.2B_0$ LRP. A reference removal rate of $U_{0.4B_0} = 10.5\%$ of the vulnerable population annually, which is equivalent to an annual removal of approximately 4.4 kt, was estimated to take the stock to $0.4B_0$ in the long term (50 years) assuming that the low recruitment estimated from 2010 to 2019 continues.

The size of catches and discards prior to 1996, the lack of random-stratified surveys prior to 2005 that together cover the entire coast, the estimation of maturity and selectivity curves, the assumed magnitude of recruitment variability, and the estimation of B_0 are major sources of uncertainty in this assessment that make it challenging to estimate the size and productivity of the stock. The use of a stitched geostatistical survey to replace the separate synoptic survey indices could help resolve some issues fitting the Queen Charlotte Sound Synoptic

survey index, which has a lower rate of decline than the other survey indices. After evaluating ecosystem considerations and known biology of the stock, there are no clear indications that current environmental conditions should modify the catch advice in this assessment. Given the stock is estimated slightly below the USR in the base model and close to the LRP under one sensitivity model with higher recruitment variation, as well as declining estimated spawning stock biomass, declining survey indices, and declining estimated recruitment, it is suggested that this stock assessment be updated with new data in approximately two years when one additional survey has been run in each area of the coast.

1. INTRODUCTION

Arrowtooth Flounder (*Atheresthes stomias*, Family Pleuronectidae, also commonly called Turbot), is a species of flatfish that occurs in the offshore waters of British Columbia. Arrowtooth Flounder are primarily taken by the groundfish bottom trawl fishery, although they are also encountered by hook and line fisheries, particularly those targeting Pacific Halibut (*Hippoglossus stenolepis*). Prior to the introduction of freezer trawlers in the British Columbia groundfish fleet in the mid-2000s, most of the historical catch of Arrowtooth Flounder is understood to have been discarded at sea. Proteolysis occurs in the muscle tissue of this species a short time after it is caught, making the flesh mushy and unpalatable. In the past five years, markets have been established for fillets that have been frozen at sea as soon as possible after capture to reduce proteolysis. There is also a market for the frills. The stock was last assessed by Grandin and Forrest (2017), who presented an age-structured Bayesian model using the ISCAM platform (Martell 2011). This stock assessment covers the combined Pacific Marine Fisheries Commission (PMFC) major areas 3CD and 5ABCDE off the west coast of British Columbia.

1.1. PURPOSE OF DOCUMENT

Arrowtooth Flounder is managed as a coastwide stock in British Columbia with the majority of the catch coming from PMFC major areas 3CD; West Coast Vancouver Island, 5AB; Queen Charlotte Sound Synoptic Survey and 5CD; Hecate Strait (Figures 1–3, Table 3). The Strait of Georgia (management area 4B) is not included in this stock assessment. The Total Allowable Catch (TAC) has been 5,000 t since February 21, 2020. The TAC was 15,000 t for many years prior to the reduction in 2020. February 21 is the start date for the groundfish trawl fishery each year.

The purpose of this stock assessment is to update management advice for Arrowtooth Flounder stocks in British Columbia as requested by the Pacific Groundfish Management Unit (GMU). This assessment identifies reference points for Arrowtooth Flounder that are consistent with the DFO Decision-Making Framework Incorporating the Precautionary Approach (DFO 2009) and characterizes stock status relative to these reference points using a Bayesian, age-structured stock assessment model. Management advice is provided in the form of decision tables, which forecast the impacts of a range of harvest levels on Arrowtooth Flounder stock status relative to these reference points.

1.2. BIOLOGICAL BACKGROUND

Arrowtooth Flounder are distinguished by their large mouth and arrow-shaped teeth, for which the species is named. Their distribution ranges from Baja California to the eastern Bering Sea (Hart 1973). In British Columbia, the species inhabits depths from 50–900 m (Fargo and Starr 2001).

Arrowtooth Flounder exhibit sexual dimorphism. After sexual maturity, females grow faster than males and reach a larger maximum size (Appendix A, Figure A.4). Theoretical maximum length, L_{∞} , is estimated to be 61.8 cm for females and 47.2 cm for males in British Columbia although the maximum sizes that have been observed are 97 cm for females and 79 cm for males (Figures A.1 and A.4). Age-at-50%-maturity for females is thought to occur around age 5.6 y for females and 4.1 y for males (Figure A.5). The maximum observed age is 27 y for females and 23 y for males. There were few observations of fish over 20 y in the dataset, and this assessment assumes a plus group of 20 y (Figure A.2).

Arrowtooth Flounder are batch spawners with peak spawning occurring at depths deeper than 350 m in the fall and winter months, although the timing of spawning may vary inter-annually

(Rickey 1995). The species produces pelagic eggs, followed by a pelagic larval stage that may last several months (Rickey 1995). Fecundity of this species is poorly understood (Cosimo 1998). One- and two-year-old fish occupy shallower depths than adults, but by the age of three or four years old, they are generally found in deeper water with adults (Fargo and Starr 2001). Arrowtooth Flounder appear to occupy separate spawning (winter) and feeding (summer) areas, and undergo seasonal bathymetric movement from shallower to deeper water in the fall and winter (Fargo and Starr 2001).

Arrowtooth Flounder have a diet comprised of zooplankton, fish, and benthic invertebrates. Juveniles feed primarily on mobile prey such as euphausiids, cumaceans, carideans, and amphipods. Adults are more piscivorous and cannibalistic, feeding on Pacific Herring (*Clupea pallasii*), juvenile Walleye Pollock (*Theragra chalcogramma*), and Pacific Sandlance (*Ammodytes hexapterus*), among other species (Fargo et al. 1981; Yang 1993).

1.3. FISHERY AND MANAGEMENT HISTORY

Prior to 2006 there were no limits on the amount of Arrowtooth Flounder that could be caught. In 2006 a TAC of 15,000 t was established and it remained at this level until 2017. In 2017, the TAC was increased to 17,500 t and remained there for two years until it was reduced to 14,000 t in 2019 as a precautionary measure to address concerns raised by the commercial trawl fleet about their observations of reduced abundance in the Arrowtooth Flounder fishery. In 2020 the TAC was decreased to 5,000 t to address industry concerns regarding declining Arrowtooth Flounder abundance on traditional fishing grounds (DFO 2020).

1.3.1. Fishery Management Impacts on Catch and Reporting

The increase in catch seen from 2010–2014 (Figures 4 and 5) was due to new market opportunities. There has been an overall decline in annual catches since 2017, with a particularly large decrease occurring in 2019 (Figure 4) and continuing through 2021. The large decrease is due to the quota reduction which was based on survey abundance index and commercial CPUE declines.

Prior to the introduction of freezer trawlers, most of the historical catch of Arrowtooth Flounder is understood to have been released at sea in unknown quantities due to proteolysis of the flesh if catches were not landed and frozen quickly after capture. Before the introduction of 100% at-sea observer coverage in the British Columbia groundfish fleets in 1996, reporting of Arrowtooth Flounder discards in fishery logbooks was mandatory, but since Arrowtooth Flounder were not given a TAC until 2005, there was little incentive for skippers to record discards accurately until at-sea observers were present aboard vessels starting in 1996. The quantity of discards in the pre-1996 period is highly uncertain and no catch reconstruction prior to 1996 could be made for this assessment. Figure 3 shows the boundaries of the commercial trawl sector (for all species) with the Synoptic surveys overlaid.

U.S. and foreign catches were not accounted for in this assessment.

2. STOCK ASSESSMENT MODELLING

We applied a two-sex two-fleet statistical catch-at-age model in a Bayesian estimation framework to assess the coastwide stock of Arrowtooth Flounder. Analysis of the sex composition of the commercial and survey sample data indicated that the stock is composed of approximately 79% females; see Appendix B, Table B.1. All models in this assessment, including the base model, bridging models, sensitivity models, and retrospective models, were run using 0.79 as the proportion of females in the stock. Bridging models 1 and 2, prior to the addition of data up to 2021 used 0.70 for the proportion female, which is what was used in the 2015 assessment.

The model was fit to commercial catch data from two fleets, six indices of abundance with associated coefficients of variation, and to age composition data from the commercial trawl fleets and four of the six surveys. Biological parameters used in the model, including growth, weight-at-age, and maturity schedules, were estimated independently for each sex (Appendix A) and input into the assessment model as fixed parameters that were assumed to remain constant over time.

Reference points based on estimated equilibrium unfished spawning biomass, B_0 , were estimated (Section 3). A harvest decision table (Table 15) was created by projecting the assessment model into the future under a range of constant catch levels. For each level of catch, the probabilities that projected spawning biomass will be less than B_0 -based reference points are provided (Section 3). Reference points based on Maximum Sustainable Yield (MSY), including the spawning biomass (B_{MSY}) and the annual harvest rate producing MSY (U_{MSY}), were estimated but not included in the decision table as they are not being presented for advice. They were estimated to show that the F_{MSY} (and U_{MSY}) values are unreasonably high, due to selectivity being estimated greater than maturity, as described in Section 2.4.5.

2.1. DATA INPUTS

2.1.1. Data Sources

Data were extracted using the R package `gfdata`, found on GitHub, in the `pbs-assess` organization's repository list. Functions in the `gfdata` package apply standard SQL routines to several databases and reconstruct the various time series accordingly. The databases accessed for this assessment were:

1. GFBioSQL: Contains all modern biological sample data for surveys and commercial fisheries. This database includes most of the groundfish specimen data collected since the 1950s.
2. PacHarvTrawl: Contains Canadian trawl landing data from 1996 to March 31, 2007.
3. GFFOS: Contains Canadian trawl landings from April 1, 2007 to present. This database is essentially a copy of the Fisheries and Oceans Canada (DFO) Fishery Operations (FOS) database with a slightly different structure that makes it easier for our assessment needs.

2.1.2. Catch Data

Commercial fishing data are presented for the period February 21, 1996 to February 20, 2021. Coastwide landings and discards are shown in Table 1 and by fleet in Table 2. The current assessment fits a two-sex Bayesian age-structured model to catch, survey, and age-composition data from the years 1996 to 2021, for management areas 3CD (West Coast Vancouver Island), 5AB (Queen Charlotte Sound), 5CD (Hecate Strait), and 5E (West Coast Haida Gwaii).

Prior to the introduction of freezer trawlers into the British Columbia groundfish trawl fleet in 2005, most of the historical catch of Arrowtooth Flounder is understood to have been

discarded at sea in large quantities due to flesh proteolysis, as discussed above. In many cases entire tows were discarded, precluding the use of ratio estimators or other statistical methods of estimating unobserved discards. All catch data prior to the introduction of 100% at-sea observer coverage in 1996 were therefore omitted from this assessment, on the recommendation of our industry advisors and technical working group, and follows what was done in the 2015 assessment (Grandin and Forrest 2017).

2.1.3. Abundance Indices

Six fishery independent indices of abundance were used in this assessment:

1. Queen Charlotte Sound Synoptic Survey (QCS Synoptic)
2. Hecate Strait Multispecies Assemblage Survey (HS Multi)
3. Hecate Strait Synoptic Survey (HS Synoptic)
4. West Coast Vancouver Island Synoptic Survey (WCVI Synoptic)
5. West Coast Haida Gwaii Synoptic Survey (bridging only)
6. Discard CPUE Index (DCPUE)

Queen Charlotte Sound Synoptic Survey

The Queen Charlotte Sound Synoptic Survey has been conducted from July–August in 2003, 2004, and in odd years starting in 2005. The survey area is divided into 2 km × 2 km blocks and each block is assigned one of four depth strata based on the average bottom depth in the block. The four depth strata for this survey are 50–125 m, 125–200 m, 200–330 m, and 330–500 m. Each year blocks are randomly selected within each depth strata. In addition, for the purposes of allocating blocks, the survey is divided into northern and southern spatial strata.

Hecate Strait Multispecies Assemblage Survey

A series of multi-species groundfish bottom trawl surveys were conducted in Hecate Strait in May–June of 1984, 1987, 1989, 1991, 1993, 1995, 1996, 1998, 2000, 2002, and 2003 (Westrheim et al. (1984); Fargo et al. (1984); Fargo et al. (1988); Wilson et al. (1991); Hand et al. (1994); Workman et al. (1996); Workman et al. (1997); Choromanski et al. (2002); Choromanski et al. (2005)). The present assessment only uses observations from 1996 until the survey ended in 2003. The original design of this survey assigned fishing locations by 10 fathom depth intervals within a 10 nautical mile grid of Hecate Strait. The survey was post-stratified using 10 fathom depth intervals for the entire survey area, thereby treating each depth interval as a single stratum. Despite attempts to apply post-sampling stratification, this approach had high survey variance (Sinclair et al. 2007). In 2004 the Hecate Strait Multispecies Assemblage Survey was discontinued in favour of the Hecate Strait Synoptic Survey (described below).

Hecate Strait Synoptic Survey

The Hecate Strait Synoptic Survey is part of a coordinated set of long-term surveys that together cover the continental shelf and upper slope of most of the British Columbia coast. The Queen Charlotte Sound Synoptic Survey and West Coast Vancouver Island Synoptic Survey described in this section are part of the same set of surveys. All the synoptic surveys follow a random depth stratified design. The relative allocation of blocks among depth strata was determined by modelling the expected catches of groundfish and determining the target number of tows per stratum that would provide the most precise catch rate data for as many species as possible. The Hecate Strait Synoptic Survey has been conducted from May–June in odd years starting in 2005. The survey area is divided into 2 km × 2 km blocks and each block is assigned one of four depth strata based on the average bottom depth in the block. The four

depth strata for this survey are 10–70 m, 70–130 m, 130–220 m, and 220–500 m. Each year blocks are randomly selected within each depth strata.

West Coast Vancouver Island Synoptic Survey

The West Coast Vancouver Island Synoptic Survey has been conducted from May–June in even years starting in 2004. The survey area is divided into 2 km × 2 km blocks and each block is assigned one of four depth strata based on the average bottom depth in the block. The four depth strata for this survey are 50–125 m, 125–200 m, 200–330 m, and 330–500 m. Each year blocks are randomly selected within each depth strata. In addition, for the purposes of allocating blocks, the survey is divided into northern and southern spatial strata.

West Coast Haida Gwaii Synoptic Survey

The West Coast Haida Gwaii Synoptic Survey has been conducted from August–September in even years starting in 2006. The survey area is divided into 2 km × 2 km blocks and each block is assigned one of four depth strata based on the average bottom depth in the block. The four depth strata for this survey are 180–330 m, 330–500 m, 500–800 m, and 800–1,300 m.

Discard CPUE Index

A standardized commercial CPUE index, as has been used in other recent DFO Pacific assessments, was not used due to the behaviour of the fishery. Arrowtooth Flounder are targeted on known grounds, and the location information is shared among fishermen, so there is a bias towards a high CPUE. Instead, a Discard CPUE Index was suggested by stakeholders as an approach to create an index of abundance that would span every year in the assessment and be less influenced by changes in targeting behaviour than a standard commercial CPUE index. The index was constructed using CPUE for a defined ‘fleet’ of vessels and only included tows in which 100% of Arrowtooth Flounder were discarded. See Appendix C for more details.

Swept Area Analysis for Indices of Abundance

For all surveys, the swept area estimate of biomass in year y was obtained by summing the product of the CPUE and the area surveyed across the surveyed strata i :

$$B_y = \sum_{i=1}^k C_{y_i} A_i = \sum_{i=1}^k B_{y_i} \quad (1)$$

where C_{y_i} is the mean CPUE density (kg/km²) for species in stratum i , A_i is the area of stratum i , B_{y_i} is the biomass of Arrowtooth Flounder in stratum i for year y , and k is the number of strata.

CPUE (C_{y_i}) for Arrowtooth Flounder in stratum i for year y was calculated as a density in kg/km² by:

$$C_{y_i} = \frac{1}{n_{y_i}} \sum_{j=1}^{n_{y_i}} \frac{W_{y_i,j}}{D_{y_i,j} w_{y_i,j}} \quad (2)$$

where $W_{y_i,j}$ is the catch weight in kg for Arrowtooth Flounder in stratum i , year y , and tow j , $D_{y_i,j}$ is the distance travelled in km for tow j in stratum i and year y , $w_{y_i,j}$ is the net opening in km by tow j , stratum i , and year y , and n_{y_i} is the number of tows in stratum i .

The variance of the survey biomass estimate V_y for Arrowtooth Flounder in year y is calculated in kg² as follows:

$$V_y = \sum_{i=1}^k \frac{\sigma_{y_i}^2 A_i^2}{n_{y_i}} = \sum_{i=1}^k V_{y_i} \quad (3)$$

where $\sigma_{y_i}^2$ is the variance of the CPUE in kg^2/km^4 for year y in stratum i , V_{y_i} is the variance of Arrowtooth Flounder in stratum i for year y , where $\sigma_{y_i}^2$ was obtained from bootstrapped samples (see below).

The CV for Arrowtooth Flounder for each year y was calculated as follows:

$$CV_y = \frac{V_y^{1/2}}{B_y} \quad (4)$$

where CV_y is the CV for year y .

One thousand bootstrap replicates with replacement were constructed from the survey data to estimate bias-corrected 95% confidence intervals for each survey year (Efron 1982). Mean survey biomass estimates obtained from Eq. 1 with CVs (Eq. 4) are presented for the fishery-independent indices in Table 4.

We also included a set of geostatistical-model-standardized indices in our sensitivity analyses (Appendix D).

2.1.4. Age Data

Ages for the years 1996–2019 are included in this assessment from the two commercial fleets and three synoptic surveys. The samples were aged by the bake-and-break method, which involves placing a large number of otoliths in a tray, baking them in a specially designed oven, then breaking them to perform age reads. During this process, if the person ageing the otoliths finds one that is not baked enough, they will burn the otolith manually to give it the right contrast for age reading. This extra burning step makes this method equivalent to the traditional break-and-burn method in which the age-reader burns each otolith individually (S. Wischniowski, Sclerochronology Laboratory, Pacific Biological Station, Pers. Comm.).

Age composition data represented the whole coast for the following years:

1. Freezer trawlers (Figure A.2), 2013–2019
2. Shoreside (Figure A.2), 1996–2019
3. Queen Charlotte Sound Synoptic Survey (Figure A.2), 2003–2019
4. Hecate Strait Synoptic Survey (Figure A.2), 2005–2019
5. West Coast Vancouver Island Synoptic Survey (Figure A.2), 2004–2019
6. West Coast Haida Gwaii Synoptic Survey (Figure A.2), 2016–2018, (bridging models only)

Age composition data were input to the assessment models as weighted proportions-at-age. Weighting was based on a stratified scheme that adjusted for unequal sampling effort across depth strata and tow biomass density (surveys) or quarterly period within a year and tow catch weight (commercial). Details are given in Holt et al. (2016) (page 160) and the 2015 assessment (Grandin and Forrest 2017). The methods used are from the `gfplot` package, found on GitHub, in the `pbs-assess` organization's repository list. The 2015 assessment used custom code as the `gfplot` package was not yet available.

Commercial ageing requests included randomly chosen samples from many vessels across both commercial fleets.

2.1.5. Length data

Length data from the freezer trawler and shoreside fleets and from the synoptic surveys are shown in Figure A.1. Survey lengths are shown by sex and commercial lengths are aggregated. Some of the commercial length histograms are bimodal illustrating the sexual dimorphism of this species.

Females did not vary in length significantly between the two fleets, with both having an overall median of 52 cm. Males had a median of 45 cm for the Freezer trawler fleet and 43 cm for the Shoreside fleet. Females had a median of 54 cm for the Freezer trawler fleet and 52 cm for the Shoreside fleet.

Females have been sampled more often than males in both fleets. This difference in sampling is due to the proportion of females in the population being higher than males. Appendix B describes in detail how the proportion female was calculated.

2.1.6. Growth parameters

Growth parameters were estimated outside the ISCAM framework. They were input into data files for the stock assessment model. Appendix A contains details including equations and the estimated growth parameter values for the base model in Table A.1.

2.2. STATISTICAL CATCH-AT-AGE MODEL

2.2.1. Model Description

A two-sex, Bayesian statistical catch-at-age model was applied to assess the coastwide stock status of Arrowtooth Flounder. The model is based on the Integrated Statistical Catch Age Model (ISCAM) framework, Martell et al. (2011). Full model details are provided in Appendix G.

We define a base model with fixed and estimated parameters described in Table 5. A total of 147 model parameters were estimated by the base model (Table 5 shows most of these). The model estimated time series of log recruitment anomalies and log fishing mortality rates; and time-invariant values of unfished recruitment, steepness of the Beverton-Holt stock-recruit relationship, natural mortality, average recruitment, and logistic selectivity parameters for the two commercial fisheries and the four synoptic surveys. Prior probability distributions for the base model are shown in Table 5 and Figure 36 and described in Section 2.2.2. Model sensitivity to fixed parameters and to assumed prior probability distributions are presented in Section 2.5.

The model was conditioned on observed catch data (1996–2021), which were assumed to be known without error. The model was fit to four survey indices of abundance, the Discard CPUE index, and to age composition data from the two commercial fisheries, and three synoptic surveys. Biological parameters determining weight-at-age and maturity-at-age schedules were estimated independently (Appendix A) and input into the assessment model as fixed parameters that remained constant over time (Table A.1).

Survey biomass indices were treated as relative abundance indices that are directly proportional to the survey vulnerable biomass at the beginning of each year. Observation errors in relative abundance indices were assumed to be log-normally distributed. The catchability parameter q_k was estimated for each index k . Prior probability distributions for $\ln(q_k)$ are described in Section 2.2.2.

Age-composition observations were assumed drawn from a Dirichlet-multinomial distribution. It was assumed ages were read without error.

Selectivity-at-age for the trawl fisheries, four surveys, and Discard CPUE index was modelled using a two-parameter logistic function with asymptote at 1. Age-at-50%-vulnerability (\hat{a}_k) and the standard deviation of the logistic selectivity curve ($\hat{\gamma}_k$) for each gear k were estimated for the trawl fisheries and the three synoptic surveys. No age composition data were available for the Hecate Strait Multispecies Assemblage Survey and Discard CPUE Index so selectivity was fixed with $\hat{a}_k = 9$ and $\hat{\gamma}_k = 0.5$, similar to estimated values for the other gears. Additional sensitivity runs not included in this assessment document indicated that there was little model sensitivity to this assumption.

Variance components of the model were partitioned into observation and process errors. The key parameter is the total variance (i.e., ϑ^2 , total precision). The total variance is partitioned into observation and process error components by the model parameter ρ , which represents the proportion of the total variance that is due to observation error (Punt and Butterworth 1999; Deriso et al. 2007). The total variance is partitioned into observation errors (σ) and process errors (τ) using Eq. G.32 from Appendix G. The parameters ϑ^2 and ρ were fixed in the current assessment (Table 5) at values that gave $\sigma = 0.2$ and $\tau = 0.8$. See Section 2.5.1 for sensitivity analyses to this assumption. See Appendix for further details on the treatment of variance in this assessment.

2.2.2. Prior Probability Distributions

Prior probability distributions for the base model are shown in Figure 36 and Table 5. Model sensitivities to assumed prior distributions are presented in Sections 2.5.1, 2.5.3, and 2.5.4.

Uniform prior probability distributions were assumed for $\ln(R_0)$, $\ln(\bar{R})$, $\ln(R_{\text{init}})$ and selectivity parameters (Table 5). A Beta distribution was assumed for the steepness (h) of the stock-recruit relationship, with shape parameters that resulted in a distribution with mean = 0.85 and CV = 0.10 (Beta($\alpha = 13.4$, $\beta = 2.4$)). This prior was based on a literature review on steepness parameters for Pacific flatfish species done by Holt et al. (2016) and was used in the 2015 assessment for Arrowtooth Flounder. A review of steepness estimates for flatfish species by Maunder (2012) suggested that flatfish steepness using a Beverton-Holt stock-recruit relationship may be around 0.94 (where h approaching 1.0 implies recruitment is independent of spawning biomass).

A normal distribution was assumed for $\ln(M)$ for both sexes with mean = $\ln(0.20)$ and SD = 1.22 for females and mean = $\ln(0.35)$ and SD = 1.22 for males (in log space). Holt et al. (2016) reviewed the literature and stock assessments and assumed a prior probability distribution for M with mean = 0.2 in their assessment of British Columbia Rock Sole (*Lepidopsetta spp.*). Shotwell et al. (2021) assumed a value of $M = 0.2$ for females and $M = 0.35$ for males in the assessment of Gulf of Alaska Arrowtooth Flounder; the same was done for the Bering Sea Aleutian Islands stock (Spies and W. 2019).

Normal prior probability distributions were assumed for the log survey catchability parameters $\ln(q_k)$ for each survey k . Normal distributions with mean = $\ln(0.499999990279973)$ and SD = 1 in log space were selected because the survey estimates of biomass were derived from swept area analysis (Eqs. 1, 2, and 3) and could therefore reasonably be expected to be within 1–2 orders of magnitude of unity. A large standard deviation was used to reflect ignorance of the scale of the swept area analysis compared with the true biomass.

2.3. FISHERY REFERENCE POINTS

The DFO Fishery Decision-Making Framework Incorporating the Precautionary Approach (PA) policy (DFO 2009) requires stock status to be characterized using three reference points:

1. A Reference Removal Rate
2. An Upper Stock Reference point (USR)
3. A Limit Reference Point (LRP)

Provisional values of $\text{USR} = 0.8B_{\text{MSY}}$ and $\text{LRP} = 0.4B_{\text{MSY}}$ are suggested in the absence of stock-specific reference points. The framework suggests a reference removal rate of F_{MSY} . A harvest control rule based on these reference points that is coincident with the choice of LRP, USR, and removal reference would apply a linear reduction in fishing mortality as the stock falls below the USR and would cease fishing when the stock reaches the LRP (e.g., Figure 6 in Grandin and Forrest 2017).

The F_{MSY} (and annual harvest rate U_{MSY}) are estimated to be very large in this model due to selectivity being greater than maturity, as described in Section 2.4.5. We therefore present B_0 -based reference points for Arrowtooth Flounder that are less reliant on estimated selectivity and maturity at age. We suggest an LRP = $0.2B_0$ and USR = $0.4B_0$. These are the reference points agreed to in the last assessment for Arrowtooth Flounder in British Columbia (Grandin and Forrest 2017); we further elaborate on our reasoning below.

2.3.1. Limit Reference Point (LRP)

We suggest an LRP of $0.2B_0$ as a proxy for recruitment overfishing. A value of $0.2B_0$ is a threshold below which there is typically at least some reduction in per-capita recruitment (Myers et al. 1994; Sainsbury 2008). This threshold has been recommended in recent national guidance (Barrett et al. 2022). Furthermore, this threshold is consistent with recommendations in other jurisdictions: a limit value of $0.2B_0$ is the default recommendation (and minimum acceptable value) under Australia’s Commonwealth Fisheries Harvest Strategy Policy (Department of Agriculture and Water Resources, Australian Government 2018) and is the default trigger for rebuilding plans under New Zealand’s Harvest Strategy (Ministry of Fisheries, New Zealand Government 2008).

2.3.2. Upper Stock Reference Point (USR)

Under the PA Policy, the USR can perform two functions: (1) a ‘threshold below which removals must be progressively reduced in order to avoid reaching the LRP’ (an operational control point or ‘OCP’) and (2) a ‘target reference point determined by productivity objectives for the stock, broader biological considerations, and social and economic objectives for the fishery’ (DFO 2009). Marentette and Kronlund (2020) emphasize that the primary role of the USR is its first role, as an OCP, to avoid the LRP. The PA Policy describes how the USR is meant to be developed by fishery managers with consultation with interested parties and advice from Science. We therefore provide the following science advice regarding the USR.

First, one rationale for choosing $0.4B_0$ is that under a Schaefer surplus production model, B_{MSY} is $0.5B_0$ and since $0.8B_{MSY}$ is the provisional USR and $0.8 \times 0.5 = 0.4$, $0.4B_0$ is the equivalent B_0 -based USR. A similar rationale applies to $0.2B_0$ as the LRP: $0.4B_{MSY}$ is the provisional LRP and $0.4 \times 0.5 = 0.2$ resulting in $0.2B_0$ as the LRP.

In addition, there is a rationale regarding the USR’s role in triggering fishery reductions to reduce risk of the stock breaching the LRP. The PA Policy notes that *‘while socio-economic factors may influence the location of the USR, these factors must not diminish its minimum function in guiding management of the risk of approaching the LRP’*. We suggest the following scientific factors should be considered with respect to the timing of adjusting fishing intensity as the stock approaches the LRP: (1) the level of uncertainty around the relative spawning biomass; (2) the frequency of assessment; (3) the availability of important data sources; and (4) plausible future rates of decline. We present the following advice with respect to these factors for Arrowtooth Flounder (as will be shown in the results):

1. The level of uncertainty around relative biomass is reasonably high with the 95% CIs roughly spanning the width between $0.2B_0$ and $0.4B_0$. Greater uncertainty means the USR would need to be spaced further from the LRP to ensure an equivalent risk tolerance.
2. Although it has been several years since the last assessment, we recommend the stock assessment be updated approximately every two years, when an additional year of data is available from each survey. Longer gaps between assessments would require the USR to be further spaced from the LRP to ensure an equivalent risk.
3. Commercial age samples have not been available for this stock since 2019 and it unclear when this sampling will resume. These data provide a critical source of information about

recruitment and selectivity. The assessment results show that declines in estimated recruitment from 2009–2019 are responsible for a large part of the recent estimated declines in SSB. The lack of age samples may introduce uncertainty going forward, which would suggest a larger gap between the LRP and USR for an equivalent risk compared to having this information.

4. Although the stock is estimated to have undergone a relatively rapid decline in SSB from about 2012 to 2020, this was associated with higher F 's than are currently estimated and this past trajectory is not necessarily indicative of future possible trajectories. A closed-loop simulation analysis would be a rigorous way of evaluating plausible stock trajectories and the ability for a given USR to provide sufficient time to avoid the stock biomass falling below the LRP. We therefore have little information currently about plausible future rates of decline.

Several other jurisdictions worldwide suggest or legislate targets near $0.4B_0$ when status is assessed relative to B_0 ; however, these jurisdictions also use this 'target' as an Operational Control Point (OCP) below which fishing mortality F is to be reduced to avoid hitting a lower limit reference point (Punt et al. 2008, and references therein). It is our understanding that the North Pacific Fishery Management Council (NPFMC) in Alaska would use an upper OCP of $0.4B_0$ for this Arrowtooth Flounder stock with F ramped down when biomass is below this level ('Tier 3 3b,' p. 19 in NPFMC 2020). The US West Coast Pacific Fishery Management Council (PFMC) also uses $0.4B_0$ as a standard groundfish OCP to ramp down F (PFMC 2022), although a flatfish-specific OCP of $0.25B_0$ was added in 2010 (Amendment 16-5 NMFS 2010). However, this is under the assumption that flatfish stocks are often more productive than other groundfish stocks, which may not bear out for this BC stock with low estimated recruitment over the last decade. Australia uses maximum economic yield (MEY) as their legislated objective, which they suggest can be approximated as $0.4B_0 \times 1.2 = 0.48B_0$; this then acts as an OCP with exploitation rate ramped down below $0.48B_0$ (p. 9 and 22 in Department of Agriculture and Water Resources, Australian Government 2018). In other words, in these jurisdictions, their 'target' matches the primary definition of the Canadian USR (Marentette and Kronlund 2020) as an OCP. This interpretation would suggest that, despite the use of the term 'target' elsewhere, a USR would be equivalent in function to these jurisdictions. Most equivalent in function to these jurisdictions would be to consider $0.4B_0$ both a 'target' and a USR OCP rather than how they are separated in the PA Policy diagram.

Finally, from a science perspective, we note that $0.4B_0$ was previously accepted as the USR for Arrowtooth Flounder (Grandin and Forrest 2017). We caution that reducing reference points when there is evidence of declining recruitment and declining stock trends would be inconsistent with the precautionary approach as outlined in the DFO PA Policy. Such 'moving the reference point goalposts' can have considerable implications for fisheries sustainability (Silvar-Viladomiu et al. 2021).

2.3.3. Reference removal rate

Although the PA Policy recommends F_{MSY} as a provisional reference removal, for reasons outlined above, we suggest B_0 -based reference points for this stock. We suggest that an equivalent reference removal rate would be the fishing mortality F that would take the stock to $0.4B_0$ at equilibrium given recently observed recruitment. We determined this by projecting the stock 50 years into the future with recruitment deviations randomly drawn with replacement from 2010–2019 (omitting the poorly estimated 2020 and 2021 deviations), using an optimization routine to find the constant catch that would generate SSB matching $0.4B_0$ within a tolerance of 50 t. We report the associated F at the end of 50 years. Given sufficient projection years, performing the projections with a constant F or a constant catch should render the same conclusion.

2.3.4. Dynamic B_0

A dynamic B_0 was calculated by recreating the population dynamics model in R with parameter estimates from the fitted base model. The fishing mortality was set to zero but estimated recruitment deviations were included. Figure 10 shows the estimated dynamic B_0 from this exercise. The figure illustrates that the model explains a portion of the recent decline by a sequence of poor recruitment.

2.4. RESULTS

2.4.1. Bridge Models

A set of bridging models was run to determine the effects of incremental model modifications while moving from the single-sex, single-fleet 2015 assessment model to the two-sex, two-fleet model used in this assessment.

The base model from the 2015 assessment (Grandin and Forrest 2017) was run with the newest version of the ISCAM (Martell 2011) code and the original data files. The parameter estimates, reference points, estimated trajectories, index fits, and age composition fits were determined to be identical. The 2015 model was a female-only catch-at-age model with four indices of abundance, which included the three Synoptic surveys and the Hecate Strait Multispecies assemblage survey.

The Technical Working Group (TWG) for Arrowtooth Flounder was formed prior to the data preparation and assessment modelling to determine which data should be used in the model, survey index suitability for the stock, and the best model parameterization to use for this year's assessment. The group was made up of external and DFO scientists, industry advisors, and fisheries managers who have insight into the Arrowtooth Flounder stock and fishery.

The TWG agreed that the model should be two-sex, based on the sexual dimorphism observed in the age and length data for this species, and there being eight more years of data since the 2015 assessment, which allowed for a larger number of age proportion specimens for each sex.

All bridge models were run using MCMC (Markov chain Monte Carlo) sampling with a chain length of 10,000,000, retaining every 5,000th sample, giving 2,000 samples, which were then burned in by 1,000 giving a total of 1,000 samples used for inference.

Each model in this list is based on the previous one with only one change made so incremental changes can be tracked.

1. 2015 Base model (Grandin and Forrest 2017).
2. Extracted the data for the 2015 model using the `gfdata` and `gfplot` packages, which have been used in several assessments and in the `gfsynopsis` package/report [Anderson2019synopsis; DFO2022synopsis]. The packages can be found on GitHub, in the `thepbs-assess` organization's repository list.
3. Using the same data extraction methods as in the previous step, appended data up to and including 2021. The proportion female was changed in this step from 0.70 to 0.79.
4. Added the West Coast Haida Gwaii Synoptic Survey index and age composition data. This was tried to determine how the additional survey years since 2015 contributed to the model fit.
5. Switched the age composition likelihood from multinomial to the saturating parameterization of the Dirichlet-multinomial (Thorson et al. 2016). We did this because in more complex model configurations, the multivariate normal logistic had convergence issues and the standard multinomial would have required manually re-weighting the age proportions for each model run (Francis 2016).

-
6. Changed the model from one to two commercial fleets. This splits the commercial trawl catch into catch from Freezer Trawlers and Shoreside fleets. This was done on the recommendation of the Technical Working Group (TWG) since the large freezer trawlers may fish differently and have different selectivity than the shoreside vessels.
 7. Added a Discard CPUE index. This was suggested by the TWG and is an index of catch per unit effort for vessels that were not fishing for Arrowtooth Flounder and therefore were discarding all that they caught incidentally. The selectivity could not be estimated for this index since there are no age composition data for it, so its selectivity was fixed to values representative of other estimated selectivities from other gears. See Appendix C for details on how this index was generated.
 8. Converted the model from female-only to a two-sex model. In this model, the two natural mortality parameters for male and female were estimated.
 9. Changed fishing year to start on February 21 (vs. January 1), which is the date currently used by Fisheries Management for the fishing year.
 10. Removed the West Coast Haida Gwaii Synoptic Survey index and age comps. The survey was not contributing meaningfully to the assessment and the estimated selectivities were not viable due to too few samples. Its removal was suggested by the TWG.
 11. Fixed both male and female natural mortality parameters. The estimated values were quite low for this species based on assessments in neighbouring jurisdictions (Spies et al. 2017, 2019; Shotwell et al. 2020, 2021).

Bridge models group 1 (models 1-4)

Figure 29 shows the absolute and relative spawning biomass for the first four bridging models in the list above (list items 1–4). Changing the data extraction method for all data up to 2014 had minimal effect, with only a small difference in 2015 absolute biomass and a very small difference in 2015 relative biomass. Small changes in data are mainly due to changes in survey indices, which are caused by survey blocks being removed from the entire survey series. These blocks were found to be unfishable or inappropriate for the index in the surveys since 2014 and were removed from the entire series, changing the historical indices slightly from those included in the 2015 assessment.

Adding the data from 2015–2021 caused a large change in the biomass trajectories (Figure 29). The biomass began dropping more rapidly starting in 2002, with a relatively steep drop from 2010–2020. This decline in the biomass is caused mainly by the declining indices of abundance in that time period. From 2021–2022 the model shows the beginnings of an upward trend. Credible intervals (CIs) became much narrower with the addition of the 2015–2021 data. However, the estimated parameters (except steepness) are all moderately to highly correlated (Figure 30). All the bridging models that follow have high correlation between parameters, except for the last one in which the natural mortalities for both sexes were fixed.

Adding the West Coast Haida Gwaii Synoptic Survey age compositions and index into the model had a scaling effect in the earlier part of the trajectory, but both absolute and relative biomasses were nearly identical for 2022 (Figure 29).

Bridge models group 2 (models 5-8)

Figure 31 shows the absolute and relative spawning biomass for the second group of four bridging models (list items 5–8). Changing the age data weighting to the saturated Dirichlet multinomial (DM) (Thorson et al. 2016), caused a drop in absolute biomass and B_0 . The B_0 median for the first model in Figure 31, when compared to the B_0 median for the last model in Figure 29 shows a difference of 16,000 t (from 203,000 to 187,000 t). However, the biomass estimates were also scaled down, so the 2022 relative biomass only dropped a small amount (from 0.45 to 0.42).

For the next bridging model, the commercial trawl fishery was split into two fleets: the Freezer trawlers and Shoreside fleets. This changed the model internals but had negligible effect on the biomass and relative biomass trajectories (Figure 31).

Adding the Discard CPUE Index (DCPUE) to the model had almost no effect on the absolute biomass and B_0 estimates. It did, however, reduce the credible interval (Figure 31) on the absolute spawning biomass time series.

The next step in the bridging was to convert the model into a two-sex model. All previous bridge models were female-only. This step involved significant modifications to the ISCAM model code. This change caused a drop in final-year biomass and relative biomass, and some overall scaling up of the historical relative biomass trajectory (Figure 31). The selectivity age-at-50% estimates (\hat{a}) for females in the West Coast Haida Gwaii Synoptic Survey for this model were unreasonable at NA (NA–NA) years.

Bridge models group 3 (models 9–13)

The biomass plots for the final group of bridging models (list items 9-13) can be found in Figure 32. For the first of these models, the fishing year was changed from what it was in the 2015 assessment, January 1–December 31 to February 21–February 20. This change was made to reflect the start date for the fishery each year in Canada (February 21). The effect of this is the median B_0 and relative biomass being the same as the two-sex base model found in Figure 31. The credible interval of the absolute biomass is the same size but moves slightly from 49–93 (width 44) to 47–91 (width 44). The credible interval on the relative biomass is the same in size and position for the base model and the model with the fishery timing change (Figure 32).

The West Coast Haida Gwaii Synoptic Survey was removed (it was also removed in the 2015 assessment) as it had poor selectivity estimates.

The natural mortality estimates from the model at this point were 0.21 for males and 0.14 for females with credible intervals of 0.20–0.22 (width 0.01) and 0.13–0.15 (width 0.01) respectively. The female estimate of natural mortality was close to the fixed value for females in assessments done in neighbouring jurisdictions (0.20), but the male estimate was much lower than what was used in neighboring stocks (0.35). Based on the estimated natural mortality values and the high correlation between estimated parameters for this model (Figure 35), we decided to fix the natural mortalities at the same values as the Gulf of Alaska and Bering Sea and Aleutian Islands assessments (Spies et al. 2019; Spies and W. 2019; Shotwell et al. 2020, 2021); 0.20 for females and 0.35 for males.

2.4.2. Model diagnostics

The joint posterior distribution was numerically approximated using the Metropolis Hastings Markov Chain Monte Carlo (MCMC) sampling algorithm in AD Model Builder (Fournier et al. 2012). For the base model and all sensitivity cases, posterior samples were drawn every 5,000 iterations from a chain of length 10,000,000, resulting in 2,000 posterior samples (of which the first 1,000 were dropped as burn-in). Convergence was diagnosed using visual inspection of the traceplots (Figures 37 and 39) and examination of autocorrelation in posterior chains (Figures 38 and 40). Autocorrelation was low at lag values up to 1,000 for all parameters after thinning. Correlation between parameters appeared low overall, with only some moderate correlations between catchability parameters and \bar{R} (Figures 41 and 42). There was no strong evidence for lack of convergence in the base model.

2.4.3. Fits to Data

Catch was constrained by standard deviation value of 0.2 for the first phase of minimization and by 0.051 for the last phase, so the predicted catch fit the data very well (Figure 6).

The model generally fit the indices of abundance well (Figure 14). The West Coast Vancouver Island Synoptic Survey has a large fluctuation high and low for successive years of the survey from 2008–2016, which is difficult for the model to fit. The Queen Charlotte Sound Synoptic Survey was difficult to fit, due to fluctuations from high to low abundance from year to year early in the time series, and the lack of the recent drop in biomass seen in all other data sources. A sensitivity was done to attempt a better fit on this index, while retaining the good fits on the others (Section 2.5.6).

The Discard CPUE Index fit particularly well and is the only index to have a value for every year in the assessment. Standardized residuals show mostly even distribution of positive and negative residuals, with evidence of some autocorrelation in the Discard CPUE Index residuals (Figure 15). For all indices, the log index residuals (Figure 15) were good, with all being in the $[-2, 2]$ range.

Fits to age compositions for each gear, and log standardized residuals are shown in Figures 16–26. Fits were reasonable and there were no strong patterns in the residuals.

2.4.4. Parameter Estimates

Prior and posterior probability distributions of estimated parameters are shown in Figure 36. The median and 95% CI (2.5th and 97.5th percentile) posterior parameter estimates are shown in Table 6. With the exception of steepness, the posterior estimates did not appear to be strongly influenced by the prior probability distributions. The posterior probability distribution for steepness, h , was similar to the prior distribution, suggesting that there was little information about this parameter in the data. Sensitivity to the assumed prior for steepness is tested in Section 2.5.2.

Normal prior probability distributions were used for the log catchability parameters $\ln(q_k)$ for the indices of abundance (Figure 36). Posterior estimates tended to overlap with the left-hand tail of the prior distributions for each index. Sensitivity analyses (discussed in Section 2.5) indicated that posterior estimates of catchability were sensitive to the mean and standard deviation of the prior distribution.

2.4.5. Selectivity

Selectivity-at-age was estimated for the two fisheries and the synoptic surveys (Figure 27). The Discard CPUE Index and Hecate Strait Multispecies Assemblage Survey fixed selectivities are also shown in Figure 27.

Posterior estimates of age-at-50%-harvest (\hat{a}_k) and the standard deviation in the logistic selectivity ogive ($\hat{\gamma}_k$) are provided in Table 6. The median posterior estimates of age-at-50%-harvest were higher for females than males for all gears except for the Hecate Strait Synoptic Survey, which had a higher estimate for males. The estimates of standard deviation were similar between sexes by gear.

These estimates were further to the right than expected, but were consistent with the available age composition data (Figure A.2), which indicate fewer observations of younger fish, especially in the latter part of the time series. Numerous tests of alternative model configurations did not result in a lower estimate of age-at-50%-harvest for any gear/sex combination.

Arrowtooth Flounder are thought to mature at around 5.6 years of age for females and 4.1 years of age for males (Figure A.5, Table A.1). Therefore, it appears that individuals have several opportunities to spawn before they become vulnerable to the fishery. This in turn resulted in estimates of maximum sustainable harvest rate U_{MSY} approaching 1 (discussed in Section 2.4.6), implying that under theoretical equilibrium conditions, all of the vulnerable (i.e., fully selected) biomass could be harvested because the population could be sustained by younger spawners that are invulnerable to the fishery. This is a theoretical condition subject to

the assumptions in the stock assessment model and the data limitations therein. We strongly advise against this as a harvest strategy and suggest that the age-at-50% selectivity in the commercial trawl fleets are a primary axis of uncertainty in this stock assessment.

2.4.6. Fishery Reference Points

Posterior estimates of fishery reference points from the base model are provided in Table 7 and Figure 28. The posterior unfished spawning biomass (SB_0) (abbreviated to B_0 herein) had a median 184,155 t and 95% CI ranging from 128,212 t to 263,786 t (Table 7). Posterior 95% CIs for the LRP $0.2B_0$ and USR $0.4B_0$ are also provided in Table 7.

Reference points based on maximum sustainable yield MSY were strongly impacted by estimates of selectivity in the trawl fisheries described in the previous section. Because the selectivity ogives were estimated to the right of the maturity ogive, the median estimates of F_{MSY} were 1.52 for the Freezer trawler fleet and 4.77 for the Shoreside fleet (Table 7). The CI on these values is large, 0.34-3.92 for the Freezer trawlers fleet and 0.86-15.35 for the Shoreside fleet. These instantaneous fishing mortalities convert to an annual harvest rate approaching 1 for the Shoreside fleet (Figure 28), through the equation $U_{MSY} = 1 - e^{-F_{MSY}}$, implying that all of the vulnerable biomass (i.e., the biomass that is selected by the fishing gear) could be harvested because the population can be sustained by the spawning biomass that is invulnerable to the fishery (i.e., fish that are between 5.6 and 8.4 years for females and 4.1 and 8.3 for males). The relationship between age at maturity and age at first harvest and its effect on fishery reference points was discussed by Myers and Mertz (1998), who described a fishing strategy where overfishing could be avoided by allowing all fish to spawn before they were available to be caught. Froese (2004) also discusses reduction in risks of overfishing by allowing fish to spawn before they are caught.

It is important to understand the distinction between vulnerable biomass and spawning biomass. The fishery reference points F_{MSY} and U_{MSY} refer to catch of the vulnerable biomass VB_t , which is determined by the selectivity function

$$VB_{t,k} = \sum_a N_{a,t} w_{a,t} v_{a,t,k}, \quad (5)$$

where a is age, t is year, k is the trawl fishery (Freezer trawlers or Shoreside), N is the population number, w is the average weight-at-age, and v is the vulnerability-at-age in the trawl fisheries (i.e., selectivity).

When the selectivity ogive is located to the right of the maturity ogive, this means that a larger proportion of the total population is mature than vulnerable to the fishery (Figure 11). A comparison between vulnerable biomass and spawning biomass is provided in Section 2.4.7.

The median posterior estimate of B_{MSY} (and 95% CI), conditional on estimated trawl selectivities and resulting F_{MSY} values, was 30,957 t (16,067–60,828) (Table 7). Posterior CIs for the default LRP $0.4B_{MSY}$ and USR $0.8B_{MSY}$ are also provided in Table 7. The B_0 -based LRP and USR were approximately four times as large as the B_{MSY} -based reference points. I.e., B_0 -based reference points were more precautionary than the B_{MSY} -based reference points (Table 7).

2.4.7. Biomass

The base model estimates the spawning biomass to have been on a decreasing trajectory since 2011, with a flattening trend from 2020-2022 (Figure 7, Table 8). The posterior median (and 95% CI) spawning biomass in 2022 is projected to be 67,955 t (56,137–83,830) (Table 7). The median projected beginning-of-year 2022 spawning biomass, which incorporates fishing mortality arising from the observed 2021 catch, is considerably higher than median estimates

of both the default USR of $0.8B_{\text{MSY}}$ and the default LRP of $0.4B_{\text{MSY}}$ (Figure 7, Table 7). The 2022 spawning biomass was projected to be slightly below the USR $0.4B_0$ and above the LRP $0.2B_0$ (Figure 9, Table 7).

For comparison, posterior estimates of vulnerable biomass and spawning biomass are shown together in Figure 11. The two estimated vulnerable biomasses are considerably smaller than the spawning biomass, due to the relatively early age at maturity compared to the estimated age-at-50%-harvest, discussed in Sections 2.3 and 2.4.6.

Given the choice to base reference points on B_0 , some participants at the regional peer review meeting expressed interest in comparing biomass to a dynamic B_0 that reconstructs what biomass would be expected through time without fishing mortality. A dynamic B_0 was calculated by recreating the population dynamics model in R with parameter estimates from the fitted base model. The fishing mortality was set to zero but estimated recruitment deviations were included. Figure 10 shows the estimated dynamic B_0 from this exercise.

This figure illustrates that the model explains a portion of the recent decline by a sequence of poor recruitment.

2.4.8. Recruitment

Median posterior estimates of age-1 recruits are shown in Figure 12 and Table 10. The 95% CIs are large around the estimates of 2020 and 2021 recruitment. This is expected since there is no information in the data about the strength of this year class (also seen in other assessments such as Figure 28 of Edwards et al. 2022).

Projected recruitment anomalies for 2021 and 2022 were drawn randomly from a normal distribution, $N(0, \tau^2)$. For most of the time series prior to 2008, recruitment was estimated to fluctuate around the long-term average, with little variation around R_0 . However, since 2009, annual recruitment has been below average.

2.4.9. Fishing mortality

Median posterior estimates of fishing mortality are shown in Figure 13 and Table 11. The median posterior estimate of fishing mortality is estimated to have peaked in 2005 in the Shoreside fishery at 0.327 (0.275–0.388) as a result of higher effort due to a new market as described in Section 1.3.1. Fishing mortality rates converted to annual harvest rates can be found in Table 12.

2.4.10. Relative spawning biomass

Median posterior estimates of relative spawning biomass B_t/B_0 are shown in Figure 9. The size of the 95% CI is amplified when compared to the absolute spawning biomass due to large uncertainty in the estimate of B_0 (Figure 8, Table 7). The median posterior projected estimate of 2022 relative biomass is 0.373 (0.262–0.514) (Figure 9, Table 9).

2.5. SENSITIVITY ANALYSES

We tested sensitivity of the model outputs as follows:

1. Decrease σ from 0.2 to 0.135 (changes ϑ^2 and ρ) and estimate ϑ^2
2. Increase initial value of τ from 0.8 to 1.0 (changes ϑ^2 and ρ) and estimate ϑ^2
3. Decrease initial value of τ from 0.8 to 0.6 (changes ϑ^2 and ρ) and estimate ϑ^2
4. Decrease mean of h prior from 0.85 to 0.72
5. Estimate M_{female} with a narrow prior (SD = 0.2)
6. Estimate M_{female} with a broad prior (SD = 1.6)

-
7. Estimate M_{male} with a narrow prior (SD = 0.2)
 8. Estimate M_{male} with a broad prior (SD = 1.6)
 9. Increase mean of priors for catchabilities from 0.499999990279973 to 1 (q_k for all gears k)
 10. Broader catchability priors, from SD = 1 to 1.5 (q_k for all gears k)
 11. Selectivity curves equal maturity ogive for all gears
 12. Estimate time-varying selectivity for the Queen Charlotte Sound Synoptic Survey, to try to improve the survey index fit
 13. Geostatistical model-based survey indices (Section D)
 14. Remove Discard CPUE
 15. Modify maturity ogive to not include 'developing' or 'resting' specimens
 16. Fix selectivity for the Discard CPUE index to be equal to the Shoreside fishery selectivity
 17. Fix all survey's selectivity to be equal to the Shoreside fishery selectivity

This list of sensitivity scenarios with more details is provided in Table 13. Base model parameter settings are provided in Table 5. All sensitivity models were run using MCMC with a chain length of 10,000,000, a sample frequency of 5,000, giving 2,000 samples, which were then burned in by 1,000 giving a total of 1,000 samples retained for inference.

2.5.1. Decreasing σ and adjusting τ

ISCAM uses an error parameterization which includes two parameters, ϑ^2 and ρ . They represent the total variance and the proportion of total variance associated with observation errors, respectively (Martell 2011). Observation error SD (σ) and process error SD (τ) cannot be estimated directly, instead there is a calculation done to translate those values to and from ϑ^2 and ρ (Appendix G, Eq. G.32). The values of σ and τ were fixed in the base model (Grandin and Forrest 2017) at 0.2 and 0.8 respectively. By calculation, ϑ^2 and ρ were fixed at 1.47 and 0.0588.

Reducing the observation error by decreasing σ from 0.2 to 0.135 and estimating ϑ^2 increased the value of ϑ^2 from 1.47 to 1.52 while approximately halving ρ from 0.059 to 0.028. The median and 95% CI of the posterior for ϑ^2 was 0.37 (0.27–0.48). There was little effect on the absolute biomass trajectory (Figure 43), but the estimate of B_0 was increased from 184,000, to 446,000 t (Figure 43). The increase in the B_0 estimate caused a scaling downward of the relative biomass trajectory (Figure 44). There were no substantial changes to the index fits, age fits, or selectivities.

Setting the value for τ to 1.0 had a similar effect to reducing the assumed index observation error and lowered the relative biomass trajectory. For this value of τ , the values of ϑ^2 and ρ were 0.96 and 0.038 respectively (Appendix G, Eq. G.32).

Setting the initial value for τ to 0.6 also had little effect on absolute biomass. For this value of τ , the initial values of ϑ^2 and ρ were 2.49 and 0.100 respectively. The estimate for ϑ^2 was 1.11 (0.80–1.54).

The estimates of B_0 were increased for both of these models when compared to the base model, which resulted in scaling down of the relative biomass trajectory and putting the status in 2021/2022 to be estimated just below the LRP for the $\tau = 1.0$ model and just below the USR for the $\tau = 0.6$ model (Figure 44). The increase of B_0 was much greater, and had a much larger CI for the $\tau = 1.0$ model when compared to the $\tau = 0.6$ model.

2.5.2. Decreasing the mean of the steepness prior

Decreasing the steepness prior mean from 0.85 to 0.72 and changing the prior SD from 0.10 to 0.15 produced little change in both absolute biomass and B_0 (Figure 43), despite having a different posterior (Figure 45, compare to base model Figure 36). The prior for h is very influential on the posterior, but the value of h does not have a large effect on the absolute or relative biomass (Figure 44).

2.5.3. Modifying priors on M_{female} and M_{male}

In the base model, the natural mortality parameters M_{female} and M_{male} are fixed to 0.20 and 0.35 respectively. Four sensitivity models were run, to estimate each M parameter with broad and narrow prior SDs. Figure 46 shows the absolute biomass trajectories for these models. The relative spawning biomass trajectories are shown in Figure 47. Estimating M_{female} with narrow and broad priors produced estimates for M_{female} of 0.28 (0.25–0.30) and 0.29 (0.27–0.31) respectively. M_{male} remained fixed for those models, at 0.35. Figure 46 shows that the model is sensitive to the female natural mortality parameter, as both absolute biomass trajectories and B_0 estimates are inflated. The estimates are quite different from the fixed value of 0.20, causing this scaling effect. If the female mortality is higher, the model must adjust the starting point (B_0) higher in order to fit all parameters including the indices with the drop in biomass in 2019 (Figure 14).

The sensitivity models that estimate M_{male} with narrow and broad priors produced estimates of 0.24 (0.21–0.28) and 0.23 (0.20–0.26) respectively. These estimates were also substantially different than the fixed values of the parameter (0.35). However, males only make up 21% of the spawning stock biomass and estimated male selectivity is generally farther to the right of maturity than females (Figure 27). This implies that males removed from the stock will have lower overall impact to the stock biomass, since there are not as many older male fish in the stock to be caught, and the selectivity is higher on those fewer fish. The lack of older males can be seen in the length and age data (Figures A.1 and A.2).

This model is sensitive to natural mortality values whether fixed or estimated. The base model uses fixed values as used by several nearby jurisdictions (Spies et al. 2017, 2019; Spies and W. 2019; Shotwell et al. 2020, 2021).

2.5.4. Modifying catchability priors

The catchability parameters are $\ln(q_k)$ where k is the gear, one for each trawl fleet and survey index (Freezer trawlers, Shoreside, QCS Synoptic, HS Multi, HS Synoptic, WCVI Synoptic, Discard CPUE). These parameters have an associated normal prior with a log mean and SD set in the ISCAM control files. In the base model those are $\ln(0.5)$ and 1.0, respectively.

Two sensitivity models were run to test the influence of the priors for $\ln(q_k)$. In the first, the means for all gears were increased from $\ln(0.5)$ to $\ln(1.0)$, and the SD remained at 1.0. In the second, the prior was broadened by setting the SD for all the gears to 1.0. The means for that model remained at $\ln(0.5)$.

The absolute and relative biomasses were almost identical to the base model for these models (Figures 48 and 49). The catchability estimates were also almost identical between these models and the base model (Figure 50).

2.5.5. Setting selectivities equal to maturity

This sensitivity came about in the 2015 assessment cycle, where it was found that the estimated selectivity curves were all to the right of the maturity ogive (Figure 17, Grandin and Forrest 2017). This caused the value of F_{MSY} to be very large and essentially give the advice that an

unlimited amount of catch could be taken without affecting the stock. We repeat it here, as the same situation has arisen with the current base model and to compare this model with the single sex model from the 2015 assessment.

For this model structure, the absolute biomass and B_0 estimates are much larger than for the base model (Figure 51). The median of the posterior for B_0 was estimated to be 356,000 t with a broad CI of 231–529 (width 298) thousand t. For comparison, the base model had a B_0 estimate of 184,000 t with a CI of 128–264 (width 136) thousand t. The absolute biomass trajectory is also high, so the relative biomass is higher than the base model (Figure 52). The index fits all reflect this, as they all show a one-way trip downwards (Figure 54).

The vulnerable biomass for this model is substantially higher than for the base model (Figure 53), and exactly equal for the two fleets (one is overlapping the other and we cannot see it in the figure). This is due to selectivity being exactly the same for both fleets, not because they are equal to the maturity. The ratio of the sum of the two fleets' vulnerable biomasses to the spawning biomass is 2.00. For the base model, this ratio is 1.22. Moving the selectivity to the left increases the vulnerable biomass relative to the spawning biomass.

2.5.6. Using TV selectivity for the Queen Charlotte Sound Synoptic Survey

In an attempt to improve the fit of the Queen Charlotte Sound Synoptic Survey index (Figure 14), we implemented time-varying selectivity in ISCAM and ran the model with the Queen Charlotte Sound Synoptic Survey having three blocks of selectivity, 2003–2010, 2011–2016, and 2017–2021. We tried many combinations of both number of selectivity blocks and range of each block and this particular combination fit the data the best.

The absolute and relative biomass trajectories both show a lower value in 2022 than the base model (Figures 51 and 52). The index fit was better overall than for the base model, especially in the latter part of the series (Figure 54). The improved fit to the QCS index was the goal of this sensitivity run but came at the expense of poor estimates of selectivity. The selectivity estimates for the three-year blocks can be seen in Figure 55. The male selectivity for the early years (left panel) is far to the right, much further than the time-invariant selectivities in the base model (Figure 27). The other two time periods have even more unreasonable estimates of selectivity, making this model unusable for any form of advice.

There was also some autocorrelation in the MCMC samples for the Queen Charlotte Sound Synoptic Survey selectivity parameters in this model (Figure 56) and the trace plots for those parameters are not adequate for valid inference (Figure 57).

2.5.7. Using survey indices calculated using geostatistical modelling

This sensitivity case involved replacing the index data for the three synoptic surveys: (Queen Charlotte Sound Synoptic Survey, Hecate Strait Synoptic Survey, and West Coast Vancouver Island Synoptic Survey). These data are calculated using a standard design-based estimator in the base model. Here, they were replaced with geostatistical-based indices (Appendix D). Both absolute and relative biomass are similar to the base model, with a slightly higher estimate of B_0 and a slightly higher absolute biomass trajectory (Figures 58 and 59).

The index fit is shown in Figure 60. The fit to the geostatistical-based index is approximately visually equivalent to the fit to the index in the base model (Figure 14) but they are not shown on the same plot together due to the base indices being different.

2.5.8. Removal of the Discard CPUE index from the model

We tested the impact of removing the Discard CPUE index. The relative biomass trajectory remained similar, with only a slight increase in end year biomass and slightly lower overall

relative biomass (Figure 62). The fits for the survey indices showed only minor departures from the base model fits (Figure 63).

2.5.9. Modification of the maturity ogive

Arrowtooth Flounder spawn during the winter, and the surveys take place during the summer. Many of the maturities recorded in the summer are therefore in the 'resting' phase which can be difficult to distinguish from immature. There is also some ambiguity in the classification of 'developing' fish (codes 2 and 3 in the DFO maturity codes for flatfish).

Removing 'developing' and resting' from the maturity ogive produced a better-fitting ogive (Figure A.5) and resulted in slightly lower overall B_0 estimate and absolute biomass compared to the base model, which resulted in a similar relative biomass (Figures 61 and 62). This maturity should be considered for the base model in the next assessment. Since it made no qualitative difference on the results, and because it was worked up following the initial review meeting, we did not include it in the base model for this assessment.

The biomass vulnerable to the two fleets compared to the spawning biomass is shown in Figure 64. The vulnerable biomass is lower for each fleet than the spawning biomass, as it should be when only the mature portion of the stock is available to catch.

2.5.10. Fixing selectivities

There were two sensitivities for which selectivities were fixed to the estimated value of the shoreside fishery in the base model:

1. Fix selectivity of the Discard CPUE index to the shoreside fishery selectivity
2. Fix selectivity of all surveys to the shoreside fishery selectivity

Fixing the Discard CPUE selectivity resulted in a slightly lower absolute and relative biomass for the final year compared to the base model. There were no substantial index fit differences.

Fixing the survey selectivities produced a large change in the model, with a much higher B_0 estimate (Figure 61) resulting in a large scaling down in relative biomass (Figure 62). There was also a pronounced upward swing in biomass at the end of the time series implying sudden exponential growth of the stock, which is an unrealistic outcome. The index fits were slightly different with this model, with a pronounced lower estimate for the Queen Charlotte Sound Synoptic Survey in 2010.

2.6. RETROSPECTIVE ANALYSES

The base model was tested for retrospective patterns. This was done by successively removing all catch, age, and index data for 1 year from the end of the time series in the data files and refitting the model. We attempted to run the retrospective model back 10 years, but only the first 8 years would converge. It is likely that attempting to remove too much data led to too few data sources for this two-sex, two-fleet model. This is the reason the 2015 assessment was parameterized as a single-sex model.

All retrospective models were run using MCMC with a chain length of 10,000,000, a sample frequency of 5,000, giving 2,000 samples, which were then burned in by 1,000 giving a total of 1,000 samples retained for inference. This was the same as all other models in this assessment.

Figures 65 and 66 show the absolute biomass for the base model compared with the retrospective models. Following the subtraction of years by looking at the trajectories, we see that the -4 years model (ending in 2018) follows a different path than the years following (2019–present). This is due to the large drop in biomass seen in 2019 in the West Coast Vancouver Island Synoptic Survey, Hecate Strait Synoptic Survey, and Discard CPUE Index (Figure 14). The

model is highly sensitive to these drops in the indices, all of which occur in the same year. If this assessment had taken place prior to 2019 with this model, the outcome would have been notably different than it is now.

The B_0 estimates are also segregated into two distinct groups by the -4 year model, with those from 2019–present being lower than those prior to 2019. When the absolute trajectories are divided by these B_0 values we can inspect the relative biomass trends (Figure 67). The high B_0 estimates for the models prior to 2019 force the relative biomass downwards giving the impression of a more depleted stock in earlier years when compared to the more recent models.

Comparing recruitment estimates (Figures 68 and 69), most appear similar between models; however, there is an obvious outlier—the 2014 recruitment for the 2014 model (the -7 year line). This can also be seen in in Figure 21 of the 2015 assessment (Grandin and Forrest (2017)). The 2014 cohort was highly uncertain at that time with the data that was available, even with the single-sex model. The R_0 estimates follow the same grouping seen in the absolute biomass figure.

There is a decrease in fishing mortality for the models prior to 2019 (Figure 70), which corresponds to the increasing biomass trend in those models.

The fits to the indices of abundance (Figure 71) show a clear divergence for the models prior to 2019. The log standardized residuals (Figure 72) show that indices for those models fit neither better nor worse overall than the post-2019 models.

In order to quantify the uncertainty in retrospective patterns, and therefore retrospective bias, Mohn's ρ statistic was calculated for all 8 retrospective models compared to the base model to be 0.099.

Hurtado-Ferro et al. (2015) suggests that Mohn's ρ should fall between -0.15 and 0.2, which are the lower and upper bounds of the 90% simulation intervals for the longer-lived flatfish base case they examined. For shorter-lived species, those values are -0.22 and 0.30. Since the calculated value of 0.099 lies within the limits given, we can say that there is no indication of retrospective patterns or bias in this model.

3. RECOMMENDATIONS AND YIELD OPTIONS

3.1. REFERENCE REMOVAL RATE

As outlined in Section 2.3.3, the reference removal rate was calculated as the amount of constant catch taken each year for the long term to bring the relative spawning biomass to $0.4B_0$. The long-term annual catch calculated was 4,406 t. Table 14 gives the values including the associated instantaneous fishing mortality and annual exploitation rate values.

3.2. PROJECTIONS AND DECISION TABLE

Projections were run 4 years into the future with alternative constant catch levels ranging from 0 to 15,000 t in 1,000 t increments for the years 2022–2025. Projected log recruitment deviations in the years 2022–2025 were drawn randomly with replacement from the estimated 2010–2019 deviations (omitting the poorly estimated 2020 and 2021 deviations).

The projected relative biomass trajectory (medians of the posteriors with 95% CI) and a closeup view of it are shown in Figures 73 and 74 respectively. The 95% CI in the trajectory becomes larger the further into the future the projections are run. Using 10,000 t catch in 2024 as an example, the 95% CI for the 2025 biomass spans from 0.173 to 0.571, which represents a range of 0.397. This is almost twice the size of the difference between the USR and the LRP

(0.2). The large amount of uncertainty should be taken into account when evaluating these projections.

Figures 75–78 show the medians of the posterior, 50% CI and 95% CI for the relative spawning biomass in the projected years, for each catch level applied. The B_0 reference points are also shown along with a reference line for $0.35B_0$. These figures give another view of the medians and uncertainties shown in Figures 73 and 74, but with each figure representing one projected year only so that each posterior can be more clearly seen.

Posterior estimates of reference points and benchmarks are provided in Table 7. A decision table is presented showing predicted probabilities of undesirable states under the projected catch levels (Table 15). An undesirable biomass-based performance measure is defined to occur when the projected spawning biomass is below the reference point or benchmark, e.g. the ratio $B_{2023}/B_{\text{ReferencePoint}} < 1$. Probabilities in the decision tables are measured as the proportion of posterior samples that meet the above criteria.

As Table 15 shows, the model-predicted probability of the 2023 relative spawning biomass being below the 2022 relative spawning biomass ranged from 0.044 under 0 t of catch to 0.977 under 15,000 t of catch. The catch that is closest to 0.5 probability of the biomass declining from 2022 to 2023 while still being below 0.5 is 3,000 t, at a probability of 0.418.

The probability of being below the USR of $0.4B_0$ was from 0.543 to 0.892 over the range of catch levels considered; the probability of being below the LRP of $0.2B_0$ for the same catch range was from 0.000 to 0.006.

All catch levels including zero had a probability of greater than 0.5 of the 2023 biomass being under the $0.4B_0$ reference point.

3.3. SOURCES OF UNCERTAINTY AND FUTURE RESEARCH

As with all stock assessments, there are two major types of uncertainty in the advice presented in this document:

1. Uncertainty in the estimates of model parameters within the assessment
2. Structural uncertainty arising from processes and data that were not included in the assessment

The first type, parameter uncertainty, is presented in terms of posterior credible intervals for parameters and state variables such as biomass, recruitment, and fishing mortality. This uncertainty was captured in the decision tables and was further explored using sensitivity analyses. The second type, structural uncertainty, was tested through sensitivity tests of model structure and the inclusion/removal of data.

The magnitude of catch and discards prior to 1996 is a major source of structural uncertainty in this assessment. As discussed in Section 2.1.2, all catch data prior to 1996 were omitted from this assessment on the recommendation of industry advisors and Technical Working Group, as was done in the 2015 assessment. Arrowtooth Flounder is known to have been discarded at sea in large quantities due to proteolysis of the flesh if catches were not landed and frozen quickly after capture. Applications of ratio estimators or models to estimate historical discard rates were rejected as analytical tools due to discarding of whole tows and changes to discarding behaviour over time.

Stock structure of Arrowtooth Flounder is poorly understood in British Columbia. Several approaches are available to improve understanding of stock structure including genetic analysis, analysis of otolith microchemistry, and analysis of life-history traits such as growth and maturity. Arrowtooth Flounder is managed as a coastwide stock. If there are distinct stocks within British Columbia waters, there may be risks associated with taking a large proportion of the TAC from one area. In particular, the less steep decline in the Queen Charlotte Sound

Synoptic Survey compared to the declines seen in the other survey indexes raises questions about stock structure.

The assessment model was able to fit all indices of abundance well with the possible exception of the Queen Charlotte Sound Synoptic Survey. Although the index has declined since 2015 (and in particular in 2021 after the initial Technical Working Group meetings), the decline has been somewhat less pronounced than the other surveys or the Discard CPUE Index. We attempted to better fit the Queen Charlotte Sound Synoptic Survey with survey-specific time-varying selectivity, but we were unable to obtain satisfactory estimates of selectivity and MCMC diagnostics on this model and so used time-invariant selectivity in the base model. It is possible Queen Charlotte Sound represents a nursery ground for Arrowtooth Flounder or factors affecting local distribution or movement (such as environmental conditions) have resulted in a moderately different index pattern in the Queen Charlotte Sound Synoptic Survey compared to the other surveys. Overall, the congruence between the coastwide 'stitched' synoptic survey and the Discard CPUE Index give us some confidence that both data sources are capturing underlying biomass dynamics.

We suggest future research consider the use of the 'stitched' stock-wide geostatistical index as a replacement for considering each of the synoptic surveys as independent samples from the same overall stock (sometimes with different selectivities). The distinct age composition data precluded us from doing that in this assessment, but future research could consider the impact of considering these composition data as independent samples from the same overall stock (perhaps with area and density expansion) or standardizing these data as well with a similar multivariate geostatistical model.

The relationship between DNA and spatial area is unknown for Arrowtooth Flounder. In future it is recommended that a genetic study take place to determine differences between Arrowtooth Flounder found in the Strait of Georgia, Queen Charlotte Sound, Hecate Strait, and WCVI.

There is a lack of age structures sampled from the commercial fleets from 2020 onwards. This would have had a minimal effect on this assessment given the last year of data was 2021. However, this may have an increasingly large impact on the assessment in terms of estimating selectivity, recruitment, and tracking age-cohorts within the composition data. Retrospective analyses could be conducted excluding existing commercial age data to partially evaluate this impact. Simulation analyses, possibly including closed-loop simulation, could also evaluate this impact. However, we think it is reasonable to assume that some level of continued age structure sampling from the commercial fleet will be important to this assessment going forward. It is suggested that collecting maturity data from winter samples (from commercial fisheries or surveys) could help reconcile the position of the maturity ogives with respect to selectivity curves because this species is a winter spawner while all the structured surveys operate in the spring/summer/fall months. In addition, future work could investigate various treatments of dynamic B_0 (e.g., Berger, A.M. (2019)).

Taking into account the ecosystem considerations in Appendix F and known biology of Arrowtooth Flounder, there are no clear indications that current environmental conditions should modify the catch advice in this assessment. Future research could evaluate incorporating environmental variables into the Arrowtooth Flounder stock advice more explicitly. It is not clear what mechanism this should entail, although options may include linking environmental indices to natural mortality or recruitment processes (e.g., Stock and Miller 2021). Other options would include adjusting target fishing mortality based on ecosystem modelling (Howell et al. 2021) or through closed-loop simulation that aims to find management procedures that are robust to uncertainties about future environmental conditions (e.g., Anderson et al. 2020).

Given the stock is estimated slightly below the USR in the base model and close to the LRP under one sensitivity model with higher recruitment variation, as well as declining estimated

spawning stock biomass, declining survey indices, and declining estimated recruitment, it is suggested that this stock assessment be updated with new data on a relatively short interval. We suggest an appropriate interval would be two years once one additional survey will have been conducted for each subregion and new commercial biological samples will hopefully be available for aging.

Ageing error was not used for this assessment. It is recommended that an ageing error matrix be included in the assessment model, to determine model sensitivity to ageing error.

Selectivity is an issue in this assessment, and one contributing factor could be catchability changing over time. It is recommended that time-varying catchability be explored in future assessments if the model framework allows for it.

It is recommended that there be a more detailed review of recruitment variance and initial biomass assumptions in future assessments. This includes recruitment assumptions into the projection years.

4. ACKNOWLEDGEMENTS

We thank members of the Arrowtooth Flounder Technical Working Group (Robyn Forrest, Rowan Haigh, Paul Starr, Diedre Finn, Rob Tadey, Bruce Turriss, and Brian Mose) for their valuable advice and insights throughout this project. We thank members of the Sclerochronology Laboratory at the Pacific Biological Station for their processing of Arrowtooth Flounder otoliths.

We thank the reviewers for their careful reviews, which uncovered structural issues that would have otherwise been missed. This highlights the importance of independent peer review in the advisory process.

We thank participants of the CSAS review meetings which took place on Oct. 19–20 and December 5, 2022 for their studious and thoughtful comments and requests. Thanks to Shannon Obradovich for chairing the meeting.

5. FIGURES

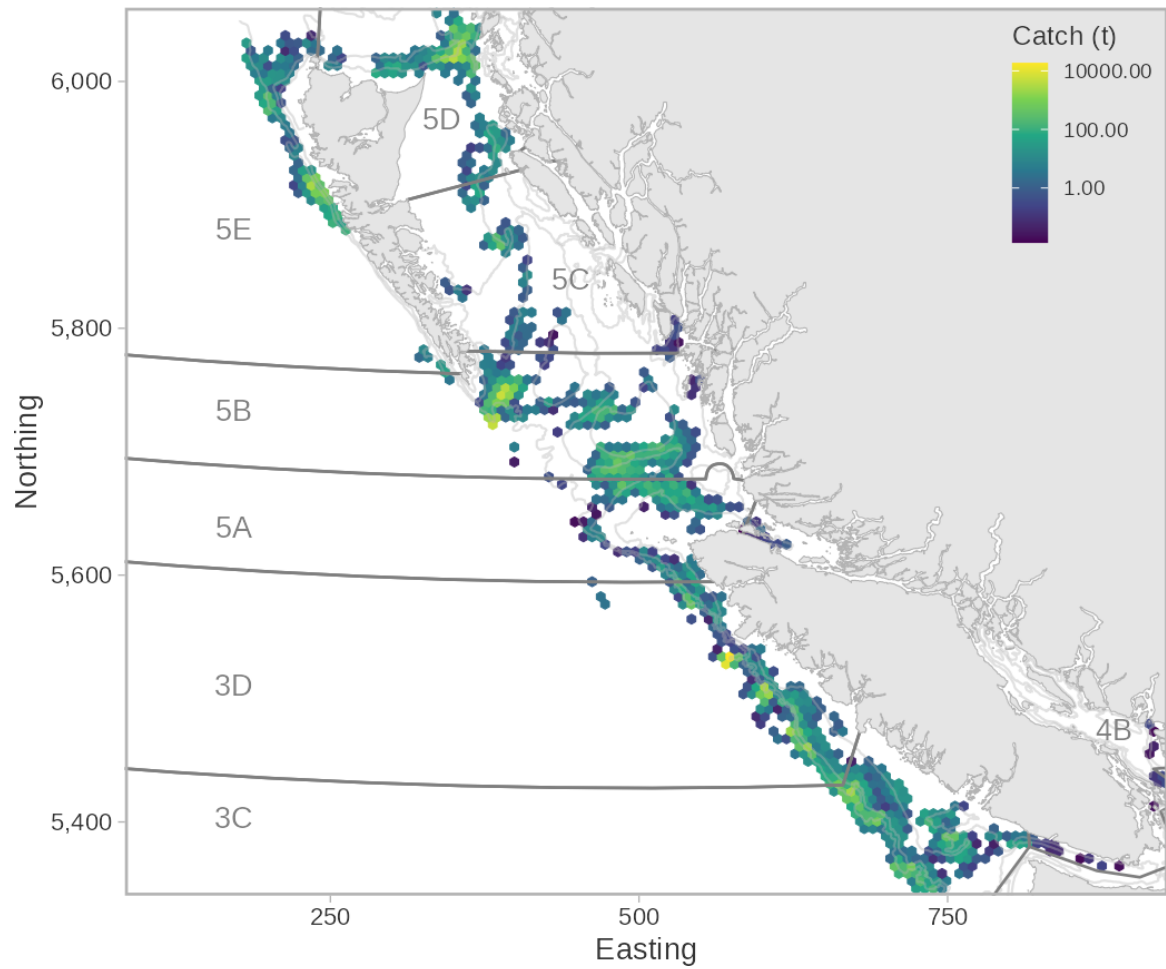


Figure 1. Spatial distribution of commercial catch from 1996 to 2021 for Arrowtooth Flounder. The colour scale is log10 transformed. Cells are 7 km wide and are only shown in cases where there are at least 3 unique vessels in a given cell to meet privacy requirements.

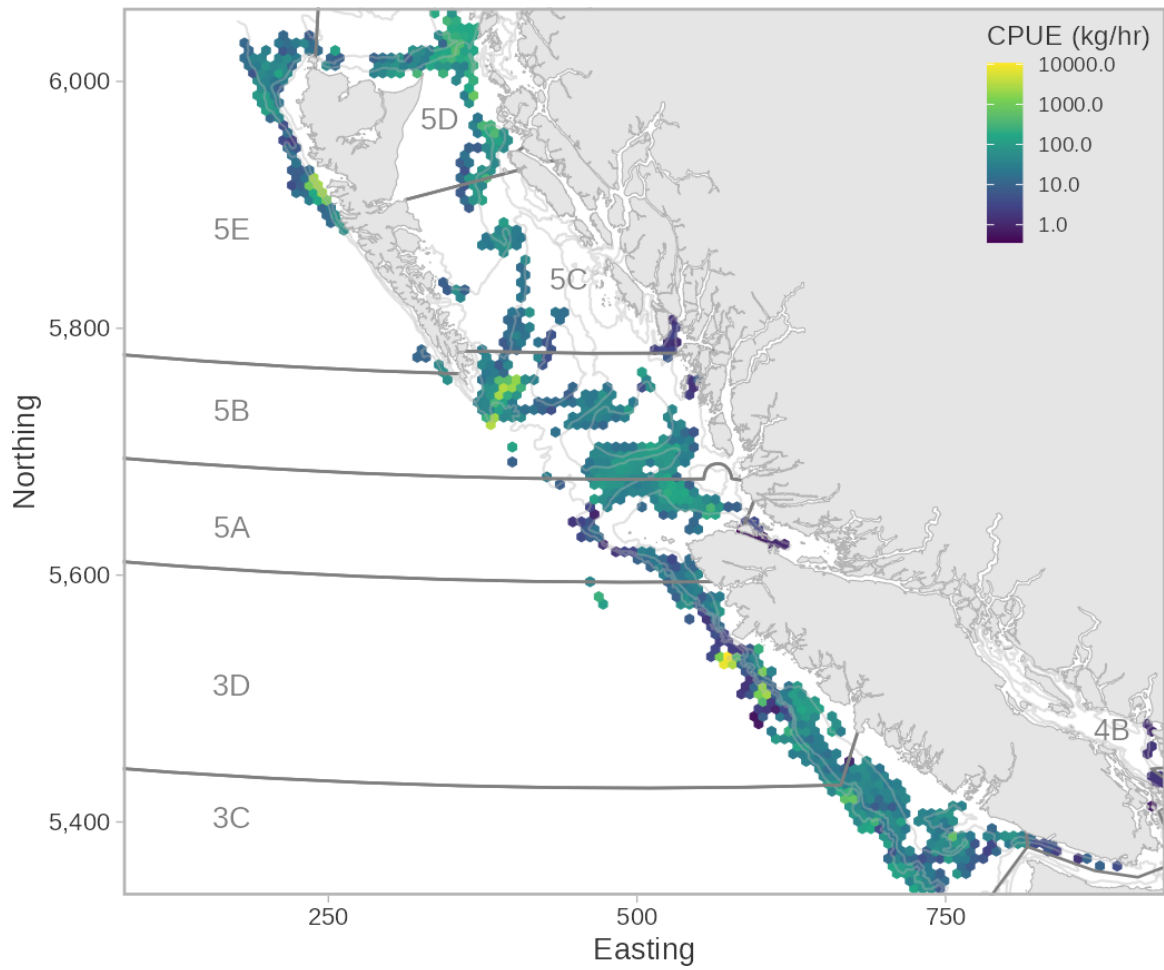


Figure 2. Spatial distribution of commercial CPUE from 1996 to 2021 for Arrowtooth Flounder. The colour scale is log10 transformed. Cells are 7 km wide and are only shown in cases where there are at least 3 unique vessels in a given cell to meet privacy requirements.

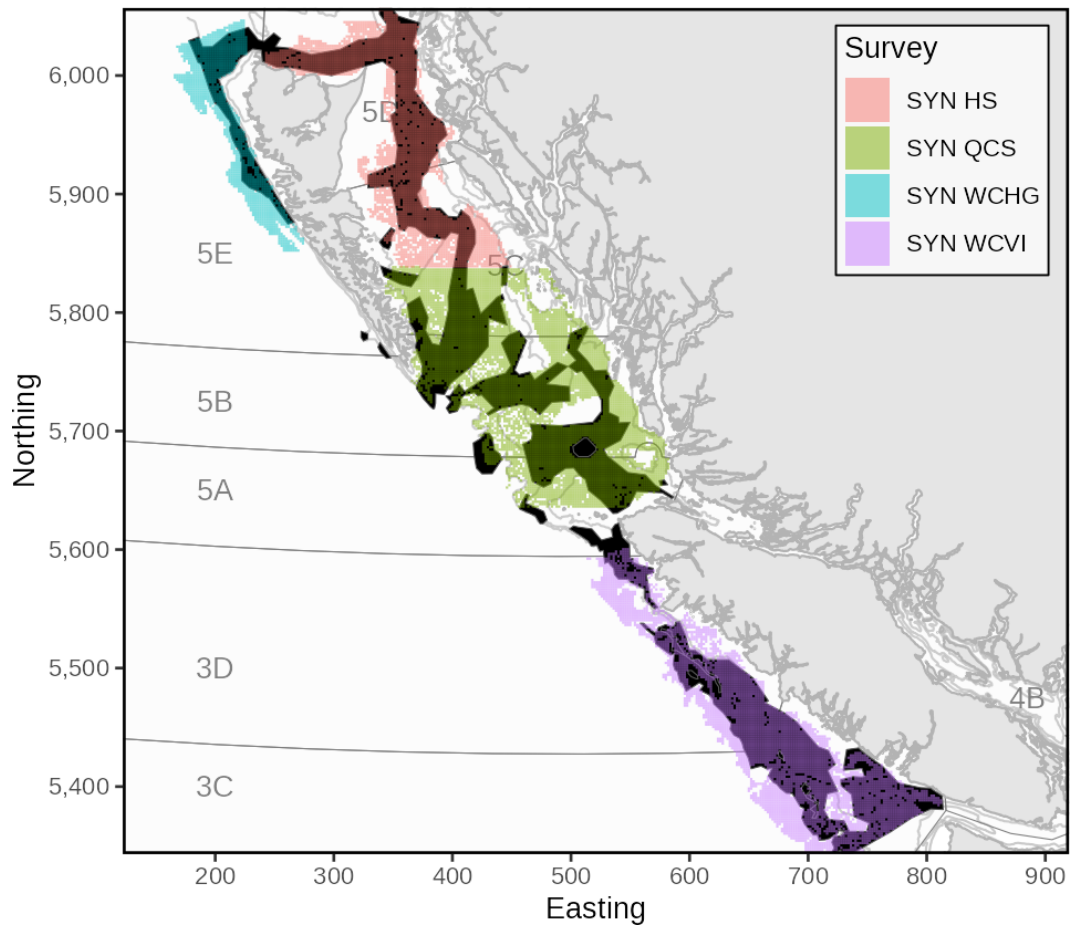


Figure 3. Spatial coverage of the commercial trawl sector for all species (black polygons) overlaid with the coverage by the four synoptic surveys (colors). Synoptic surveys are shown as a grid of 2km x 2km blocks, which represent 'active blocks' in the survey design. The presence of a block in this figure does not mean that it has been surveyed, only that it is in the set of blocks that can be surveyed as detailed in the survey design.

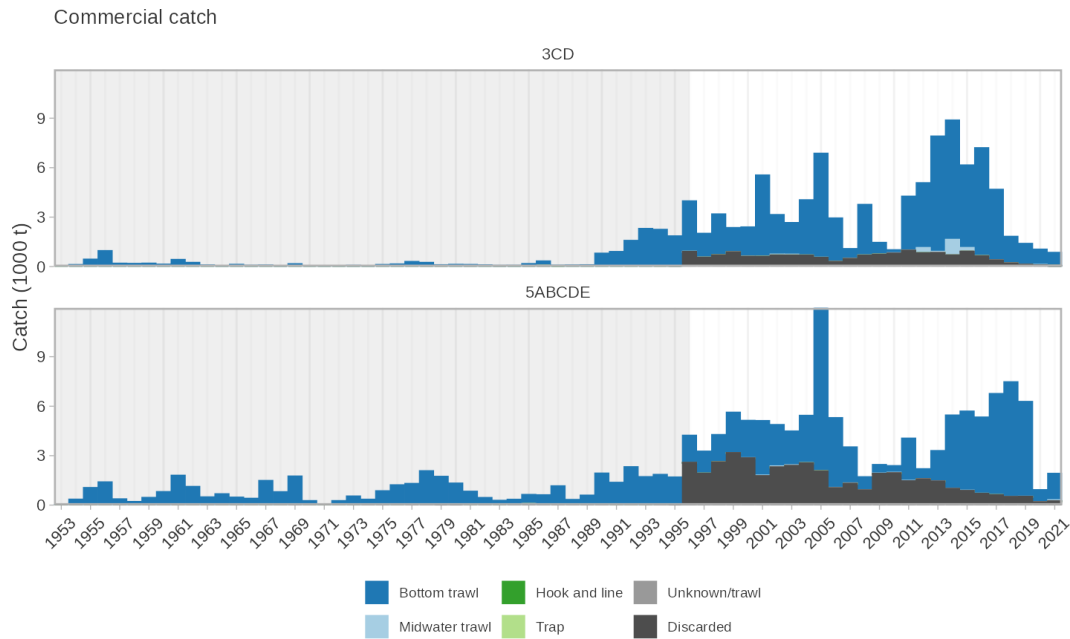


Figure 4. Commercial catch of Arrowtooth Flounder by area and gear type. Each year of catch starts on Feb. 21 and ends on Feb. 20. e.g. the year 2005 catch is all catch between Feb. 21, 2005 to Feb. 20, 2006. The shaded grey area from the beginning of the time series to 1996 indicate unreliable data. In the years prior to 1996, many tows of Arrowtooth Flounder were discarded without logs being kept.

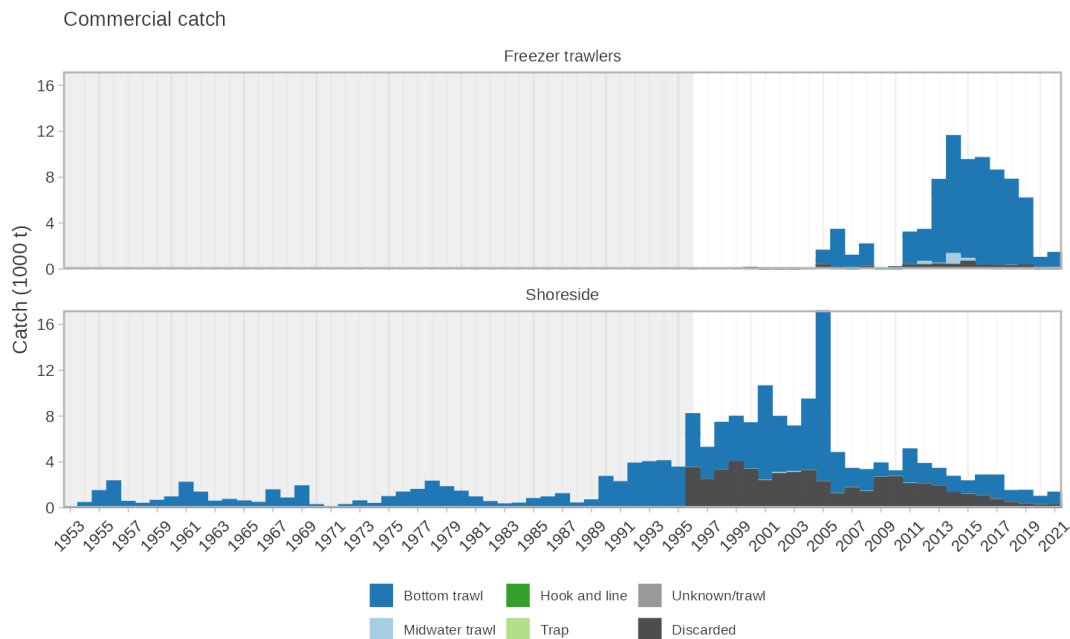


Figure 5. Commercial catch of Arrowtooth Flounder by fleet and gear type. Each year of catch starts on Feb. 21 and ends on Feb. 20. See the previous figure for an explanation of the shaded grey area.

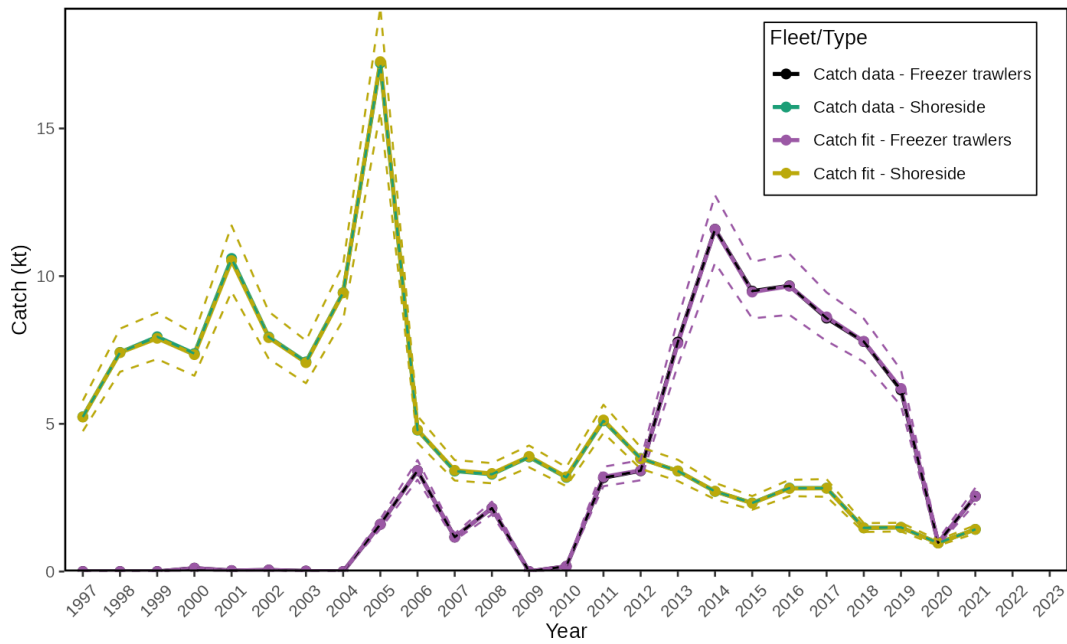


Figure 6. Predicted catch compared to the observed catch data for the two commercial fleets used in the model. The solid lines are either the observed catches or the median catch by fleet; the dotted lines are the 95% CI for the posterior of the catch fits.

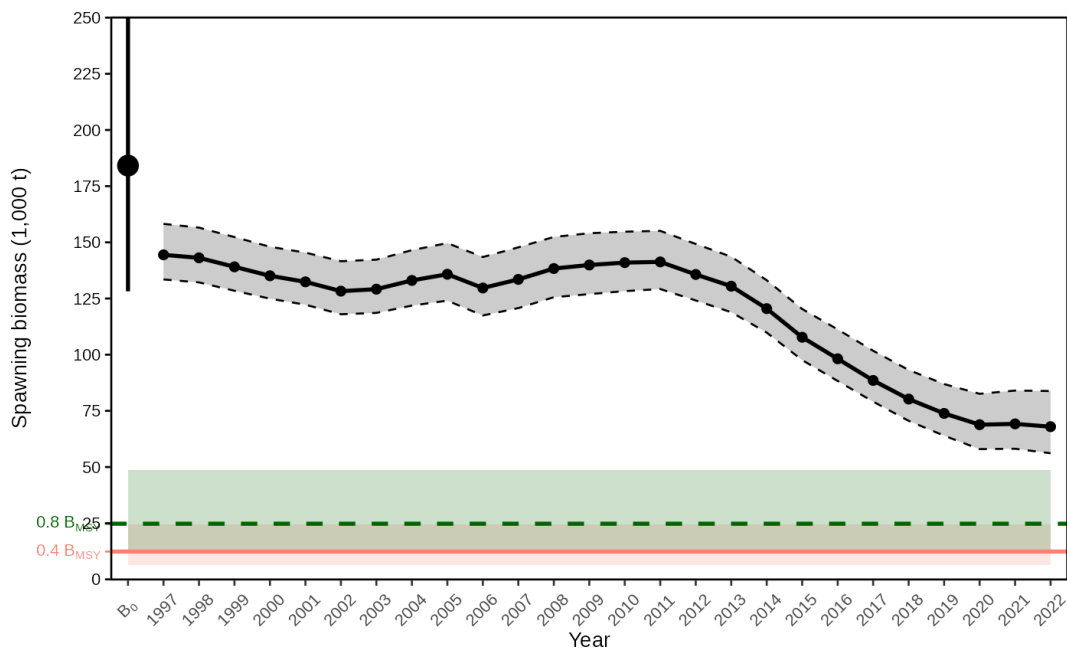


Figure 7. Spawning biomass of Arrowtooth Flounder for the base model with B_{MSY} reference points. The solid black line with points show the medians of the posteriors, the shaded ribbon encapsulated by dashed lines covers the 95% CI for the posteriors, the point at B_0 is the median estimate for the unfished biomass, and the vertical line over that point is the 95% CI for that parameter. The upper part of the CI is not shown for reasons of clarity for the trajectory, the median and CI for B_0 here is 184, 128–264 (width 136) thousand t. The B_{MSY} reference point lines are shown here for reference only, they are not advised for use in decision making for this stock. See section 2.3 for more details.

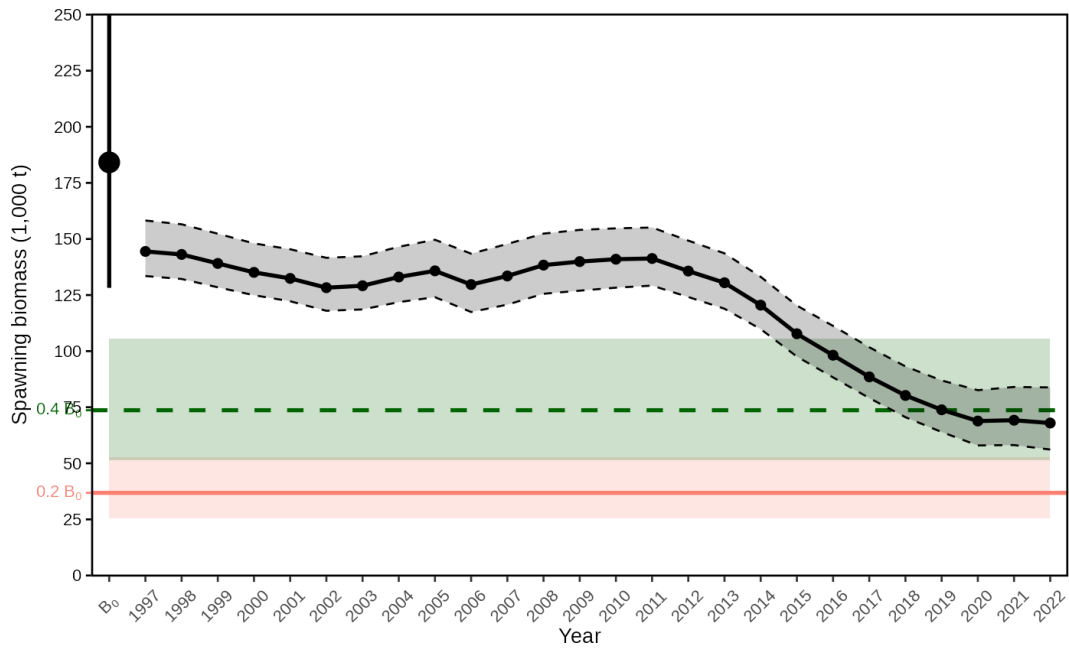


Figure 8. Spawning biomass of Arrowtooth Flounder for the base model with B_0 reference points. See Figure 7 for more information. The upper part of the CI is not shown for reasons of clarity for the trajectory, the median and CI for B_0 here is 184, 128–264 (width 136) thousand t.

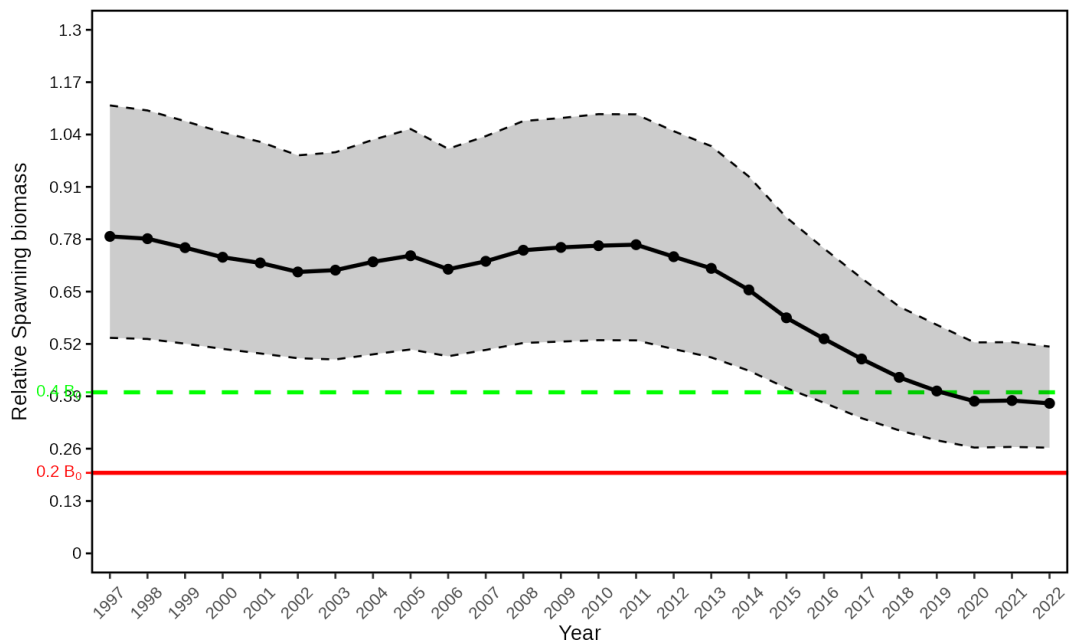


Figure 9. Relative spawning biomass for the base model. The shaded area represents the 95% CI. Horizontal lines indicate the $0.2 B_0$ (solid, red) and $0.4 B_0$ (dashed, green) reference points. Because the ribbon represents relative spawning biomass (depletion) and the reference points are with respect to B_0 , all uncertainty about the ratio of the spawning biomass to the reference points is captured in the ribbon and the reference points are shown as point values.

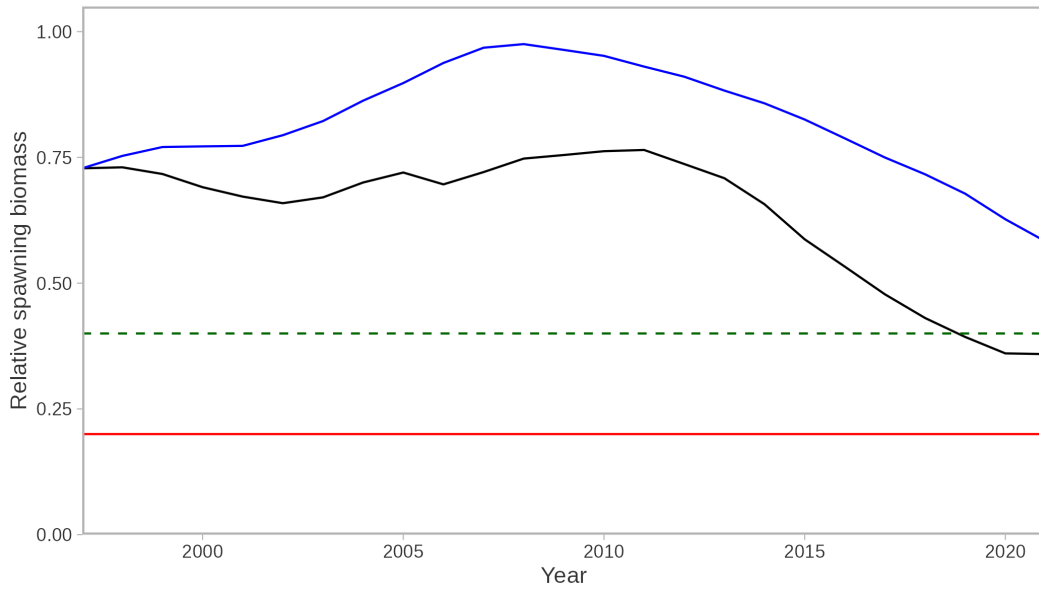


Figure 10. Relative spawning biomass of the base model (black line) compared to relative spawning biomass of the base model calculated with fishing mortality set to zero but estimated recruitment deviations, i.e. a dynamic B_0 (blue). The black line is not exactly equal to the ISCAM model output median line as seen in Figure 9 because this figure was created with a separate code base using only mean parameter estimates from the fitted base model as an approximation illustration.

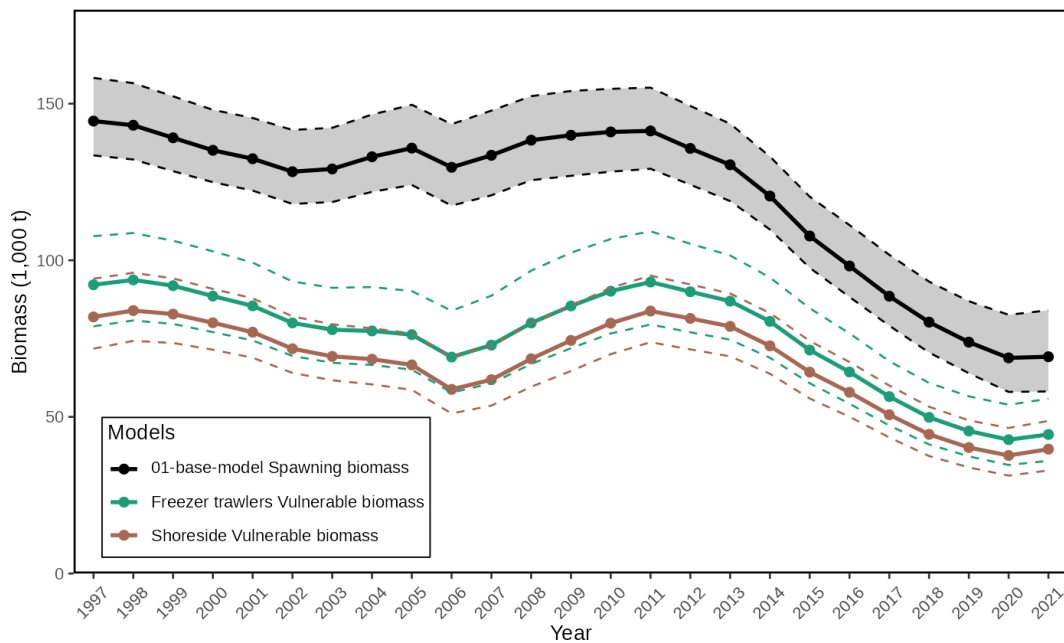


Figure 11. Spawning biomass of Arrowtooth Flounder for the base model compared with vulnerable biomass for the trawl fisheries for the base model. The spawning biomass is in black and has its 95% CI shaded. The two vulnerable biomass trajectories have their 95% CI contained within the dotted lines of their respective colours.

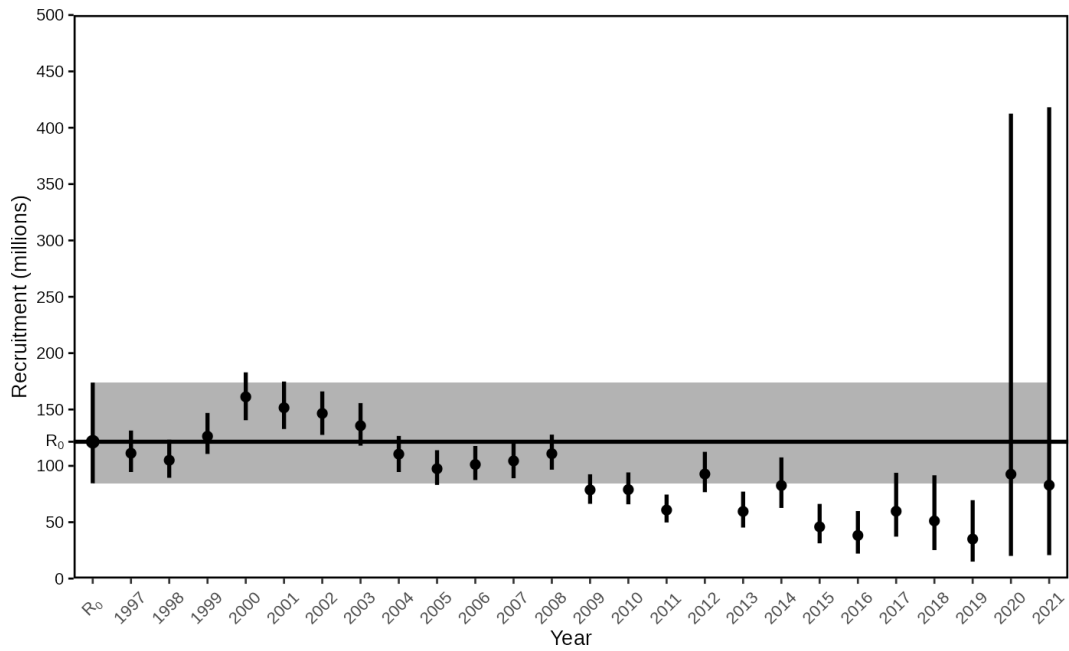


Figure 12. Recruitment of Arrowtooth Flounder for the base model. The black points are the medians of the posteriors, the vertical black lines are the 95% CIs for the posteriors, the point at R_0 is the median estimate for the initial recruitment parameter R_0 , and the vertical line over that point and shaded ribbon across the time series is the 95% CI for R_0 .

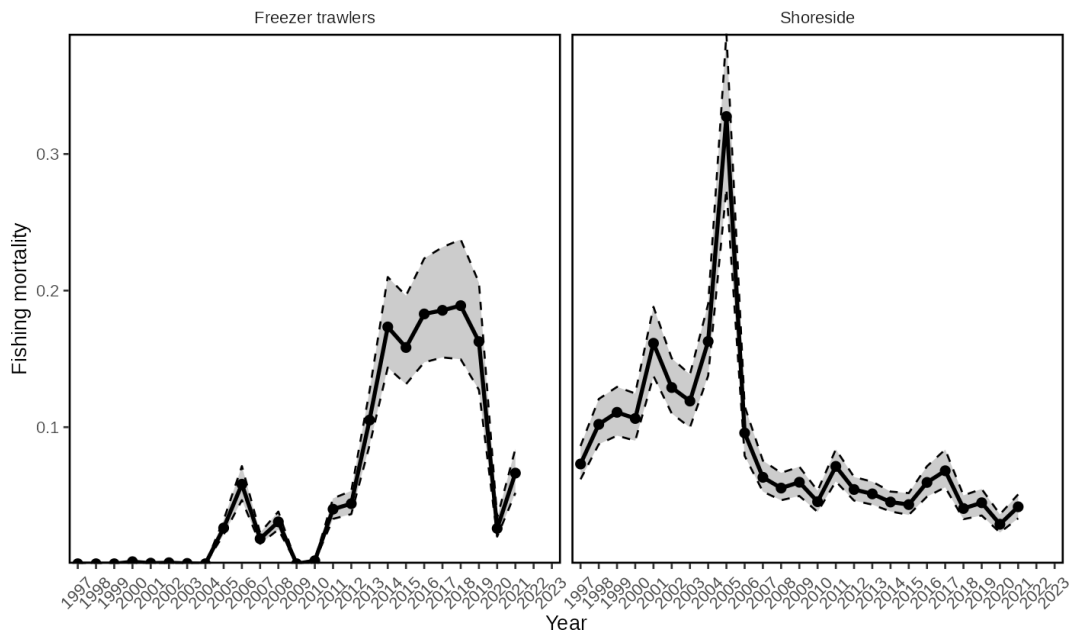


Figure 13. Fishing mortality for the base model for the two trawl fisheries for females only. The plots for the males are not shown, because they are the same. The shaded area represents the 95% CI.

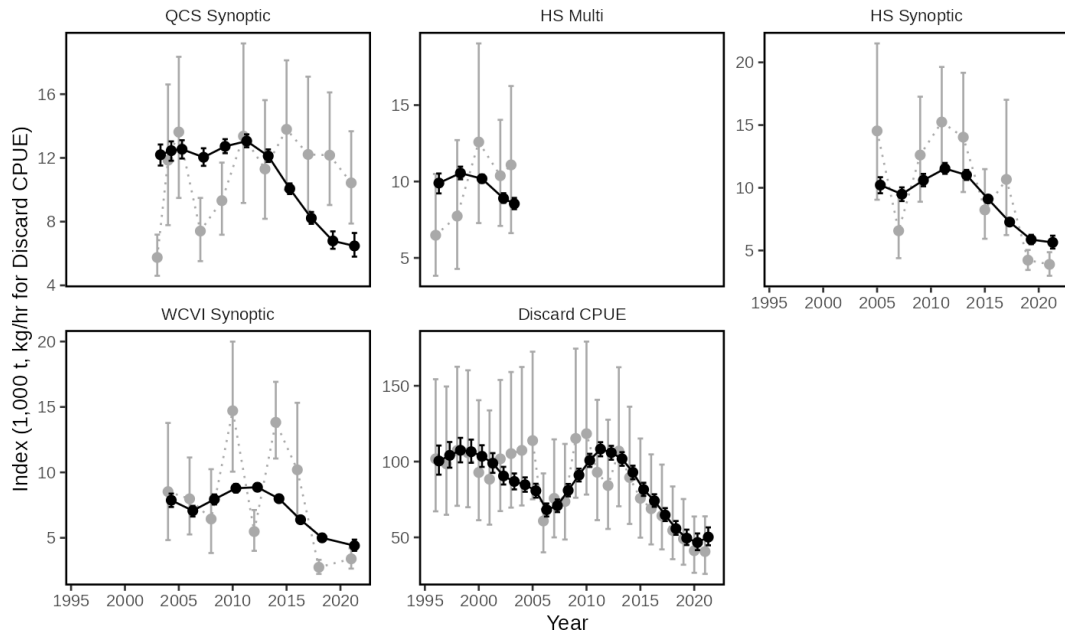


Figure 14. Index fits for the base model. The light grey points and vertical lines show the index values and 95% CIs; the black points show the medians of the posteriors; the black solid vertical lines show the 95% CIs of the posteriors.

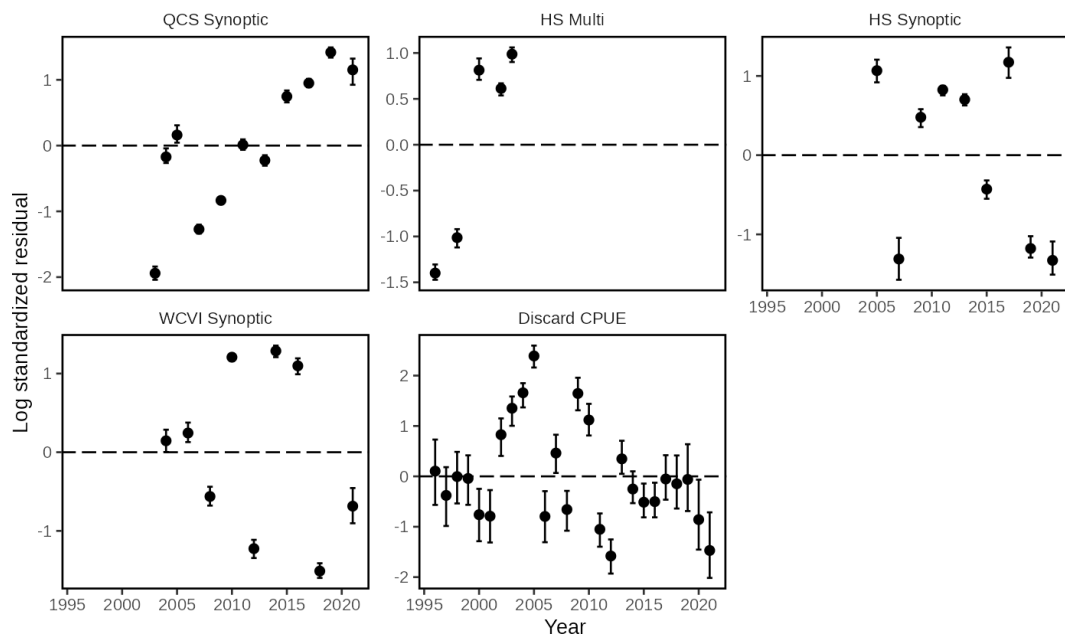


Figure 15. Index log standardized residuals. The points are the median of the posteriors for the $\epsilon_{k,t}$ parameters in ISCAM. The vertical lines represent the 95% CIs for those posteriors.

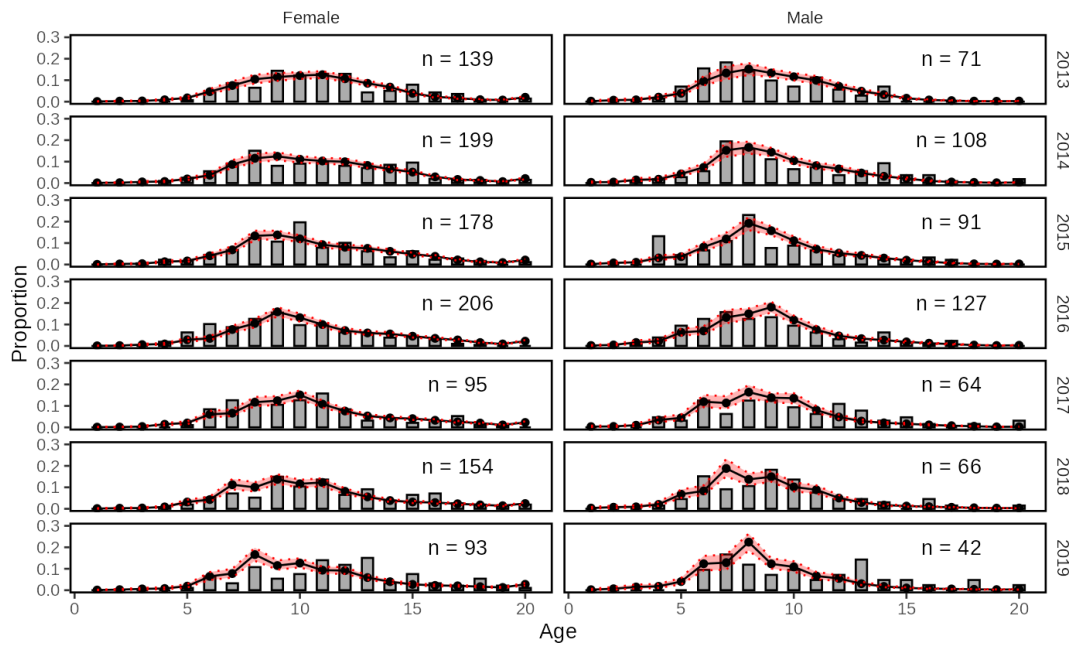


Figure 16. Age composition fits for each sex for the Freezer trawler fleet. The vertical bars are the age composition data points. The sum of the bar values equals 1 for each year/sex combination. The black points are the medians of the posteriors for each age. The red shaded area with dotted edges represents the 95% CIs. The panel labels are the total number of specimens (sex aggregated) fit for the year.

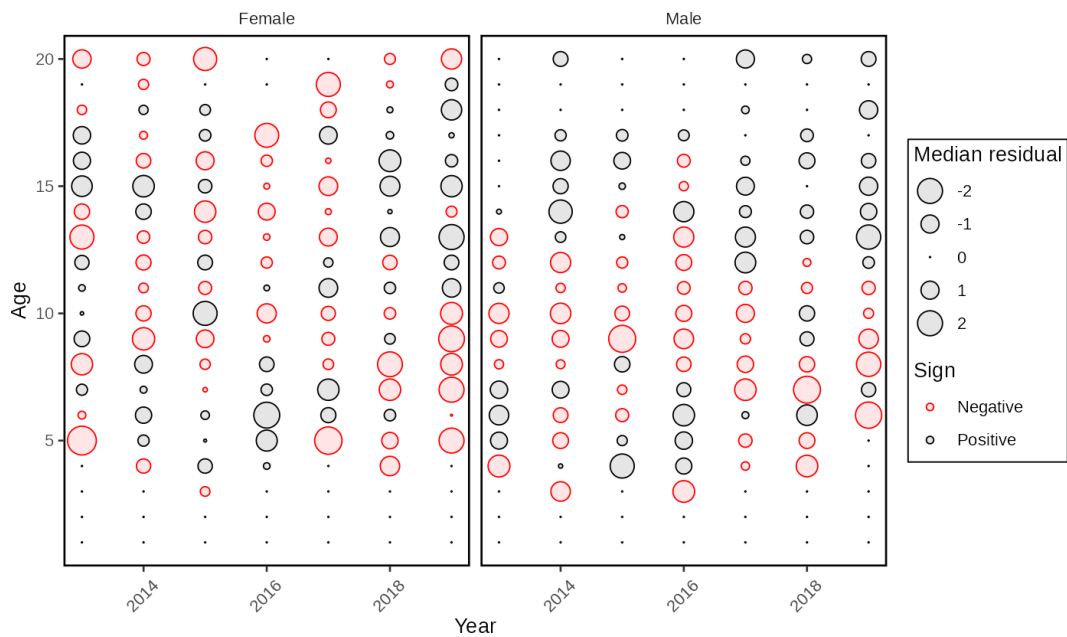


Figure 17. Pearson residuals for the age composition fits for each sex for the Freezer trawler fleet. The bubbles represent the median of the posterior for Pearson residuals. Red bubbles are negative residuals, black are positive, and dots represent zero residuals.

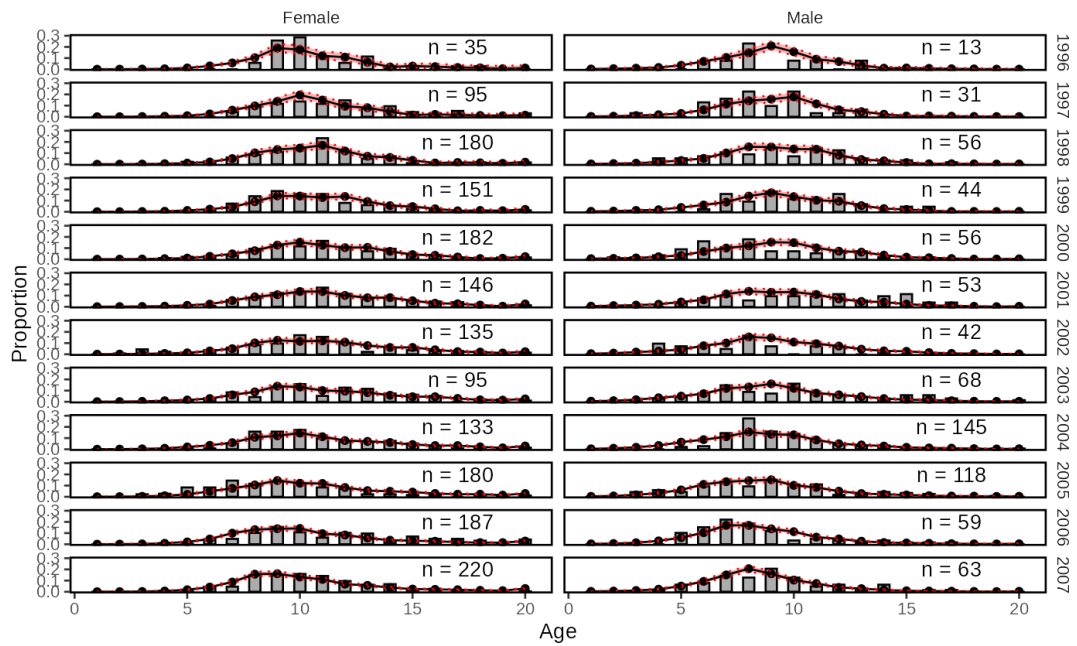


Figure 18. Age composition fits for each sex for the Shoreside fleet from 1996–2007. See Figure 16 for plot details.

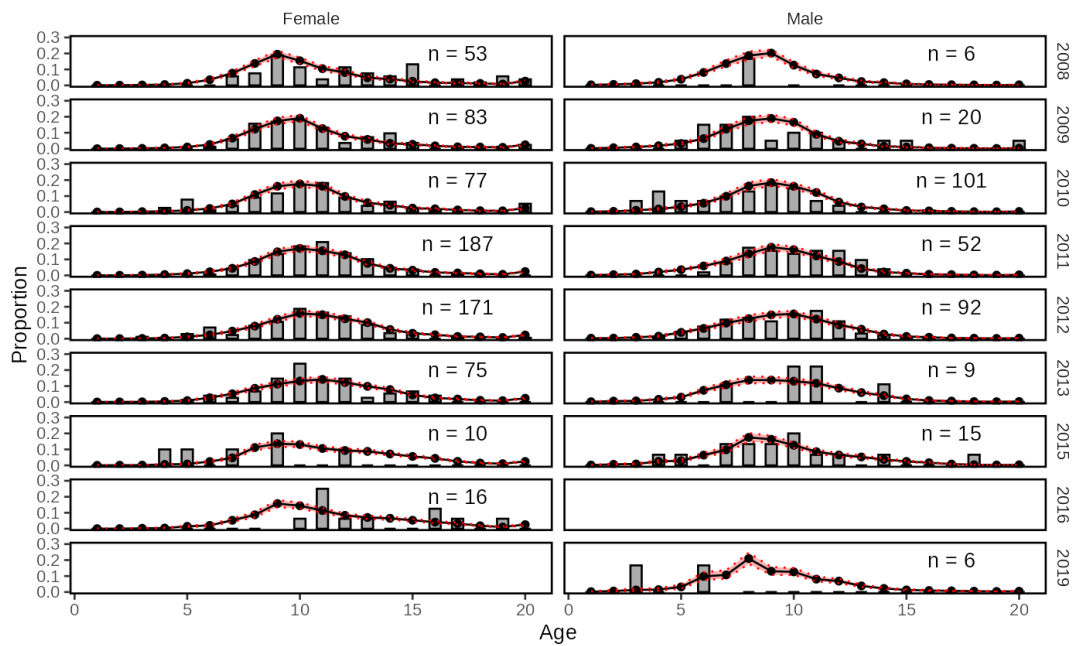


Figure 19. Age composition fits for each sex for the Shoreside fleet from 2008–2019. See Figure 16 for plot details.

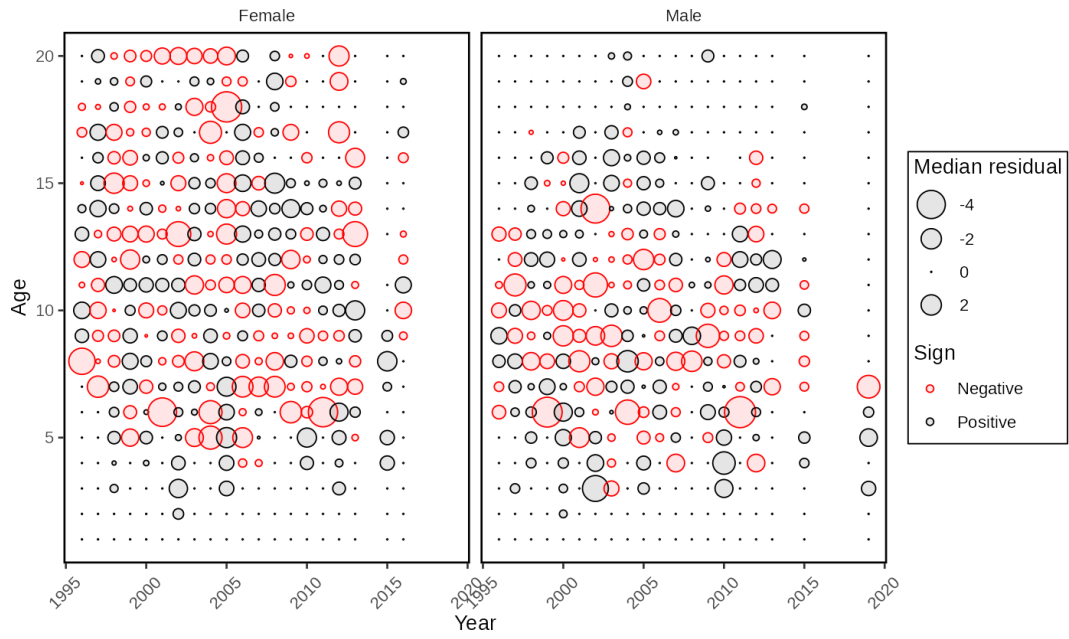


Figure 20. Pearson residuals for the age composition fits for each sex for the Shoreside fleet. The bubbles represent the median of the posterior for Pearson residuals. Red bubbles are negative residuals, black are positive, and dots represent zero residuals.

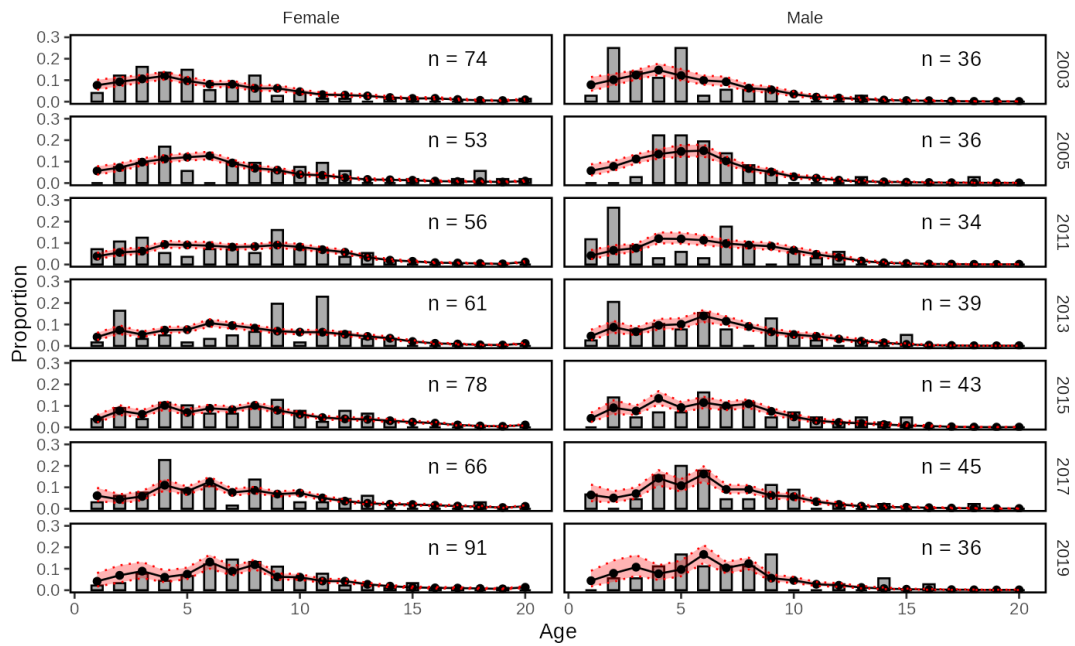


Figure 21. Age composition fits for each sex for the Queen Charlotte Sound Synoptic Survey. See Figure 16 for plot details.

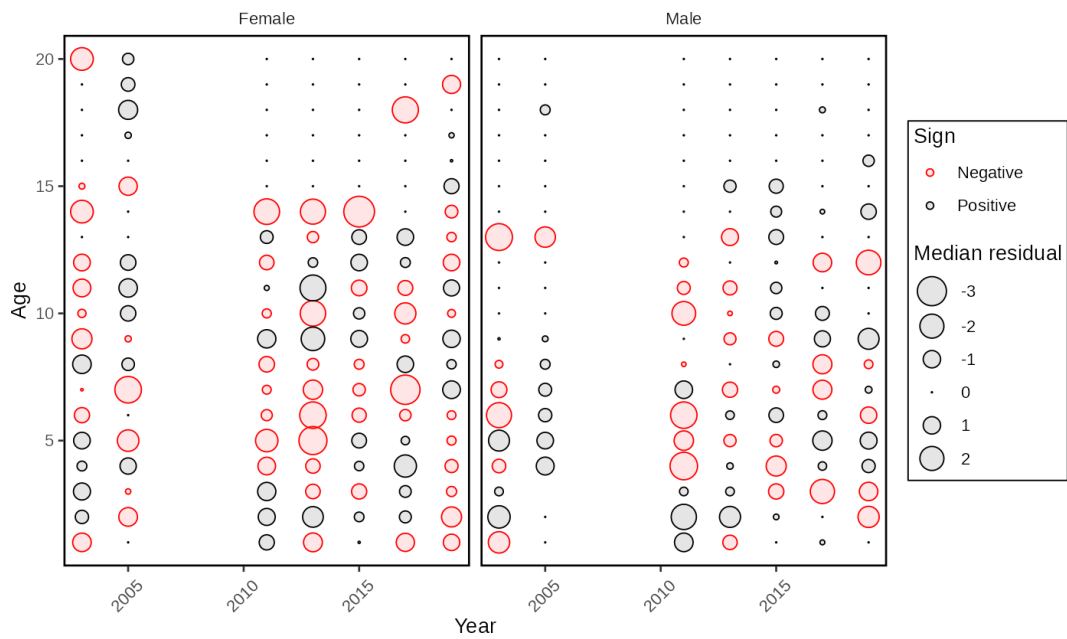


Figure 22. Pearson residuals for the age composition fits for each sex for the Queen Charlotte Sound Synoptic Survey. The bubbles represent the median of the posterior for Pearson residuals. Red bubbles are negative residuals, black are positive, and dots represent zero residuals.

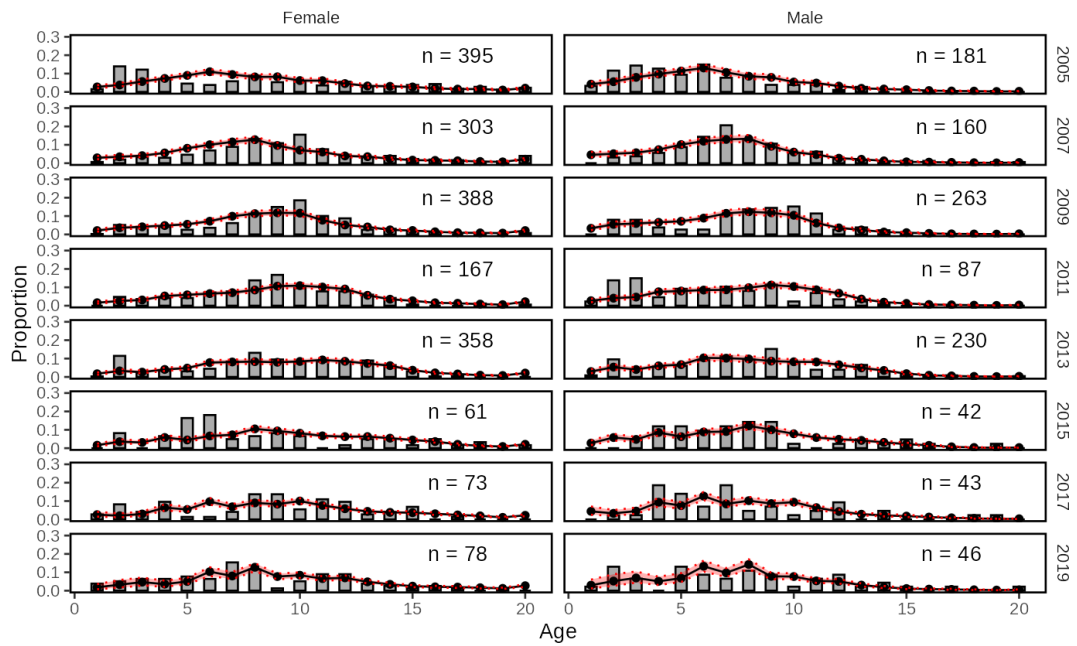


Figure 23. Age composition fits for each sex for the Hecate Strait Synoptic Survey. See Figure 16 for plot details.

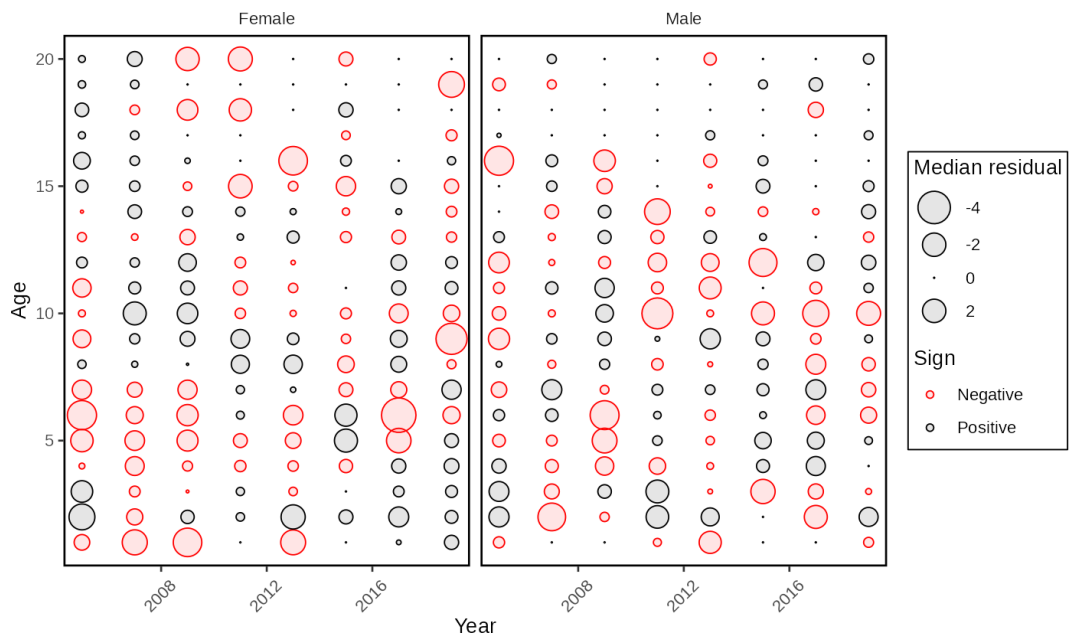


Figure 24. Pearson residuals for the age composition fits for each sex for the Hecate Strait Synoptic Survey. The bubbles represent the median of the posterior for Pearson residuals. Red bubbles are negative residuals, black are positive, and dots represent zero residuals.

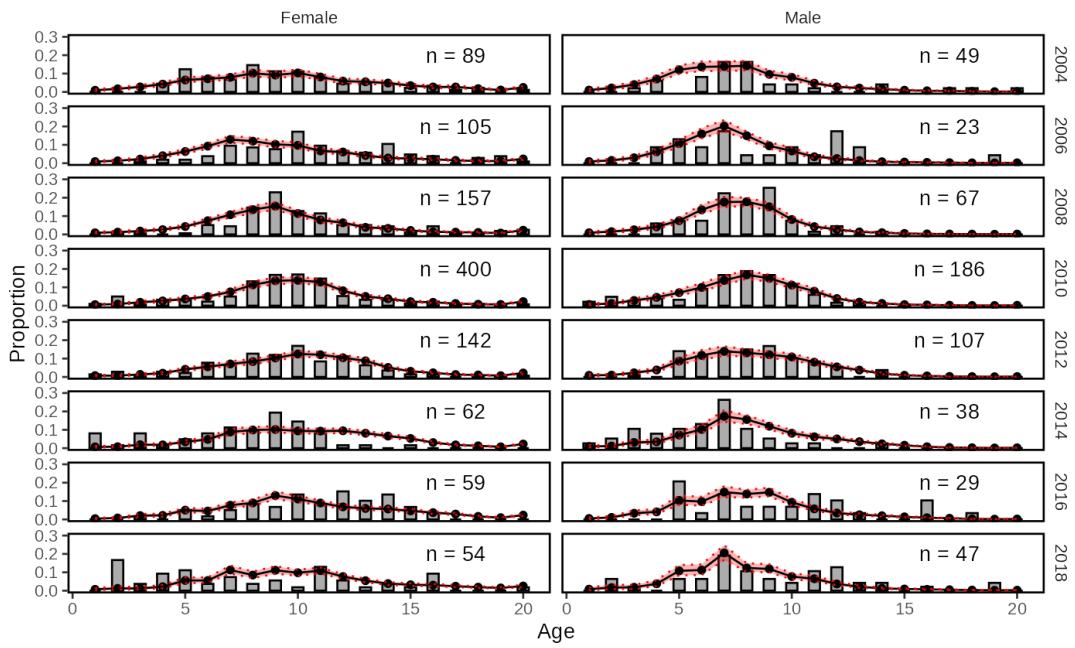


Figure 25. Age composition fits for each sex for the West Coast Vancouver Island Synoptic Survey. See Figure 16 for plot details.

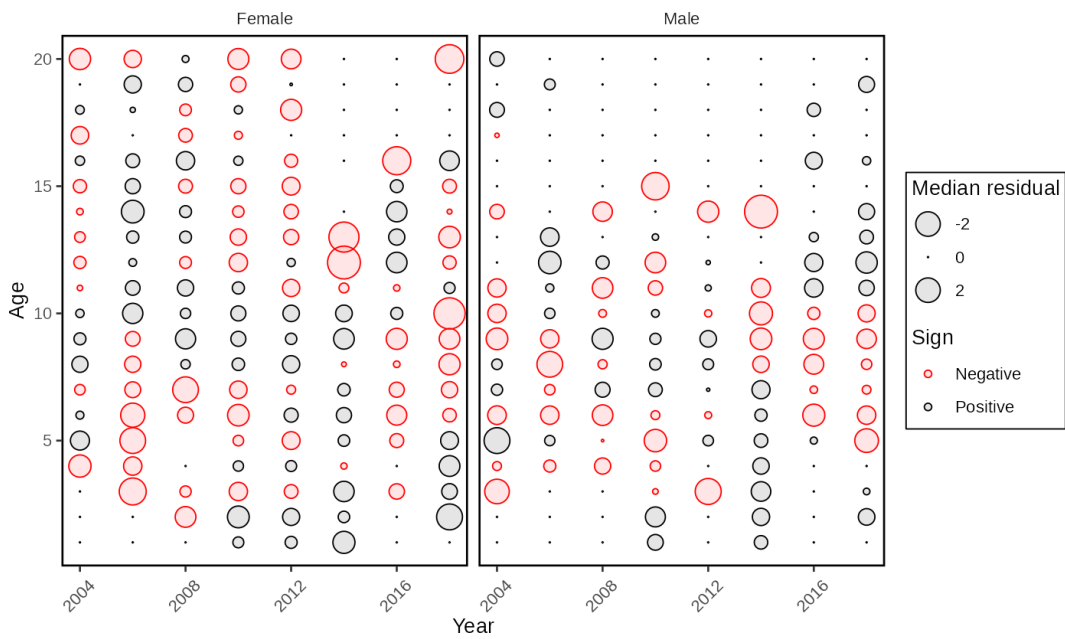


Figure 26. Pearson residuals for the age composition fits for each sex for the West Coast Vancouver Island Synoptic Survey. The bubbles represent the median of the posterior for Pearson residuals. Red bubbles are negative residuals, black are positive, and dots represent zero residuals.

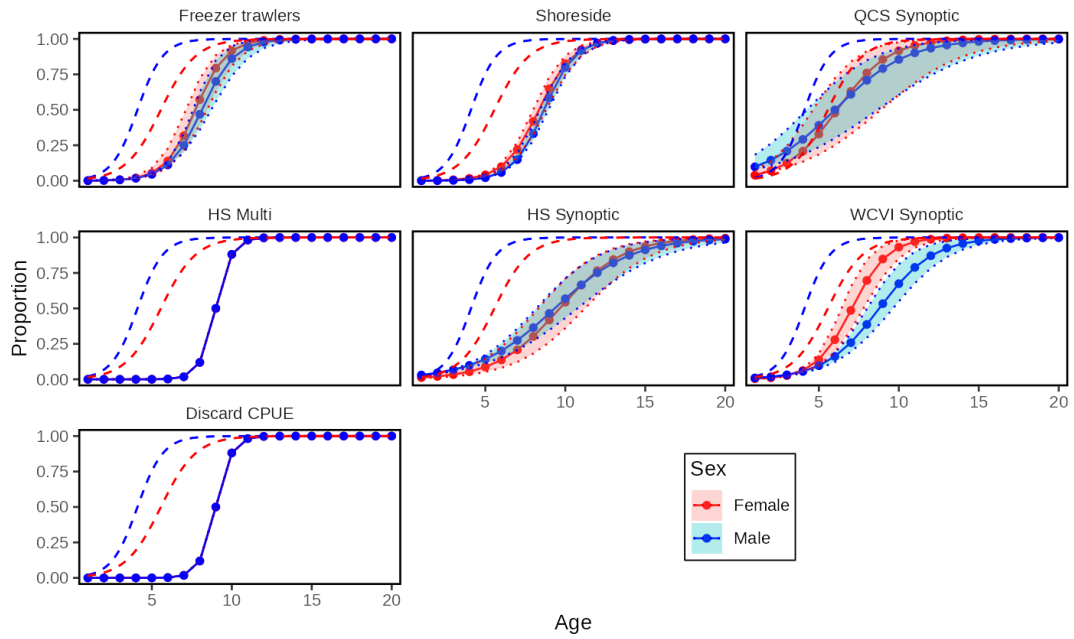


Figure 27. Estimated and fixed selectivities by sex for the base model. The dots show estimated median selectivity-at-age, and the shaded areas show the 95% credible intervals (CI). Single dotted lines with no CI (HS Multi, Discard CPUE) represent fixed selectivities. Dashed lines represent maturity-at-age based on logistic curves fit to the proportion of mature fish at age.

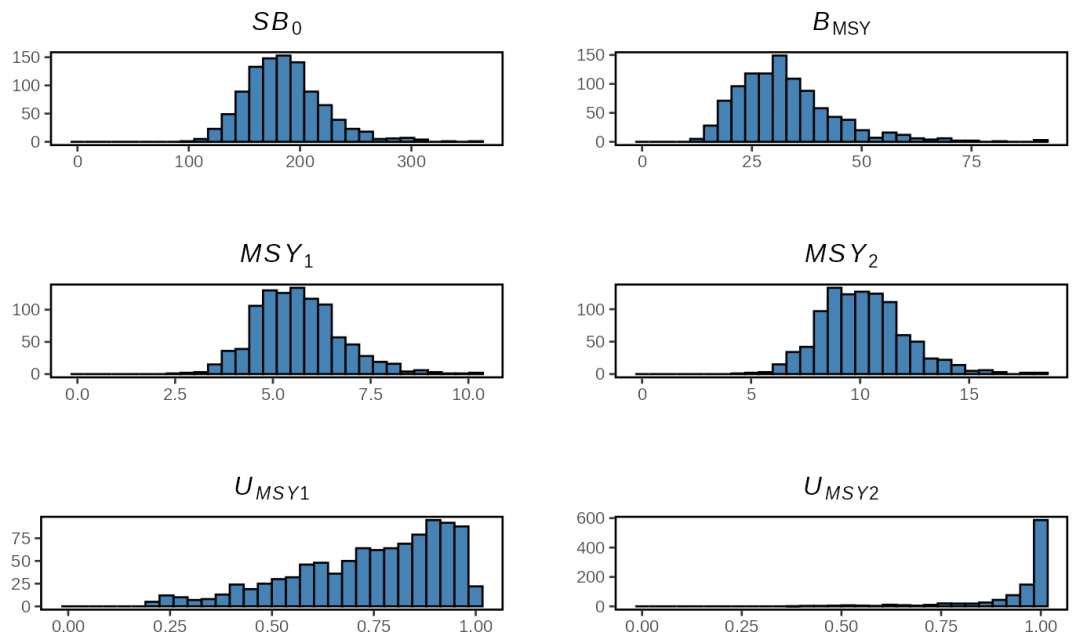


Figure 28. Posterior distributions for reference points and other values of interest for the base model. Subscripts are 1 = Freezer trawlers and 2 = Shoreside.

5.1. BRIDGE MODEL FIGURES

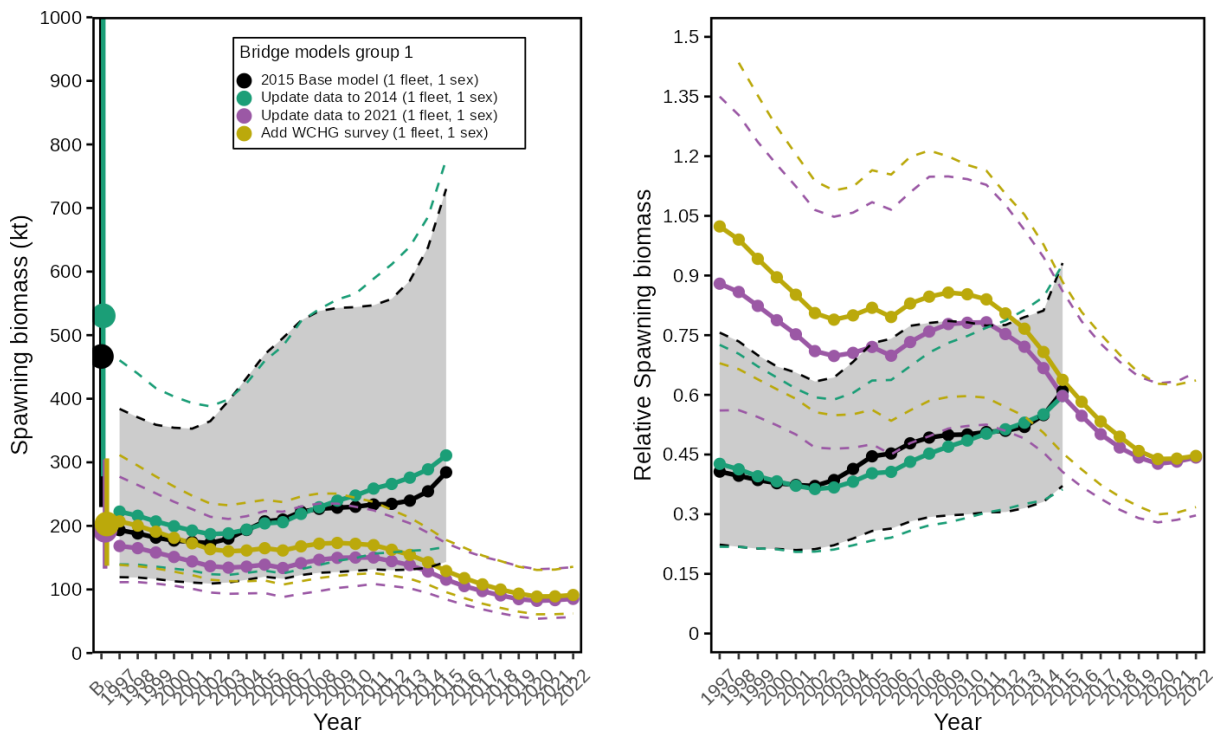


Figure 29. MCMC estimates of spawning biomass (left panel) and relative spawning biomass (right panel) for the first four bridging models. Points and bars on the left in the left panel represent B_0 values and 95% credible interval. The first model in the legend has a shaded ribbon representing the credible interval (CI), the others have dotted lines the same colour as the medians which represent the CI.

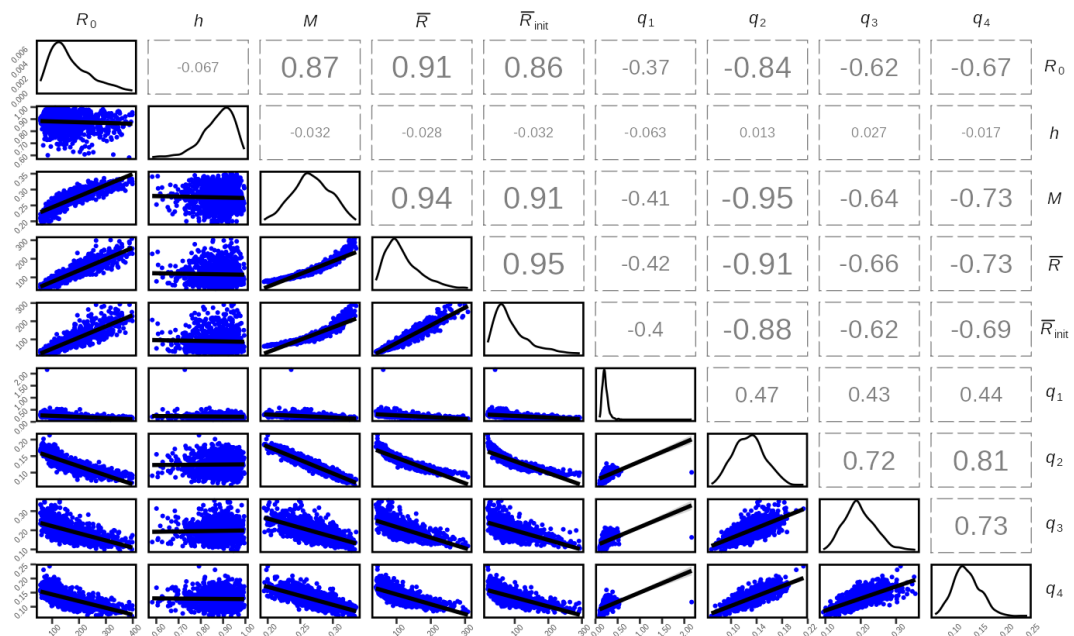


Figure 30. Pairs plots for MCMC estimated parameters in the bridging model in which data from 2015–2021 are added. See Figure 36 for q subscript descriptions.

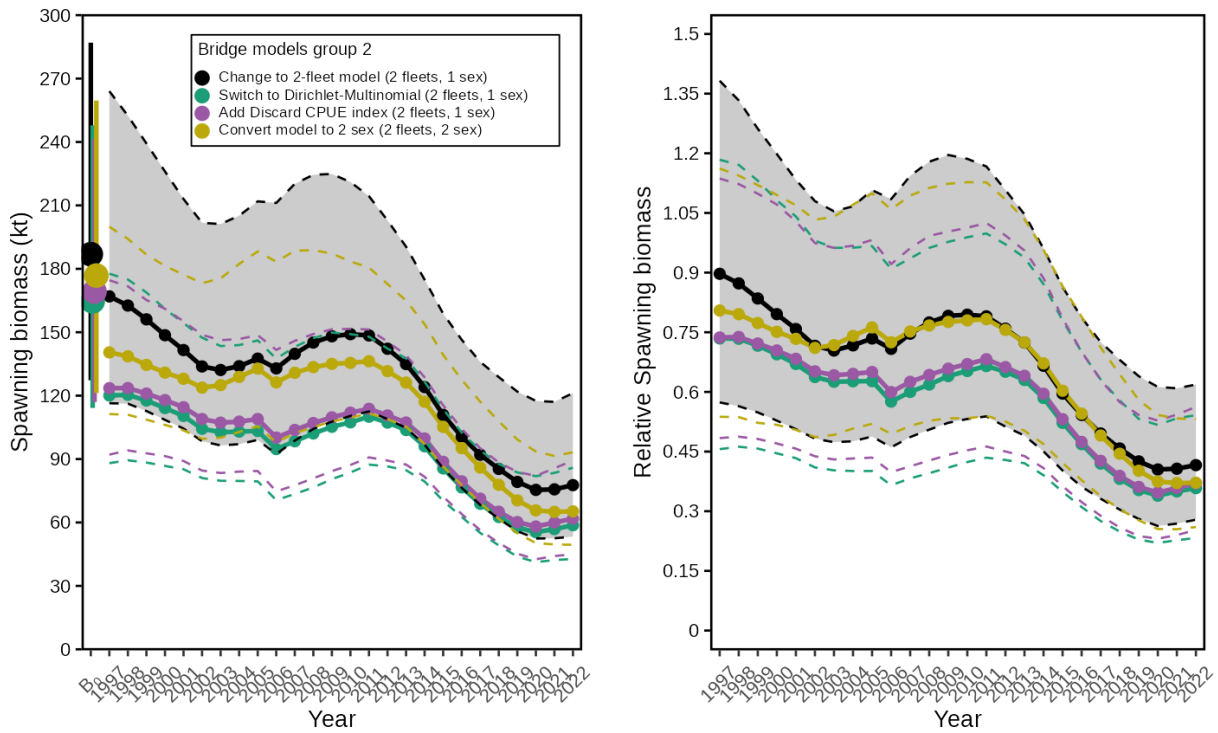


Figure 31. MCMC estimates of spawning biomass (left panel) and relative spawning biomass (right panel) for the second group of bridging models. See Figure 29 for more information.

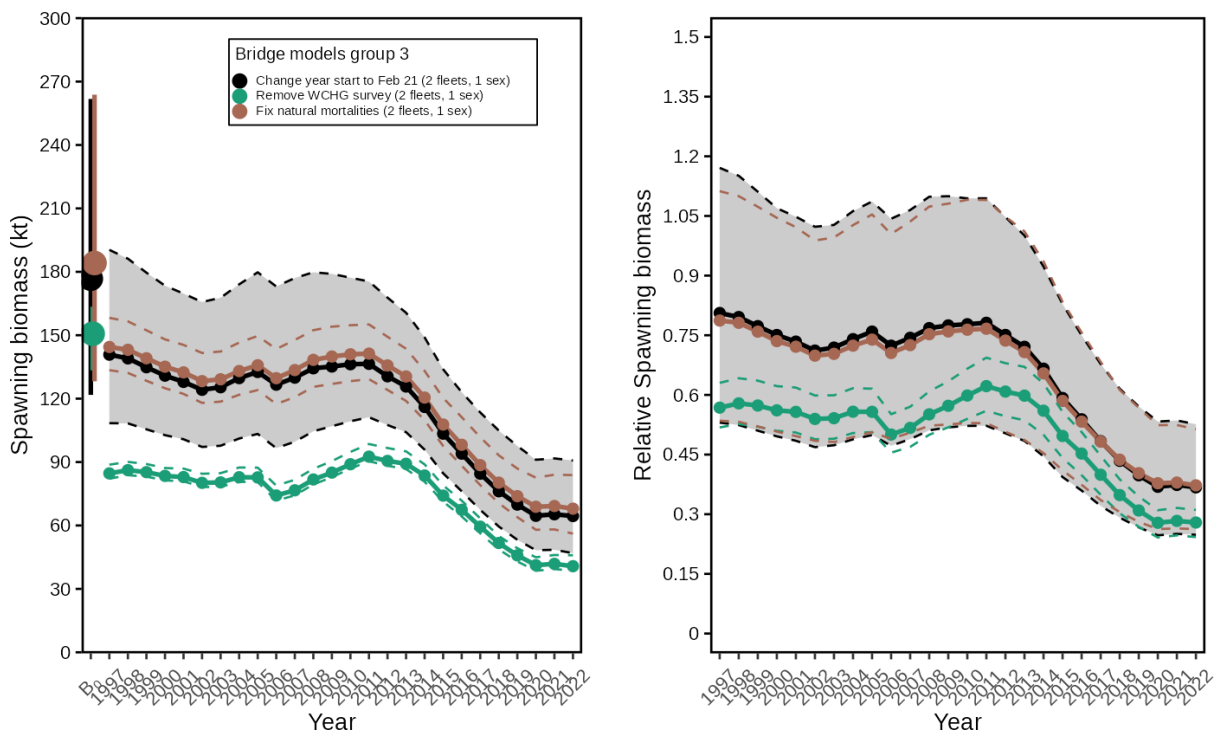


Figure 32. MCMC estimates of spawning biomass (left panel) and relative spawning biomass (right panel) for the third group of bridging models. See Figure 29 for more information.

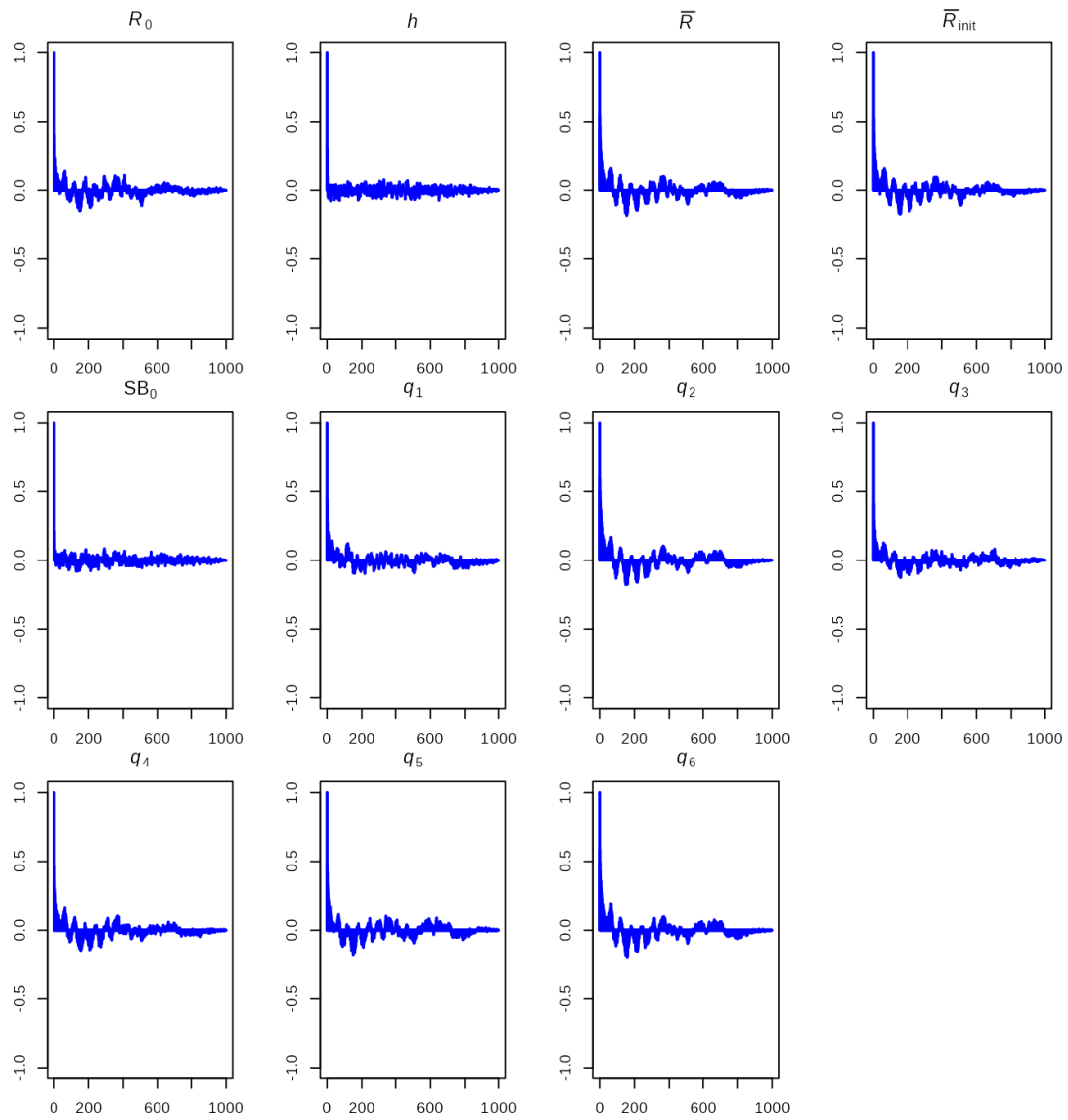


Figure 33. Autocorrelation plots for MCMC estimated lead parameters in the bridge model that has a modified fishing year. See Figure 36 for q subscript descriptions.

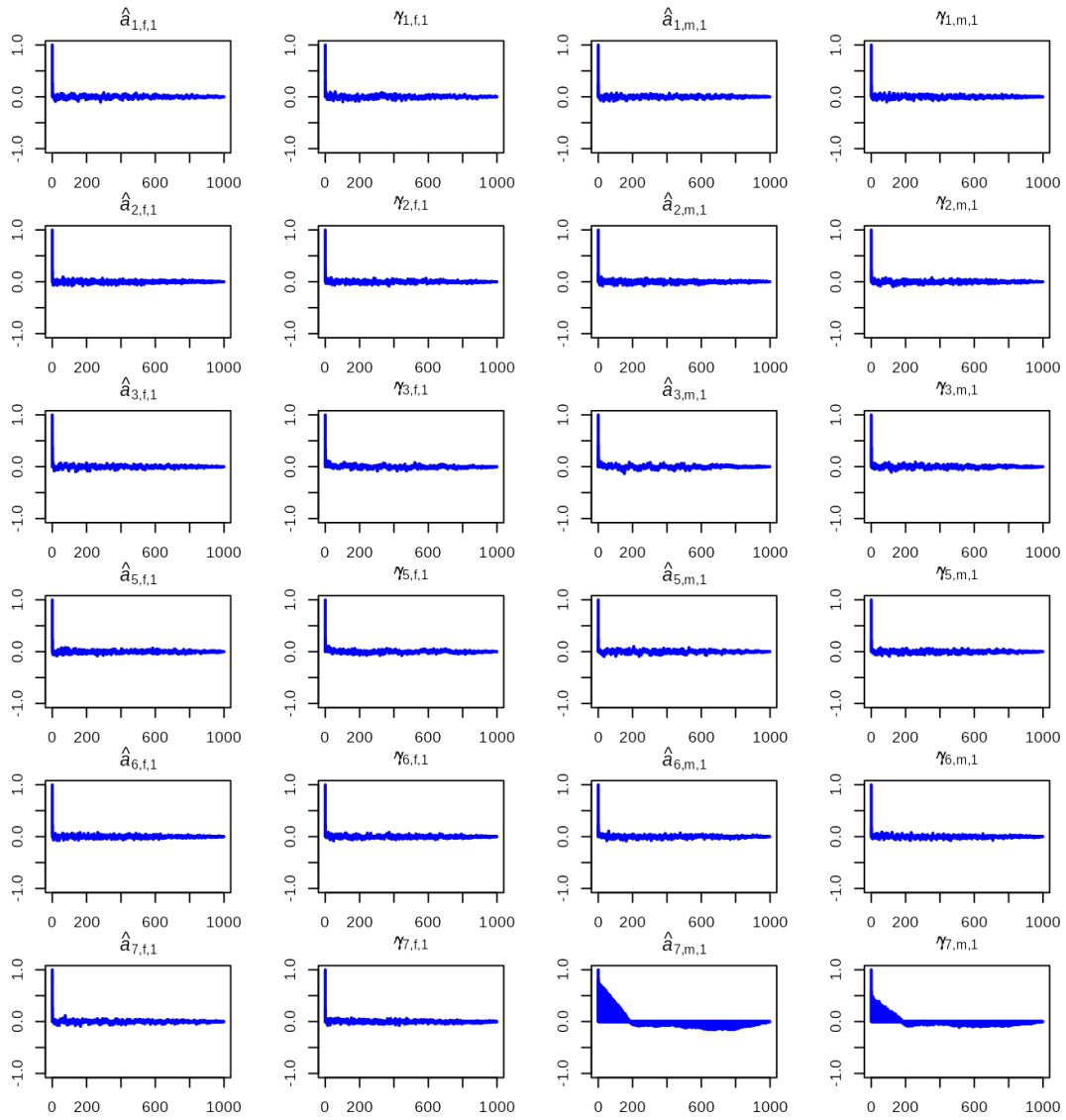


Figure 34. Autocorrelation plots for MCMC estimated lead parameters in the bridge model that has a modified fishing year. See Figure 36 for q subscript descriptions.

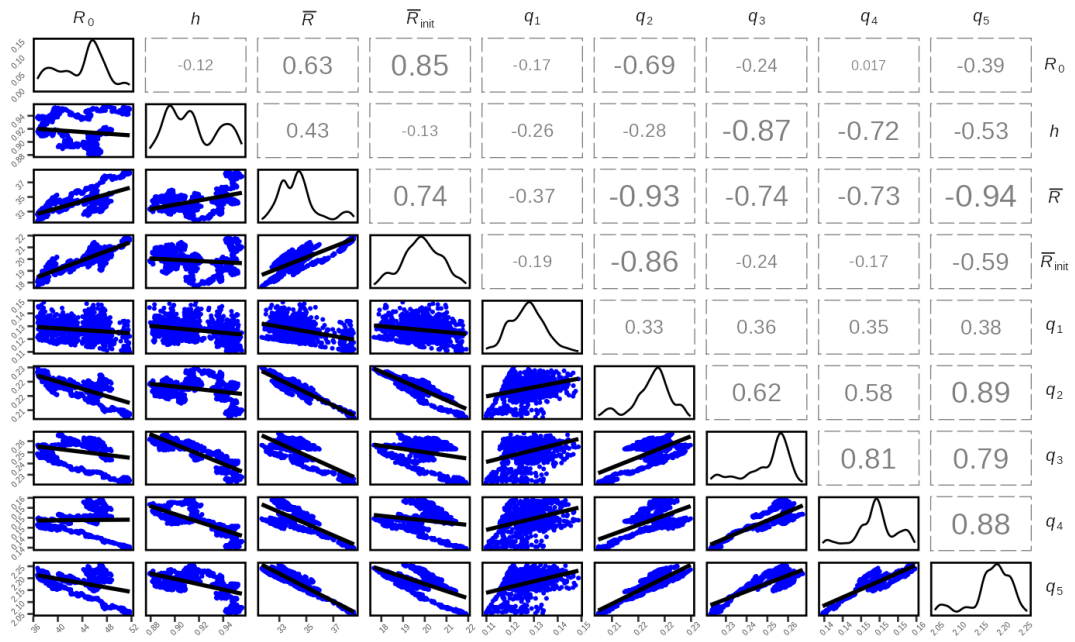


Figure 35. Pairs plots for MCMC estimated parameters in the bridging model for which the WCHG index was removed. See Figure 36 for q subscript descriptions.

5.2. MCMC DIAGNOSTIC FIGURES FOR THE BASE MODEL

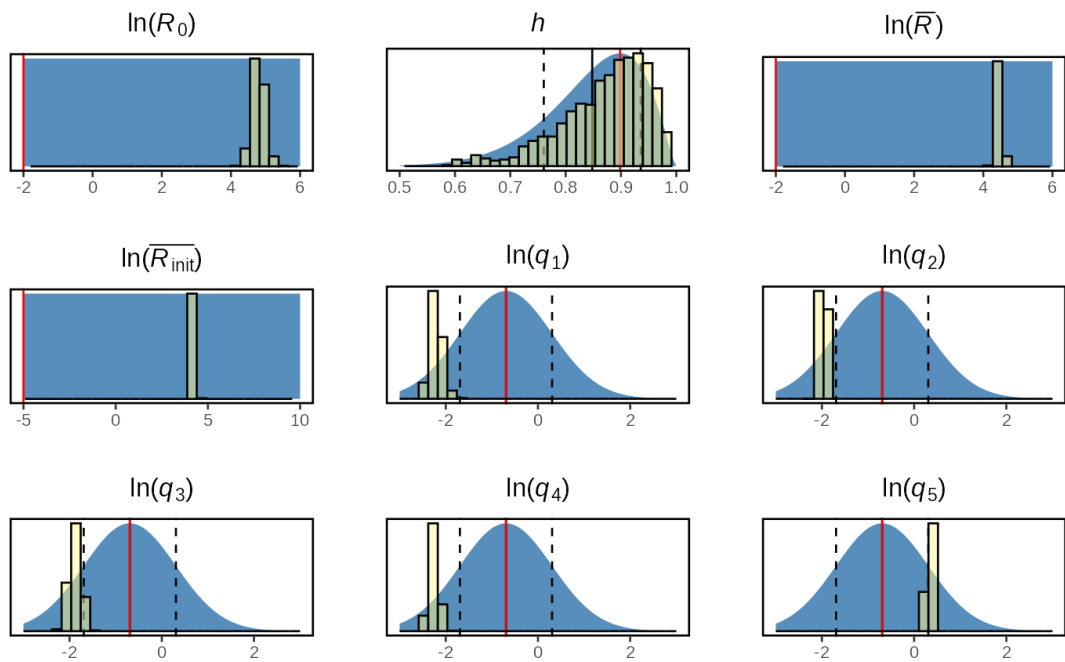


Figure 36. Prior probability distributions used in the base model (blue shaded areas) overlaid with posterior distribution histograms. The solid red line is the mode of the prior distribution, the vertical solid black line is the mean of the prior, and the vertical dashed black lines represent one standard deviation from the mean. Plots that are entirely shaded blue represent uniform priors. Catchability (q) parameters for the survey indices have numerical subscripts which are: 1 = QCS Synoptic, 2 = HS Multi, 3 = HS Synoptic, 4 = WCVI Synoptic, 5 = Discard CPUE.

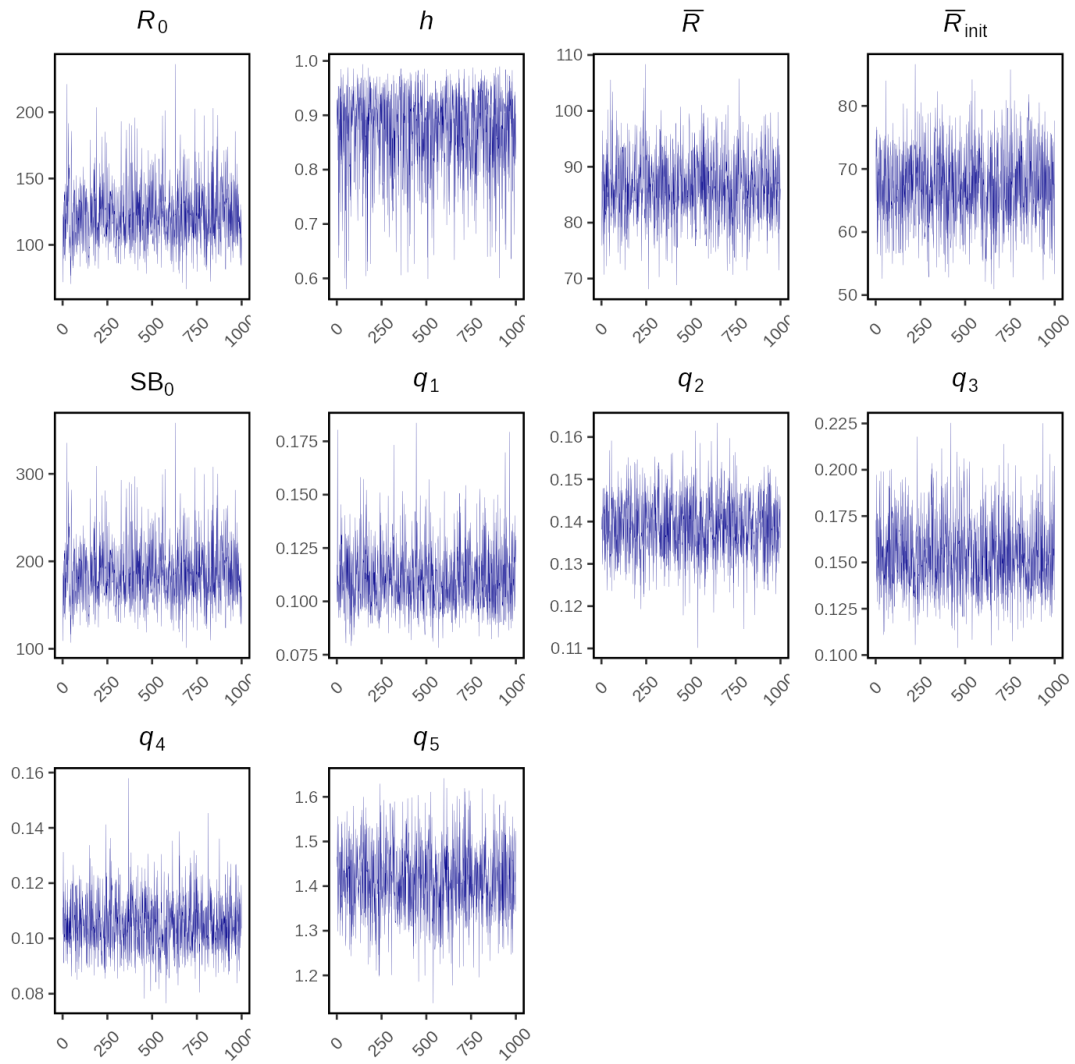


Figure 37. Trace plots for MCMC output of estimated lead parameters in the base model. The MCMC run has chain length 10,000,000 with a sample taken every 5,000th iteration. Of the 2,000 samples taken, the first 1,000 were removed as a burn-in period. See Figure 36 for q subscript descriptions.

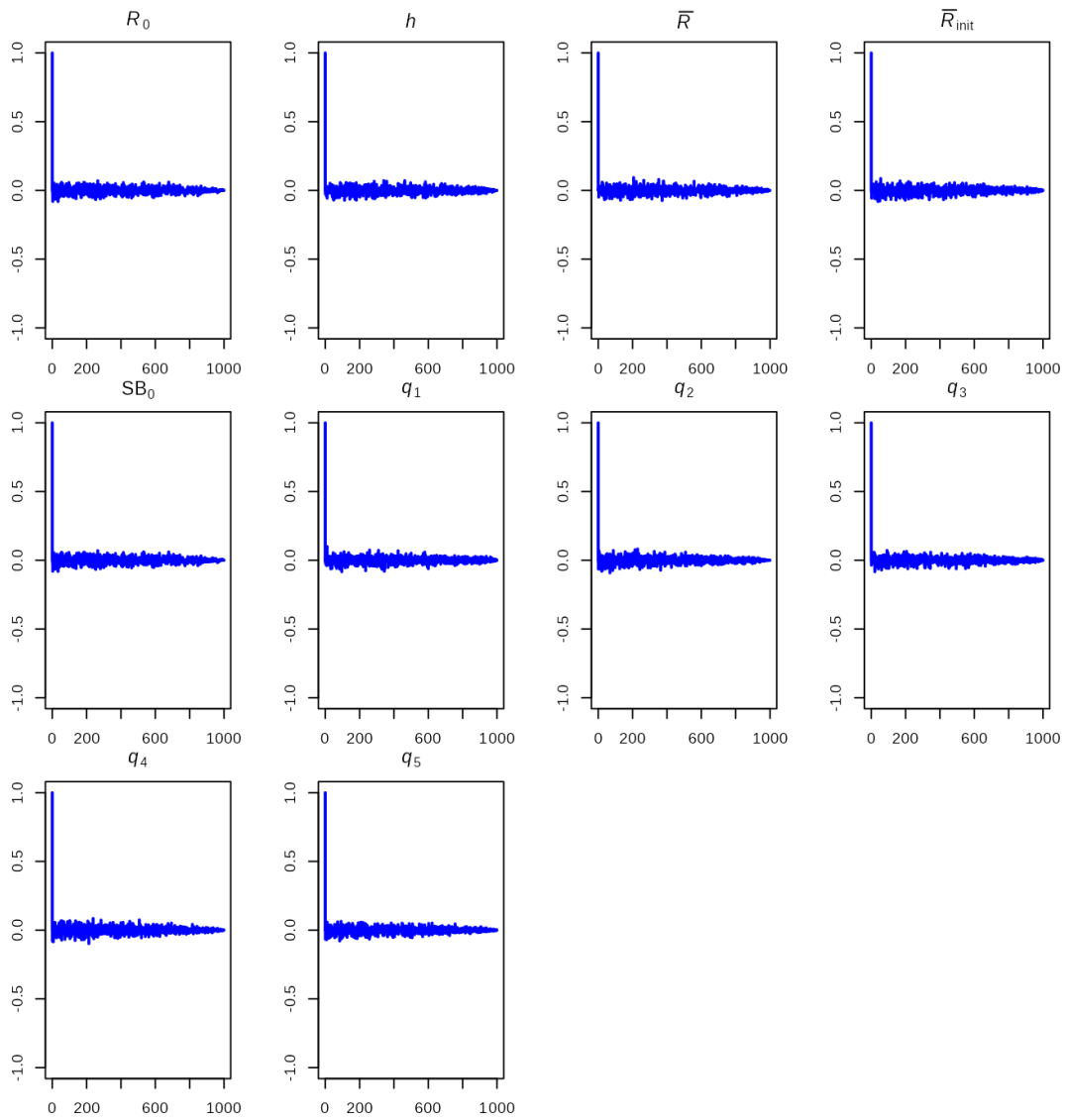


Figure 38. Autocorrelation plots for MCMC output of estimated lead parameters in the base model. The x-axis values are the lag between posteriors. See Figure 36 for q subscript descriptions.

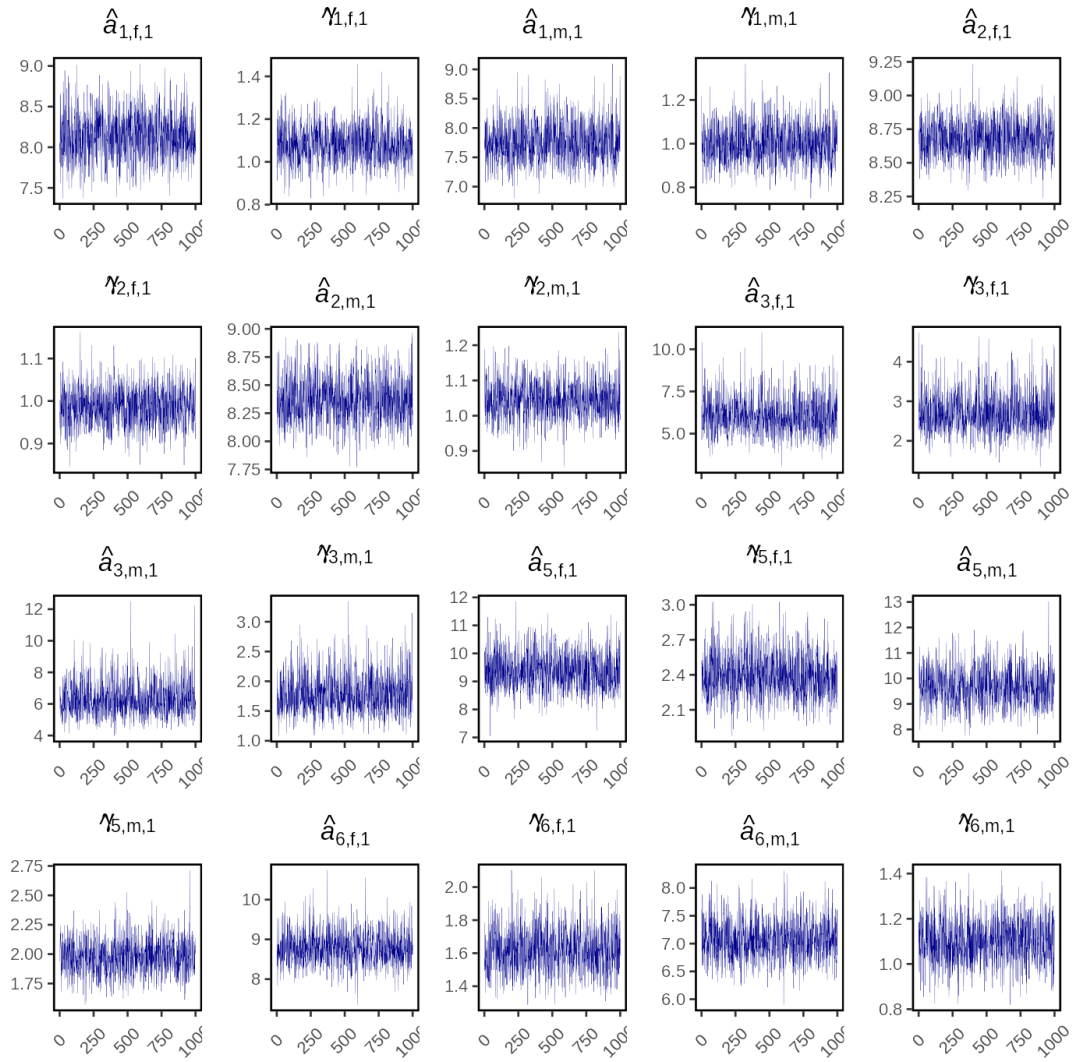


Figure 39. Trace plots for MCMC output of estimated selectivity parameters in the base model. \hat{a} are the estimates of selectivity-at-age-50%, $\hat{\gamma}$ are the estimated standard deviations on selectivity-at-age-50%. The first numerical subscript is the gear number which are: 1 = Freezer trawlers, 2 = Shoreside, 3 = QCS Synoptic, 4 = HS Multi, 5 = HS Synoptic, 6 = WCVI Synoptic, 7 = Discard CPUE. The letter subscripts 'f' and 'm' correspond to female and male, and the second numerical subscripts represent the year block for selectivity. For the base model, there is only the subscript '1' for all parameters shown, because time-varying selectivity was not implemented.

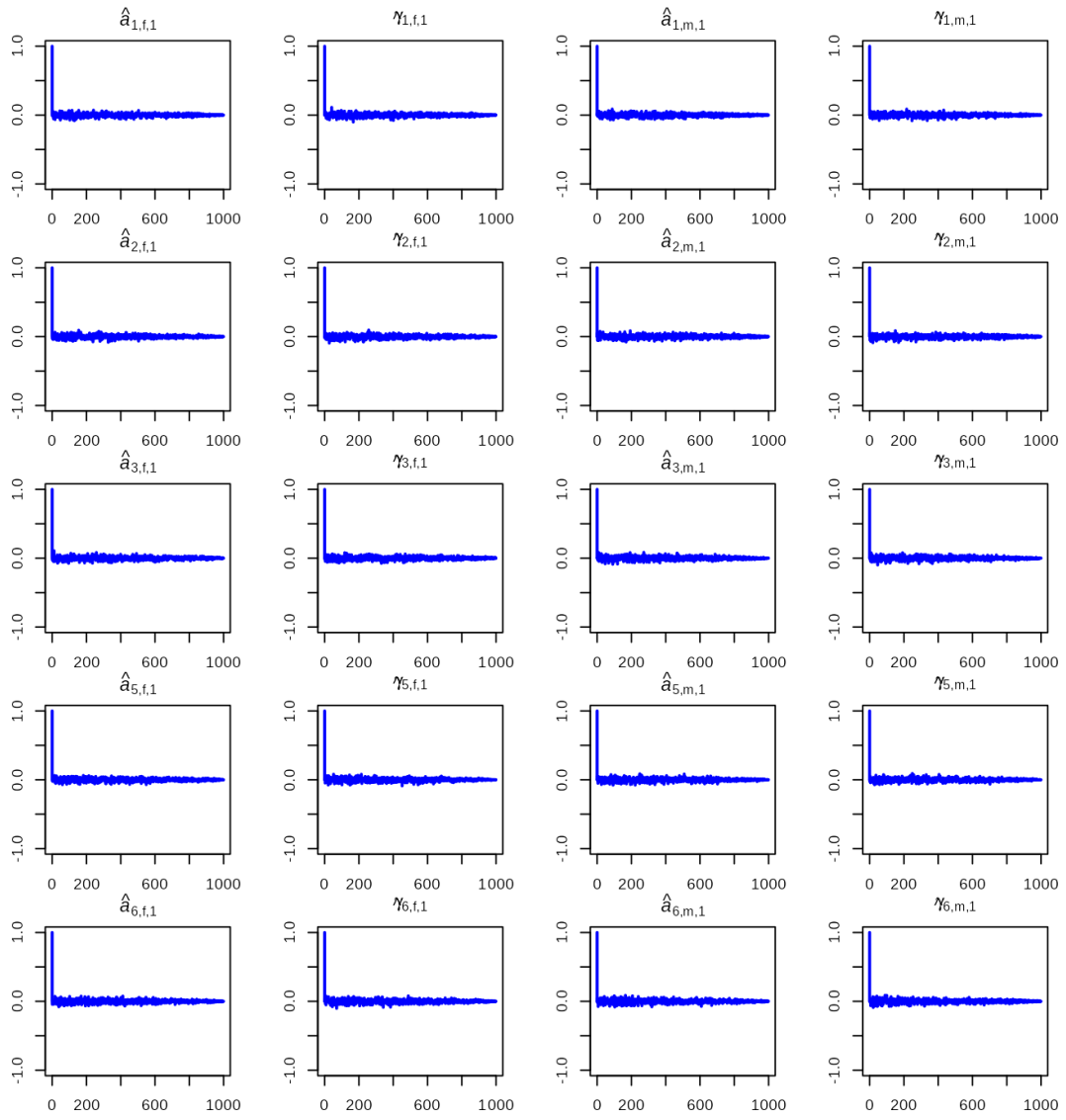


Figure 40. Autocorrelation plots for MCMC output of estimated selectivity parameters in the base model. The x-axis values are the lag between posteriors. See Figure 39 for descriptions of the parameter subscripts.

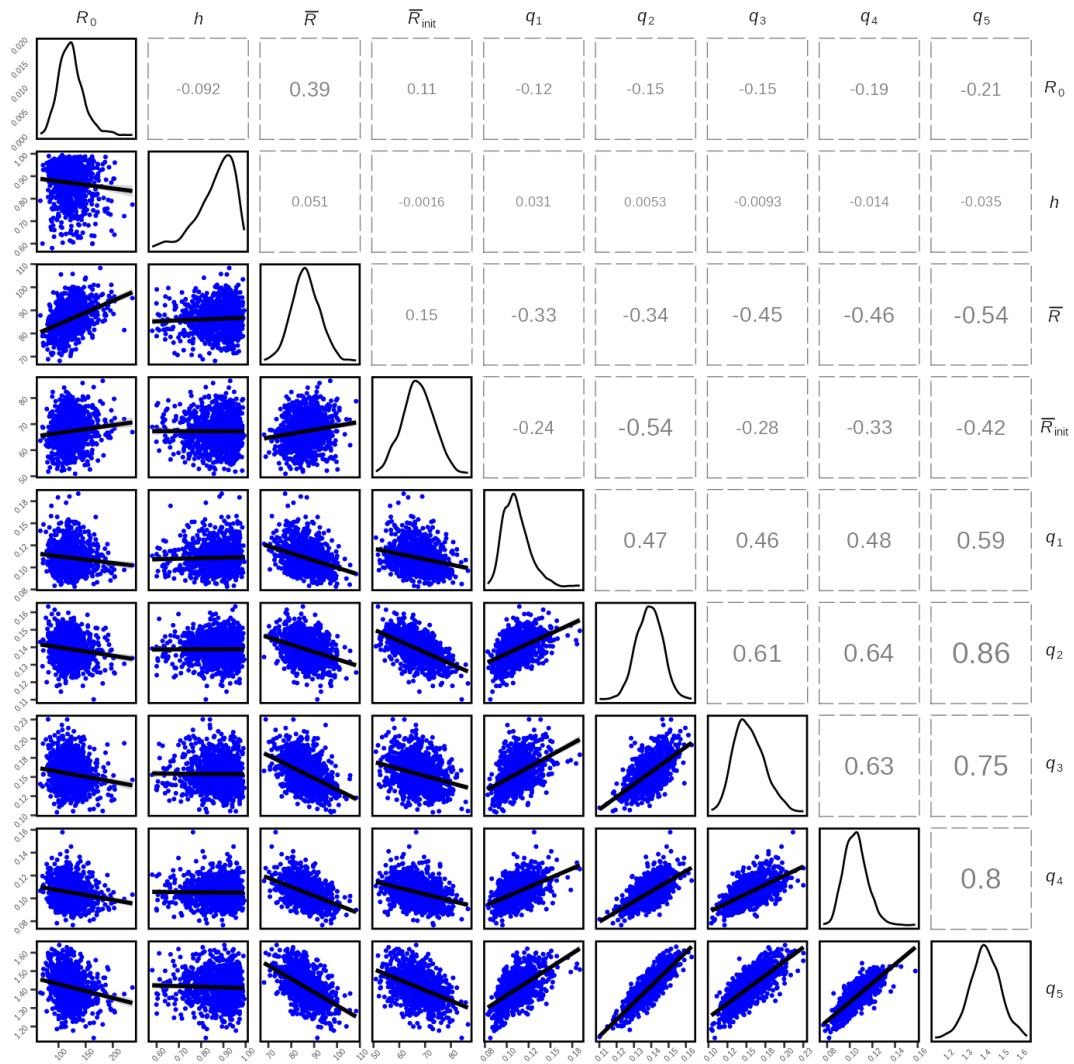


Figure 41. Pairs plots for MCMC estimated parameters in the base model. The lines in the points plots in the lower triangular panels are linear models with shaded 95% confidence intervals. The line plots in the diagonal panels represent density of the parameter values, and the values in the upper triangular panels are the correlations between parameters with text size being directly proportional to the absolute value of those values. See Figure 36 for q subscript descriptions.

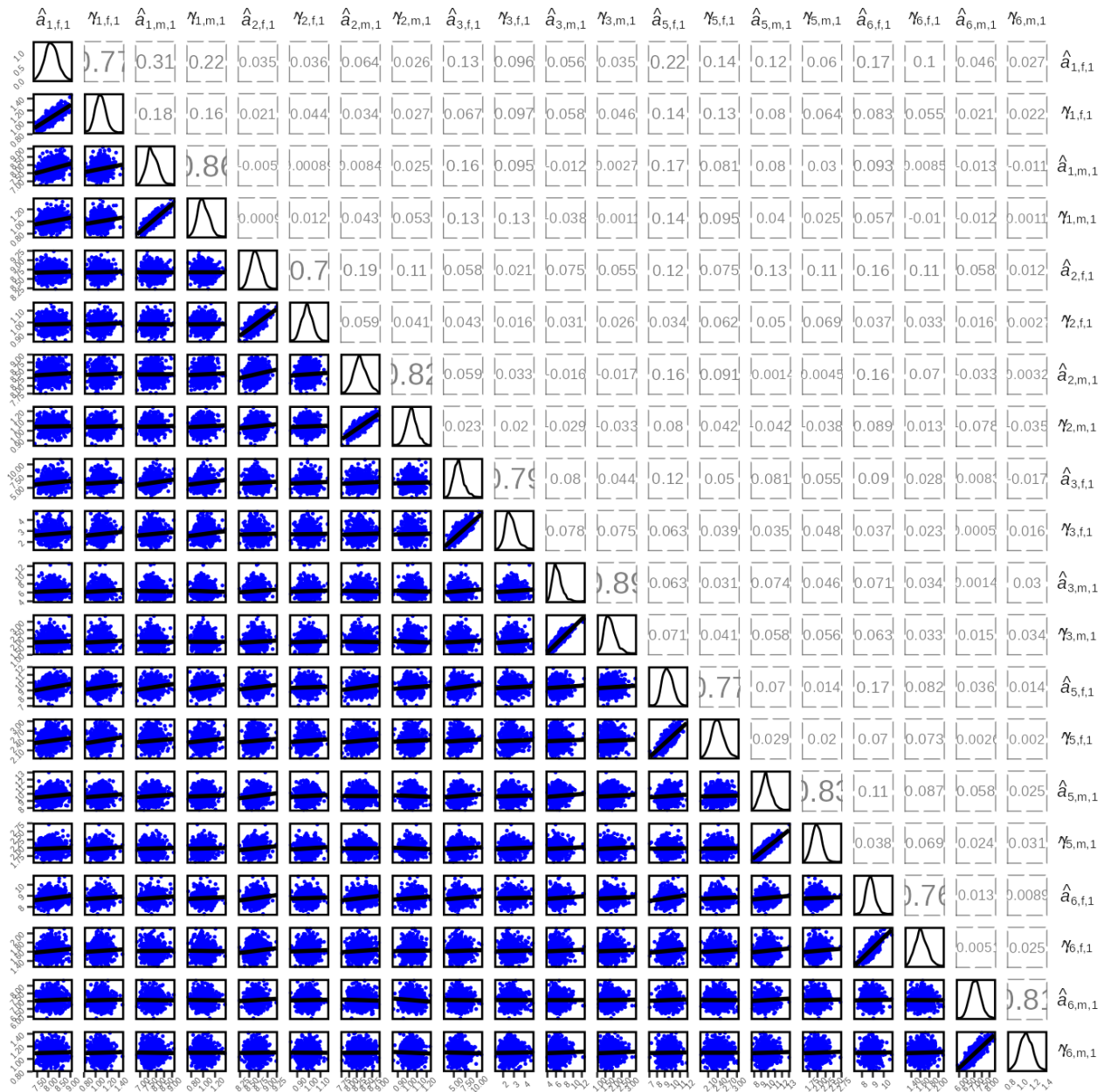


Figure 42. Pairs plots for MCMC estimated selectivity parameters in the base model. The lines in the points plots in the lower triangular panels are linear models with shaded 95% confidence intervals. The line plots in the diagonal panels represent density of the parameter values, and the values in the upper triangular panels are the correlations between parameters with text size being directly proportional to the absolute value of those values. See Figure 39 for descriptions of the parameter subscripts.

5.3. SENSITIVITY MODEL FIGURES

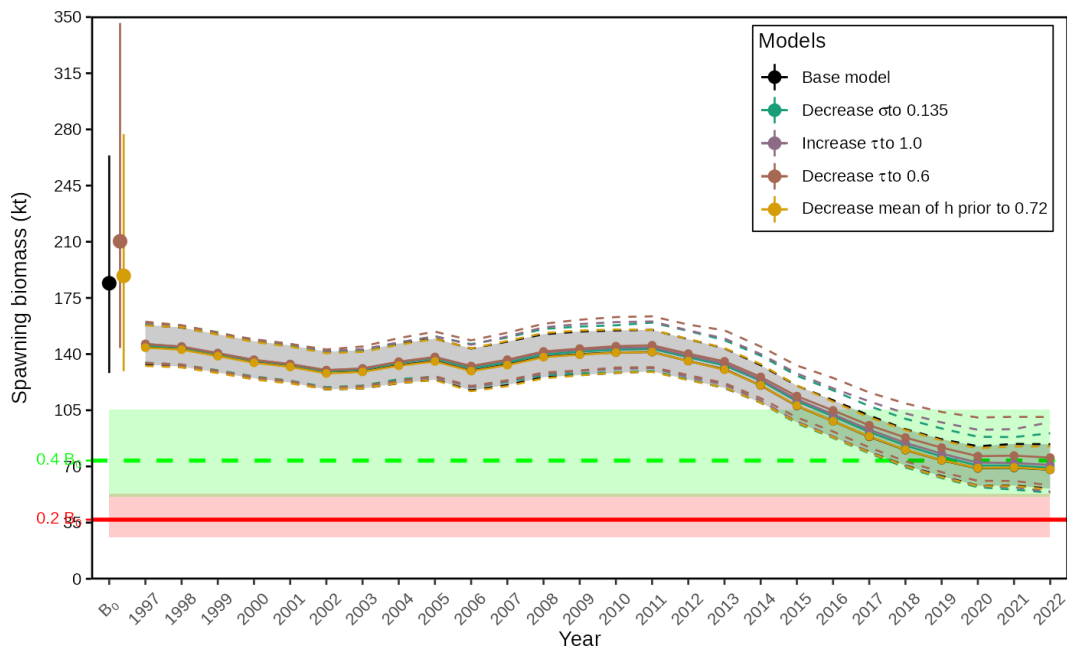


Figure 43. Spawning biomass for sensitivities to changes in the ϑ^2 and ρ parameters (due to changes to σ and τ), and steepness (h) parameter. The B_0 estimates for the ‘Decrease σ to 0.135’ and ‘Increase τ to 1.0’ models are outside the axis limits. For the sake of clarity of the trajectories, they were left off the plot. They are estimated as 446 (252–605) thousand t and 372 (190–588) thousand t respectively.

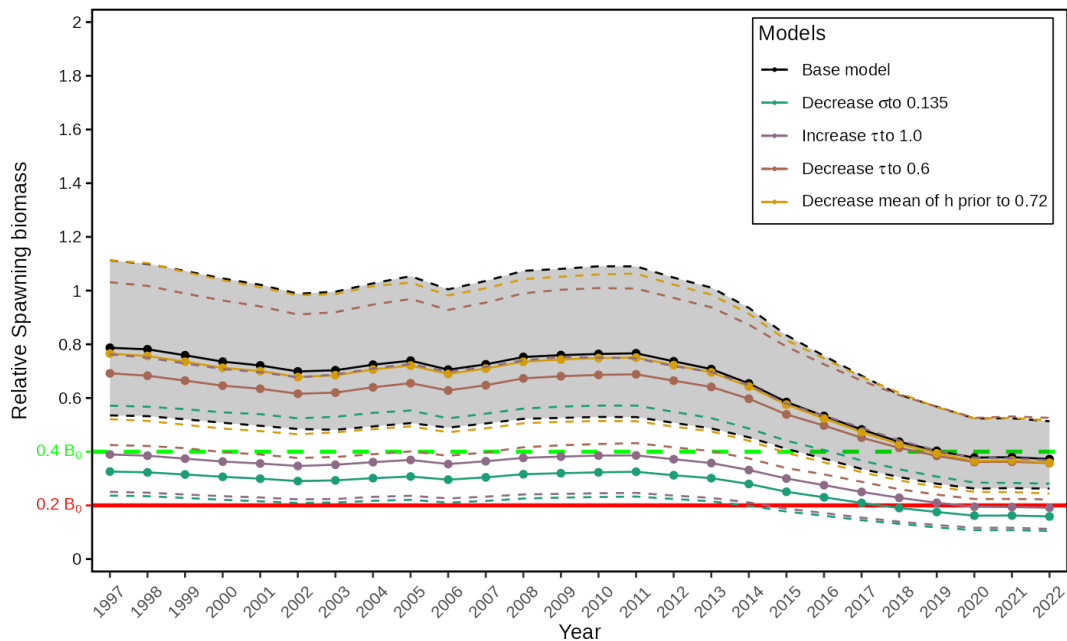


Figure 44. Relative spawning biomass for sensitivities to changes in the ϑ^2 and ρ parameters (due to changes to σ and τ), and steepness (h) parameter.

Decrease mean of h prior to 0.72

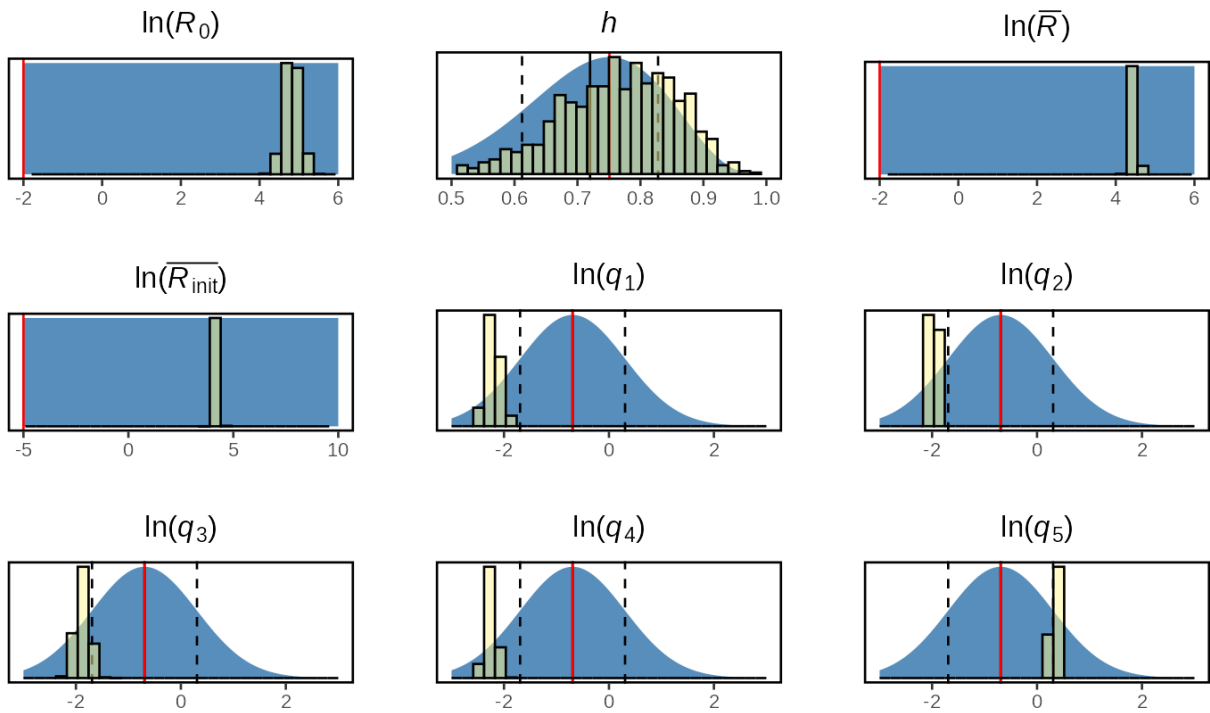


Figure 45. Priors and posteriors for the sensitivity in which the steepness prior was changed. This can be compared to the base model in Figure 36.

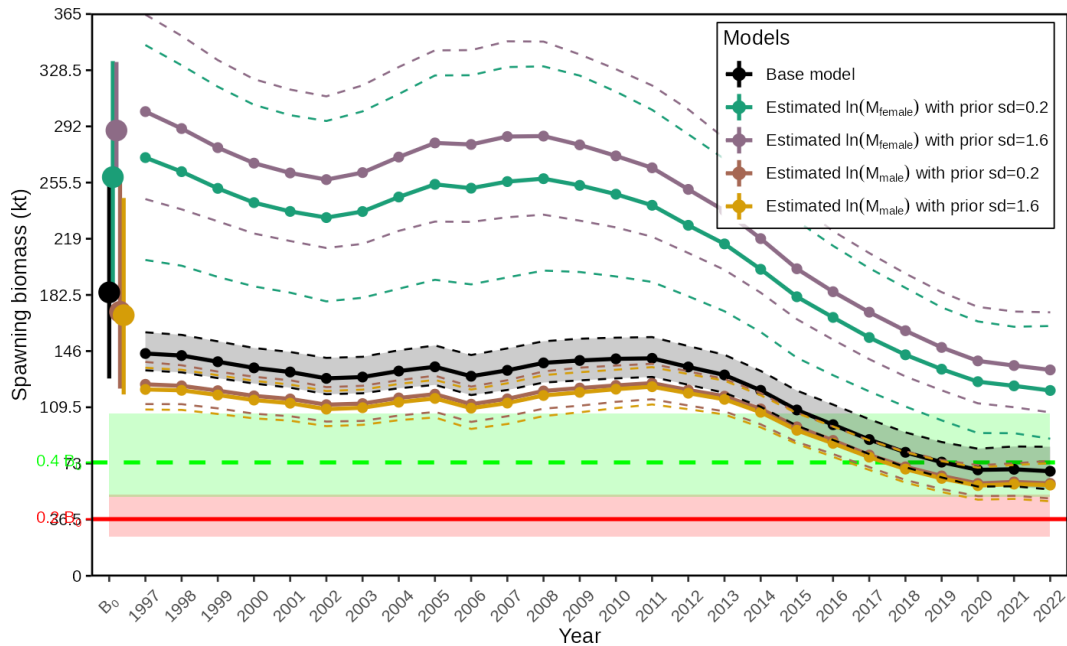


Figure 46. Spawning biomass for sensitivities to changes in the natural mortality (M) parameters. In the base model, this parameter is fixed for both male and females. In these sensitivities, M is estimated for the sex in question in addition to the changes in prior, while the parameter for the opposite sex remains fixed.

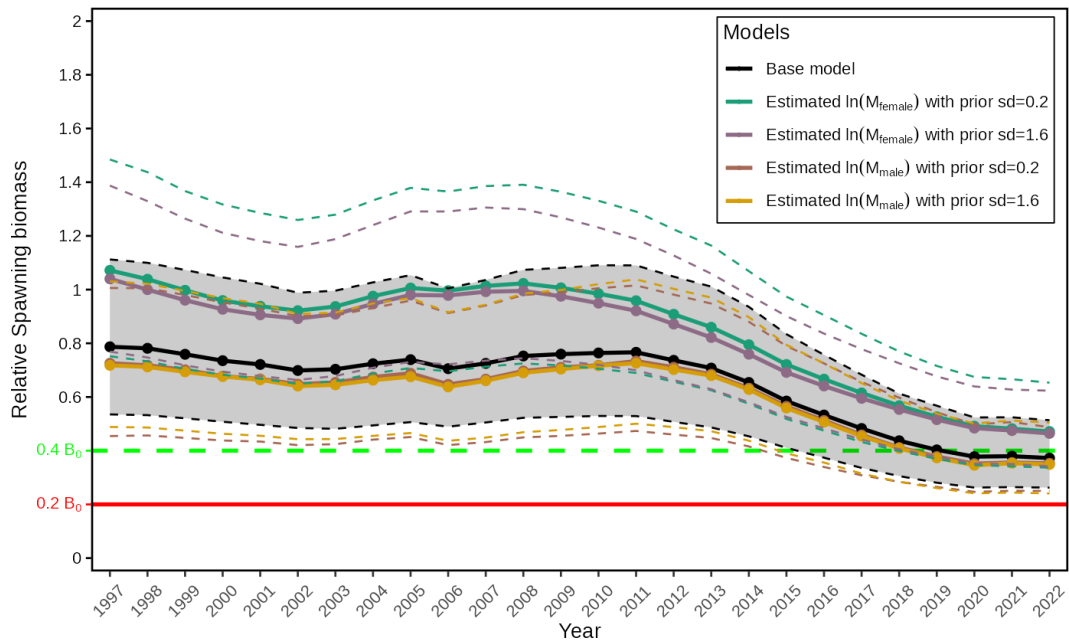


Figure 47. Relative spawning biomass for sensitivities to changes in the natural mortality (M) parameters.

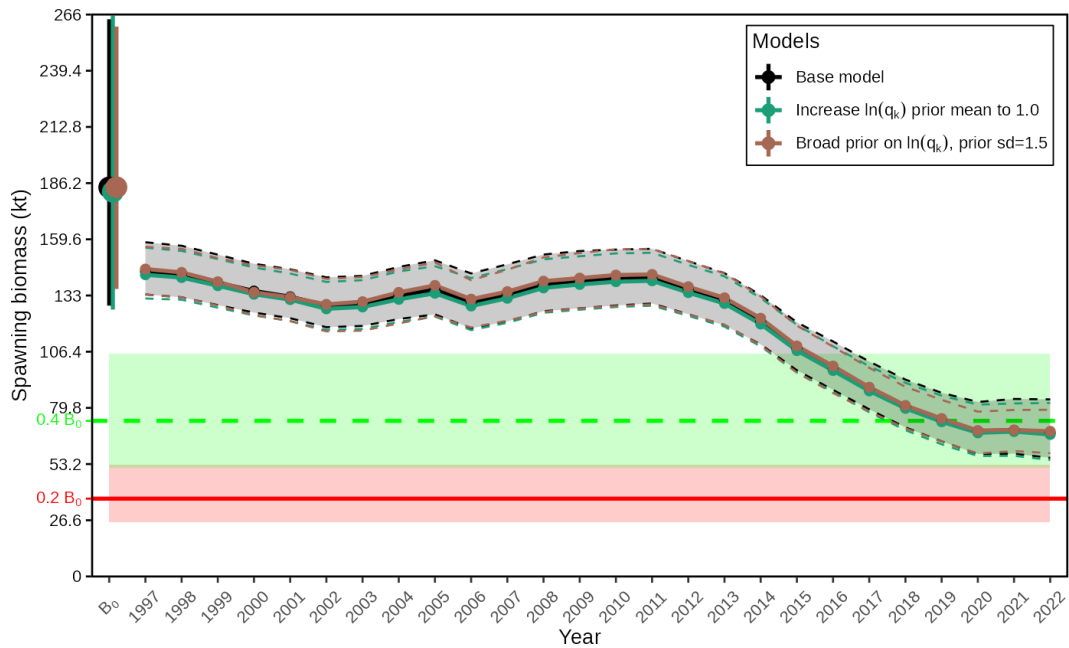


Figure 48. Spawning biomass for the sensitivities to changes in the catchability (q_k) parameters. For these sensitivities the priors for all gears (k) are modified in the same way.

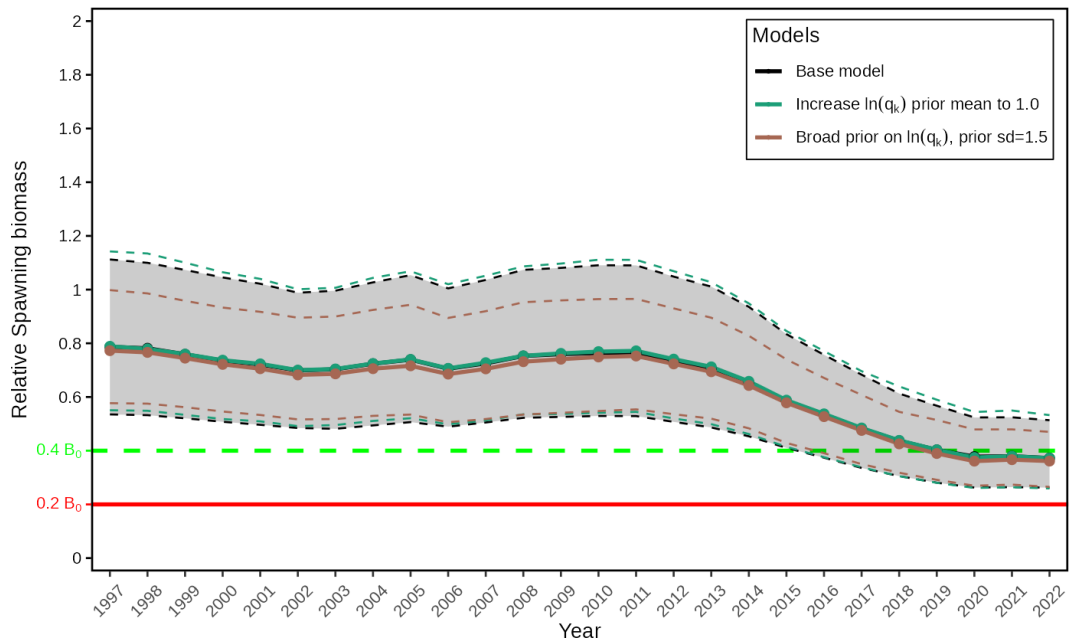


Figure 49. Relative spawning biomass for the sensitivities to changes in the priors for the catchability (q_k) parameters. For these sensitivities the priors for all gears (k) are modified in the same way.

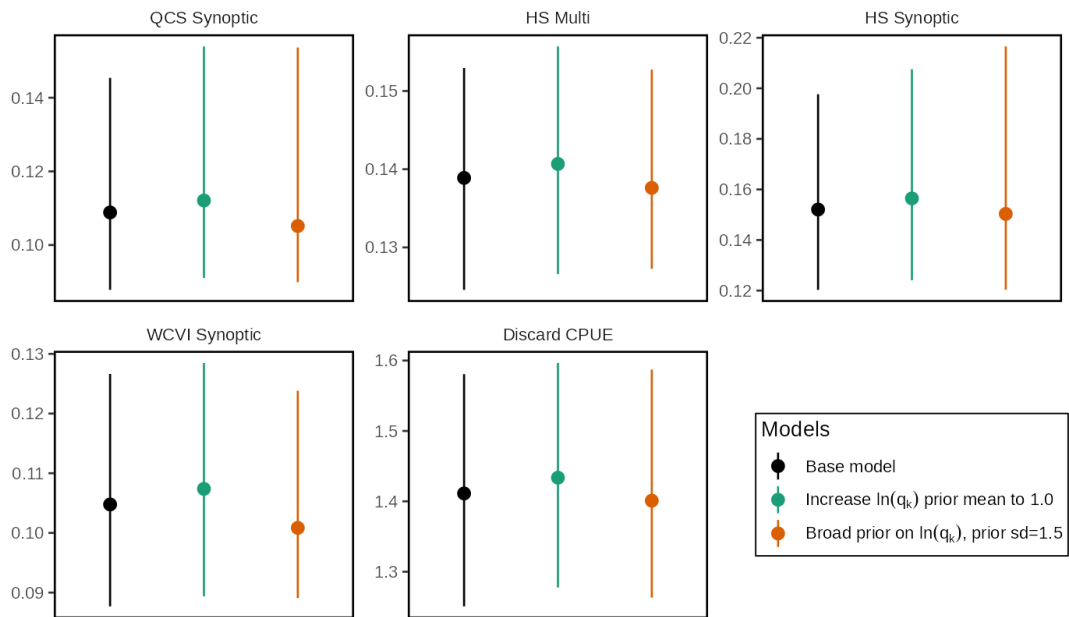


Figure 50. Catchability estimates for the sensitivities to changes in the priors for the catchability (q_k) parameters. The points are the median of the posterior and the vertical lines are the 95% CI.

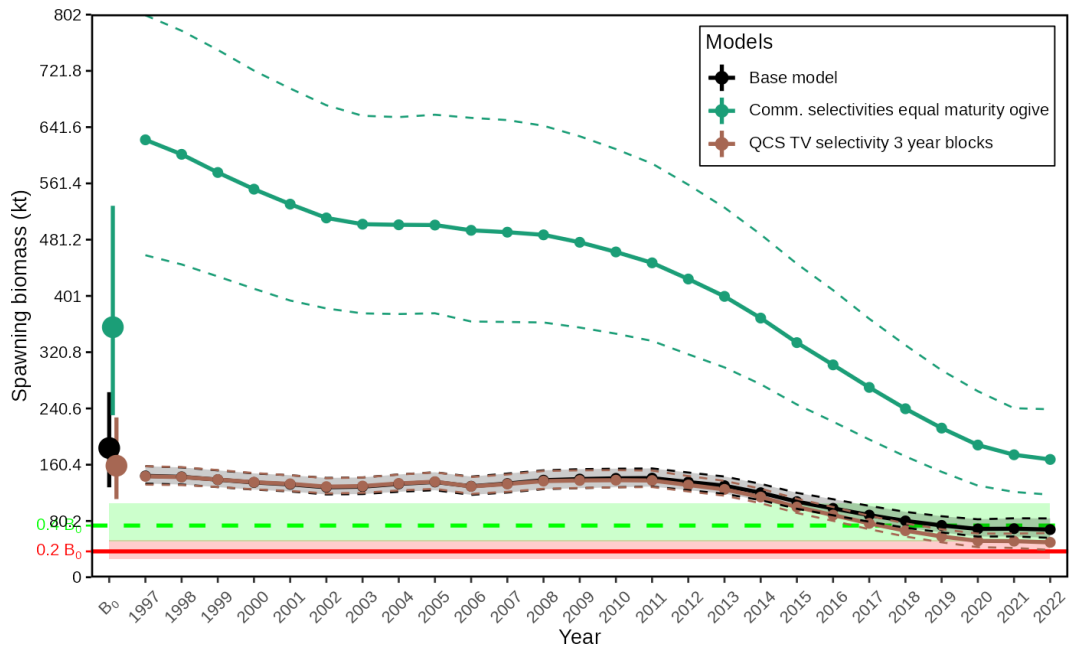


Figure 51. Spawning biomass for the sensitivities to changes in the selectivity parameters (\hat{a}_k and γ_k). For the first sensitivity, the selectivities for the two commercial trawl fisheries are fixed to the maturity for the two commercial trawl gears (k). For the second, the Queen Charlotte Sound Synoptic Survey has three year blocks or time-varying selectivity, 2003–2010, 2011–2016, and 2017–2021.

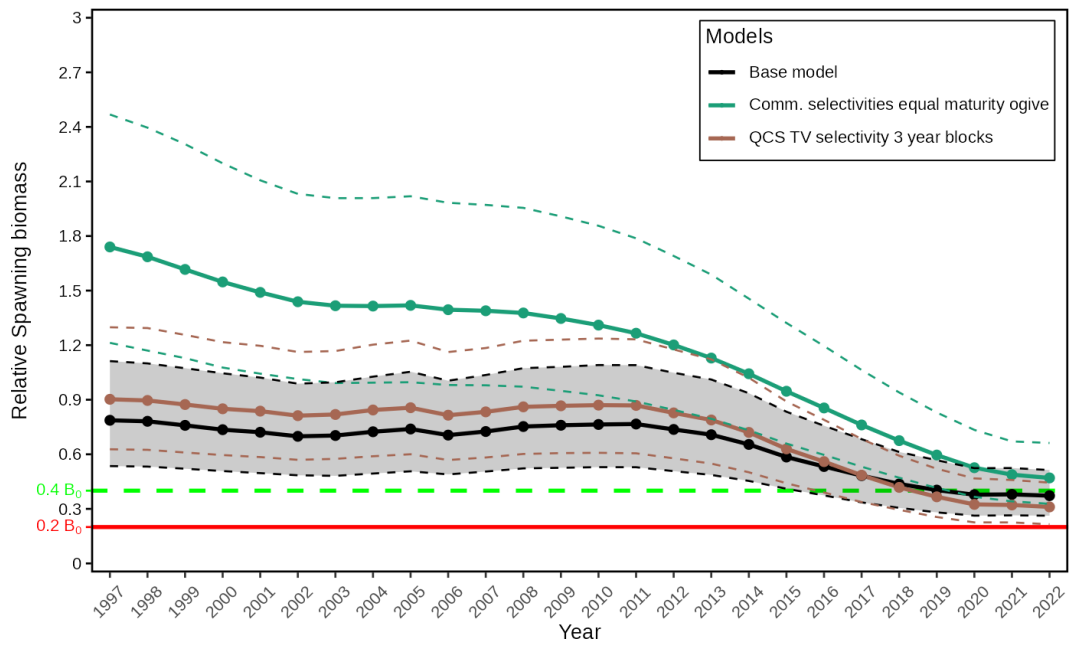


Figure 52. Relative spawning biomass for the sensitivities to changes in the selectivity (\hat{a}_k and γ_k) parameters. See Figure 51.

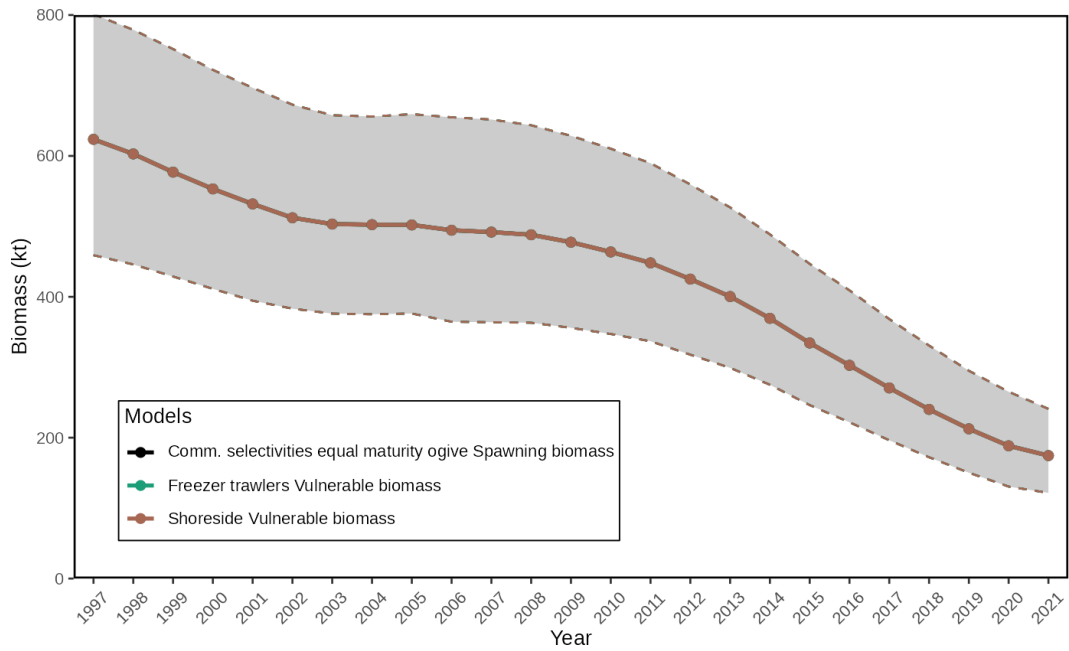


Figure 53. Spawning biomass and vulnerable biomass for the sensitivity model for which the selectivity has been set equal to the maturity for the two commercial trawl fleets. The spawning biomass is in black and has its 95% CI shaded. The two vulnerable biomass trajectories have their 95% CI contained within the dotted lines of their respective colours. The three trajectories are identical because the selectivity is set to match the maturity so that 100% of the biomass is available to the fisheries. This plot is presented as a check to ensure the model is specified correctly.

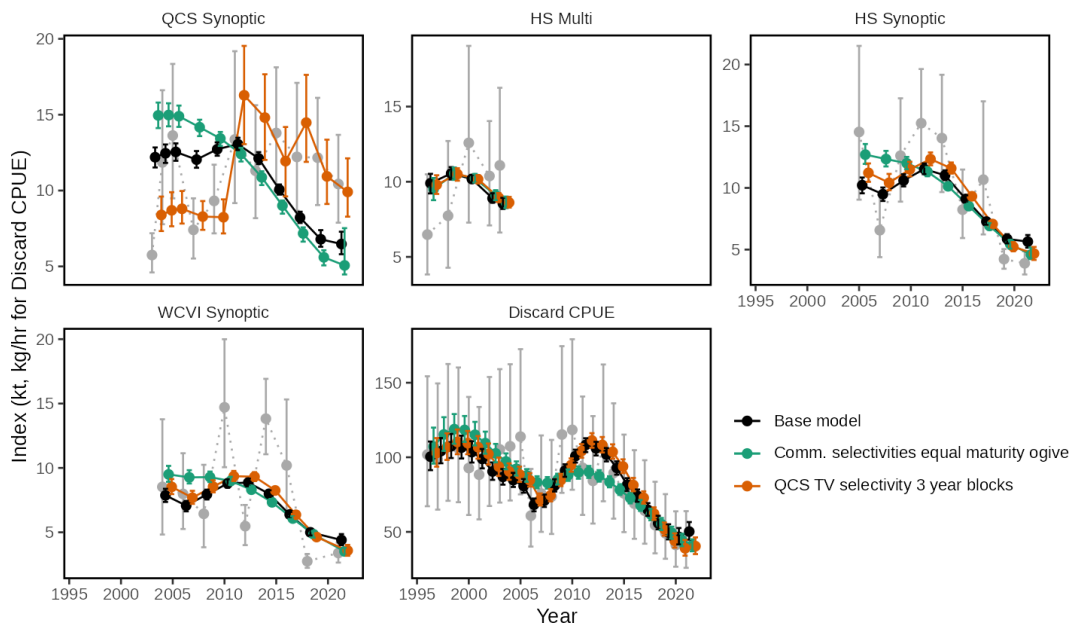


Figure 54. Index fits for the sensitivity where the Queen Charlotte Sound Synoptic Survey has time-varying selectivity.

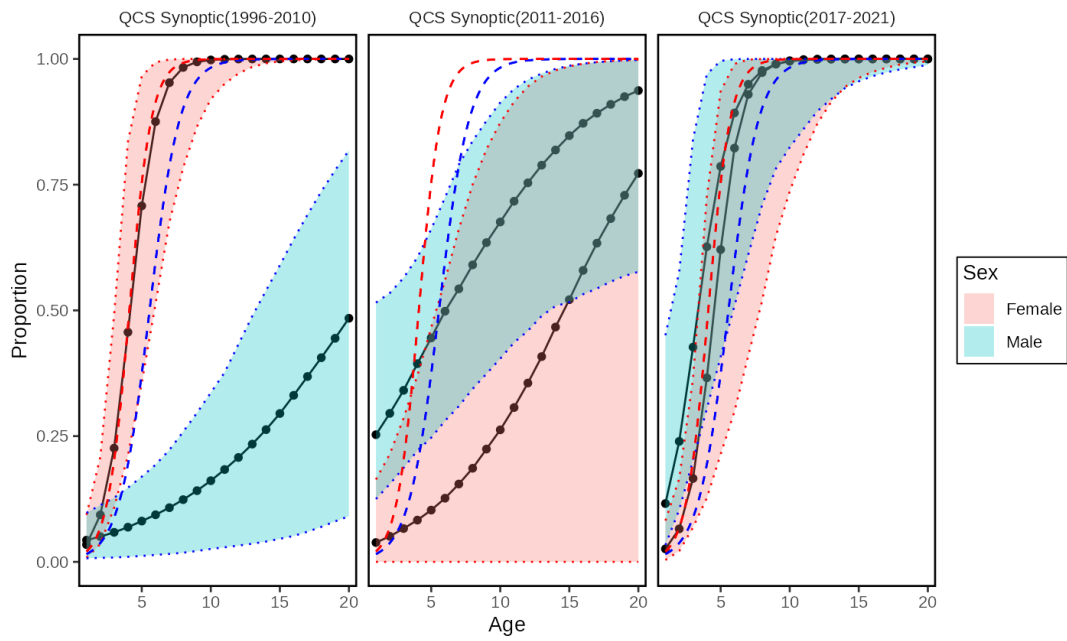


Figure 55. Time-varying selectivity for the Queen Charlotte Sound Synoptic Survey, where the panels are blocks of years: 2003–2010 (left), 2011–2016 (middle), and 2017–2021 (right). The dots are median selectivity-at-age estimates; the shaded areas are the 95% CI for those estimates. Dashed lines are maturity curves, where the colours represent sex as shown in the legend.

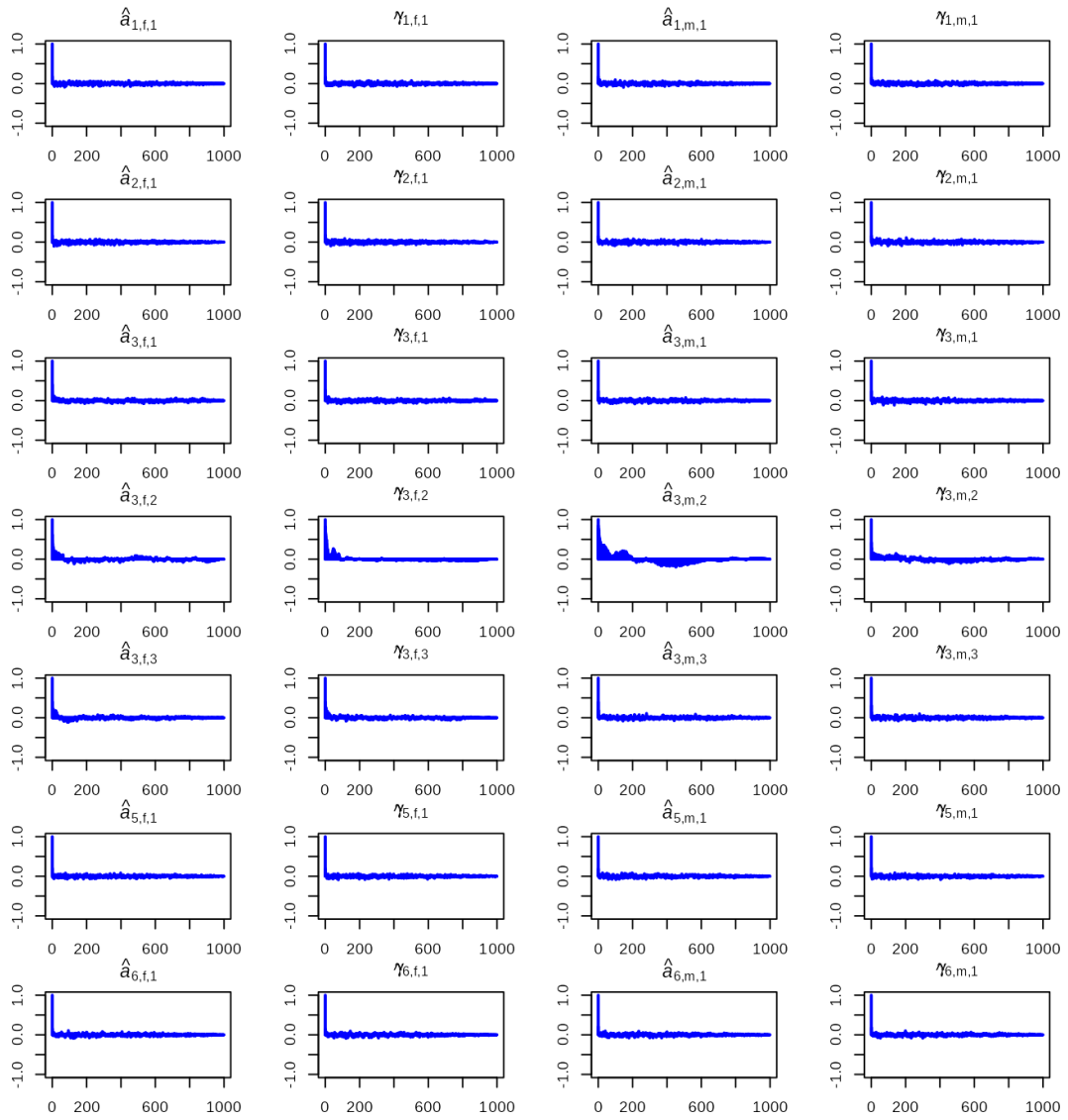


Figure 56. Autocorrelation for estimated selectivity parameters for the sensitivity model which has time-varying selectivity for the Queen Charlotte Sound Synoptic Survey. See Figure 39 for descriptions of the parameter subscripts.

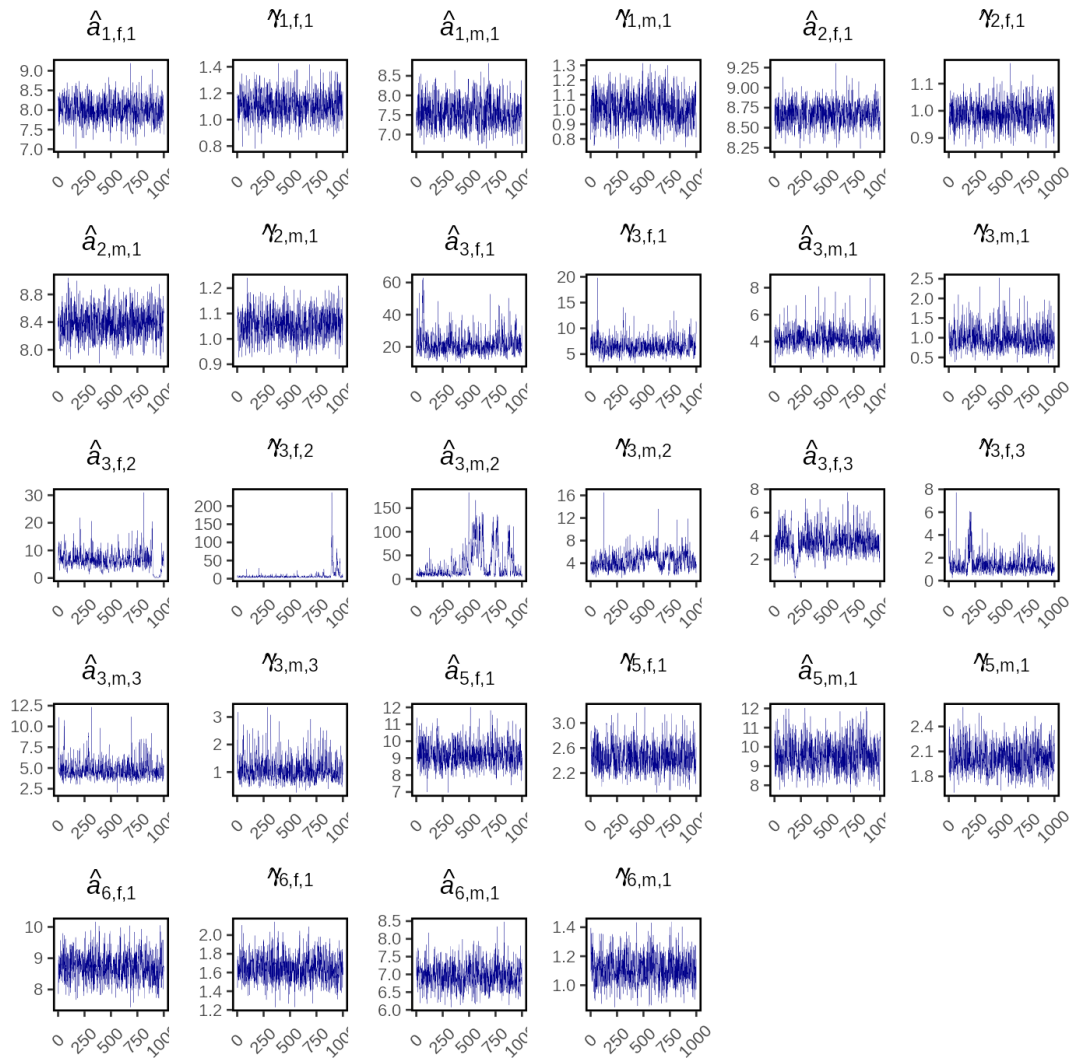


Figure 57. Trace plots for selectivity parameters for the sensitivity model which has time-varying selectivity for the Queen Charlotte Sound Synoptic Survey. See Figure 40 for parameter and subscript descriptions.

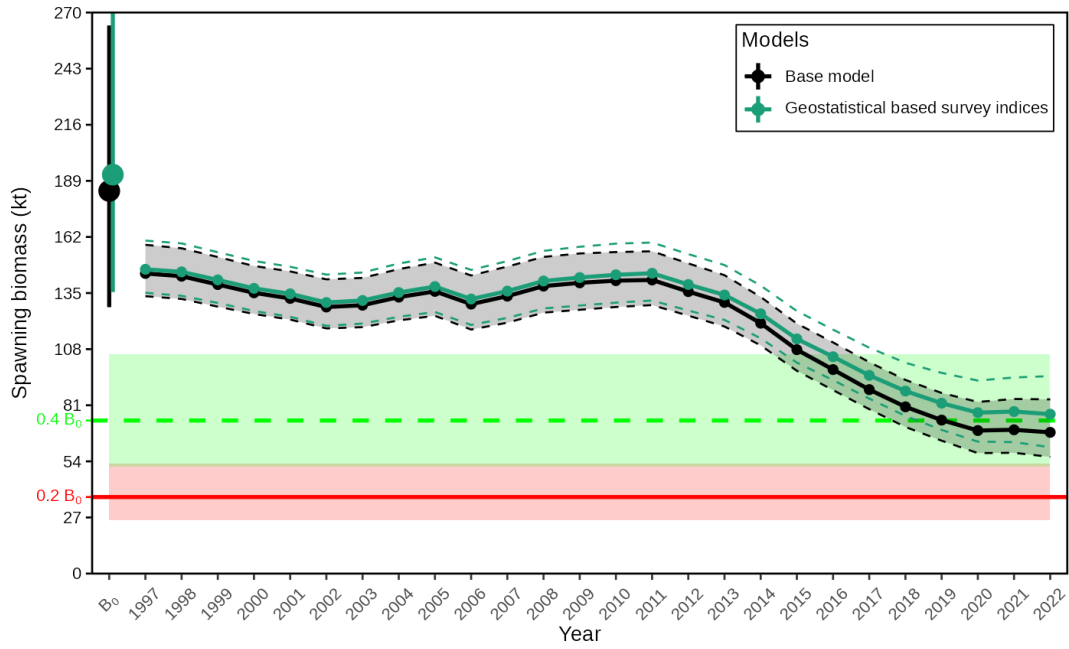


Figure 58. Spawning biomass for the sensitivity in which the design-based survey index data has been replaced with geostatistical-based survey indices. See Appendix D.

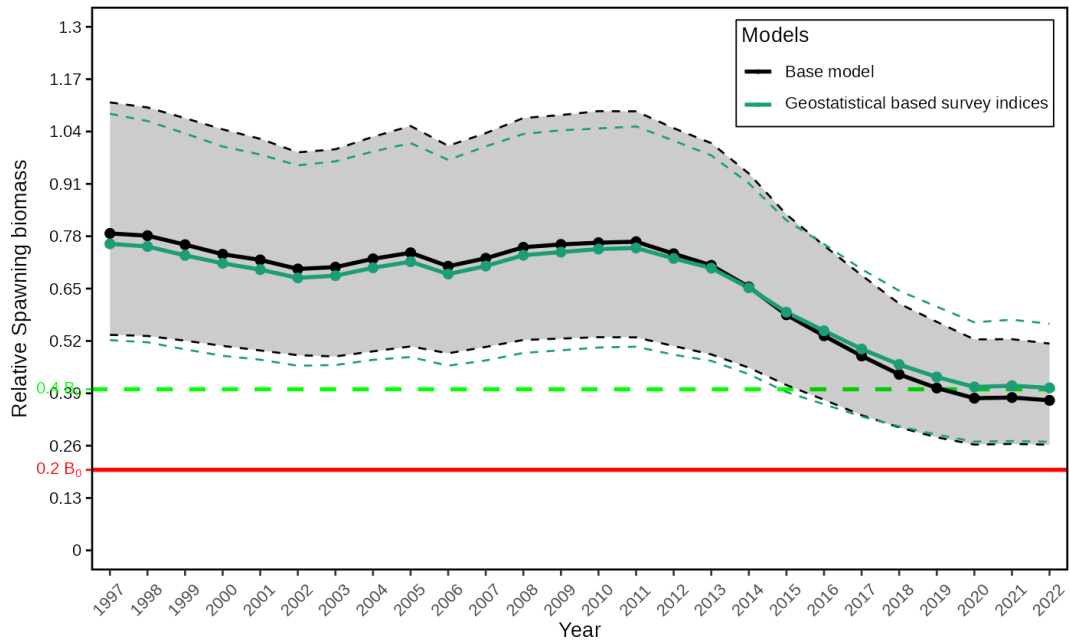


Figure 59. Relative spawning biomass for the sensitivity in which the design-based survey index data has been replaced with geostatistical-based survey indices. See Appendix D.

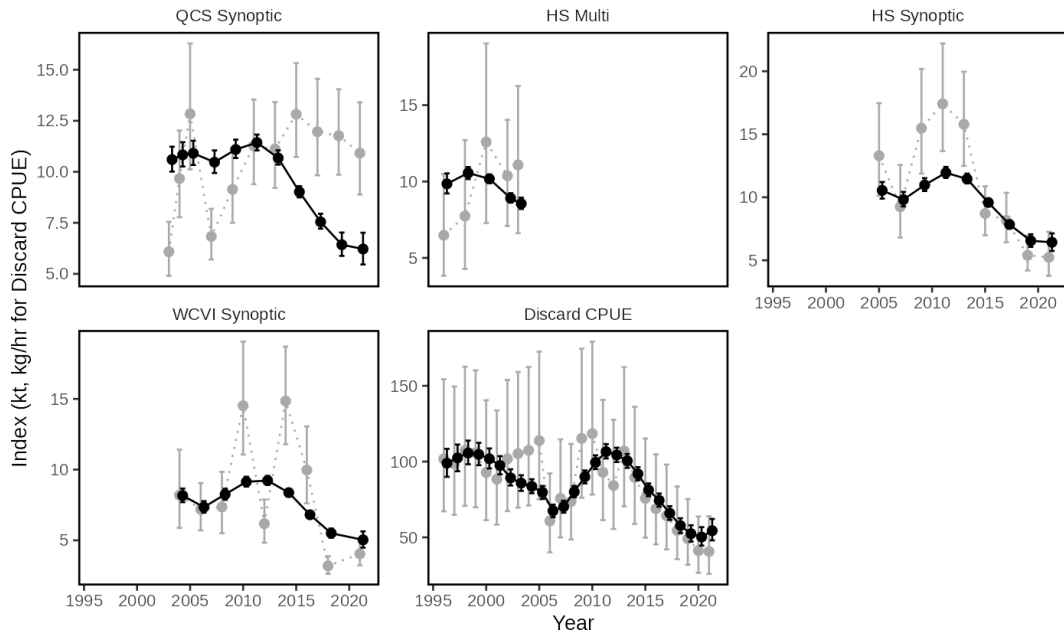


Figure 60. Index fits for the sensitivity in which the design-based survey index data has been replaced with geostatistical-based survey indices. See Appendix D.

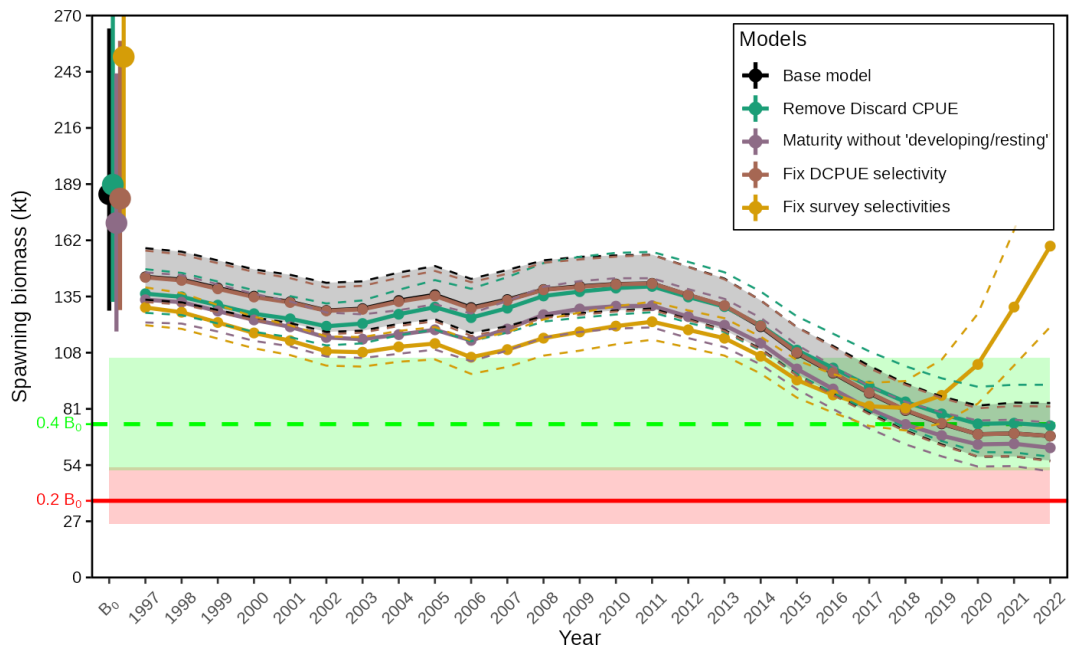


Figure 61. Spawning biomass for the sensitivities involving removing the DCPUE index, fixing selectivities and maturities, and modifying the maturity ogive. These sensitivities were added during the formal review meeting in October 2022.

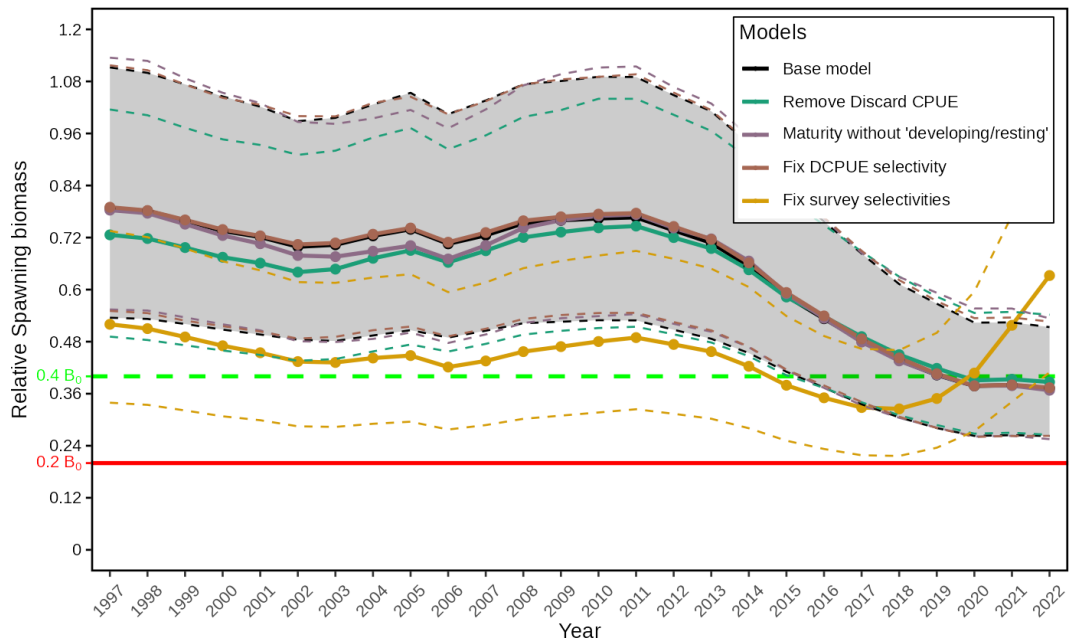


Figure 62. Relative spawning biomass for the sensitivities involving removing the DCPUE index, fixing selectivities and maturities, and modifying the maturity ogive. These sensitivities were added during the formal review meeting in October 2022.

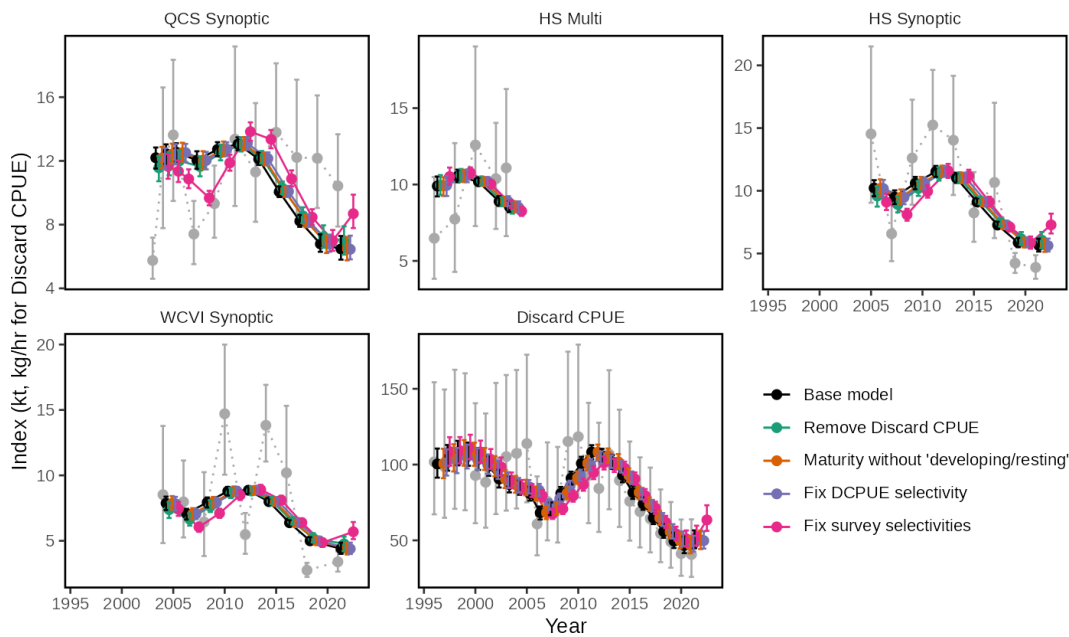


Figure 63. Index fits for the sensitivities involving removing the DCPUE index, fixing selectivities and maturities, and modifying the maturity ogive.

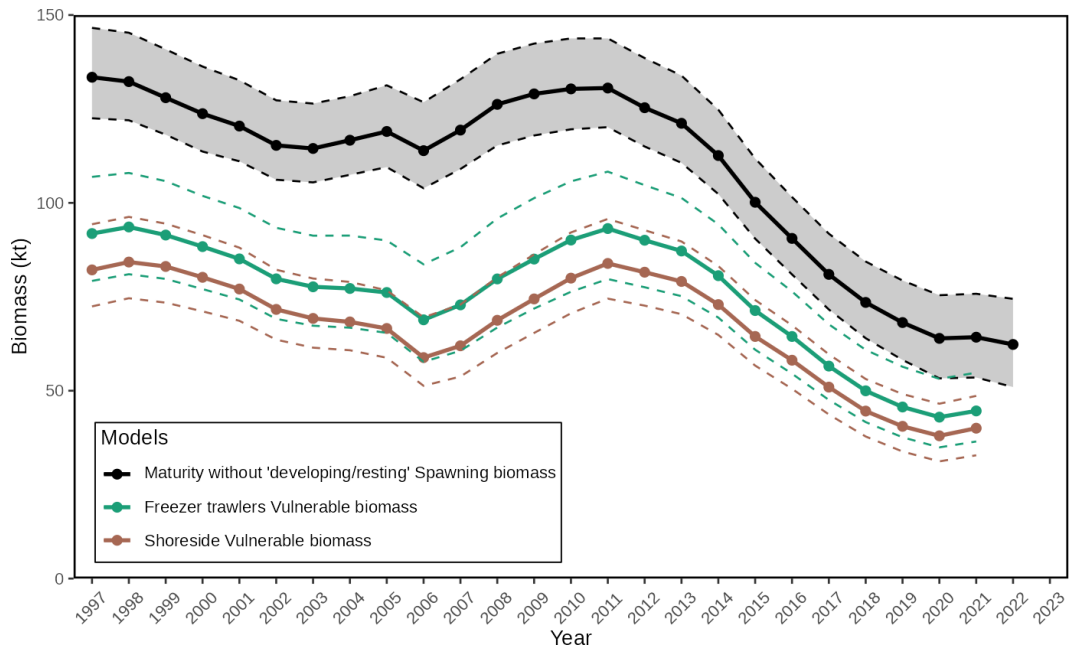


Figure 64. Spawning biomass and vulnerable biomass for the sensitivities involving removing resting and developing stages of maturity, by modifying the maturity ogive.

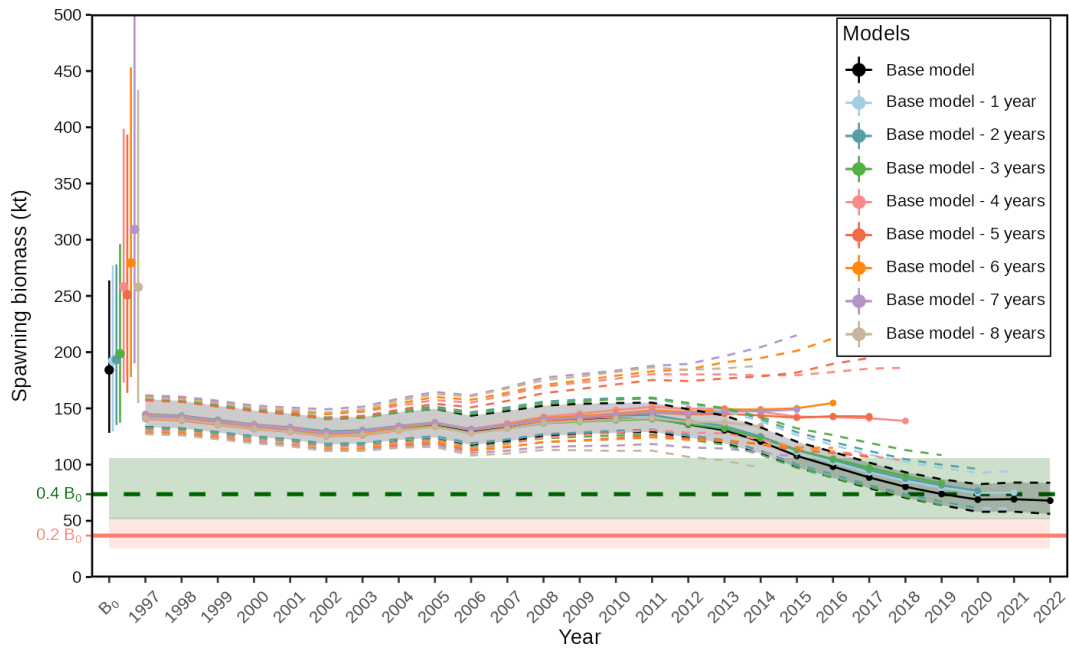


Figure 65. Spawning biomass for retrospective models comparing the base model with models with successively removed years of data. All models have the same parameterization, and were run as MCMCs in exactly the same way as the base model.

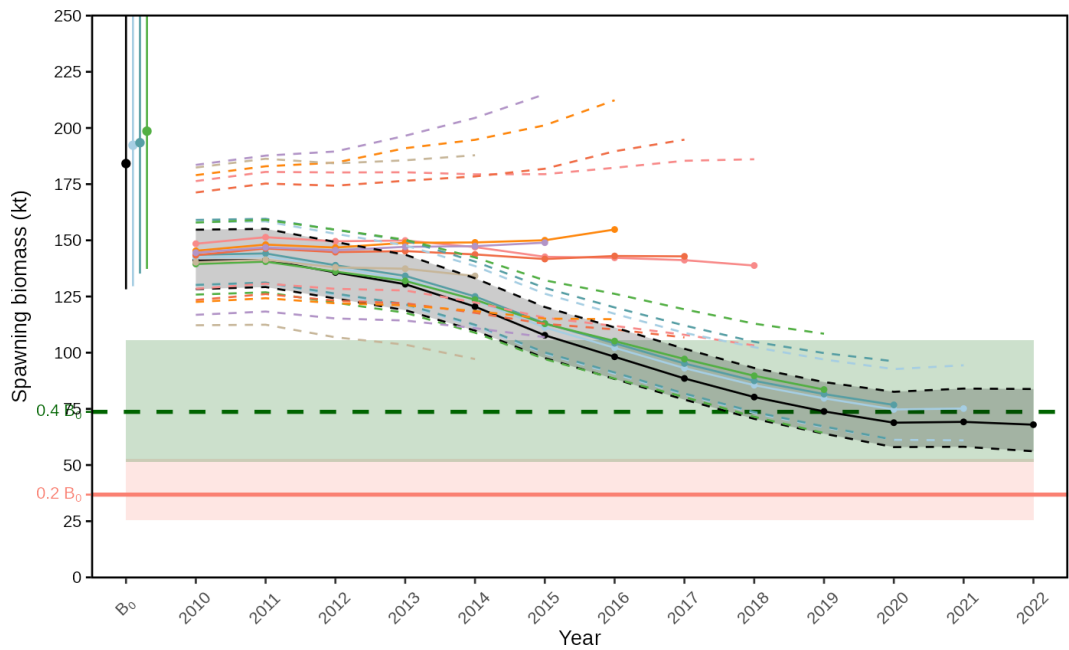


Figure 66. A closer view of Figure 65.

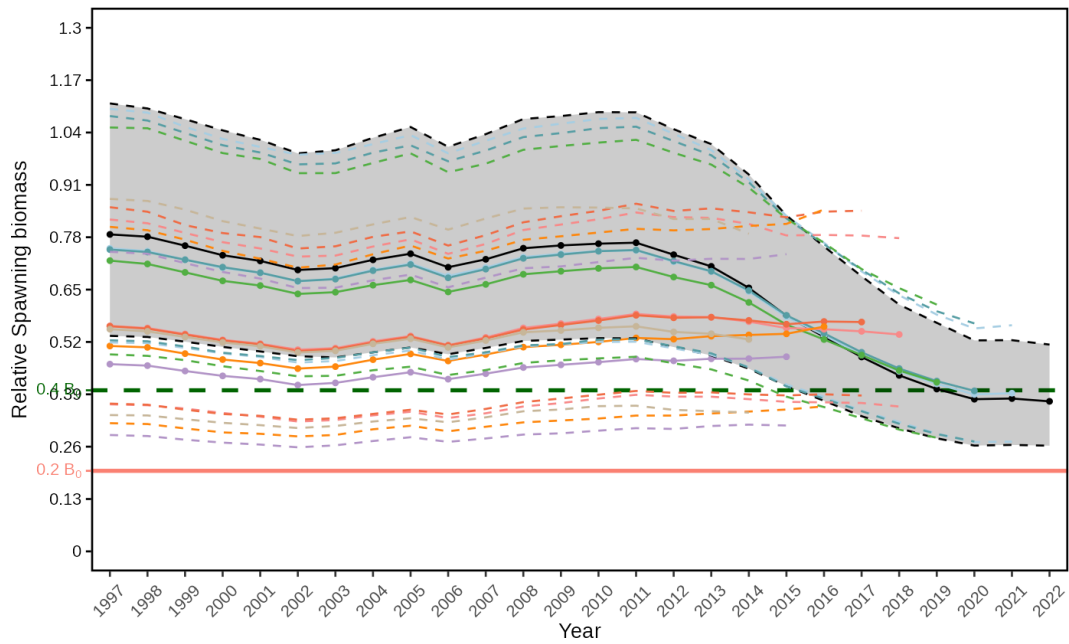


Figure 67. Relative spawning biomass for retrospective models. See Figure 65 for legend.

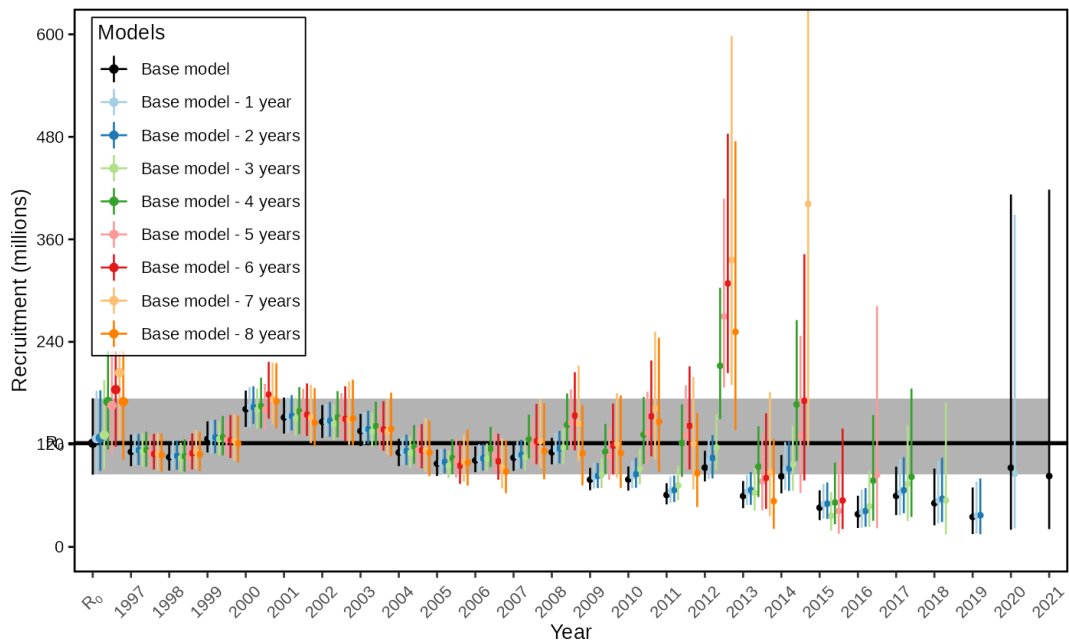


Figure 68. Recruitment of Arrowtooth Flounder for the retrospective models. The points are the medians of the posteriors, the vertical lines are the 95% Credible intervals for the posteriors, the points at R_0 are the median estimates for the initial recruitment parameters R_0 , and the vertical lines over those points is the 95% Credible interval for R_0 . The shaded ribbon is the R_0 credible interval across the whole time series for the base model. The models are slightly offset from each other for ease of viewing.

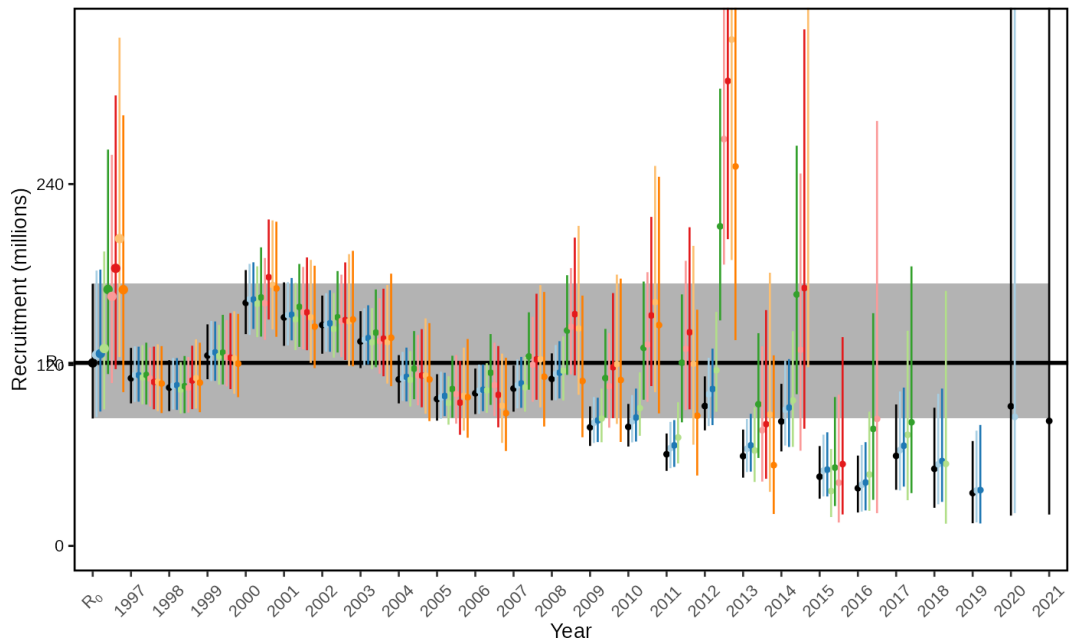


Figure 69. Recruitment of Arrowtooth Flounder for the retrospective models. The points are the medians of the posteriors, the vertical lines are the 95% CIs for the posteriors, the points at R_0 are the median estimates for the initial recruitment parameters R_0 , and the vertical lines over those points is the 95% CI for R_0 . The shaded ribbon is the R_0 CI across the whole time series for the base model. The models are slightly offset from each other for ease of viewing.

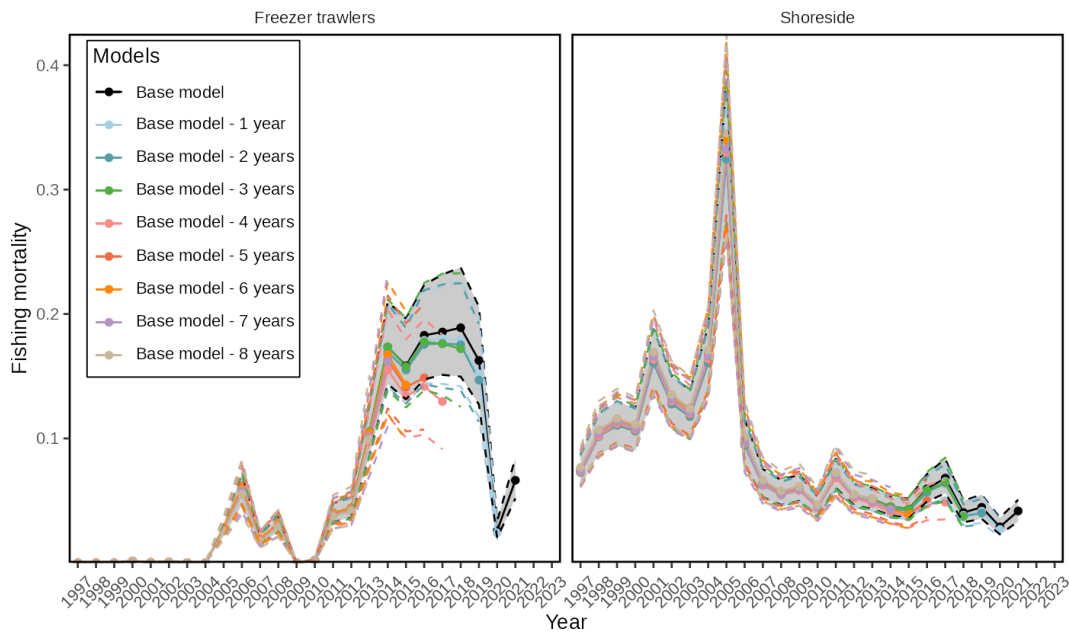


Figure 70. Fishing mortality for the base and retrospective models for the two trawl fisheries. The shaded area represents the 95% CI for the base model, the dotted lines represent the 95% CI for the retrospective models.

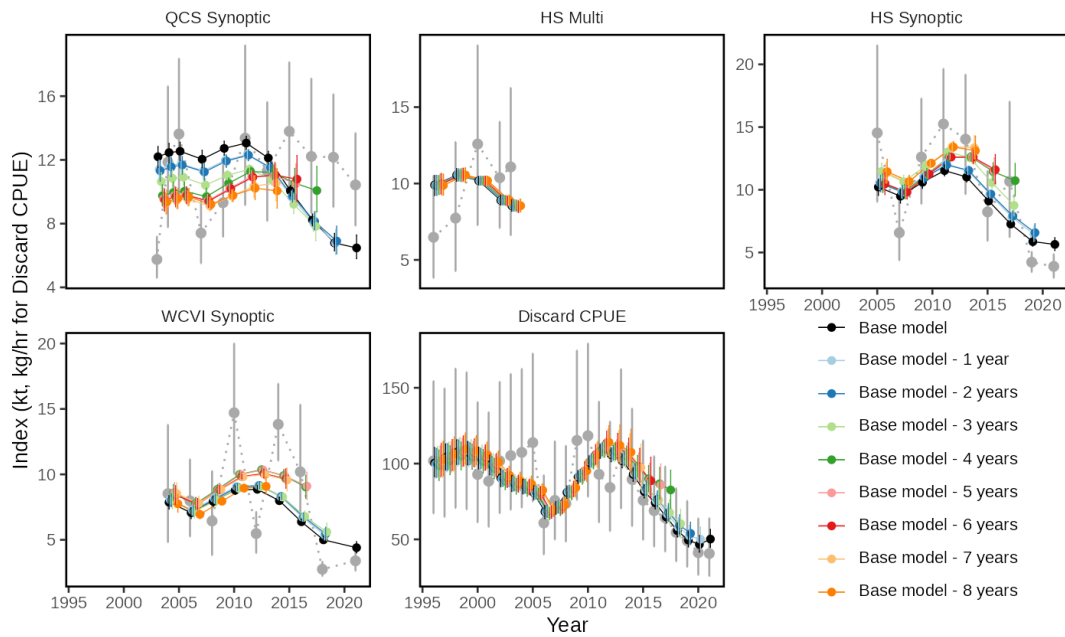


Figure 71. Index fits for the base and retrospective models. The light grey points and vertical lines show the index values and 95% CIs. The other coloured points show the medians of the posteriors; the solid vertical lines show the 95% CIs for the posteriors. The lines connecting points along the time series are only present for aesthetic value.

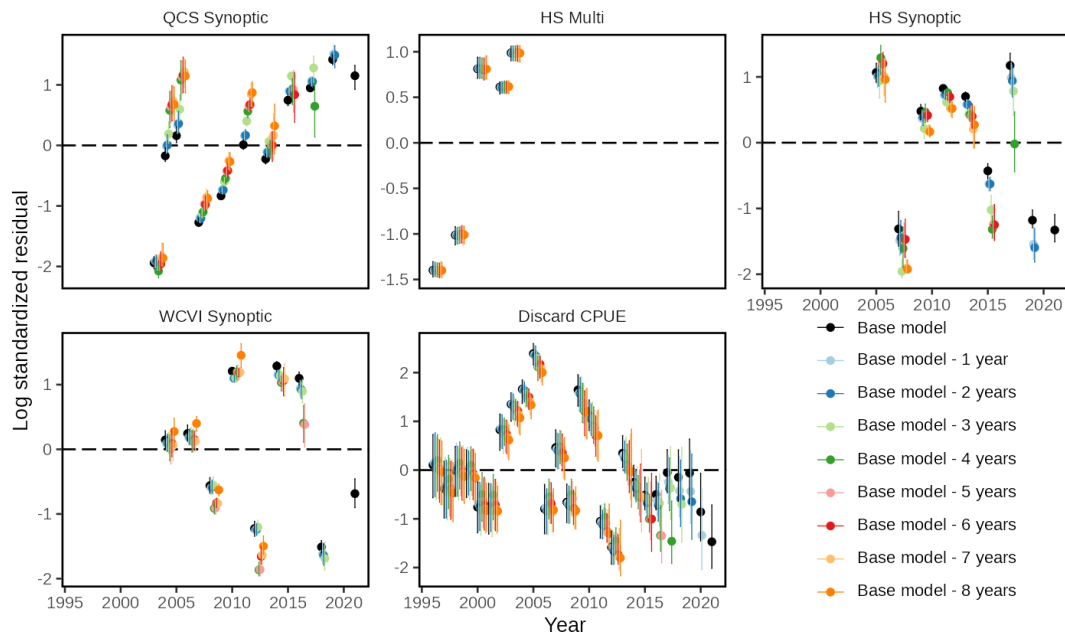


Figure 72. Log standardized residuals for the base and retrospective model index fits. See Figure 71 for description.

5.4. PROJECTION FIGURES FOR THE BASE MODEL

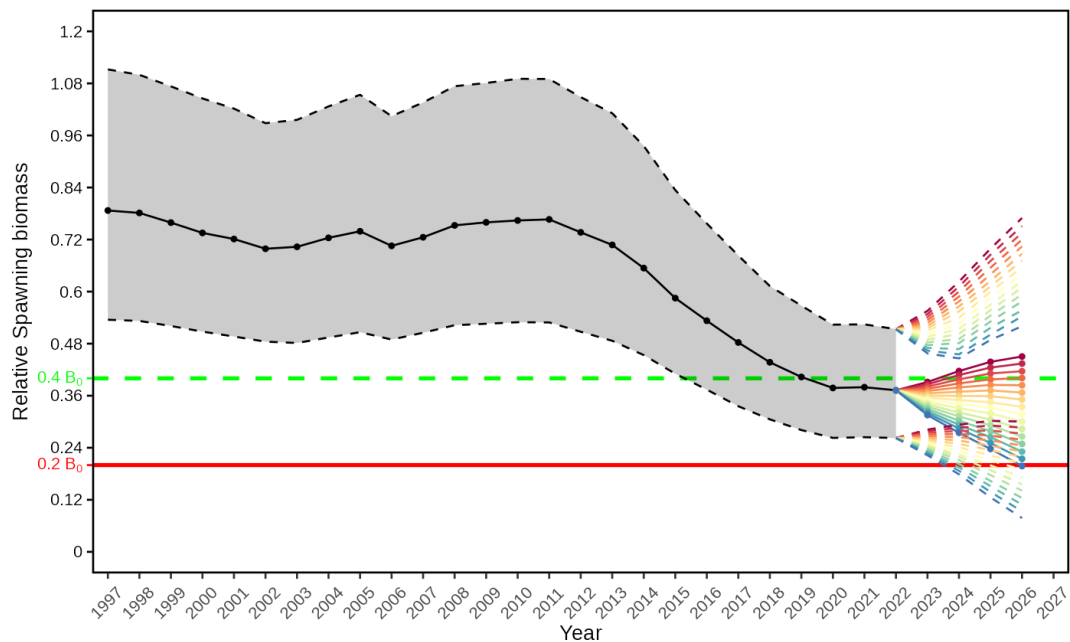


Figure 73. Estimated relative spawning biomass (B_t/B_0) for the base model. The shaded area represents the 95% credible interval (CI) and the solid line with points represents the median. Horizontal lines indicate the $0.2B_0$ (solid red) and $0.4B_0$ (dashed green) reference points. The colored dots from 2023 to 2026 are the medians of the posteriors for the projected catch levels, with solid lines connecting them; the dashed lines from 2023 to 2026 represent the 95% CIs for those posteriors. The constant catch values are shown as text on the right of the end points of each projected trajectory. See the decision table (Table 15) for probabilities of being under reference points and of the stock declining for each catch level.

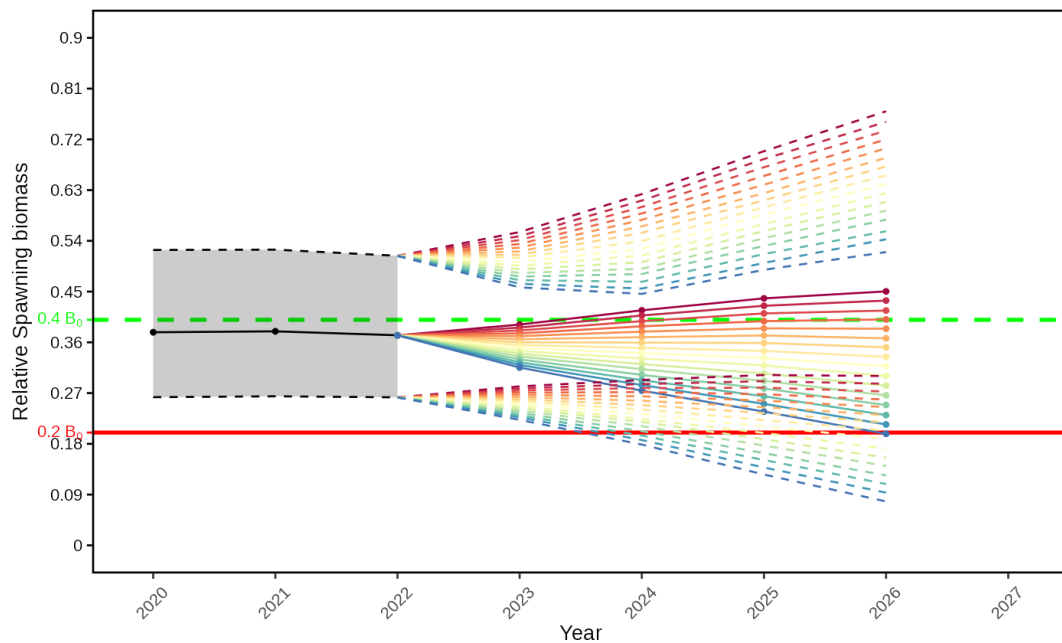


Figure 74. Closeup view of relative spawning biomass for the Arrowtooth Flounder base model with B_0 -based reference points and projections into the future. The constant catch values are shown as text on the right of the end points of each projected trajectory. See the decision table (Table 15) for probabilities of being under reference points and of the stock declining for each catch stream.

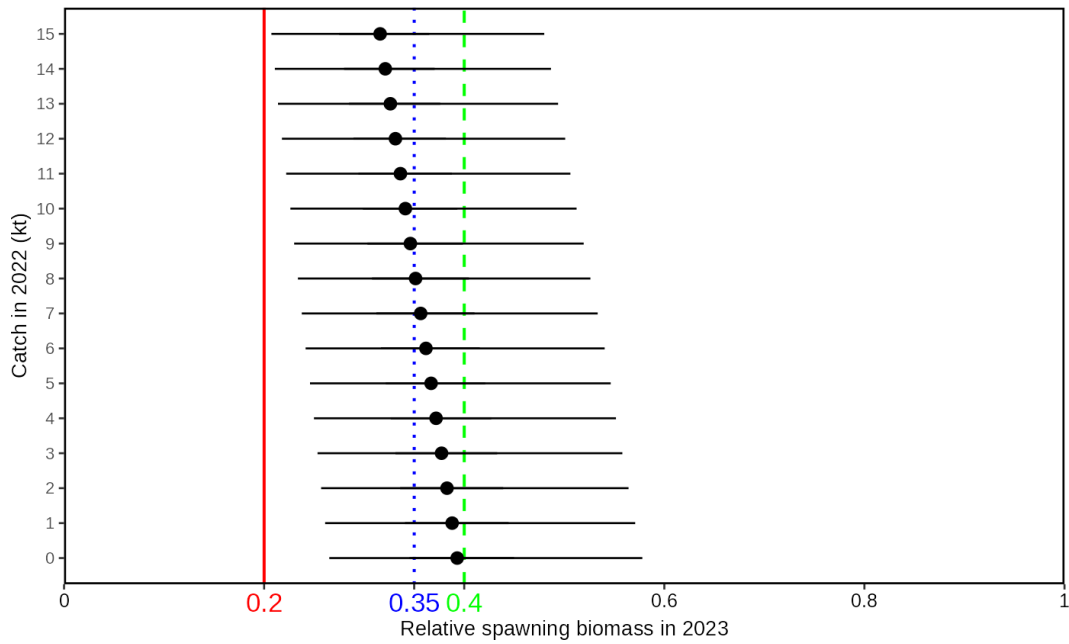


Figure 75. Projected 2023 relative spawning biomass for catch occurring in 2022. Black points are medians of the posterior, thick lines are the 50% CI (25%–75%), and thin lines are the 95% CI (2.5%–97.5%). The solid red line is the LRP, $0.2B_0$, the dotted blue line is the $0.35B_0$ line, and the dashed green line is the USR, $0.4B_0$.

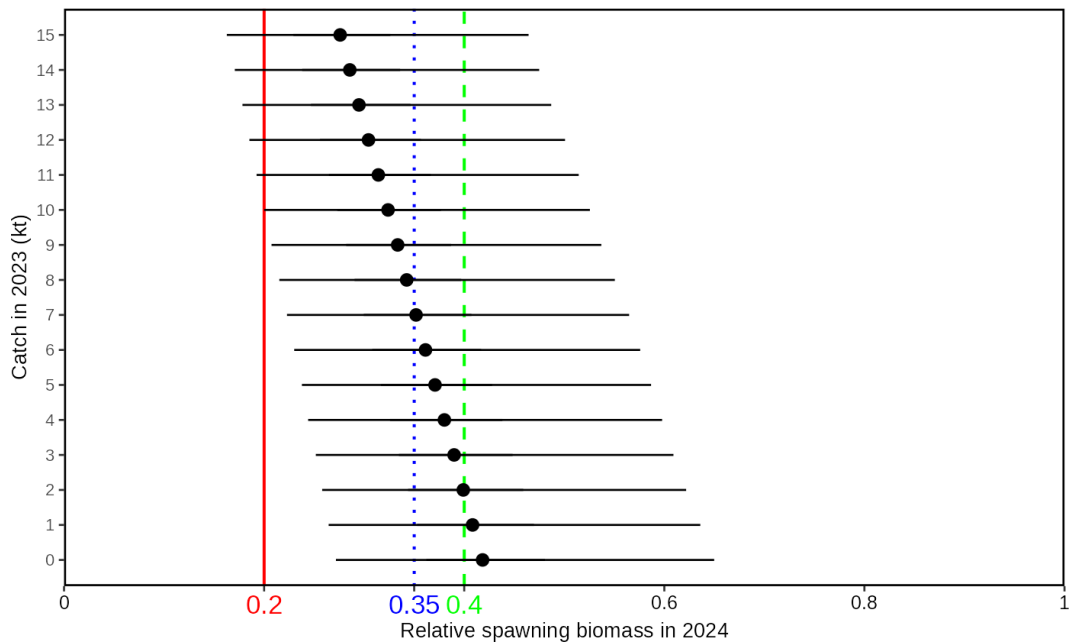


Figure 76. Projected 2024 relative spawning biomass for catch occurring in 2023. Black points are medians of the posterior, thick lines are the 50% CI (25%–75%), and thin lines are the 95% CI (2.5%–97.5%). The solid red line is the LRP, $0.2B_0$, the dotted blue line is the $0.35B_0$ line, and the dashed green line is the USR, $0.4B_0$.

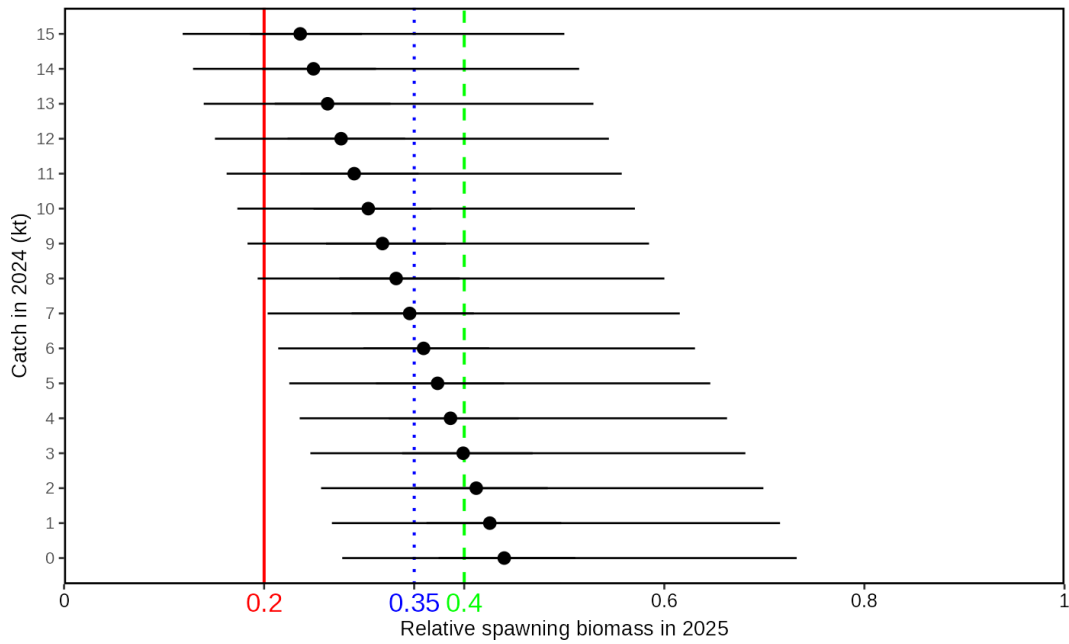


Figure 77. Projected 2025 relative spawning biomass for catch occurring in 2024. Black points are medians of the posterior, thick lines are the 50% CI (25%–75%), and thin lines are the 95% CI (2.5%–97.5%). The solid red line is the LRP, $0.2B_0$, the dotted blue line is the $0.35B_0$ line, and the dashed green line is the USR, $0.4B_0$.

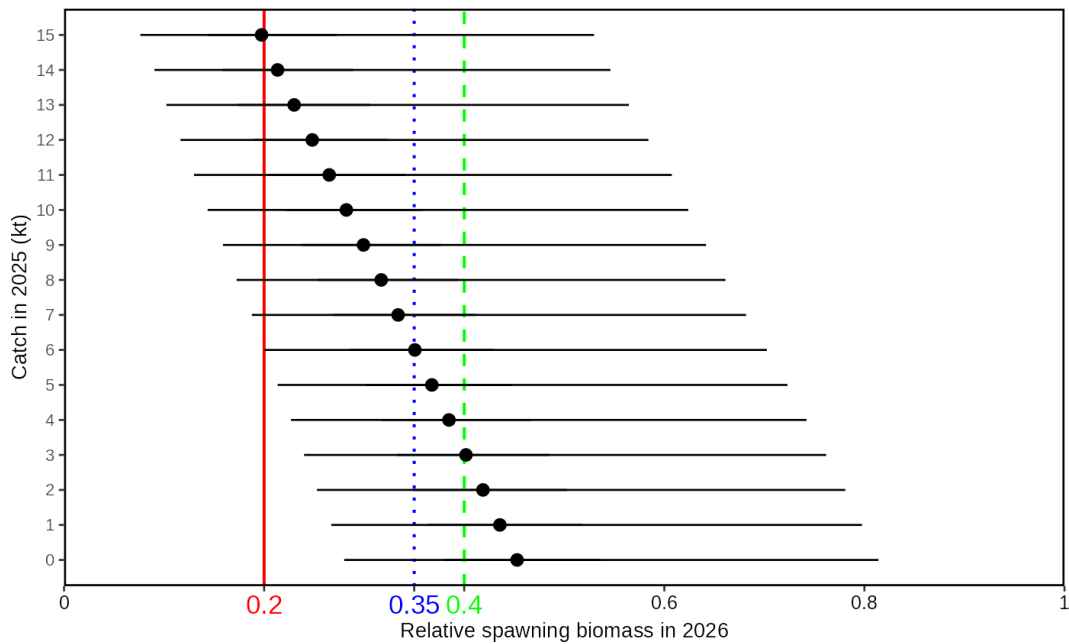


Figure 78. Projected 2026 relative spawning biomass for catch occurring in 2025. Black points are medians of the posterior, thick lines are the 50% CI (25%–75%), and thin lines are the 95% CI (2.5%–97.5%). The solid red line is the LRP, $0.2B_0$, the dotted blue line is the $0.35B_0$ line, and the dashed green line is the USR, $0.4B_0$.

6. TABLES

Table 1. Recent coastwide commercial fishery landings and discards (t) for Arrowtooth Flounder.

Year	Landings	Discarded
1996	4,711.5	3,459.6
1997	2,795.8	2,442.5
1998	4,145.9	3,272.3
1999	3,927.9	4,019.9
2000	4,061.6	3,429.4
2001	8,289.3	2,340.4
2002	5,031.4	2,957.6
2003	4,067.4	3,046.0
2004	6,239.3	3,204.2
2005	16,237.4	2,576.4
2006	6,901.3	1,300.0
2007	2,819.1	1,747.9
2008	3,876.1	1,562.6
2009	1,259.2	2,619.0
2010	646.1	2,714.9
2011	5,872.6	2,407.3
2012	4,869.7	2,370.0
2013	8,913.1	2,257.8
2014	12,641.3	1,658.7
2015	10,050.2	1,762.6
2016	11,184.9	1,312.9
2017	10,430.2	973.5
2018	8,575.8	687.8
2019	7,027.6	615.1
2020	1,692.8	247.1
2021	2,459.6	276.0

Table 2. Recent coastwide commercial fishery landings and discards (t) of Arrowtooth Flounder by fleet.

Year	Freezer Trawlers			Shoreside			Total Catch
	Landings	Discards	Total	Landings	Discards	Total	
1996	0.0	0.7	0.7	4,711.5	3,459.0	8,170.4	8,171.1
1997	0.0	0.0	0.0	2,795.8	2,442.5	5,238.3	5,238.3
1998	0.0	0.0	0.0	4,145.9	3,272.3	7,418.2	7,418.2
1999	0.0	0.0	0.0	3,927.9	4,019.9	7,947.8	7,947.8
2000	6.8	106.3	113.1	4,054.9	3,323.1	7,377.9	7,491.1
2001	12.5	18.9	31.4	8,276.9	2,321.5	10,598.4	10,629.8
2002	28.0	22.4	50.4	5,003.5	2,935.2	7,938.7	7,989.0
2003	6.7	9.4	16.1	4,060.7	3,036.5	7,097.2	7,113.4
2004	0.4	0.0	0.4	6,238.9	3,204.2	9,443.1	9,443.5
2005	1,257.8	340.8	1,598.6	14,979.5	2,235.5	17,215.1	18,813.7

Year	Landings	Discards	Total	Landings	Discards	Total	Total Catch
2006	3,302.5	113.5	3,416.0	3,598.8	1,186.5	4,785.3	8,201.3
2007	1,123.4	41.8	1,165.3	1,695.7	1,706.1	3,401.8	4,567.0
2008	1,956.0	189.8	2,145.8	1,920.1	1,372.8	3,292.9	5,438.7
2009	0.0	2.1	2.1	1,259.2	2,616.8	3,876.1	3,878.2
2010	140.5	34.5	175.0	505.6	2,680.4	3,186.0	3,361.0
2011	2,841.8	335.3	3,177.1	3,030.8	2,072.1	5,102.8	8,279.9
2012	3,085.2	326.6	3,411.8	1,784.6	2,043.4	3,827.9	7,239.7
2013	7,375.2	392.6	7,767.8	1,537.9	1,865.2	3,403.1	11,170.8
2014	11,231.9	355.9	11,587.8	1,409.4	1,302.9	2,712.3	14,300.1
2015	8,855.3	637.3	9,492.6	1,194.9	1,125.3	2,320.3	11,812.8
2016	9,367.2	305.2	9,672.4	1,817.7	1,007.8	2,825.5	12,497.9
2017	8,286.9	292.9	8,579.8	2,143.3	680.6	2,823.8	11,403.6
2018	7,527.5	257.3	7,784.8	1,048.3	430.5	1,478.9	9,263.6
2019	5,836.1	312.4	6,148.5	1,191.5	302.7	1,494.2	7,642.7
2020	947.3	26.4	973.7	745.5	220.7	966.2	1,939.9
2021	1,376.7	28.2	1,404.8	1,082.9	247.8	1,330.7	2,735.5

Table 3. Recent commercial fishery landings and discards (t) for Arrowtooth Flounder by area.

Year	Area			
	3CD		5ABCDE	
	Landings	Discarded	Landings	Discarded
1996	3,068.0	892.0	1,643.5	2,567.7
1997	1,453.9	537.3	1,341.9	1,905.1
1998	2,486.2	680.4	1,659.7	2,591.9
1999	1,474.8	864.9	2,453.1	3,155.1
2000	1,789.7	588.8	2,272.0	2,840.6
2001	4,943.0	586.9	3,346.4	1,753.5
2002	2,457.1	672.1	2,574.4	2,285.5
2003	1,974.1	670.5	2,093.3	2,375.5
2004	3,356.1	669.0	2,883.2	2,535.2
2005	6,317.7	531.5	9,919.6	2,044.8
2006	2,645.2	278.2	4,256.1	1,021.8
2007	605.6	459.4	2,213.5	1,288.5
2008	3,075.6	669.0	800.5	893.6
2009	722.8	719.3	536.4	1,899.6
2010	208.1	786.4	438.0	1,928.5
2011	3,284.9	960.3	2,587.7	1,447.0
2012	4,253.2	807.5	616.5	1,562.5
2013	7,067.7	822.8	1,845.4	1,435.0
2014	8,188.0	675.8	4,453.4	982.9
2015	5,234.8	902.6	4,815.4	860.1
2016	6,556.2	626.6	4,628.8	686.4
2017	4,289.4	372.9	6,140.7	600.6
2018	1,619.1	190.0	6,956.8	497.8

Year	Landings	Discarded	Landings	Discarded
2019	1,270.7	109.7	5,756.8	505.4
2020	954.0	77.0	738.7	170.1
2021	790.0	45.4	1,669.6	230.5

Table 4. Indices of abundance and CVs for the base model.

Year	QCS Synoptic		HS Multi		HS Synoptic		WCVI Synoptic		Discard CPUE	
	Index	CV	Index	CV	Index	CV	Index	CV	Index	CV
1996	–	–	6.48	0.26	–	–	–	–	101.81	0.21
1997	–	–	–	–	–	–	–	–	98.50	0.22
1998	–	–	7.73	0.28	–	–	–	–	107.29	0.21
1999	–	–	–	–	–	–	–	–	105.80	0.21
2000	–	–	12.58	0.23	–	–	–	–	92.80	0.21
2001	–	–	–	–	–	–	–	–	88.36	0.21
2002	–	–	10.38	0.17	–	–	–	–	101.78	0.21
2003	5.75	0.11	11.09	0.23	–	–	–	–	105.26	0.21
2004	11.86	0.19	–	–	–	–	8.53	0.26	107.39	0.21
2005	13.63	0.17	–	–	14.53	0.23	–	–	113.84	0.21
2006	–	–	–	–	–	–	7.98	0.19	60.83	0.21
2007	7.41	0.14	–	–	6.57	0.19	–	–	75.70	0.21
2008	–	–	–	–	–	–	6.44	0.28	73.64	0.21
2009	9.32	0.13	–	–	12.61	0.17	–	–	115.27	0.21
2010	–	–	–	–	–	–	14.71	0.17	118.39	0.21
2011	13.37	0.19	–	–	15.24	0.14	–	–	92.93	0.21
2012	–	–	–	–	–	–	5.48	0.14	84.20	0.21
2013	11.3	0.17	–	–	14.03	0.17	–	–	106.95	0.22
2014	–	–	–	–	–	–	13.82	0.11	89.52	0.22
2015	13.79	0.15	–	–	8.23	0.18	–	–	75.76	0.22
2016	–	–	–	–	–	–	10.2	0.23	68.91	0.22
2017	12.22	0.19	–	–	10.67	0.26	–	–	64.21	0.22
2018	–	–	–	–	–	–	2.75	0.1	54.55	0.22
2019	12.17	0.15	–	–	4.23	0.1	–	–	49.05	0.22
2020	–	–	–	–	–	–	–	–	41.21	0.23
2021	10.43	0.14	–	–	3.89	0.12	3.39	0.12	40.66	0.23

Table 5. Parameters and prior probability distributions used in the base model.

Parameter	Number estimated	Bounds [low, high]	Prior (mean, SD) (single value = fixed)
Log recruitment [$\ln(R_0)$]	1	[-2, 6]	Uniform
Steepness [h]	1	[0.2, 1]	Beta($\alpha = 13.4, \beta = 2.4$)
Log natural mortality (female) [$\ln(M_{\text{female}})$]	0	Fixed	-1.609
Log natural mortality (male) [$\ln(M_{\text{male}})$]	0	Fixed	-1.050
Log mean recruitment [$\ln(\bar{R})$]	1	[-2, 6]	Uniform
Log initial recruitment [$\ln(\bar{R}_{\text{init}})$]	1	[-5, 6]	Uniform

Parameter	Number estimated	Bounds [low, high]	Prior (mean, SD) (single value = fixed)
Variance ratio, observation error [ρ]	0	Fixed	0.059
Total variance [ϑ^2]	0	Fixed	1.471
Fishery age at 50% logistic selectivity (\hat{a}_k)	2	[0, 1]	Uniform
Fishery SD of logistic selectivity ($\hat{\gamma}_k$)	2	[0, 1]	Uniform
Survey age at 50% logistic selectivity (\hat{a}_k)	3	[0, 1]	Uniform
Survey SD of logistic selectivity ($\hat{\gamma}_k$)	3	[0, 1]	Uniform
Survey catchability (q_k)	5	[0, 1]	Normal(0.5, 1)
Log fishing mortality values ($\Gamma_{k,t}$)	52	[-30, 3]	[-30, 3]
Log recruitment deviations (ω_t)	26	None	Normal(0, τ)
Initial log recruitment deviations ($\omega_{\text{init},t}$)	19	None	Normal(0, τ)

Table 6. Posterior median and 95% credible interval estimates of key parameters for the base model.

Parameter	Gear	Sex	2.5%	50%	97.5%
R_0	–	–	84.52	121.40	173.89
h	–	–	0.66	0.89	0.98
M_1	–	female	0.20	0.20	0.20
M_2	–	male	0.35	0.35	0.35
\bar{R}	–	–	74.75	86.14	98.03
\bar{R}_{init}	–	–	55.75	67.23	79.11
SB_0	–	–	128.21	184.16	263.79
B_{MSY}	–	–	16.07	30.96	60.83
MSY_1	Freezer trawlers	–	3.78	5.55	8.08
F_{MSY_1}	Freezer trawlers	–	0.34	1.52	3.92
U_{MSY_1}	Freezer trawlers	–	0.29	0.78	0.98
MSY_2	Shoreside	–	6.80	9.98	14.55
F_{MSY_2}	Shoreside	–	0.86	4.77	15.35
U_{MSY_2}	Shoreside	–	0.58	0.99	1.00
q_1	QCS Synoptic	–	0.09	0.11	0.15
q_2	HS Multi	–	0.12	0.14	0.15
q_3	HS Synoptic	–	0.12	0.15	0.20
q_4	WCVI Synoptic	–	0.09	0.10	0.13
q_5	Discard CPUE	–	1.25	1.41	1.58
$\hat{a}_{1,f,1}$	Freezer trawlers	female	7.58	8.13	8.72
$\hat{\gamma}_{1,f,1}$	Freezer trawlers	female	0.92	1.08	1.26
$\hat{a}_{1,m,1}$	Freezer trawlers	male	7.13	7.73	8.45
$\hat{\gamma}_{1,m,1}$	Freezer trawlers	male	0.84	0.99	1.19
$\hat{a}_{2,f,1}$	Shoreside	female	8.41	8.67	8.95
$\hat{\gamma}_{2,f,1}$	Shoreside	female	0.90	0.98	1.08
$\hat{a}_{2,m,1}$	Shoreside	male	7.99	8.35	8.81
$\hat{\gamma}_{2,m,1}$	Shoreside	male	0.95	1.04	1.15
$\hat{a}_{3,f,1}$	QCS Synoptic	female	4.26	6.00	8.67
$\hat{\gamma}_{3,f,1}$	QCS Synoptic	female	1.86	2.65	3.98
$\hat{a}_{3,m,1}$	QCS Synoptic	male	4.64	6.15	8.88
$\hat{\gamma}_{3,m,1}$	QCS Synoptic	male	1.24	1.74	2.58
$\hat{a}_{4,f,1}$	HS Multi	female	9.00	9.00	9.00
$\hat{\gamma}_{4,f,1}$	HS Multi	female	0.50	0.50	0.50
$\hat{a}_{4,m,1}$	HS Multi	male	9.00	9.00	9.00

Parameter	Gear	Sex	2.5%	50%	97.5%
$\hat{\gamma}_{4,m,1}$	HS Multi	male	0.50	0.50	0.50
$\hat{a}_{5,f,1}$	HS Synoptic	female	8.19	9.34	10.76
$\hat{\gamma}_{5,f,1}$	HS Synoptic	female	2.05	2.38	2.81
$\hat{a}_{5,m,1}$	HS Synoptic	male	8.32	9.65	11.23
$\hat{\gamma}_{5,m,1}$	HS Synoptic	male	1.70	1.98	2.27
$\hat{a}_{6,f,1}$	WCVI Synoptic	female	8.03	8.78	9.64
$\hat{\gamma}_{6,f,1}$	WCVI Synoptic	female	1.38	1.61	1.90
$\hat{a}_{6,m,1}$	WCVI Synoptic	male	6.42	7.06	7.79
$\hat{\gamma}_{6,m,1}$	WCVI Synoptic	male	0.91	1.10	1.29
$\hat{a}_{7,f,1}$	Discard CPUE	female	9.00	9.00	9.00
$\hat{\gamma}_{7,f,1}$	Discard CPUE	female	0.50	0.50	0.50
$\hat{a}_{7,m,1}$	Discard CPUE	male	9.00	9.00	9.00
$\hat{\gamma}_{7,m,1}$	Discard CPUE	male	0.50	0.50	0.50

Table 7. Posterior median and 95% credible interval of proposed reference points for the base model. Biomass numbers are in thousands of tonnes. Subscript 1 signifies the Freezer trawler fleet, subscript 2 signifies the Shoreside fleet.

Reference point	Median	Credible interval
SB_0	184.16	128.21-263.79
$0.2B_0$	36.83	25.64-52.76
$0.4B_0$	73.66	51.28-105.51
SB_{2021}	69.20	58.13-84.03
SB_{2022}	67.95	56.14-83.83
F_{MSY_1}	1.52	0.34-3.92
F_{MSY_2}	4.77	0.86-15.35
B_{MSY}	30.96	16.07-60.83
$0.4B_{MSY}$	12.38	6.43-24.33
$0.8B_{MSY}$	24.77	12.85-48.66
MSY_1	5.55	3.78-8.08
MSY_2	9.98	6.80-14.55
F_{2021_1}	0.07	0.05-0.08
F_{2021_2}	0.04	0.03-0.05
U_{MSY_1}	0.78	0.29-0.98
U_{MSY_2}	0.99	0.58-1.00

Table 8. Posterior median and 95% credible intervals of spawning biomass for the base model. Values are in thousands of tonnes.

Year	Median	Credible interval
1996	147.74	136.58–161.42
1997	144.44	133.48–158.22
1998	143.11	132.17–156.55
1999	139.10	128.45–152.34
2000	135.12	124.93–148.03

Year	Median	Credible interval
2001	132.41	122.24–145.42
2002	128.28	117.99–141.60
2003	129.15	118.59–142.29
2004	133.04	121.85–146.52
2005	135.80	124.05–149.65
2006	129.68	117.44–143.45
2007	133.51	120.73–147.77
2008	138.34	125.57–152.39
2009	139.92	126.96–154.05
2010	140.97	128.28–154.73
2011	141.29	129.21–155.11
2012	135.70	124.13–149.27
2013	130.49	118.91–143.60
2014	120.50	109.83–133.13
2015	107.75	97.59–120.31
2016	98.18	88.30–111.24
2017	88.54	79.11–101.74
2018	80.25	70.56–93.19
2019	73.86	63.95–86.92
2020	68.84	57.98–82.59
2021	69.20	58.13–84.03
2022	67.95	56.14–83.83

Table 9. Posterior median and 95% credible intervals for relative spawning biomass for the base model.

Year	Median	Credible interval
1996	0.80	0.55–1.14
1997	0.79	0.54–1.11
1998	0.78	0.53–1.10
1999	0.76	0.52–1.07
2000	0.74	0.51–1.05
2001	0.72	0.50–1.02
2002	0.70	0.48–0.99
2003	0.70	0.48–1.00
2004	0.72	0.49–1.03
2005	0.74	0.51–1.05
2006	0.71	0.49–1.00
2007	0.73	0.51–1.04
2008	0.75	0.52–1.07
2009	0.76	0.53–1.08
2010	0.76	0.53–1.09
2011	0.77	0.53–1.09
2012	0.74	0.51–1.05
2013	0.71	0.49–1.01
2014	0.65	0.45–0.94
2015	0.58	0.41–0.83

Year	Median	Credible interval
2016	0.53	0.37–0.76
2017	0.48	0.34–0.68
2018	0.44	0.31–0.61
2019	0.40	0.28–0.57
2020	0.38	0.26–0.52
2021	0.38	0.26–0.52
2022	0.37	0.26–0.51

Table 10. Posterior median and 95% credible intervals for recruitment for the base model. Values are in millions of fish.

Year	Median	Credible interval
1997	111.21	94.55–131.31
1998	104.99	89.41–123.19
1999	126.26	110.58–146.93
2000	161.21	140.47–182.95
2001	151.55	132.70–174.80
2002	146.52	127.46–166.03
2003	135.61	117.96–155.68
2004	110.44	94.53–126.54
2005	97.43	83.09–113.88
2006	101.20	87.42–117.62
2007	104.38	89.05–119.69
2008	110.79	96.60–127.70
2009	78.68	66.31–92.52
2010	78.94	65.91–94.16
2011	60.80	49.77–74.54
2012	92.77	76.64–112.44
2013	59.55	45.27–77.15
2014	82.55	62.66–107.48
2015	45.89	31.30–66.23
2016	38.28	22.16–59.90
2017	59.72	37.21–93.81
2018	51.13	25.27–91.63
2019	35.06	15.04–69.54
2020	92.60	20.10–412.51
2021	82.87	20.80–418.16

Table 11. Posterior median and 95% credible intervals for fishing mortality for the base model.

Year	F_{Freezertrawlers}		F_{Shoreside}	
	Median	Credible interval	Median	Credible interval
1996	0.00	0.00–0.00	0.12	0.10–0.14
1997	0.00	0.00–0.00	0.07	0.06–0.09

Year	Median	Credible interval	Median	Credible interval
1998	0.00	0.00–0.00	0.10	0.09–0.12
1999	0.00	0.00–0.00	0.11	0.09–0.13
2000	0.00	0.00–0.00	0.11	0.09–0.12
2001	0.00	0.00–0.00	0.16	0.14–0.19
2002	0.00	0.00–0.00	0.13	0.11–0.15
2003	0.00	0.00–0.00	0.12	0.10–0.14
2004	0.00	0.00–0.00	0.16	0.14–0.19
2005	0.03	0.02–0.03	0.33	0.27–0.39
2006	0.06	0.05–0.07	0.10	0.08–0.12
2007	0.02	0.01–0.02	0.06	0.05–0.08
2008	0.03	0.03–0.04	0.06	0.05–0.07
2009	0.00	0.00–0.00	0.06	0.05–0.07
2010	0.00	0.00–0.00	0.05	0.04–0.05
2011	0.04	0.03–0.05	0.07	0.06–0.08
2012	0.04	0.04–0.05	0.05	0.05–0.06
2013	0.11	0.09–0.13	0.05	0.04–0.06
2014	0.17	0.14–0.21	0.05	0.04–0.05
2015	0.16	0.13–0.20	0.04	0.04–0.05
2016	0.18	0.15–0.22	0.06	0.05–0.07
2017	0.19	0.15–0.23	0.07	0.06–0.08
2018	0.19	0.15–0.24	0.04	0.03–0.05
2019	0.16	0.13–0.21	0.04	0.04–0.05
2020	0.03	0.02–0.03	0.03	0.02–0.04
2021	0.07	0.05–0.08	0.04	0.03–0.05

Table 12. Posterior median and 95% credible intervals for annual harvest rate (U_t) for the base model.

Year	$U_{\text{Freezertrawlers}}$		$U_{\text{Shoreside}}$	
	Median	Credible interval	Median	Credible interval
1997	0.00	0.00–0.00	0.07	0.06–0.08
1998	0.00	0.00–0.00	0.10	0.08–0.11
1999	0.00	0.00–0.00	0.10	0.09–0.12
2000	0.00	0.00–0.00	0.10	0.09–0.12
2001	0.00	0.00–0.00	0.15	0.13–0.17
2002	0.00	0.00–0.00	0.12	0.10–0.14
2003	0.00	0.00–0.00	0.11	0.09–0.13
2004	0.00	0.00–0.00	0.15	0.13–0.17
2005	0.00	0.00–0.00	0.28	0.24–0.32
2006	0.03	0.02–0.03	0.09	0.08–0.11
2007	0.06	0.05–0.07	0.06	0.05–0.07
2008	0.02	0.01–0.02	0.05	0.05–0.06
2009	0.03	0.02–0.04	0.06	0.05–0.07
2010	0.00	0.00–0.00	0.04	0.04–0.05
2011	0.00	0.00–0.00	0.07	0.06–0.08
2012	0.04	0.03–0.05	0.05	0.05–0.06
2013	0.04	0.04–0.05	0.05	0.04–0.06

Year	Median	Credible interval	Median	Credible interval
2014	0.10	0.08–0.12	0.04	0.04–0.05
2015	0.16	0.13–0.19	0.04	0.04–0.05
2016	0.15	0.12–0.18	0.06	0.05–0.07
2017	0.17	0.14–0.20	0.07	0.05–0.08
2018	0.17	0.14–0.21	0.04	0.03–0.05
2019	0.17	0.14–0.21	0.04	0.03–0.05
2020	0.15	0.12–0.19	0.03	0.02–0.04
2021	0.03	0.02–0.03	0.04	0.03–0.05
2022	0.06	0.05–0.08	0.00	0.00–0.00

Table 13. A summary of parameter changes to the base model for each sensitivity.

Description	Changes
Decrease σ to 0.135	$\vartheta^2 = 1.519$; $\rho = 0.028$
Increase τ to 1.0	$\vartheta^2 = 0.962$; $\rho = 0.038$
Decrease τ to 0.6	$\vartheta^2 = 2.500$; $\rho = 0.100$
Decrease mean of h prior to 0.72	$Beta(\alpha = 11.72, \beta = 4.56)$
Estimated $\ln(M_{female})$ with prior sd=0.2	$Normal(\ln(0.20), 0.5)$
Estimated $\ln(M_{female})$ with prior sd=1.6	$Normal(\ln(0.20), 2.5)$
Estimated $\ln(M_{male})$ with prior sd=0.2	$Normal(\ln(0.35), 0.5)$
Estimated $\ln(M_{male})$ with prior sd=1.6	$Normal(\ln(0.35), 2.5)$
Increase $\ln(q_k)$ prior mean to 1.0	$Normal(\ln(1.0), 0.5)$ for all gears k
Broad prior on $\ln(q_k)$, prior sd=1.5	$Normal(\ln(0.5), 1.5)$ for all gears k
Comm. selectivities equal maturity ogive	$\hat{a}_k = \hat{a}$; $\hat{\gamma}_k = \hat{\gamma}$ for both fleets k
QCS TV selectivity 3 year blocks	QCS selectivity is time-varying with year blocks 2003–2010, 2011–2016, and 2017–2021
Geostatistical based survey indices	Design-based indices replaced with Geostatistical-based indices for all surveys
Remove Discard CPUE	Remove Discard CPUE index
Maturity without 'developing/resting'	Maturity codes 2, 3, and 7 removed from the maturity-at-age estimation
Fix DCPUE selectivity	Fix DCPUE selectivity to the Shoreside estimate ($a_{k,F} = 8.67$; $\gamma_{k,F} = 1.06$; $a_{k,M} = 8.40$; $\gamma_{k,F} = 0.96$)
Fix survey selectivities	Fix all survey selectivities to the Shoreside estimate ($a_{k,F} = 8.67$; $\gamma_{k,F} = 1.06$; $a_{k,M} = 8.40$; $\gamma_{k,F} = 0.96$)

Table 14. Reference rates, calculated as the constant rate at which fishing needs to occur on an annual basis by each fleet long term (50 years) to bring the relative spawning biomass to within 50 t of $0.4B_0$ given recent average recruitment. In this case the routine was able to come within 6.4 t of $0.4B_0$. The F values are the instantaneous fishing mortalities and the U values are the annual exploitation rate. The last column shows the long term annual catch by fleet and the total. This is the value which, if caught every year for the long term would result in the biomass being close to $0.4B_0$.

Fleet	$F_{0.4B_0}$	$U_{0.4B_0}$	Catch (kt)
Freezer trawlers	0.066	0.064	1.566
Shoreside	0.042	0.041	2.840
Total			4.406

Table 15. Decision table for the base model showing posterior probabilities that projected biomass is below selected reference points and benchmarks (Table 7). An example of how to read this table is: For a catch of 10,000 t there is a 0.1% probability that the 2023 biomass will fall below the LRP of $0.2B_0$, a 78.7% probability that it will fall below the USR of $0.4B_0$, and a 92.2% probability that the biomass in 2023 will be less than the biomass in 2022. For projections beyond 2023 the catch is the same value for each projected year in each row of the table. So for the example of a constant catch each year of 10,000 t, the probability that the biomass will decline from one year to the next is 92.2% from 2022 to 2023, 78.2% from 2023 to 2024, 74.2% from 2024 to 2025, and 77.0% from 2025 to 2026.

Catch (thousand t)	P($B_{2023} < 0.2B_0$)	P($B_{2024} < 0.2B_0$)	P($B_{2025} < 0.2B_0$)	P($B_{2026} < 0.2B_0$)	P($B_{2023} < 0.35B_0$)	P($B_{2024} < 0.35B_0$)	P($B_{2025} < 0.35B_0$)	P($B_{2026} < 0.35B_0$)	P($B_{2023} < 0.4B_0$)	P($B_{2024} < 0.4B_0$)	P($B_{2025} < 0.4B_0$)	P($B_{2026} < 0.4B_0$)	P($B_{2023} < B_{2022}$)	P($B_{2024} < B_{2023}$)	P($B_{2025} < B_{2024}$)	P($B_{2026} < B_{2025}$)
0	0.000	0.000	0.000	0.000	0.262	0.171	0.118	0.107	0.543	0.410	0.352	0.315	0.044	0.093	0.161	0.233
1	0.000	0.000	0.000	0.000	0.286	0.210	0.168	0.161	0.576	0.461	0.401	0.377	0.126	0.165	0.233	0.304
2	0.000	0.000	0.000	0.001	0.307	0.260	0.227	0.236	0.602	0.512	0.447	0.434	0.262	0.251	0.307	0.373
3	0.000	0.000	0.001	0.001	0.331	0.307	0.298	0.295	0.633	0.556	0.512	0.495	0.418	0.337	0.370	0.434
4	0.000	0.001	0.001	0.001	0.362	0.349	0.355	0.367	0.657	0.606	0.573	0.574	0.570	0.429	0.427	0.508
5	0.000	0.001	0.001	0.004	0.387	0.400	0.411	0.430	0.675	0.642	0.629	0.633	0.669	0.516	0.495	0.567
6	0.001	0.001	0.001	0.010	0.436	0.440	0.466	0.496	0.701	0.689	0.685	0.687	0.748	0.587	0.565	0.624
7	0.001	0.001	0.006	0.023	0.472	0.498	0.525	0.571	0.719	0.734	0.735	0.739	0.805	0.656	0.613	0.669
8	0.001	0.001	0.013	0.050	0.500	0.552	0.597	0.644	0.741	0.790	0.777	0.780	0.856	0.710	0.671	0.707
9	0.001	0.004	0.026	0.092	0.525	0.598	0.657	0.700	0.764	0.824	0.811	0.813	0.898	0.753	0.706	0.742
10	0.001	0.008	0.047	0.143	0.559	0.646	0.713	0.745	0.787	0.843	0.847	0.836	0.922	0.782	0.742	0.770
11	0.002	0.012	0.082	0.208	0.584	0.696	0.750	0.782	0.815	0.869	0.869	0.865	0.942	0.807	0.769	0.798
12	0.003	0.022	0.125	0.268	0.619	0.742	0.796	0.821	0.836	0.892	0.882	0.884	0.954	0.831	0.789	0.820
13	0.004	0.036	0.174	0.337	0.643	0.786	0.833	0.838	0.854	0.907	0.901	0.899	0.964	0.856	0.807	0.841
14	0.004	0.054	0.230	0.421	0.673	0.827	0.853	0.862	0.881	0.923	0.914	0.909	0.971	0.875	0.829	0.862
15	0.006	0.083	0.300	0.506	0.698	0.854	0.874	0.888	0.892	0.932	0.927	0.924	0.977	0.893	0.850	0.876

REFERENCES CITED

- Aitchison, J. 1955. On the distribution of a positive random variable having a discrete probability mass at the origin. *Journal of the American Statistical Association* 50(271): 901.
- Anderson, S.C., Forrest, R.E., Huynh, Q.C., and Keppel, E.A. 2021. [A management procedure framework for groundfish in British Columbia](#). DFO Can. Sci. Advis. Sec. Res. Doc. 2021/007. vi + 139 p.
- Anderson, S.C., Keppel, E.A., and Edwards, A.M. 2019. [A reproducible data synopsis for over 100 species of British Columbia groundfish](#). DFO Can. Sci. Advis. Sec. Res. Doc. 2019/041. vii + 321 p.
- Anderson, S.C., Ward, E.J., English, P.A., and Barnett, L.A.K. 2022. sdmTMB: An R package for fast, flexible, and user-friendly generalized linear mixed effects models with spatial and spatiotemporal random fields. *bioRxiv* 2022.03.24.485545.
- Barrett, T., Marentette, J.R., Forrest, R.E., Anderson, S.C., Holt, C.A., Ings, D.W., and Thiess, M.E. 2022. [Technical Considerations for Stock Status and Limit Reference Points under the Fish Stocks Provisions](#). DFO Can. Sci. Advis. Sec. Res. Doc. 2024/029. v + 57 p.
- Berger, A.M. 2019. Character of temporal variability in stock productivity influences the utility of dynamic reference points. *Fisheries Research* 217: 185–197.
- Blood, D.M., Matarese, A.C., and Busby, M.S. 2007. Spawning, egg development, and early life history dynamics of arrowtooth flounder (*Atheresthes stomias*) in the Gulf of Alaska. U.S. Dep. Commer., NOAA Prof. Pap. NMFS 7: 28 p.
- Boldt, J.L., Javorski, A., and Chandler, P.C.(Eds.). 2021. State of the physical, biological and selected fishery resources of Pacific Canadian marine ecosystems in 2020. In *Can. Tech. Rep. Fish. Aquat. Sci.*
- Brooks, M.E., Kristensen, K., van Benthem, K.J., Magnusson, A., Berg, C.W., Nielsen, A., Skaug, H.J., Maechler, M., and Bolker, B.M. 2017. glmmTMB balances speed and flexibility among packages for zero-inflated generalized linear mixed modeling. *The R Journal* 9(2): 378–400.
- Choromanski, E.M., Fargo, J., and Kronlund, A.R. 2002. Species assemblage trawl survey of Hecate Strait, CCGS W.E. RICKER, May 31–June 13, 2000. *Can. Data Rep. Fish. Aquat. Sci.*: 1085:89.
- Choromanski, E.M., Workman, G.D., and Fargo, J. 2005. Hecate Strait multi-species bottom trawl survey, CCGS W.E. RICKER, May19–June7, 2003. *Can. Data Rep. Fish. Aquat. Sci.* 1169: 102 p.
- Cosimo, J.D.D. 1998. Groundfish of the Gulf of Alaska: A species profile. North Pacific Fisheries Management Council, 604 West 4th Avenue, Suite 306, Anchorage, Alaska, 99501.
- Department of Agriculture and Water Resources, Australian Government. 2018. Guidelines for the Implementation of the Commonwealth Fisheries Harvest Strategy Policy.
- Deriso, R.B., Maunder, M.N., and Skalski, J.R. 2007. Variance estimation in integrated assessment models and its importance for hypothesis testing. *Can. J. Fish. Aquat. Sci.* 64(2): 187–197.
- DFO. 2009. [A Fishery Decision-Making Framework Incorporating the Precautionary Approach](#).
- DFO. 2020. Changes to arrowtooth flounder fishery management in 2020/21, memorandum for the regional director general, pacific. : 4.

-
- DFO. 2021. [Trends in Abundance and Distribution of Steller Sea Lions \(*Eumetopias jubatus*\) in Canada](#). DFO Can. Sci. Advis. Sec. Sci. Rep. 2021/035.
- DFO. 2022. [A data synopsis for British Columbia groundfish: 2021 data update](#). DFO Can. Sci. Advis. Sec. Sci. Res. 2022/020.
- Doyle, M.J., Debenham, C., Barbeaux, S.J., Buckley, T.W., Pirtle, J.L., Spies, I.B., Stockhausen, W.T., Shotwell, S.K., Wilson, M.T., and Cooper, D.W. 2018. A full life history synthesis of Arrowtooth Flounder ecology in the Gulf of Alaska: Exposure and sensitivity to potential ecosystem change. *Journal of Sea Research* 142: 28–51.
- Edwards, A.M., Berger, A.M., Grandin, C.J., and Johnson, K.F. 2022. Status of the Pacific Hake (whiting) stock in U.S. and Canadian waters in 2022. Prepared by the Joint Technical Committee of the U.S. and Canada Pacific Hake/Whiting Agreement, National Marine Fisheries Service and Fisheries and Oceans Canada. : 238p.
- Efron, B. 1982. The jackknife, the bootstrap and other resampling plans. *SIAM CBMS-NSF Mon.* 38: 92.
- English, P.A., Ward, E.J., Rooper, C.N., Forrest, R.E., Rogers, L.A., Hunter, K.L., Edwards, A.M., Connors, B.M., and Anderson, S.C. 2021. Contrasting climate velocity impacts in warm and cool locations show that effects of marine warming are worse in already warmer temperate waters. *Fish and Fisheries* 23(1): 239–255.
- Fargo, J., Foucher, R.P., Saunders, M.W., Tyler, A.V., and Summers, P.L. 1988. 1988 F/V EASTWARD HO Assemblage survey of Hecate Strait, May 27-June 16, 1987. *Can. Data Rep. Fish. Aquat. Sci.*: 699:172.
- Fargo, J., Lapi, L.A., Richards, J.E., and Stocker, M. 1981. Turbot biomass survey of Hecate Strait, June 9-20, 1980. *Can. MS Rep. Fish. Aquat. Sci.*: 1630: 84p.
- Fargo, J., and Starr, P.J. 2001. [Turbot Stock Assessment for 2001 and Recommendations for Management in 2002](#). DFO Can. Sci. Advis. Sec. Advis. Rep. 2001/150.
- Fargo, J., Tyler, A.V., Cooper, J., Shields, S.C., and Stebbins, S. 1984. ARCTIC OCEAN Assemblage of Hecate Strait, May 27-June 17, 1984. *Can. Data Rep. Fish. Aquat. Sci.*: 491:108.
- Forrest, R.E., Anderson, S.C., Grandin, C.J., and J., S.P. 2020. [Assessment of Pacific Cod \(*Gadus macrocephalus*\) for Hecate Strait and Queen Charlotte Sound \(Area 5ABCD\), and West Coast Vancouver Island \(Area 3CD\) in 2018](#). DFO Can. Sci. Advis. Sec. Res. Doc. 2020/070. v + 215 p.
- Fournier, D.A., and Archibald, C. 1982. A general theory for analyzing catch at age data. *Can. J. Fish. Aquat. Sci.* 39(8): 1195–1207.
- Fournier, D.A., Skaug, H.J., Ancheta, J., Ianelli, J., Magnusson, A., Maunder, M.N., Nielsen, A., and Sibert, J. 2012. AD Model Builder: Using automatic differentiation for statistical inference of highly parameterized complex nonlinear models. *Optim. Methods Softw.* 27: 233–249.
- Francis, R.I.C.C. 2016. Revisiting data weighting in fisheries stock assessment models. *Fisheries Research*.
- Froese, R. 2004. Keep it simple: Three indicators to deal with overfishing. *Fish and Fisheries* 5(1): 86–91.
- Gavaris, S., and Ianelli, J. 2002. Statistical issues in fisheries' stock assessments. *Scan. J. Stat.* 29(2): 245–267.
-

-
- Grandin, C.J., and Forrest, R.E. 2017. [Arrowtooth Flounder \(*Atheresthes stomias*\) Stock Assessment for the West Coast of British Columbia](#). DFO Can. Sci. Advis. Sec. Res. Doc. 2017/025. v + 87 p.
- Hand, C.M., Robison, B.D., Fargo, J., Workman, G.D., and Stocker, M. 1994. 1994 R/V W.E. RICKER Assemblage survey of Hecate Strait, May 17-June 3, 1993. Can. Data Rep. Fish. Aquat. Sci.: 925:197.
- Hart, J.L. 1973. Pacific fishes of Canada. Fish Res. Board of Canada Bulletin 180: 740 p.
- Holt, K.R., Starr, P.J., Haigh, R., and Krishka, B. 2016. [Stock Assessment and Harvest Advice for Rock Sole \(*Lepidopsetta spp.*\) in British Columbia](#). DFO Can. Sci. Advis. Sec. Res. Doc. 2016/009. ix + 256 p.
- Howell, D., Schueller, A.M., Bentley, J.W., Buchheister, A., Chagaris, D., Cieri, M., Drew, K., Lundy, M.G., Pedreschi, D., Reid, D.G., and Townsend, H. 2021. Combining ecosystem and single-species modeling to provide ecosystem-based fisheries management advice within current management systems. *Frontiers in Marine Science* 7.
- Hurtado-Ferro, F., Szuwalski, C.S., Valero, J.L., Anderson, S.C., Cunningham, C.J., Johnson, K.F., Licandeo, R., McGilliard, C.R., Monnahan, C.C., Muradian, M.L., Ono, K., Vert-Pre, K.A., Whitten, A.R., and Punt, A.E. 2015. Looking in the rear-view mirror: Bias and retrospective patterns in integrated, age-structured stock assessment models. *ICES Journal of Marine Science* 72: 99–110.
- Kristensen, K., Nielsen, A., Berg, C.W., Skaug, H., and Bell, B.M. 2016. TMB: Automatic differentiation and Laplace approximation. *Journal of Statistical Software* 70(5): 1–21.
- Lindgren, F., Rue, H., and Lindström, J. 2011. An explicit link between Gaussian fields and Gaussian Markov random fields: The stochastic partial differential equation approach. *Journal of the Royal Statistical Society: Series B (Statistical Methodology)* 73(4): 423–498.
- Lindmark, M., Anderson, S.C., Gogina, M., and Casini, M. 2022. Evaluating drivers of spatiotemporal individual condition of a bottom-associated marine fish. preprint, *Ecology*.
- Marentette, J.R., and Kronlund, A.R. 2020. A Cross-Jurisdictional Review of International Fisheries Policies, Standards and Guidelines: Considerations for a Canadian Science Sector Approach. Canadian Technical Report of Fisheries and Aquatic Sciences 3342.
- Martell, S. 2011. iSCAM users guide, version 1.0. : 31.
- Martell, S.J., Schweigert, J., Cleary, J., and Haist, V. 2011. [Moving towards the sustainable fisheries framework for pacific herring: Data, models, and alternative assumptions; stock assessment and management advice for the British Columbia pacific Herring stocks: 2011 assessment and 2012 forecasts](#). DFO Can. Sci. Advis. Sec. Res. Doc. 2011/136. xii + 151 p.
- Maunder, M.N. 2012. Evaluating the stock recruitment relationship and management reference points: Application to summer flounder (*Paralichthys dentatus*) in the U.S. mid-Atlantic. *Fish. Res. Board Can. Tech. Rep.* 125-126: 20–26.
- Maunder, M.N., and Punt, A.E. 2004. Standardizing catch and effort data: A review of recent approaches. *Fisheries Research* 70(2): 141–159.
- McAllister, M.K., and Ianelli, J. 1997. Bayesian stock assessment using catch-age data and the sampling: Importance resampling algorithm. *Can. J. Fish. Aquat. Sci.* 54(2): 284–300.
- Ministry of Fisheries, New Zealand Government. 2008. Harvest Strategy Standard for New Zealand Fisheries.
-

-
- Myers, R.A., and Mertz, G. 1998. The limits of exploitation: A precautionary approach. *Ecol. Appl.* 8 Supplement s: 165–169.
- Myers, R.A., Rosenberg, A., Mace, P., Barrowman, N., and Restrepo, V. 1994. In search of thresholds for recruitment overfishing. *ICES Journal of Marine Science* 51: 191.
- Nash, R.D.M., Valencia, A.H., and Geffen, A.J. 2006. The origin of Fulton’s condition factor—Setting the record straight. *Fisheries* 31(5).
- NMFS. 2010. Fisheries Off West Coast States; Notice of Availability for Amendments 16-5 and 23 to the Pacific Coast Groundfish Fishery Management Plan. 75 Fed. Reg. 60709 (Oct. 1, 2010).
- NPFMC. 2020. Fishery Management Plan for Groundfish of the Gulf of Alaska. PFMFC. 2022. Pacific Coast Groundfish Fishery Management Plan (August 2022).
- Punt, A.E., and Butterworth, D.S. 1999. Experiences in the evaluation and implementation of management procedures. *ICES J. Mar. Sci.* 56(6): 985–998.
- Punt, A.E., Dorn, M.W., and Haltuch, M.A. 2008. Evaluation of threshold management strategies for groundfish off the U.S. West Coast. *Fisheries Research* 94(3): 251–266.
- R Core Team. 2022. R: A language and environment for statistical computing. R Foundation for Statistical Computing, Vienna, Austria.
- Richards, L.J., Schnute, J.T., and Olsen, N. 1997. Visualizing catch-age analysis: A case study. *Can. J. Fish. Aquat. Sci.* 54(7): 1646–1658.
- Rickey, M.H. 1995. Maturity, spawning, and seasonal movement of arrowtooth flounder, *atheresthes stomias*, off Washington. *Fishery Bulletin* 93:1: 127–138.
- Rue, H., Riebler, A., Sørbye, S.H., Illian, J.B., Simpson, D.P., and Lindgren, F.K. 2017. Bayesian Computing with INLA: A Review. *Annual Review of Statistics and Its Application* 4(1): 395–421.
- Sainsbury, K. 2008. Best Practice Reference Points for Australian Fisheries. Australian Fisheries Management Authority Report R2001/0999.
- Schnute, J.T., and Richards, L.J. 1995. The influence of error on population estimates from catch-age models. *Can. J. Fish. Aquat. Sci.* 52: 2063–2077.
- Shelton, A.O., Thorson, J.T., Ward, E.J., and Feist, B.E. 2014. Spatial semiparametric models improve estimates of species abundance and distribution. *Canadian Journal of Fisheries and Aquatic Sciences* 71(11): 1655–1666.
- Shotwell, S., Spies, I., Ianelli, J., Aydin, K., Hanselman, D., Pallson, W., Siwicke, K., Sullival, J., and Yasumiishi, E. 2021. Assessment of the arrowtooth flounder stock in the Gulf of Alaska. NPFMC Gulf of Alaska SAFE.
- Shotwell, S., Spies, I., and W., P. 2020. Assessment of the arrowtooth flounder stock in the Gulf of Alaska. NPFMC Gulf of Alaska SAFE.
- Silvar-Viladomiu, P., Minto, C., Halouani, G., Batts, L., Brophy, D., Lordan, C., and Reid, D.G. 2021. Moving reference point goalposts and implications for fisheries sustainability. *Fish and Fisheries* 22(6): 1345–1358.
- Sinclair, A., Krishka, B.A., and Fargo, J. 2007. Species trends in relative biomass, occupied area and depth distribution for Hecate Strait Assemblage Surveys from 1984-2003. *Can. Tech Rep. Fish. Aquat. Sci.*: 2749:141.

-
- Spies, I., Aydin, K., Ianelli, J., and Palsson, W. 2017. Assessment of the arrowtooth flounder stock in the gulf of Alaska. NPFMC Gulf of Alaska SAFE: 743–840.
- Spies, I., Aydin, K., Ianelli, J., and Palsson, W. 2019. Assessment of the arrowtooth flounder stock in the gulf of Alaska. NPFMC Gulf of Alaska SAFE: 92 p.
- Spies, I., and W., P. 2019. Assessment of the arrowtooth flounder stock in the Bering Sea and Aleutian Islands. NPFMC Bering Sea and Aleutian Islands SAFE.
- Stock, B.C., and Miller, T.J. 2021. The Woods Hole Assessment Model (WHAM): A general state-space assessment framework that incorporates time- and age-varying processes via random effects and links to environmental covariates. *Fisheries Research* 240: 105967.
- Thorson, J., Johnson, K., Methot, R., and Taylor, I. 2016. Model-based estimates of effective sample size in stock assessment models using the Dirichlet-multinomial distribution. *Fisheries Research* 192.
- Thorson, J.T. 2015. Spatio-temporal variation in fish condition is not consistently explained by density, temperature, or season for California Current groundfishes. *Marine Ecology Progress Series* 526: 101–112.
- Thorson, J.T., Shelton, A.O., Ward, E.J., and Skaug, H.J. 2015. Geostatistical delta-generalized linear mixed models improve precision for estimated abundance indices for West Coast groundfishes. *ICES Journal of Marine Science: Journal du Conseil* 72(5): 1297–1310.
- Walters, C.J., and Ludwig, D. 1994. Calculation of Bayes posterior probability distributions for key population parameters. *Can. J. Fish. Aquat. Sci.* 51: 713–722.
- Westrheim, S.J., Tyler, A.V., Foucher, R.P., Saunders, M.W., and Shields, S.C. 1984. G.B. Reed Groundfish Cruise No. 84-3, May 24-June 14, 1984. *Can. Data Rep. Fish. Aquat. Sci.*: 131.
- Wilson, S.J., Fargo, J., Hand, C.M., Johansson, T., and Tyler, A.V. 1991. 1991 R/V W.E. RICKER Assemblage survey of Hecate Strait, June 3-22, 1991. *Can. Data Rep. Fish. Aquat. Sci.*: 866:179.
- Workman, G.D., Fargo, J., Beall, B., and Hildebrandt, E. 1997. 1997 R/V W.E. RICKER Assemblage survey of Hecate Strait, May 30-June 13, 1996. *Can. Data Rep. Fish. Aquat. Sci.*: 1010:155.
- Workman, G.D., Fargo, J., Yamanaka, K.L., and Haist, V. 1996. 1996 R/V W.E. RICKER Assemblage survey of Hecate Strait, May 23-June 9, 1995. *Can. Data Rep. Fish. Aquat. Sci.*: 974:94.
- Yang, M.-S. 1993. Food Habits of the Commercially Important Groundfishes in the Gulf of Alaska in 1990. U.S. Dep. Commer., NOAA Tech. Memo. NMFS-AFSC-22: v + 150 p.

APPENDIX A. BIOLOGICAL DATA

This appendix summarizes the biological data for Arrowtooth Flounder in British Columbia. The length and age compositions collected from both surveys and commercial sources are illustrated (Figures A.1 and A.2); however, all biological parameters were estimated from synoptic survey data only. The values used in the assessment (Table A.1) were aggregated from the four synoptic surveys that are each run biennially off the West coast of British Columbia: the Queen Charlotte Sound Synoptic Survey, the Hecate Strait Synoptic Survey, the West Coast Vancouver Island Synoptic Survey, and the West Coast Haida Gwaii Synoptic Survey.

A.1. LENGTH AND WEIGHT MODEL

All valid length/weight pairs of data were extracted based on the criteria shown in table A.1. The length-weight equation used was:

$$W_s = \alpha_s L_s^{\beta_s} \quad (\text{A.1})$$

where α_s and β_s are parameters for sex s and L_s and W_s are paired length-weight observations. We applied Eq. A.1 to survey observations for the three synoptic surveys used in this assessment. Results are plotted for each survey individually, and together with data from the fourth survey West Coast Haida Gwaii Synoptic Survey to represent PMFC areas 3CD and 5ABCDE combined as 'coastwide' (Figure A.3).

A.2. VON-BERTALANFFY MODEL

We used the von-Bertalanffy function to estimate growth rates for Arrowtooth Flounder:

$$L_s = L_{\infty_s} (1 - e^{-k_s(a_s - t_{0_s})}) \quad (\text{A.2})$$

where L_{∞_s} , k_s , and t_{0_s} are parameters specific to sex s and L_s and a_s are paired length-age observations.

We applied Eq. A.2 to survey observations for the three synoptic surveys used in this assessment. Results are plotted for each survey individually, and together with data from the fourth survey West Coast Haida Gwaii Synoptic Survey to represent PMFC areas 3CD and 5ABCDE combined as 'coastwide' (Figure A.4).

A.3. MATURITY-AT-AGE MODEL

The maturity-at-age model used for Arrowtooth Flounder estimates age-at-50% maturity ($a_{s50\%}$) and standard deviation of age-at-50% maturity ($\sigma_{s50\%}$) by applying the Limited-memory Broyden Fletcher Goldfarb Shanno algorithm with Bounds (L-BFGS-B) to minimize the sum-of-squares between the observed and expected proportion mature:

$$P_{a_s} = \frac{1}{1 + e^{-\sigma_{s50\%}(a_s - a_{s50\%})}} \quad (\text{A.3})$$

where P_{a_s} is the observed proportion mature at age a_s for sex s .

A maturity code (maturity stage) of 3 or greater signifies mature fish, where the code scale is the standard flatfish scale of 1 through 7 (Holt et al. 2016).

The same equation can also be applied to lengths instead of ages. We applied Eq. A.3 to survey observations of both age and length from the three synoptic surveys used in this

assessment. Results are plotted for each survey individually, and together with data from the fourth survey West Coast Haida Gwaii Synoptic Survey to represent PMFC areas 3CD and 5ABCDE combined as 'coastwide' (Figure A.5).

A.4. FIGURES

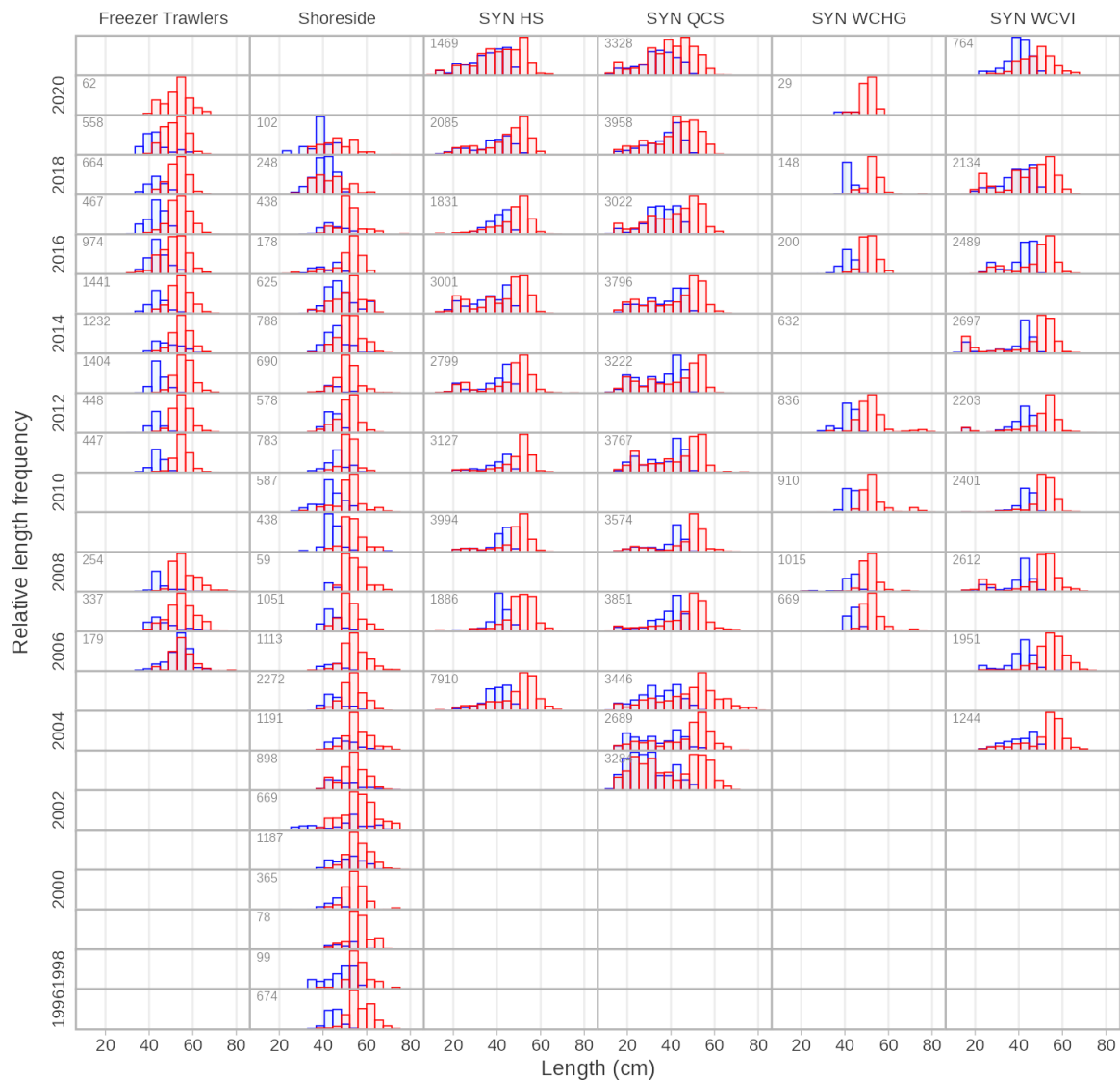


Figure A.1. Length-frequency plot where female fish are shown as red bars and male fish are shown behind as blue bars. The total number of fish measured for a given survey and year are indicated in the top left corner of each panel. Histograms are only shown if there are more than 20 fish measured for a given survey-year combination.

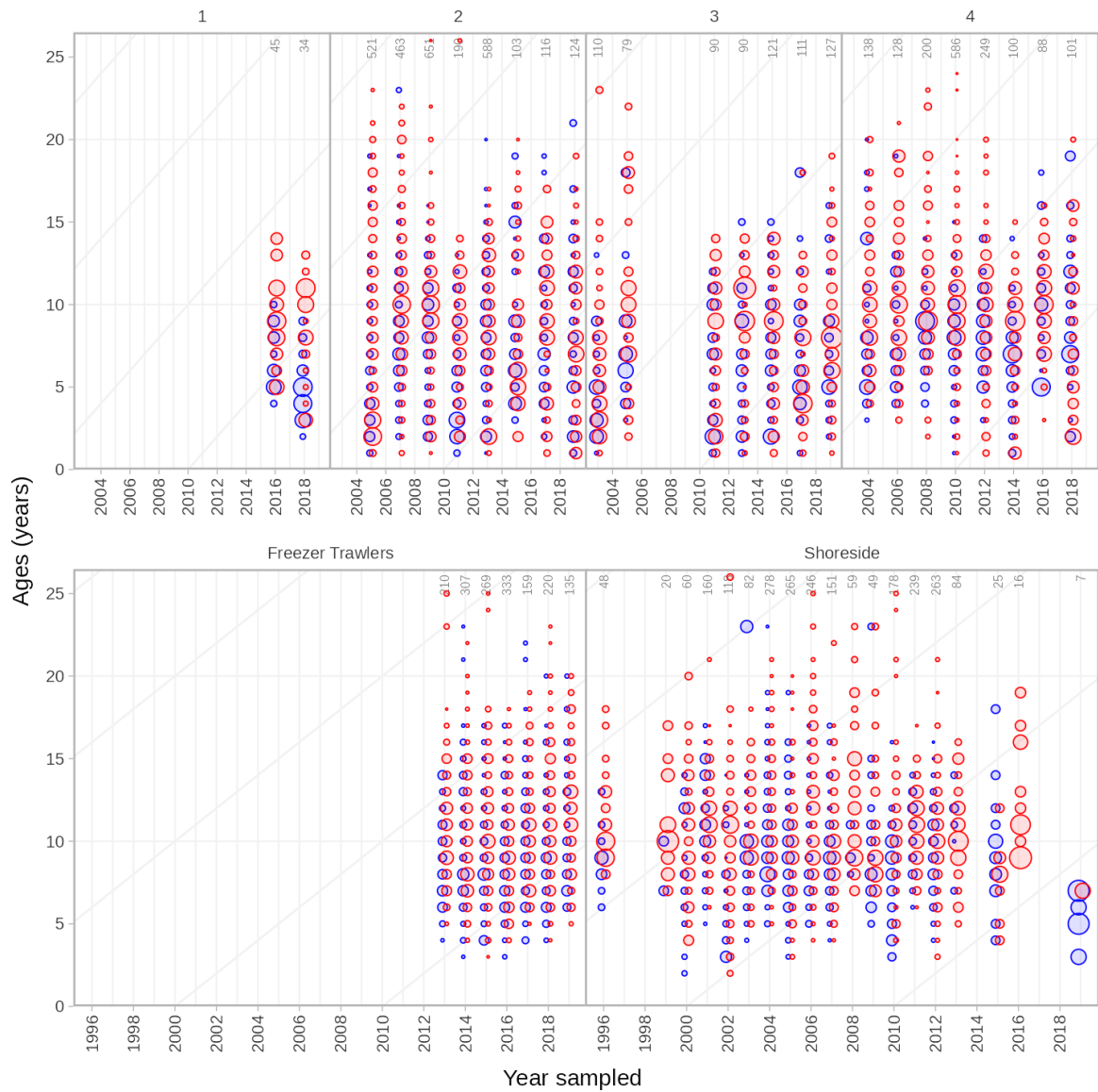


Figure A.2. Example age-frequency plot. Female fish are shown as red circles and male fish are shown behind as blue circles. The total number of fish aged for a given survey or fishery and year are indicated along the top of the panels. Diagonal lines are shown at five-year intervals to facilitate tracing cohorts through time.

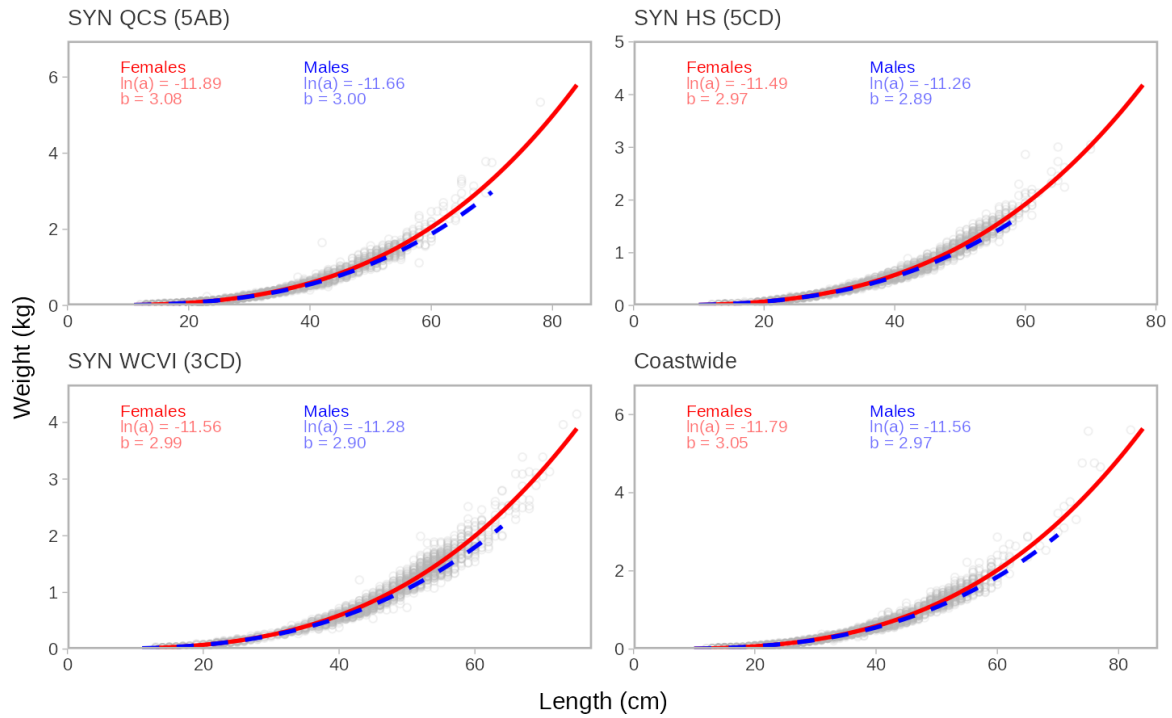


Figure A.3. Length/weight fits by sex. The length-weight curve is of the form $\log(W_i) \sim \text{Student-}t$ ($df = 3, \log(a) + b \log(L_i), \sigma$), with W_i and L_i representing the weight and length for fish i and σ representing the observation error scale. The degrees of freedom of the Student- t distribution is set to 3 to be robust to outliers. The variables a and b represent the estimated length-weight parameters. Female model fits are indicated as solid red lines and male model fits are indicated as blue lines. Text on the panels shows the parameter estimates and open circles represent individual fish that the models are fit to. These figures include all survey samples.

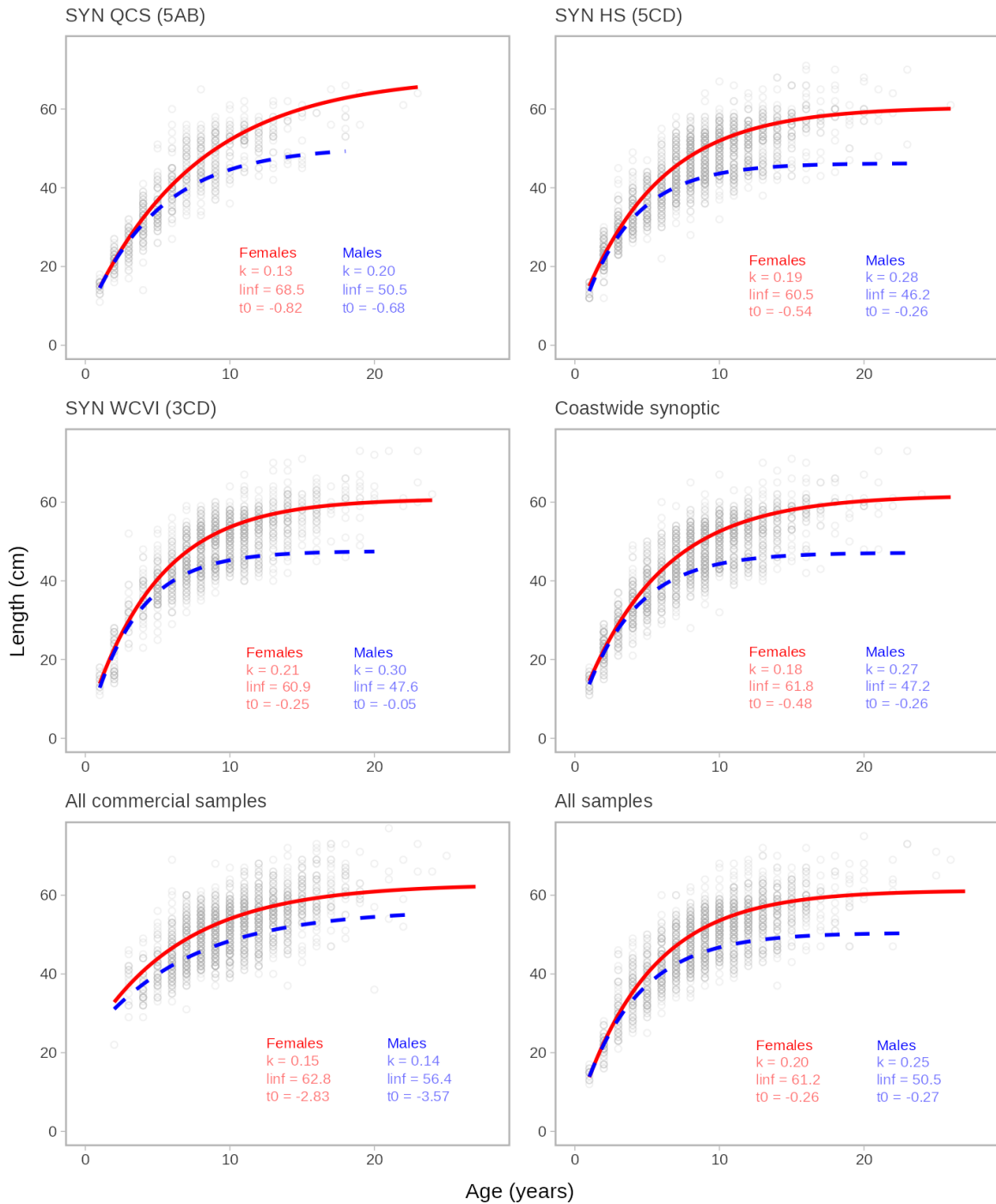


Figure A.4. The length-age growth curve is a von-Bertalanffy model of the form $L_i \sim \text{Log-normal}(\log(l_{inf}(1 - \exp(-k(A_i - t_0))))), \sigma)$ where L_i and A_i represent the length and age of fish i , l_{inf} , k , and t_0 represent the von-Bertalanffy growth parameters, and σ represents the scale parameter. Female model fits are indicated as solid red lines and male model fits are indicated as dashed blue lines. Text on the panels shows the parameter estimates and open circles represent individual fish that the models are fit to.

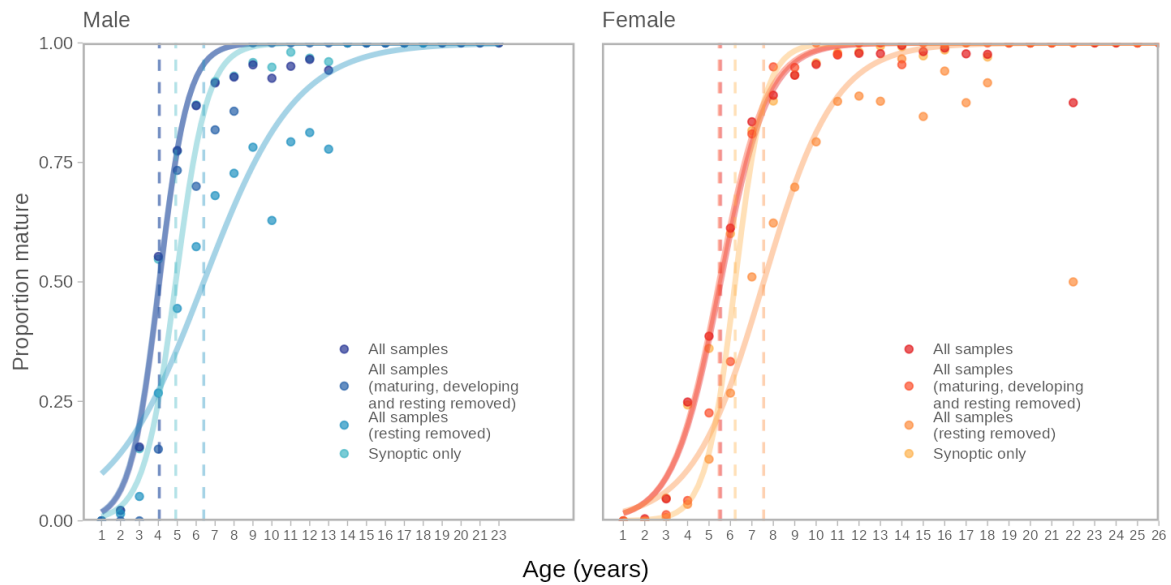


Figure A.5. Age-at-maturity ogive plots. Maturity ogives are logistic curves fit to the proportion of fish at each age that were categorized as mature vs. not mature. The dashed vertical lines indicate the estimated age at 50% maturity. Models are fit to all available samples regardless of time of year. The ogives used in the base model were based only on synoptic survey samples (male age at 50% maturity = 4.06, female age at 50% maturity = 5.55). Including all other survey and commercial samples ('All samples') doesn't not change the shape of the ogive, but we use this slightly larger dataset to check the influence of removing macroscopic maturity classifications that may be prone to misclassification and/or have uncertainty in their relationship with functional maturity ('Resting removed' and 'Maturing, developing and resting removed'). Maturing, developing and resting removed had the best fit to the data (male age at 50% maturity = 4.92, female age at 50% maturity = 6.22). These values were used as a sensitivity run.

A.5. TABLES

Table A.1. Growth parameters estimated outside the ISCAM model. All parameters were estimated using samples from the four synoptic surveys, and were filtered to include areas 3CD and 5ABCDE only. For the age-at-50% maturity estimates, the following values were used to further filter the data: maturity_convention_code = 4 (flatfish), maturity_code = 5 (Male - Spawning, testes large, white and sperm evident), (Female - Ripe, ovaries containing entirely translucent, mature ova. eggs loose and will run from oviducts under slight pressure), and usability codes = 0 (Unknown), 1 (Fully usable), 2 (Fail, but all data usable), 6 (Gear torn, all data ok).

Parameter	Female	Male
Asymptotic length (l_{inf})	61.770	47.159
Brody growth coefficient (k)	0.182	0.274
Theoretical age at zero length (t_0)	-0.479	-0.258
Scalar in length-weight allometry (α)	0.0000076	0.0000095
Power parameter in length-weight allometry (β)	3.052	2.974
Age at 50% maturity (\hat{a})	5.566	4.103
SD at 50% maturity ($\hat{\gamma}$)	1.098	0.802

APPENDIX B. PROPORTION FEMALE ANALYSIS

B.1. INTRODUCTION

The two-sex model requires a proportion of females as an input. In the Gulf of Alaska, observer length frequencies were used to determine that the stock is approximately 70% female (Shotwell et al. (2021)). In British Columbia, both commercial fishery and synoptic survey data were used to determine the proportion female. This appendix describes the weighting algorithm used, which is the same as what was used in Grandin and Forrest (2017) and based on the methods applied in Holt et al. (2016). The analysis here is based on aggregated area data for a coastwide stock.

B.2. DATA SELECTION

Both commercial and synoptic sample age data were filtered for input into the proportion female routine.

Commercial trawl fishery

The following three attributes were used to filter the age data for the commercial trawl fishery:

1. Species category
 - a. Included codes:
 - i. Unsorted
 - ii. Discards
 - b. Rejected codes:
 - i. Unknown
 - ii. Sorted
 - iii. Keepers
 - iv. Longline
2. Sample type
 - a. Included codes:
 - i. Total catch
 - ii. Random
 - iii. Random from randomly assigned set
 - iv. Random from set after randomly assigned set
 - v. Random from set requested by vessel master
 - b. Rejected codes
 - i. Selected (various codes)
 - ii. Stratified
 - iii. Unknown sample for NMFS Triennial survey
3. Gear code
 - a. Included codes:
 - i. Bottom trawl
 - ii. Unknown trawl
 - b. Rejected codes

-
- i. Unknown
 - ii. Trap
 - iii. Gillnet
 - iv. Handline
 - v. Longline
 - vi. Midwater trawl
 - vii. Troll
 - viii. Seine
 - ix. Jig
 - x. Recreational
 - xi. Various other obscure catch methods

Synoptic surveys

All available age data from the synoptic surveys were used.

Years

Age data from 1996 to 2019 were used. There was no age data available after 2019.

Quarters of the year

1 = January 1 - March 31

2 = April 1 - June 30

3 = July 1 - September 30

4 = October 1 - December 31

Areas

Coastwide, defined as areas 3CD and 5ABCDE aggregated.

Sex

Males and females only. Some records have the sex recorded as unknown or unsexed. Those records along with records with NULL sex were removed.

B.3. COMMERCIAL TRAWL FISHERY

Observations within a sample are likely to be correlated due to the small area which is trawled in a single fishing event. In addition, trip samples may be correlated due to single vessel fishing practices. This algorithm calculates a sex-specific mean weight by trip, calculated from individual sex-specific length observations converted to weight using Eq. B.1, then uses Eqs. B.2–B.8 to estimate proportion of females.

B.4. SYNOPTIC SURVEYS

For surveys, the same algorithm is followed except that the quarter of the year is not included in the calculation. This is because the surveys are single events which occur during the summer months only.

B.5. EQUATIONS

Specimens without weight data but with length data have their weights calculated as follows:

$$\hat{w}_{i,j,s} = \alpha_s l_{i,j,s}^{\beta_s} \quad (\text{B.1})$$

where α_s and β_s are parameters for sex s and $w_{i,j,s}$ and $l_{i,j,s}$ are paired length-weight observations for specimen i in sample j .

Total weight for each sample is the sum of the specimens in the sample:

$$W_{j,s,t} = \sum_{i=1}^{N_{j,s,t}} \hat{w}_{i,j,s,t} \quad (\text{B.2})$$

where $W_{j,s,t}$ is the total weight for sample j , sex s , trip t , and $N_{j,s,t}$ is the number of specimens in sample j for sex s .

Calculation of the mean sample weight by trip and sex is given by:

$$W_{s,t} = \frac{\sum_{j=1}^{K_t} W_{j,s,t} S_{j,t}}{\sum_{j=1}^{K_t} S_{j,t}} \quad (\text{B.3})$$

where $W_{s,t}$ is the mean weight for sex s and trip t , weighted by sample weight, where K_t is the number of samples in trip t , and $S_{j,t}$ is the sample weight for sample j from trip t .

To calculate the total catch weight for sampled hauls in each trip, we use the following:

$$C_t = \sum_{j=1}^{K_t} C_{j,t} \quad (\text{B.4})$$

where C_t is the total catch weight for sampled hauls for trip t , K_t is the number of samples in trip t , and $C_{j,t}$ is the catch weight associated with sample j and trip t .

The total weight in each quarter of the year by sex is given by:

$$W_{q,s} = \frac{\sum_{t=1}^{T_q} W_{q,s,t} R_{q,t}}{\sum_{t=1}^{T_q} R_{q,t}} \quad (\text{B.5})$$

where $W_{q,s}$ is the total weight for sex s and quarter of year q , $R_{q,t}$ is the trip weight for all sampled trips in quarter q , and T_q is the number of sampled trips in quarter q .

The total catch weight for sampled hauls per quarter of the year is:

$$C_q = \sum_{t=1}^{K_q} C_t \quad (\text{B.6})$$

where C_q is the total catch weight for sampled hauls for quarter q , K_q is the number of trips in quarter q , and C_t is the catch weight associated with trip t .

Now, the total weight by year and sex is calculated from:

$$W_{y,s} = \frac{\sum_{q=1}^4 W_{q,y,s} C_{q,y}}{\sum_{q=1}^4 C_{q,y}} \quad (\text{B.7})$$

where $W_{s,y}$ is the total weight for year y , sex s , $W_{q,y,s}$ is the weight in quarter q of year y , and $C_{q,y}$ is the catch in quarter q of year y .

Finally, the proportion female is given by:

$$P_y = \frac{W_{y,s=Female}}{W_{y,s=Male} + W_{y,s=Female}} \quad (\text{B.8})$$

where P_y is the proportion female by weight for year y and $W_{y,s}$ for $s = Female$ and $s = Male$ are given by Eq. B.7.

B.6. RESULTS

Table B.1 shows the proportions female for the commercial trawl fishery and the four synoptic surveys. The means of all the years included in the table are shown in the last row. There is very good agreement between the survey and commercial mean proportions and therefore it is reasonable to take the mean of the means to arrive at a single value for overall proportion of females in the Arrowtooth Flounder stock in British Columbia. The mean of the means for the synoptic surveys and the commercial fishery is 0.79. That is the proportion used as an input to all models (base, bridging, sensitivities, and retrospectives) in this assessment.

Tables B.2 and B.3 give a summary of the data used for the proportion female calculations. In most years there is a large number of weights included.

Table B.1. Proportion of female Arrowtooth Flounder in the commercial trawl fishery and four synoptic surveys coastwide. The survey acronyms stand for QCS = Queen Charlotte Sound Synoptic Survey, HS = Hecate Strait Synoptic Survey, WCVI = West Coast Vancouver Island Synoptic Survey and WCHG = West Coast Haida Gwaii Synoptic Survey.

Year	Commercial trawl	QCS	HS	WCVI	WCHG
1996	0.85	–	–	–	–
1997	0.85	–	–	–	–
1998	0.80	–	–	–	–
1999	0.79	–	–	–	–
2000	0.78	–	–	–	–
2001	0.89	–	–	–	–
2002	0.88	–	–	–	–
2003	0.78	0.84	–	–	–
2004	0.89	0.88	–	0.85	–
2005	0.85	0.90	0.82	–	–
2006	0.86	–	–	0.85	0.76
2007	0.84	0.76	0.78	–	0.81
2008	0.92	–	–	0.85	0.86
2009	0.68	0.80	0.75	–	–
2010	0.73	–	–	0.82	0.83
2011	0.74	0.75	0.79	–	–
2012	0.83	–	–	0.75	0.84
2013	0.77	0.72	0.73	–	–
2014	0.78	–	–	0.77	0.66
2015	0.76	0.74	0.74	–	–
2016	0.77	–	–	0.72	0.82
2017	0.76	0.75	0.77	–	–
2018	0.77	–	–	0.77	0.80

Year	Commercial trawl	QCS	HS	WCVI	WCHG
2019	0.78	0.77	0.78	–	–
Mean	0.81	0.79	0.77	0.79	0.81

Table B.2. Summary of samples and weights used for the calculation of proportion of female Arrowtooth Flounder in the commercial trawl fishery.

Year	Number of trips	Number of samples	Number of weights (Male)	Number of weights (Female)
1996	1	6	195	479
1997	6	6	71	194
1998	24	25	410	777
1999	27	27	411	769
2000	16	16	174	569
2001	33	34	407	1,081
2002	17	17	185	632
2003	24	26	299	810
2004	31	32	402	1,107
2005	49	53	773	1,878
2006	28	30	366	1,128
2007	28	31	432	1,088
2008	4	7	79	346
2009	11	11	165	327
2010	13	13	268	319
2011	18	24	441	789
2012	16	20	267	759
2013	29	40	631	1,463
2014	33	41	689	1,331
2015	25	40	760	1,306
2016	14	22	411	741
2017	14	19	324	581
2018	12	19	309	603
2019	10	15	231	429

Table B.3. Summary of samples and weights used for the calculation of proportion of female Arrowtooth Flounder in the synoptic surveys. See Table B.1 for survey acronym meanings.

Survey	Year	Number of samples	Number of weights (Male)	Number of weights (Female)
QCS	2003	95	1,486	1,994
QCS	2004	97	1,190	1,654
QCS	2005	86	1,464	2,142
QCS	2007	87	1,595	2,278
QCS	2009	138	1,459	2,195

Survey	Year	Number of samples	Number of weights (Male)	Number of weights (Female)
QCS	2011	160	1,614	2,237
QCS	2013	134	1,567	1,783
QCS	2015	146	1,552	2,245
QCS	2017	111	1,257	1,765
QCS	2019	130	1,412	2,546
HS	2006	30	313	445
HS	2007	22	229	467
HS	2008	29	307	708
HS	2010	41	343	594
HS	2012	50	302	534
HS	2014	25	343	318
HS	2016	11	74	164
HS	2018	6	57	91
WCVI	2005	166	3,405	5,270
WCVI	2007	43	726	1,242
WCVI	2009	75	1,572	2,436
WCVI	2011	122	1,131	2,112
WCVI	2013	112	1,106	1,693
WCVI	2015	105	1,232	1,787
WCVI	2017	68	709	1,122
WCVI	2019	75	762	1,323
WCHG	2004	38	511	951
WCHG	2006	36	567	1,432
WCHG	2008	64	930	1,811
WCHG	2010	87	774	1,627
WCHG	2012	102	865	1,364
WCHG	2014	102	1,026	1,684
WCHG	2016	97	1,009	1,480
WCHG	2018	80	816	1,318

APPENDIX C. DISCARD CPUE INDEX STANDARDIZATION

We draw on methods as written in Anderson et al. (2019) and Forrest et al. (2020), reproducing them in parts here for completeness. We sought to generate an index of Arrowtooth Flounder abundance from discard commercial trawl catch per unit effort (CPUE) data that was standardized for depth, fishing locality, month, vessel, and latitude. Fishing localities are spatial regions of similar size to Pacific Fishery Management Areas (PFMAs), and are sub-areas of the Minor statistical areas of the West Coast of British Columbia which have been traditionally fished.

C.1. DEFINING THE COMMERCIAL DISCARD FLEET

Before fitting a standardization model, we had to filter and manipulate the available catch and effort data to generate a dataset appropriate for model fitting. The unique aspect in this analysis, compared to similar CPUE analysis in other recent stock assessments done in British Columbia, is that we started by filtering all bottom trawl commercial fishing event data to only include those events for which Arrowtooth Flounder were caught and all caught were discarded. This approach was suggested by industry representatives at a Technical Working Group meeting as an approach to avoid tows targeting Arrowtooth Flounder and minimize issues related to changes in targeting behaviour over time.

Commercial groundfish bottom trawl data from 1996 to present have been recorded to the fishing-event level in the presence of on-board observers or video monitoring. Since we have data on individual vessels for this modern fleet, and in keeping with previous analyses for Pacific groundfish stocks, we defined a 'fleet' for the modern dataset that includes only vessels that qualify by passing some criteria of regularly catching (and subsequently discarding) Arrowtooth Flounder.

We follow the approach used in several recent B.C. groundfish stock assessments by requiring vessels to have caught (and discarded) the species in at least 100 tows across all years of interest, and to have passed a threshold of five trips (trips that recorded some of the species) for at least five years—all from 1996 to 2021 inclusive.

The 100% discard rule in the Discard CPUE time series means the entire tow is discarded. Figure C.1 shows the proportion of commercial tows that caught no Arrowtooth Flounder. The figure shows that the number of tows catching zero Arrowtooth Flounder has increased steadily since approximately 2014 with 2020 having approximately 40% tows with zero Arrowtooth Flounder catch.

C.2. DEFINING THE STANDARDIZATION MODEL PREDICTORS

For depth and latitude, we binned the values into a sequence of bands to allow for nonlinear relationships between these predictors and CPUE (e.g., Maunder and Punt 2004). For depth, we binned trawl depth into bands 25m wide. For latitude, we used bands that were 0.1 degrees wide. To ensure sufficient data to estimate a coefficient for each factor level, we limited the range of depth bins to those that fell within the 0.1% to 99.9% cumulative probability of positive observations and then removed any factor levels (across all predictors) that contained fewer than 0.1% of the positive observations.

Predictors that are treated as factors in a statistical model need a reference or base level—a level from which the other coefficients for that variable estimate a difference. The base level then becomes the predictor value that is used in the prediction for the standardized index. We chose the most frequent factor level as the base level. For example, we set the base month as the most common month observed in the dataset filtered for only tows where the species was caught. This choice of base level only affects the intercept or relative magnitude of our index

because of the form of our model (discussed below). This relative magnitude should not affect the outcomes of the stock assessment model because the discard CPUE index catchability is estimated with an uninformative prior.

C.3. GLMM INDEX STANDARDIZATION MODEL

Fisheries CPUE data contains both zeros and positive continuous values. A variety of approaches have been used in the fishery literature to model such data. Here, we use a Tweedie GLMM (generalised linear mixed effect model):

$$y_i \sim \text{Tweedie}(\mu_i, p, \phi), \quad 1 < p < 2, \quad (\text{C.1})$$

$$\mu_i = \exp \left(\mathbf{X}_i \boldsymbol{\beta} + \alpha_{j[i]}^{\text{locality}} + \alpha_{k[i]}^{\text{locality-year}} + \alpha_{l[i]}^{\text{vessel}} \right), \quad (\text{C.2})$$

$$\alpha_j^{\text{locality}} \sim \text{Normal}(0, \sigma_{\alpha}^2 \text{locality}), \quad (\text{C.3})$$

$$\alpha_k^{\text{locality-year}} \sim \text{Normal}(0, \sigma_{\alpha}^2 \text{locality-year}), \quad (\text{C.4})$$

$$\alpha_l^{\text{vessel}} \sim \text{Normal}(0, \sigma_{\alpha}^2 \text{vessel}), \quad (\text{C.5})$$

where i represents a single tow, y_i represents the catch (kg) per unit effort (hours trawled), \mathbf{X}_i represents a vector of fixed-effect predictors (depth bins, months, latitude bins), $\boldsymbol{\beta}$ represents a vector of associated coefficients, and μ_i represents the expected CPUE in a trip or tow. The random effect intercepts (α symbols) are allowed to vary from the overall intercept by locality j ($\alpha_j^{\text{locality}}$), locality-year k ($\alpha_k^{\text{locality-year}}$), and vessel l (α_l^{vessel}) and are constrained by normal distributions with respective standard deviations denoted by σ parameters.

We can then calculate the standardized estimate of CPUE for year t , μ_t , as

$$\mu_t = \exp(\mathbf{X}_t \boldsymbol{\beta}) \quad (\text{C.6})$$

where \mathbf{X}_t represents a vector of predictors set to the reference (r) levels with the year set to the year of interest. Because each of the α random intercepts is set to zero, the index is predicted for an average locality, locality-year, and vessel (for modern data). We estimated the fixed effects with maximum marginal likelihood while integrating over the random effects with the statistical software TMB via the R package glmmTMB (Brooks et al. 2017). We used standard errors (SE) as calculated by TMB on $\log(\mu_t)$ via the generalized delta method. We then calculated the 95% Wald confidence intervals as $\exp(\mu_t \pm 1.96\text{SE}_t)$.

For comparison, we calculated an unstandardized timeseries using a similar procedure but without any of the covariates other than a factor predictor for each year. This is similar to calculating the geometric mean of CPUE each year but with an assumed Tweedie observation model instead of a lognormal observation model that does not allow for zeros.

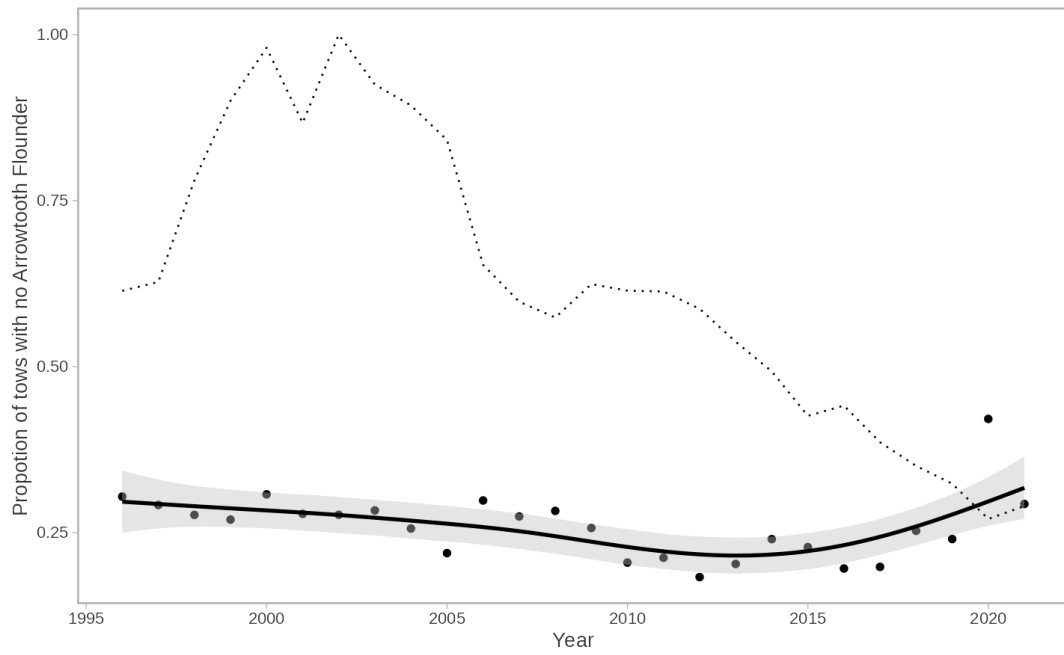


Figure C.1. Proportion of tows with no Arrowtooth Flounder from 1996 to 2021. The black dots are the actual coastwide proportions. The black line shows the output from a General Additive Model (GAM) using the points as inputs, the dotted line represents the total number of tows as a proportion of the maximum number of tows made in any given year.

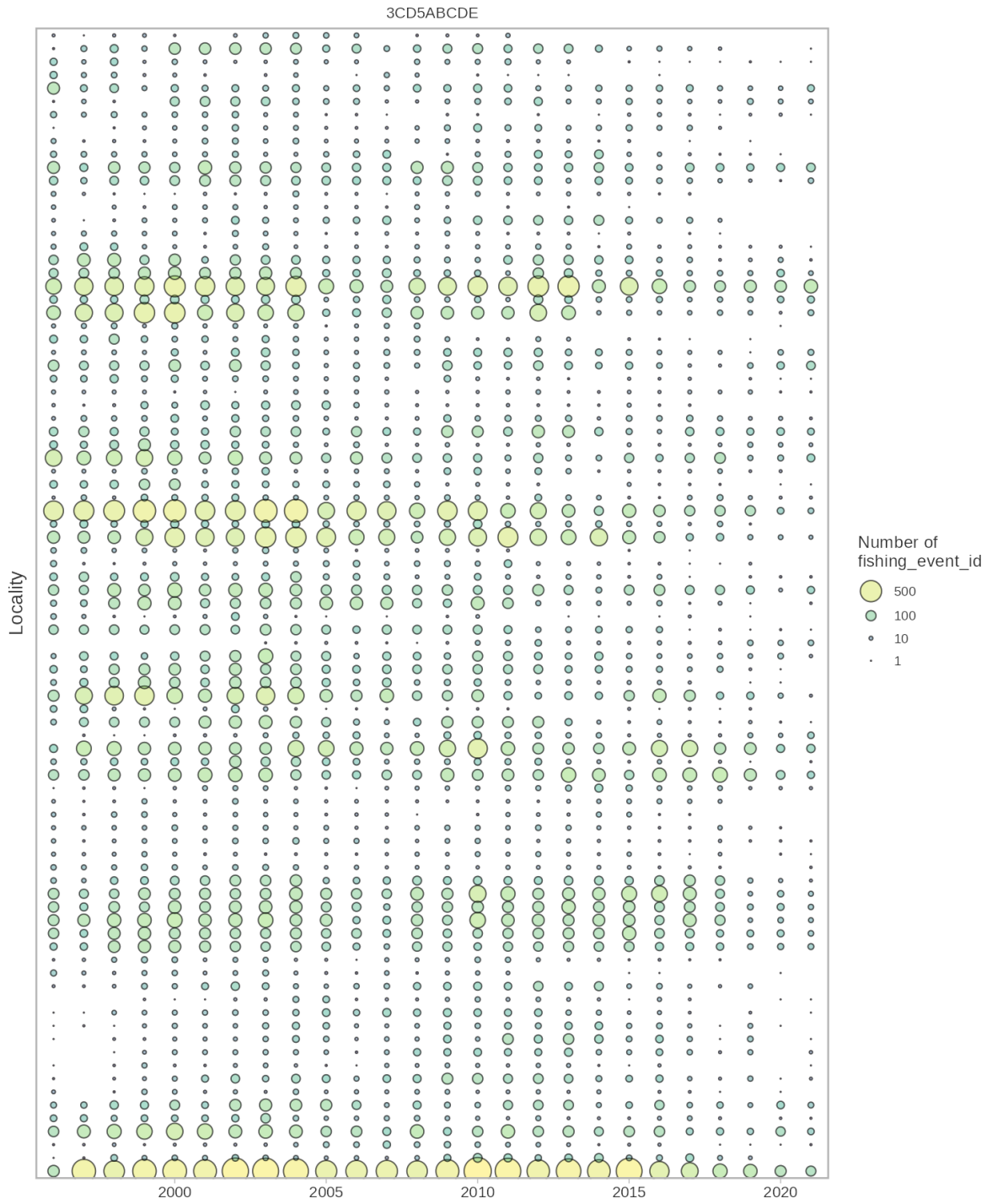


Figure C.2. Bubble plots showing distribution of the **locality** predictor by year. The area and colour of each circle represents the number of fishing events.

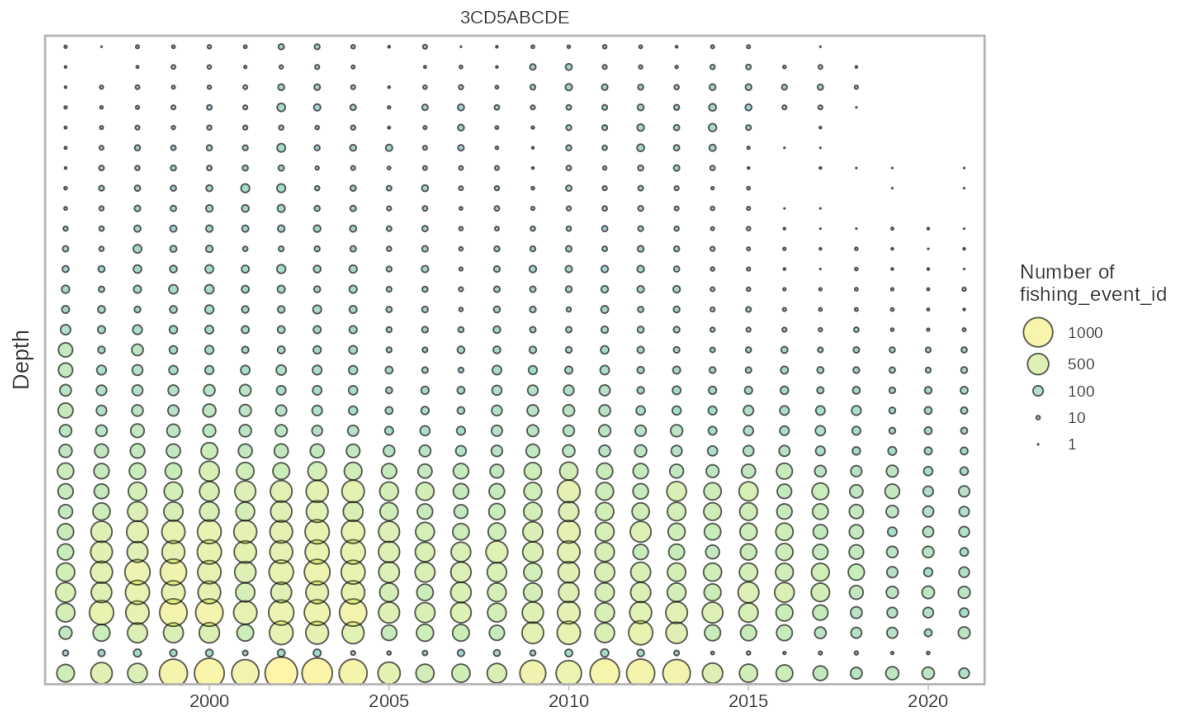


Figure C.3. Bubble plots showing distribution of the **depth** predictor by year. The area and colour of each circle represents the number of fishing events.

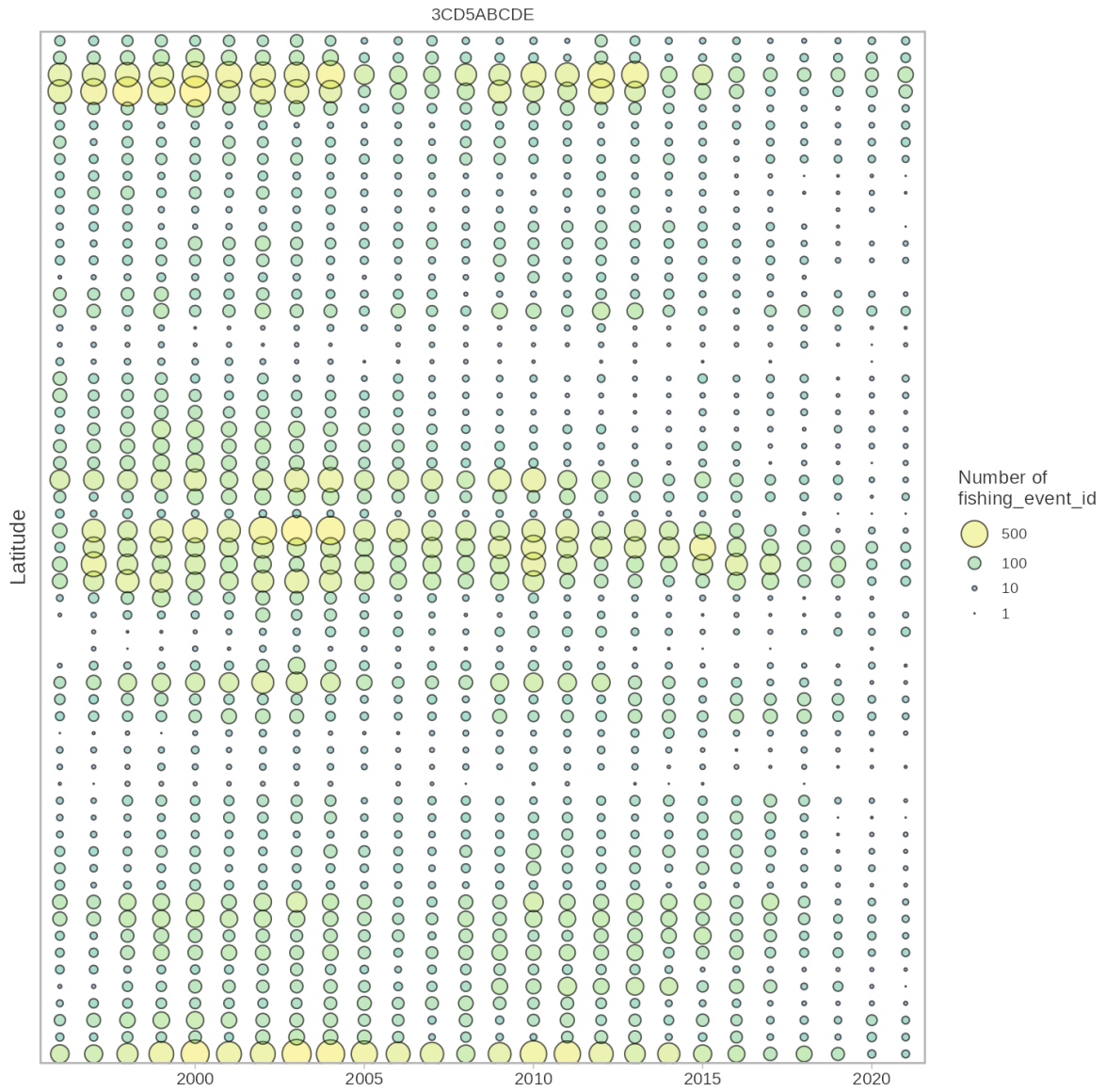


Figure C.4. Bubble plots showing distribution of the **latitude** predictor by year. The area and colour of each circle represents the number of fishing events.

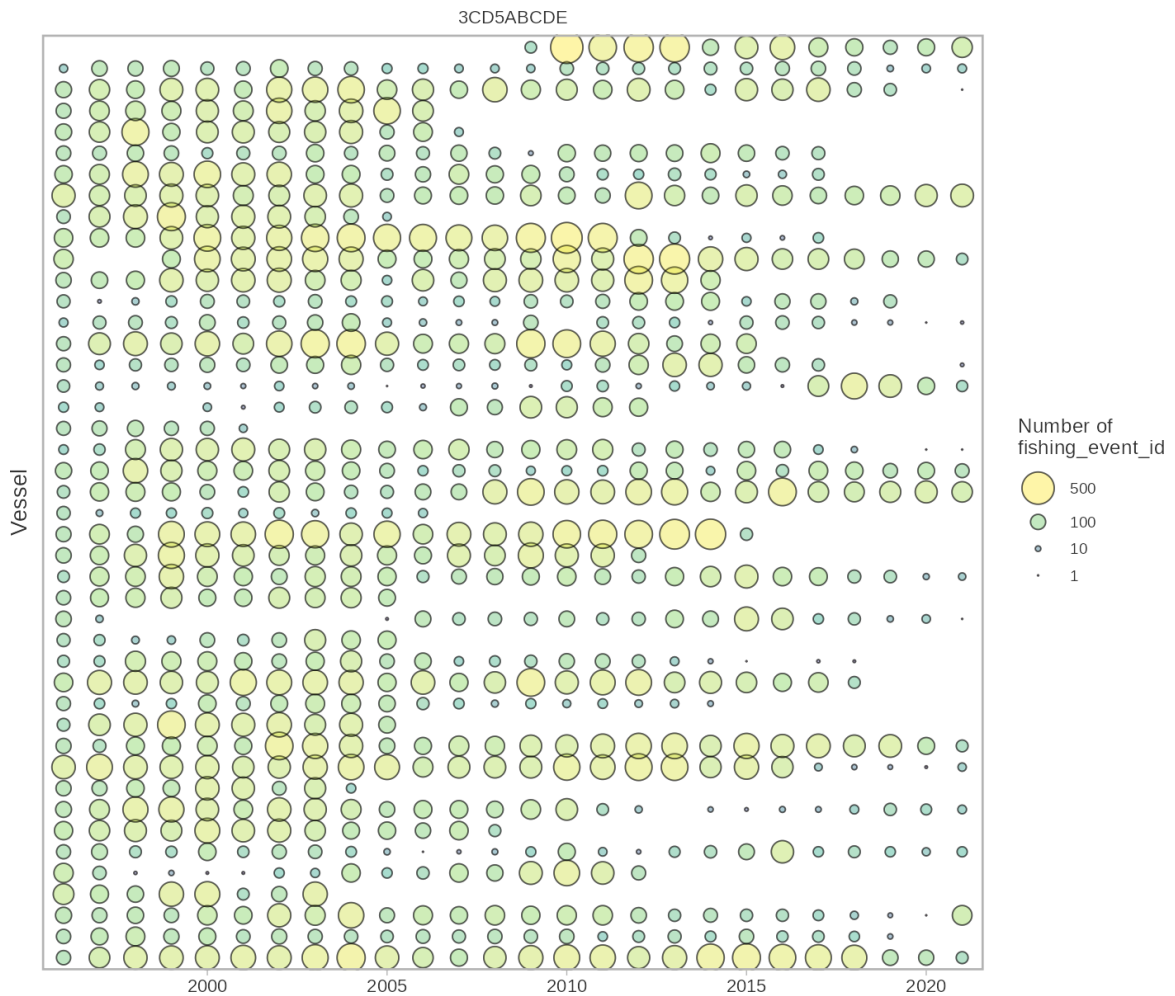


Figure C.5. Bubble plots showing distribution of the **vessel** predictor by year. The area and colour of each circle represents the number of fishing events. The vessel ID numbers of have been made anonymous by randomly sorting the vessels and assigning sequential numbers.

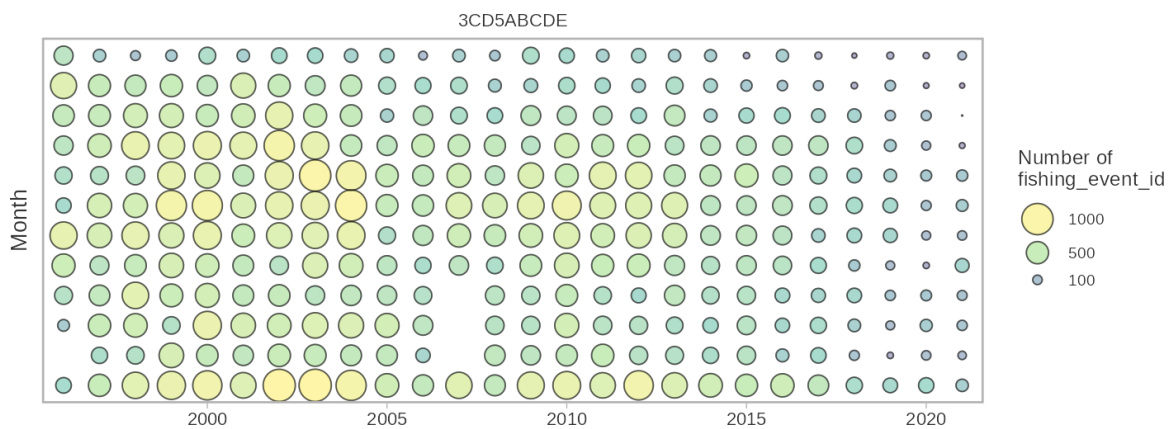


Figure C.6. Bubble plots showing distribution of the **month** predictor by year. The area and colour of each circle represents the number of fishing events.

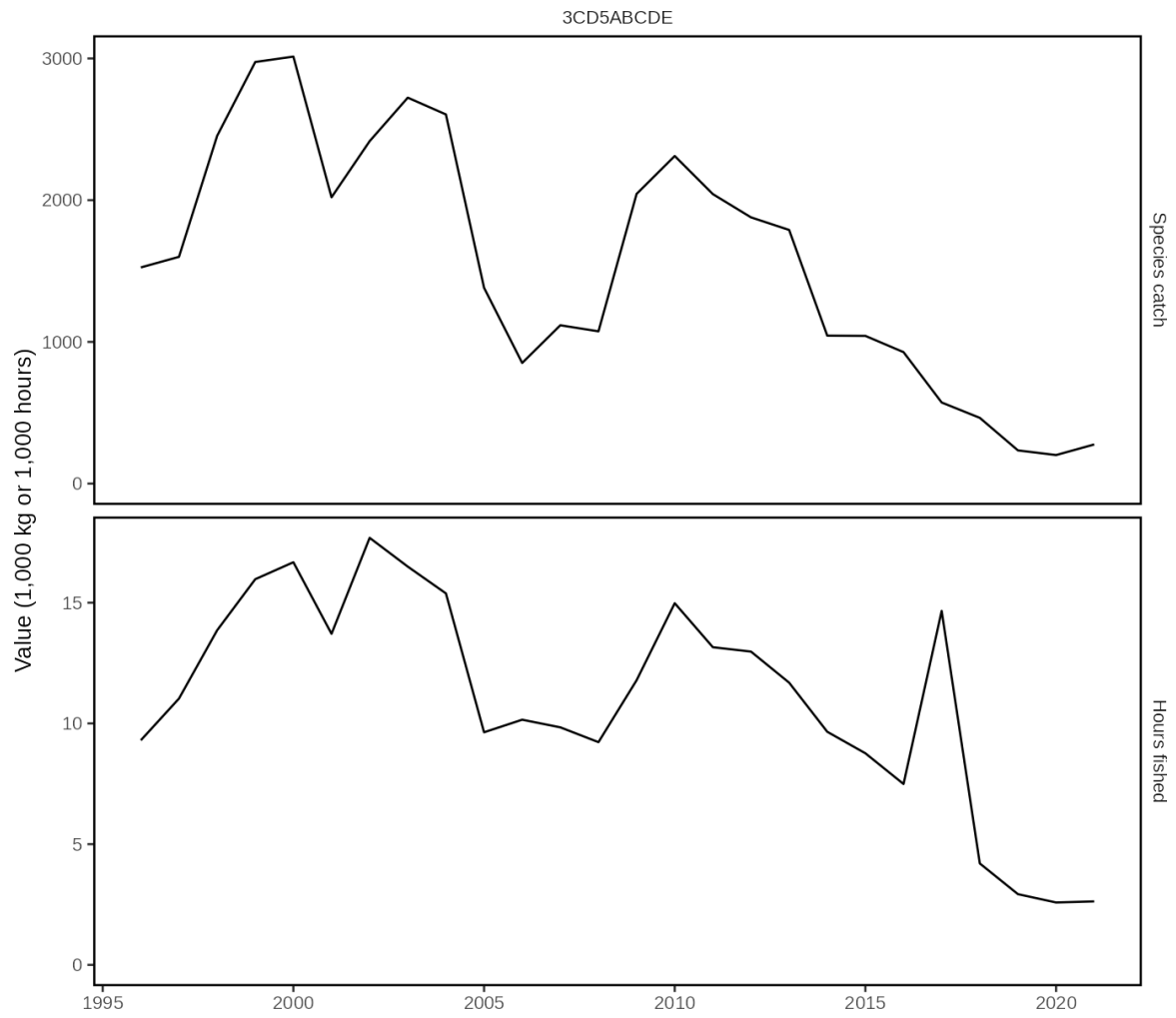


Figure C.7. Total catch and effort from the discard fleet of Arrowtooth Flounder.

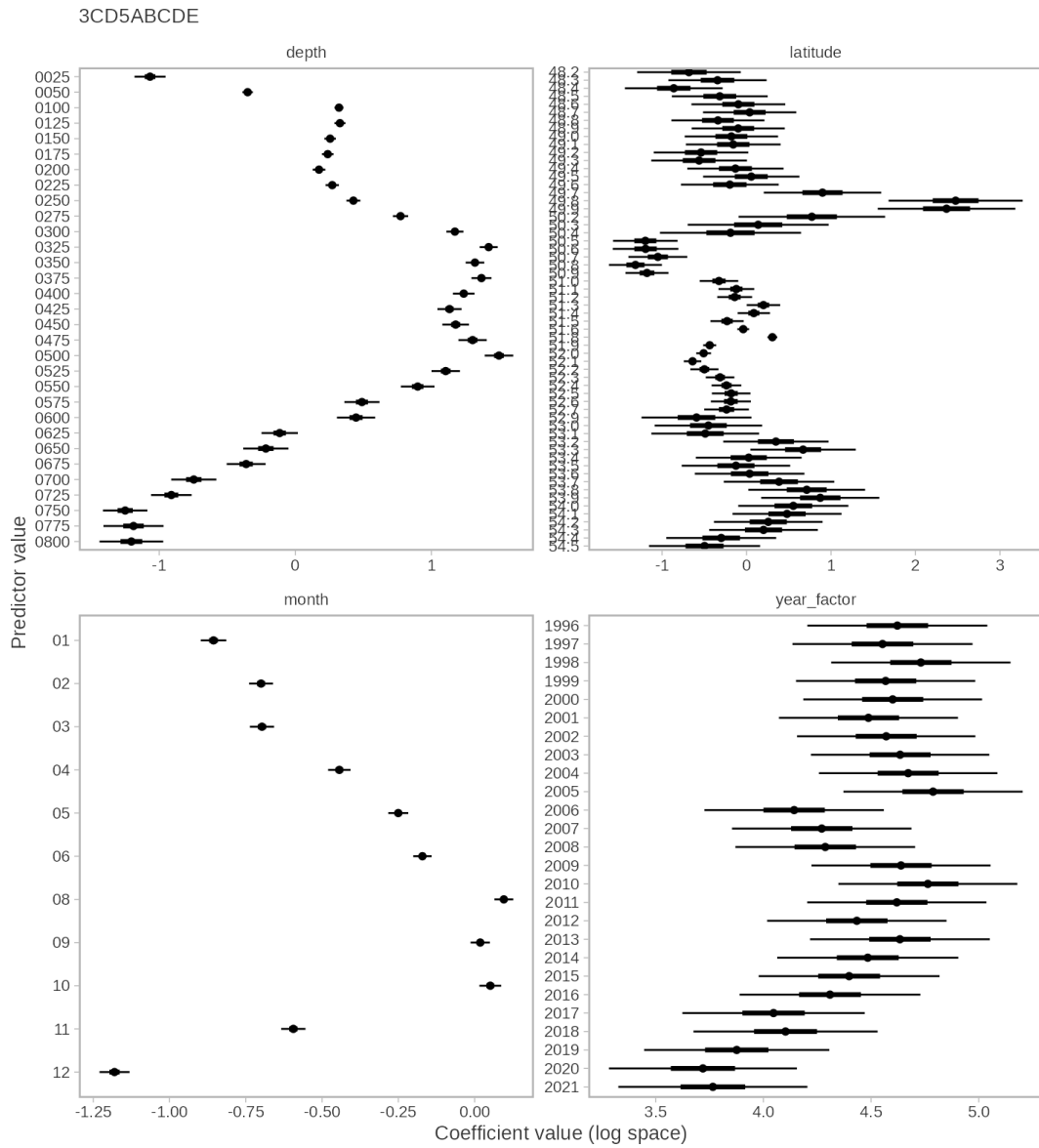


Figure C.8. Fixed effect coefficient estimates. In all cases, the values are with respect to the reference (most common) factor level (the missing factor level in each plot). Dots, thick, and thin lines represent mean, 50%, and 95% confidence intervals.

3CD5ABCDE

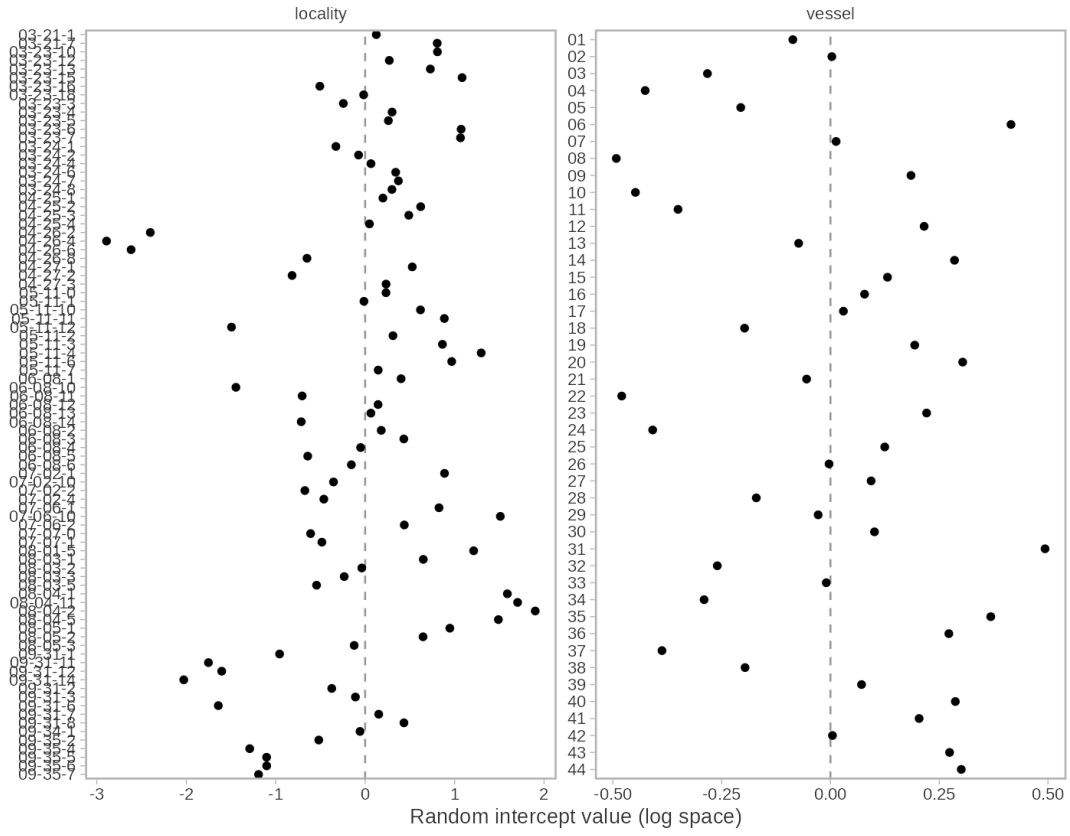


Figure C.9. Random intercept values in log space for locality and vessel.



Figure C.10. Random intercept values for the locality-year interaction effect. Panel labels represent IDs for the localities.



Figure C.11. Commercial discard CPUE indices. The red line is the standardized version, the black solid line is a version with only a year predictor with the Tweedie observation model, and the dashed line is the summed catch for the species divided by effort. The ribbons indicate the 95% (Wald) confidence intervals. The standardization process is not having a large impact on the shape of the time series here, which is likely indicative that there have not been systematic changes in the standardization factors included in the model that have impacted CPUE.

APPENDIX D. GEOSTATISTICAL STANDARDIZATION OF SURVEY INDICES

We used geostatistical spatiotemporal GLMMs (generalized linear mixed effect models) to standardize the survey indices as an alternative to design-based estimators (e.g., Shelton et al. 2014; Thorson et al. 2015; Anderson et al. 2019; Anderson et al. 2022).

We applied these models in two ways:

1. to standardize individual survey indices for use in the stock assessment model and
2. to ‘stitch’ the four synoptic trawl surveys into a single synthetic index for comparison with trends in estimated biomass from the stock assessment model and with the commercial discard CPUE index.

D.1. INDIVIDUAL SURVEY MODELLING

For the individual survey indices, we used delta/hurdle models (herein referred to as the Δ -Gamma model (Aitchison 1955)). In this model, synoptic survey catch (Figures D.1 and D.2) is defined based on a probability of encounter model and a positive catch model.

$$\Pr[C > 0] = p, \quad (\text{D.1})$$

where C is the observed catch p is the probability of encounter. The positive component given encounter is defined as

$$\Pr[C = c | C > 0] = \text{Gamma}(c, \gamma, \lambda/\gamma), \quad (\text{D.2})$$

where c is the observed catch given $C > 0$, γ is the shape parameter, λ is the expected value, and λ/γ combined is the scale parameter.

The linear component of the binomial encounter model is defined as

$$p_{s,t} = \text{logit}^{-1}(\alpha_k^{\text{Bin}} + f(\ln(D_{s,t})) + \omega_s^{\text{Bin}} + \epsilon_{s,t}^{\text{Bin}}), \quad (\text{D.3})$$

where the superscript Bin denotes binomial component parameters. The parameter α_k^{Bin} is an intercept for each survey k , $f(\ln(D_{s,t}))$ is a penalized smoother on log bottom depth, ω_s^{Bin} is a spatial random field value

$$\omega \sim \text{MVNormal}(\mathbf{0}, \Sigma_\omega), \quad (\text{D.4})$$

and $\epsilon_{s,t}^{\text{Bin}}$ is a spatiotemporal random field value

$$\epsilon \sim \text{MVNormal}(\mathbf{0}, \Sigma_\epsilon). \quad (\text{D.5})$$

The linear component of the Gamma positive catch model is defined as

$$\lambda_{s,t} = \exp(\alpha_k^{\text{Pos}} + f(\ln(D_{s,t})) + \omega_s^{\text{Pos}} + \epsilon_{s,t}^{\text{Pos}} + O_{s,t}), \quad (\text{D.6})$$

where the superscript Pos denotes positive component parameters, $O_{s,t}$ represents an offset variable (here log area swept) and the other parameters have a similar definition to the binomial model above.

D.2. SURVEY STITCHING

For the survey stitching, the models took on a similar form except that:

1. the models did not include independent intercepts for the individual years
2. the spatiotemporal random effects were instead allowed to follow a random walk (this helped constrain the model when stitching the biennial surveys)
3. we considered models that included and excluded a smoother for depth
4. we considered a Tweedie observation error model as an alternative.

The linear component of the binomial encounter model is defined as

$$p_{s,t} = \text{logit}^{-1} \left(\beta_0^{\text{Bin}} + f(d_{s,t}) + \omega_s^{\text{Bin}} + \delta_{s,t}^{\text{Bin}} \right), \quad (\text{D.7})$$

where the superscript Bin denotes binomial component parameters. The parameter β_0^{Bin} is an overall intercept, $f(d_{s,t})$ is a penalized smoother function for log depth with upper basis dimension of 5, ω_s^{Bin} is a spatial random field value

$$\omega \sim \text{MVNormal}(\mathbf{0}, \Sigma_\omega), \quad (\text{D.8})$$

and $\delta_{s,t}^{\text{Bin}}$ is a random effect drawn from a spatiotemporal random field that is assumed to follow a random walk

$$\delta_{t=1} \sim \text{MVNormal}(\mathbf{0}, \Sigma_\epsilon), \quad (\text{D.9})$$

$$\delta_{t>1} = \delta_{t-1} + \epsilon_{t-1}, \quad \epsilon_{t-1} \sim \text{MVNormal}(\mathbf{0}, \Sigma_\epsilon). \quad (\text{D.10})$$

The linear component of the Gamma positive catch model is defined as

$$\lambda_{s,t} = \exp \left(\beta_0^{\text{Pos}} + f(d_{s,t}) + \omega_s^{\text{Pos}} + \delta_{s,t}^{\text{Pos}} + O_{s,t} \right), \quad (\text{D.11})$$

where the superscript Pos denotes positive component parameters, $O_{s,t}$ represents an offset variable (here log area swept) and the other parameters have a similar definition to the binomial model above.

We also considered a Tweedie model with the linear component defined as

$$\mu_{s,t} = \exp \left(\beta_0 + f(d_{s,t}) + \omega_s + O_{s,t} + \delta_{s,t} \right), \quad (\text{D.12})$$

where the parameters have a similar definition as above in the binomial and Gamma models but the data are accounted for with a single observation distribution—the Tweedie—with associated mean, power, and scale parameters.

Furthermore, we considered versions of the above models without depth as a predictor. In total, we fit four models: Δ -Gamma with depth, Δ -Gamma without depth, Tweedie with depth, and Tweedie without depth.

Of the models considered, the models without depth made fewer assumptions. In addition, the depth data source is different from the data source used for the grid and it is possible that they represent slightly different variables. Since the trends in the models that included depth were similar to those that did not include depth, the models which do not include depth are likely better for using in the stitching process. Predictions from the Δ -Gamma model without depth are therefore shown in Figures D.3 and D.4.

D.3. CALCULATING ANNUAL STANDARDIZED BIOMASS

The total biomass b for a given year t is calculated as:

$$b_t = \sum_{j=1}^{n_j} p_{j,t} \lambda_{j,t} a_j, \quad (\text{D.13})$$

where j indexes n_j grid cells, p_j is the probability of encounter in grid cell j , λ_j is the expected catch conditional on encounter in grid cell j , and a_j is the area of grid cell j (4 km²).

D.4. MODEL FITTING

We fit our models with the R package `sdmTMB` (Anderson et al. 2019; Anderson et al. 2022), which develops input Stochastic Partial Differential Equation (SPDE) matrices using the R package `INLA` (Lindgren et al. 2011; Rue et al. 2017), calculates the model log likelihood via a TMB (Kristensen et al. 2016) template, and minimizes the negative marginal log likelihood via the R (R Core Team 2022) non-linear minimization routine `stats::nlminb()`. The Laplace approximation, as implemented in TMB, is used to integrate over random effects. We followed this optimization with a Newton optimizer, `stats::optimHess()` to further reduce the negative log likelihood.

To ensure our final optimization was consistent with convergence, we checked that all gradients with respect to fixed effects were < 0.001 and that Hessian matrices were positive-definite. We constructed our SPDE meshes such that the minimum allowed distance between vertices in the mesh (INLA ‘cutoff’) was 20 km in the coastwide model; 10 km for Queen Charlotte Sound Synoptic Survey, Hecate Strait Synoptic Survey, and the West Coast Vancouver Island Synoptic Survey; and 7 km for West Coast Haida Gwaii Synoptic Survey (smaller survey area with a sharp depth transition).

D.5. MODELLED INDICES

The geostatistical indices for individual surveys had lower CVs, on average, than the design-based indices—particularly in Queen Charlotte Sound (Fig. D.5). The Δ -Gamma and Tweedie stitched indices were similar to each other. The most noticeable difference was that including a smoother for depth slightly reduced the estimate of biomass in 2003–2004 and shrunk the confidence intervals in those years (Fig. D.6).

The geostatistical coastwide stitched survey indices all showed a strong resemblance to the commercial Discard CPUE index (Fig. D.7) with mostly overlapping confidence intervals, marked declines from 2010 to 2021, and a dip in the mid 2000s. There was some discrepancy in the initial year of the survey (2003) with the Discard CPUE being slightly higher, although the majority of the confidence intervals still overlap.

D.6. GEOSTATISTICAL INDEX FIGURES

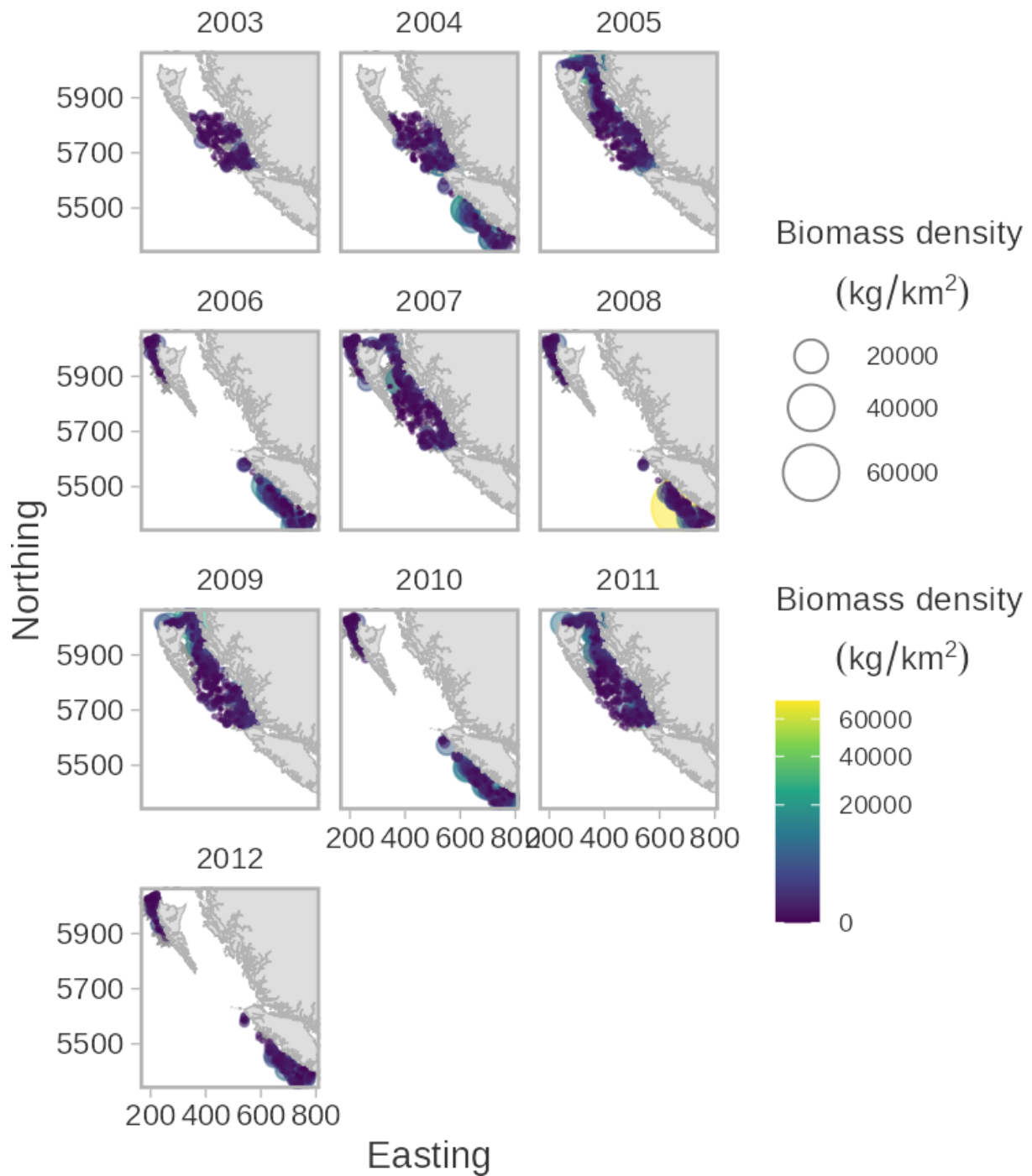


Figure D.1. Survey data bubble plot for 2003 to 2012. The area and colour of circles corresponds to set density. Sets with zero Arrowtooth Flounder catch are indicated with a grey cross.

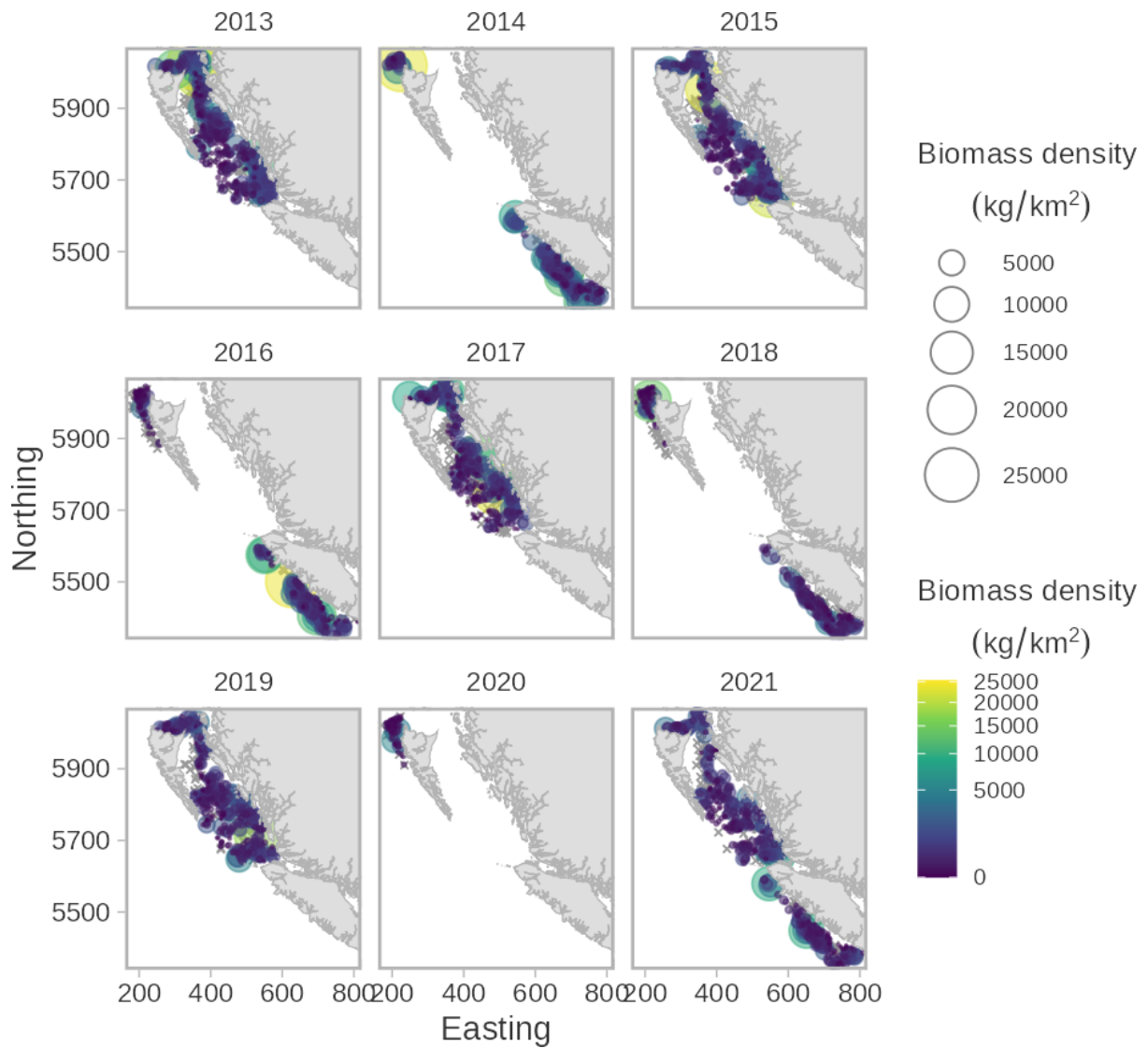


Figure D.2. Survey data bubble plot for 2013 to 2021. The area and colour of circles corresponds to set density. Sets with zero Arrowtooth Flounder catch are indicated with a grey cross.

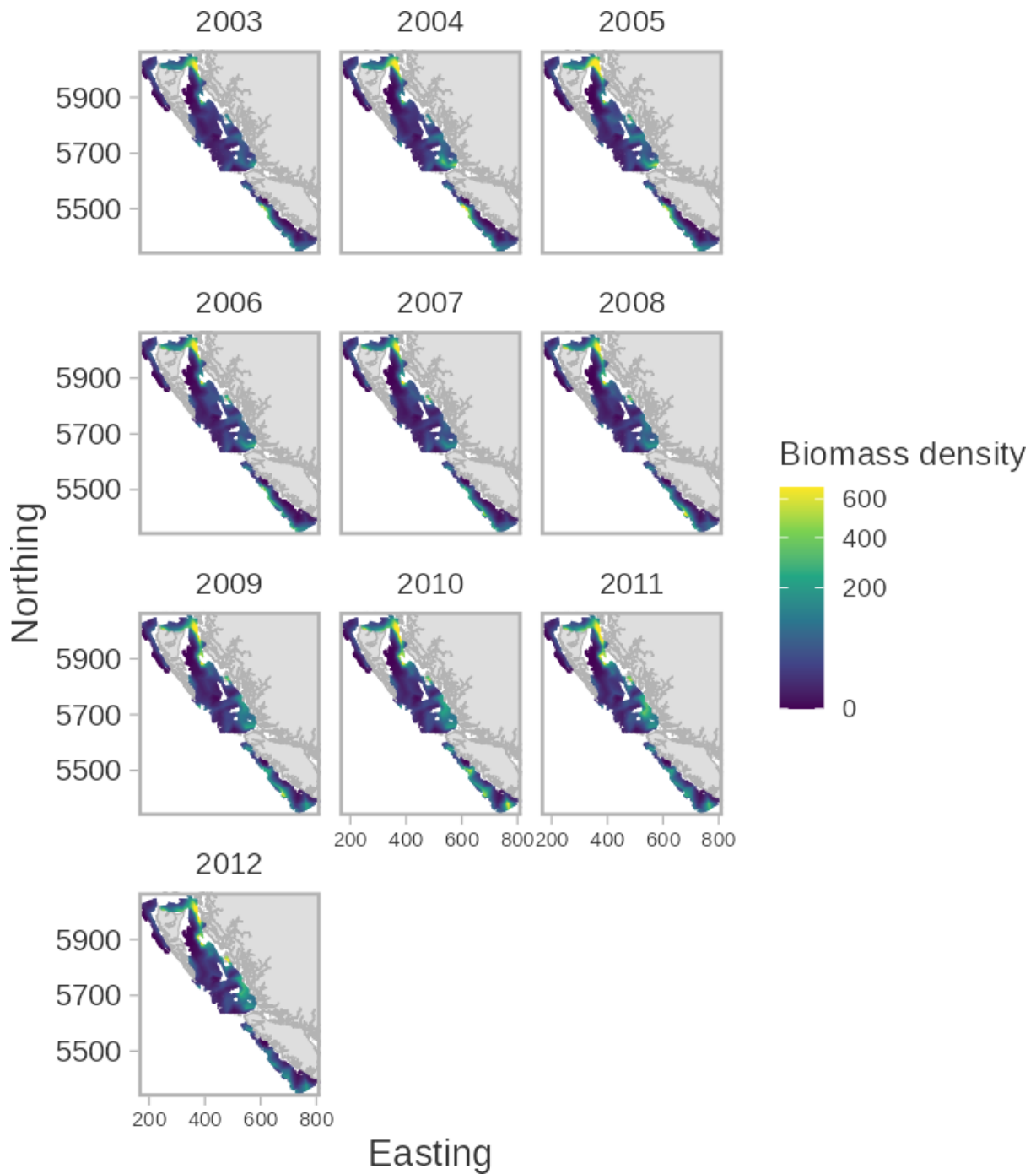


Figure D.3. Predicted Arrowtooth Flounder biomass density for 2003 to 2012 from the coastwide Δ -Gamma model without depth.

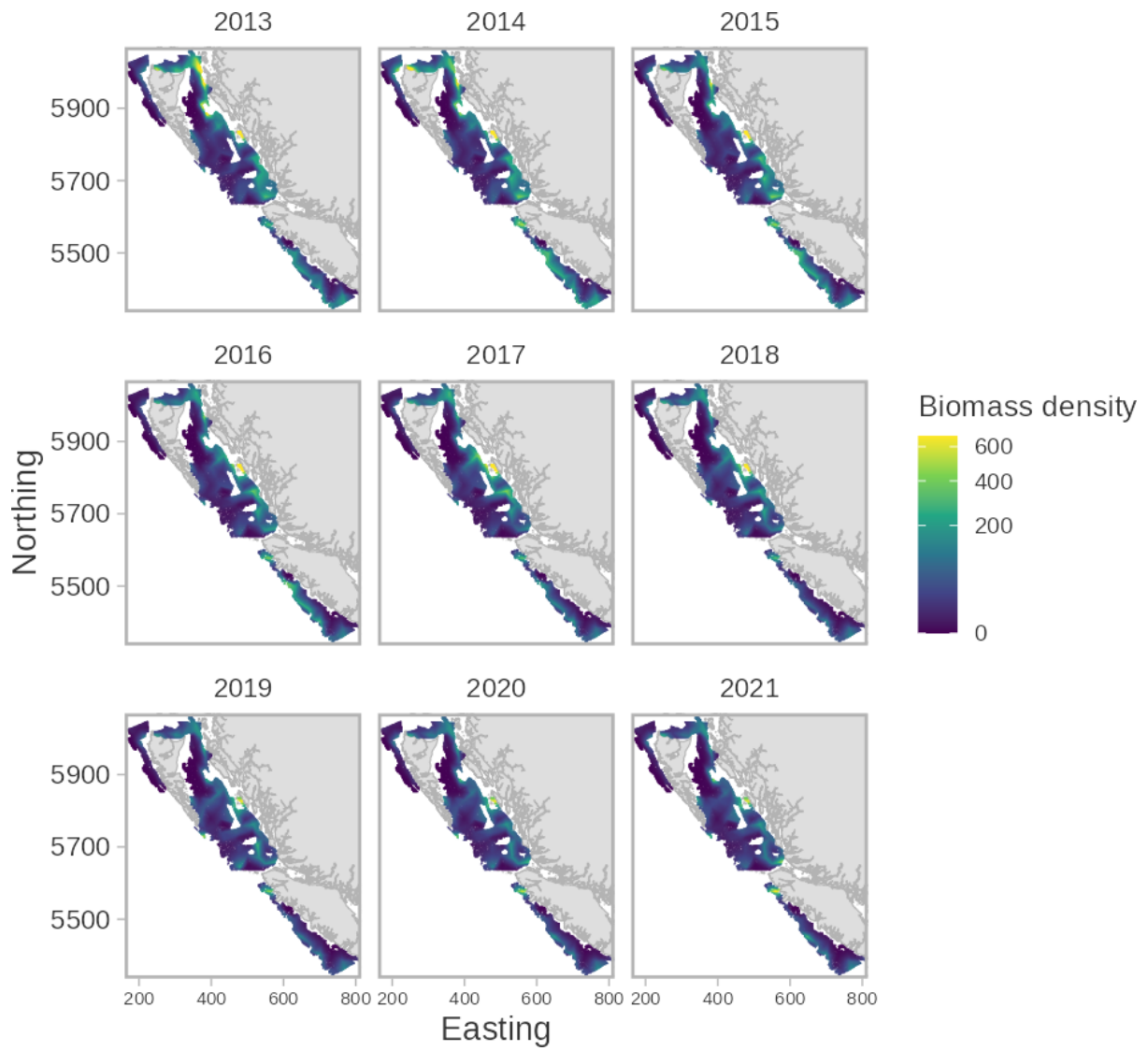


Figure D.4. Predicted Arrowtooth Flounder biomass density for 2013 to 2021 from the coastwide Δ -Gamma model without depth.



Figure D.5. Individual geostatistical indices compared to design-based indices. Lines indicate means and ribbons 95% confidence intervals.

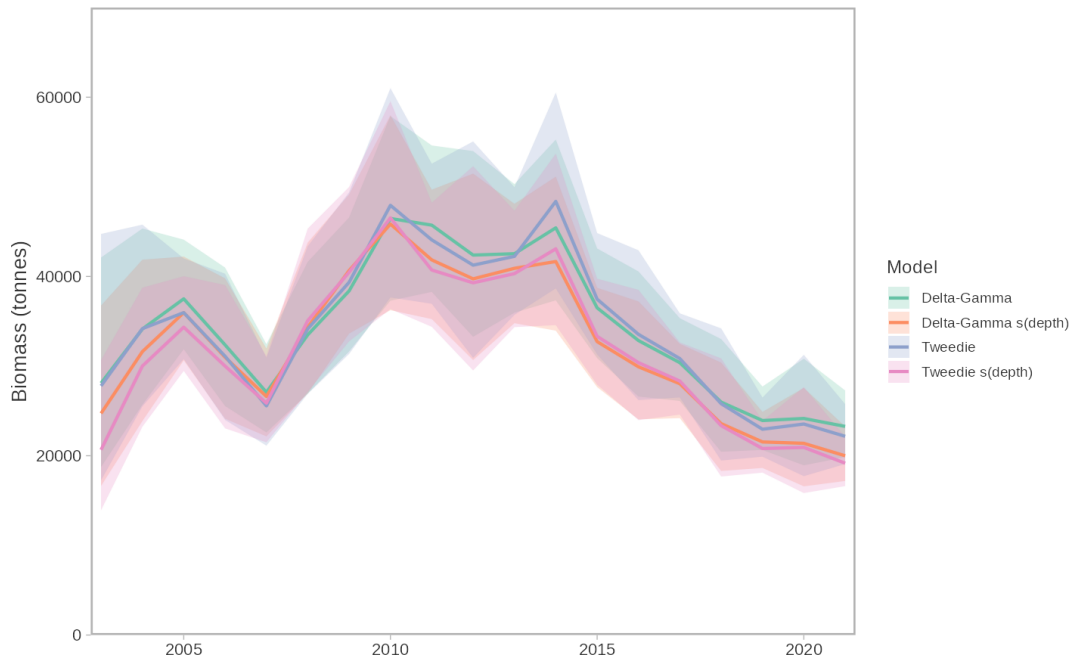


Figure D.6. Stitched indexes of abundance for Arrowtooth Flounder from four models. Lines indicate means and ribbons 95% confidence intervals.

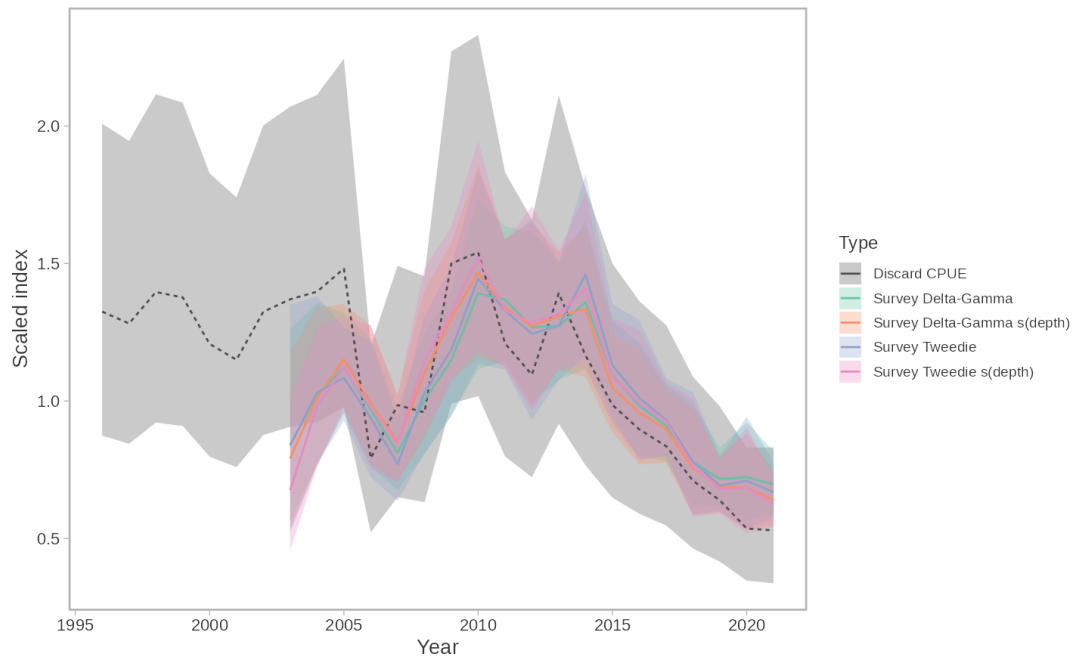


Figure D.7. Stitched indexes of abundance for Arrowtooth Flounder from four models with the commercial discard CPUE index shown in (dashed) grey. Lines indicate means and ribbons 95% confidence intervals. All indexes were centered such that their geometric means from 2003–2021 were one.

APPENDIX E. TRENDS IN BODY CONDITION

We investigated spatiotemporal patterns in Arrowtooth Flounder body condition (Nash et al. 2006) with body condition (hereafter ‘condition’) indexing the ‘plumpness’ of an organism. We do so by fitting a coastwide geostatistical model to the residuals from the Arrowtooth Flounder length-weight relationship following other recent approaches (Thorson 2015; Lindmark et al. 2022).

E.1. CONDITION MODEL

We first fit a non-spatial length-weight model of the form $\log(W_i) \sim \text{Student-t}(\text{df} = 3, \log(a) + b \log(L_i), \sigma)$, with W_i and L_i representing the weight and length for fish i and σ representing the observation error scale. The degrees of freedom (df) of the Student-t distribution is set to 3 to be robust to outliers. The variables a and b represent the estimated length-weight parameters. We fit these separately for male and female fish.

We then calculated condition factor K^{cond} as W_i/\widehat{W}_i where \widehat{W}_i refers to the predicted weight from the above weight-length model. We removed condition factor values that were greater than the 0.995 quantile or less than the 0.005 quantile to lessen the effect of outliers.

We then fit a geostatistical model following the methods in Appendix D.

Our model was of the form:

$$K_{s,t}^{\text{cond}} \sim \text{Lognormal}(\mu_{s,t}^{\text{cond}}, \sigma^{\text{cond}}), \quad (\text{E.1})$$

$$\mu_{s,t}^{\text{cond}} = \exp(\beta_0 + f(d_{s,t}) + \delta_{s,t}). \quad (\text{E.2})$$

Here, β_0 is a global intercept, $f(d_{s,t})$ is a penalized smoother for depth, and $\delta_{s,t}$ represents a spatiotemporal random field that follows a random walk

$$\delta_{t=1} \sim \text{MVNormal}(\mathbf{0}, \Sigma_\epsilon), \quad (\text{E.3})$$

$$\delta_{t>1} = \delta_{t-1} + \epsilon_{t-1}, \quad \epsilon_{t-1} \sim \text{MVNormal}(\mathbf{0}, \Sigma_\epsilon). \quad (\text{E.4})$$

We considered a model that included a spatial random field; however, the variance of this random field was estimated near zero and so we excluded it in our final model. We then calculated an annual condition-factor index as the average predicted $K_{s,t}^{\text{cond}}$ across all survey 2 km \times 2 km grid cells each year.

Finally, we also explored a model configuration where depth was included as a non-orthogonal third-order polynomial that could evolve between years via a random walk. This model included independent spatial and spatiotemporal random fields and a smoother on year, because the previous random field configuration would not converge with the increased flexibility of a time-vary depth effect.

E.2. CONDITION RESULTS

Our modeling reveals an overall decline in coastwide body condition from around 2004 until 2012, an increase until 2015, and a subsequent decline in recent years levelling off since 2019 (Fig. E.1). However, when split up by survey, we see that this overall trend masks differences that we see along the coast (Fig. E.2). The variation over time is relatively small compared to the between-region variation (Fig. E.2).

Condition within the West Coast Vancouver Island Synoptic Survey has been declining since around 2015, but condition in other survey regions has remained relatively stable in those

years (Fig. E.2). Furthermore, the coastwide index trend of an increase from 2012 to 2015 was driven largely by the Queen Charlotte Sound Synoptic Survey (Fig. E.2). We can also see these trends when looking at the spatial predictions through time (Fig. E.3).

The depth smoother indicates a higher condition factor in deeper waters (Fig. E.4), which coincides with a higher condition factor in the West Coast Vancouver Island Synoptic Survey, which covers deeper regions than the other surveys. When allowed to vary through time via a random walk, the effect of depth does not appear related to average bottom temperatures recorded on all tows at depths between 100 and 200 m for each year (Fig. E.5). This is consistent with other findings that latent unmeasured factors can explain the vast majority of spatiotemporal variability in fish condition (Lindmark et al. 2022).

There is ongoing research on this topic for all groundfish species (Philina English, Robyn Forrest pers. comm.)

E.3. CONDITION FIGURES

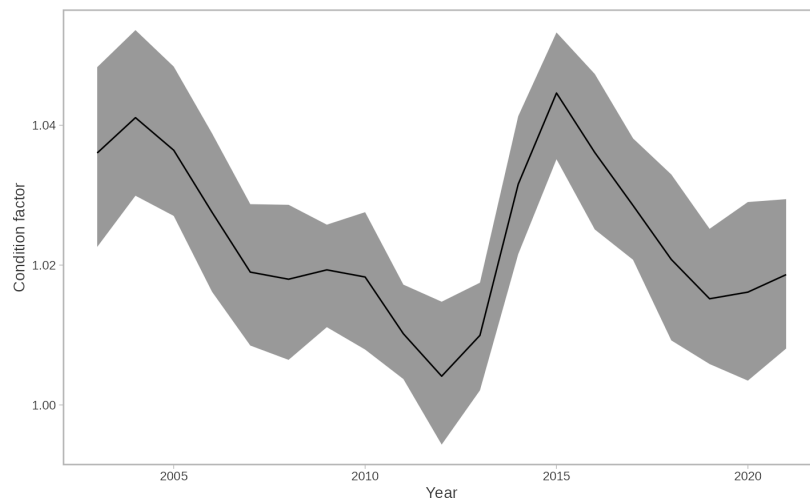


Figure E.1. Coastwide condition index. Lines and ribbons indicate means and 95% confidence intervals.

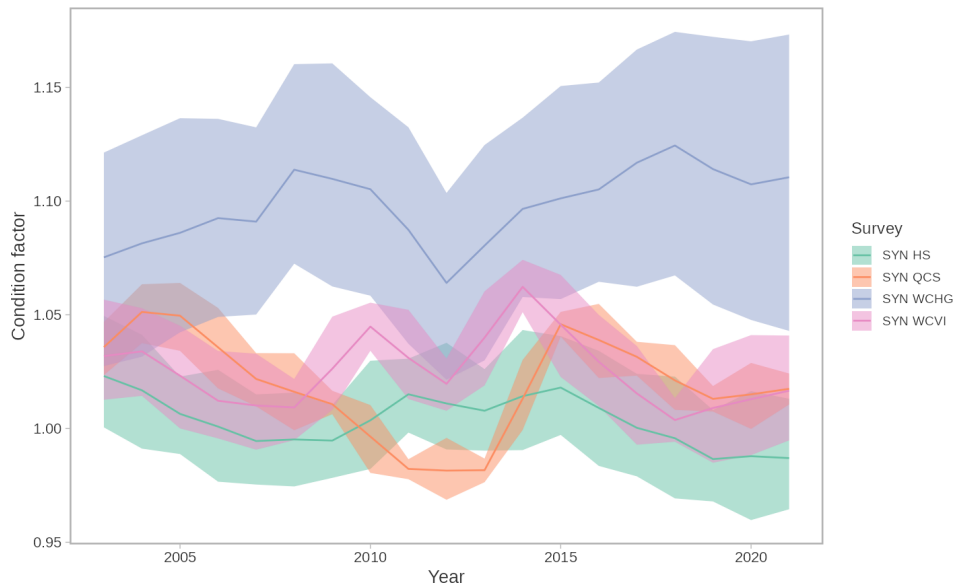


Figure E.2. Condition index split by survey region. Lines and ribbons indicate means and 95% confidence intervals.

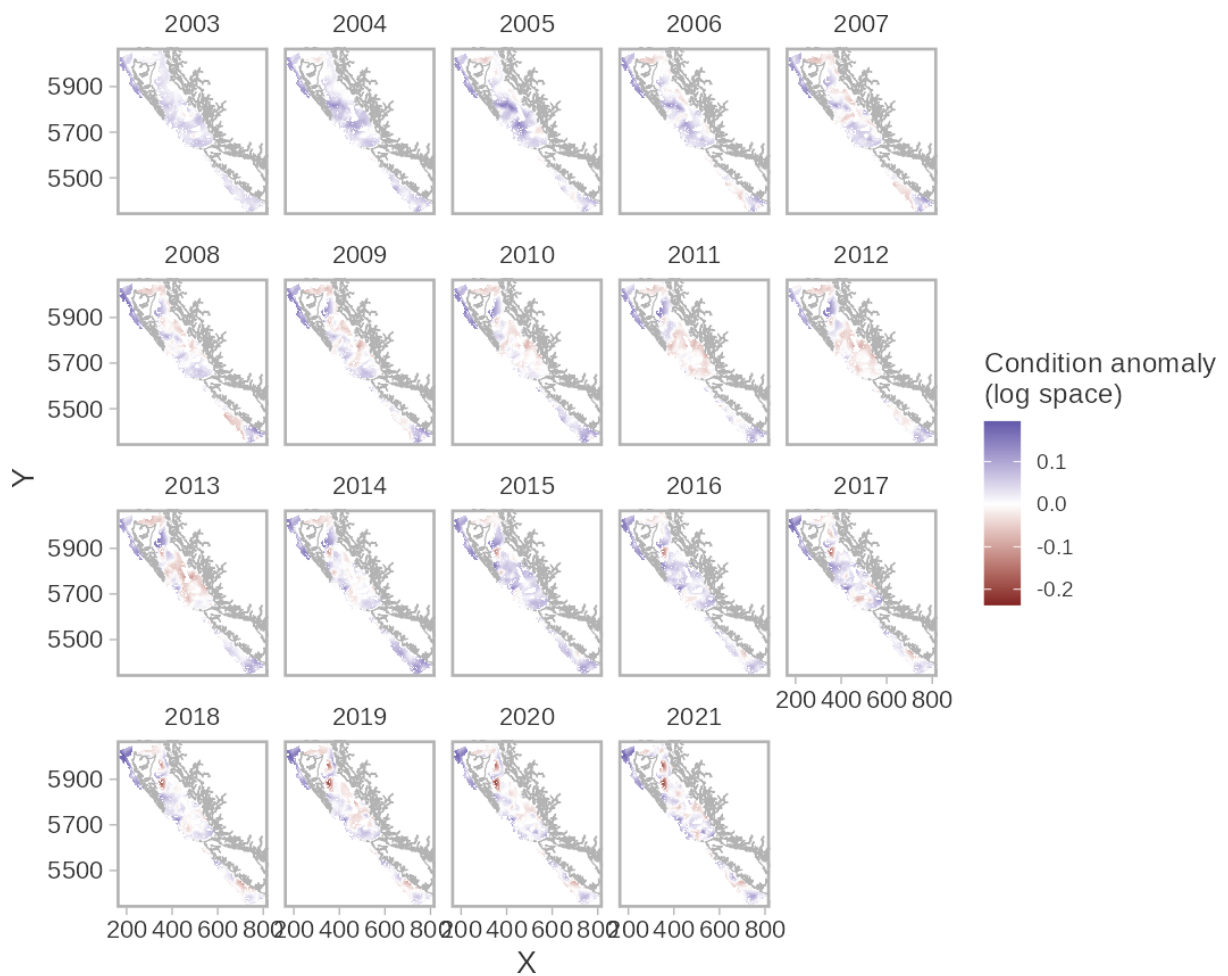


Figure E.3. Coastwide map of modelled condition anomalies. Values are shown in log space such that blue values are plumper than expected and red values less plump than expected. X and Y axes are in UTM zone 9 units of km.

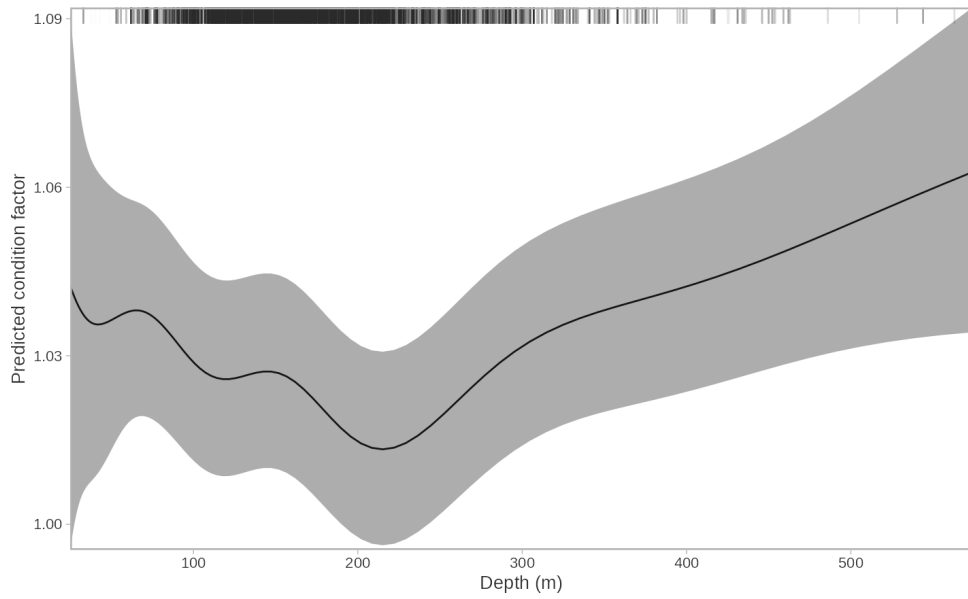


Figure E.4. Log depth smoother from the condition model. Line represents mean and the ribbon 95% confidence intervals. Horizontal rug lines are shown on the top where data are present.

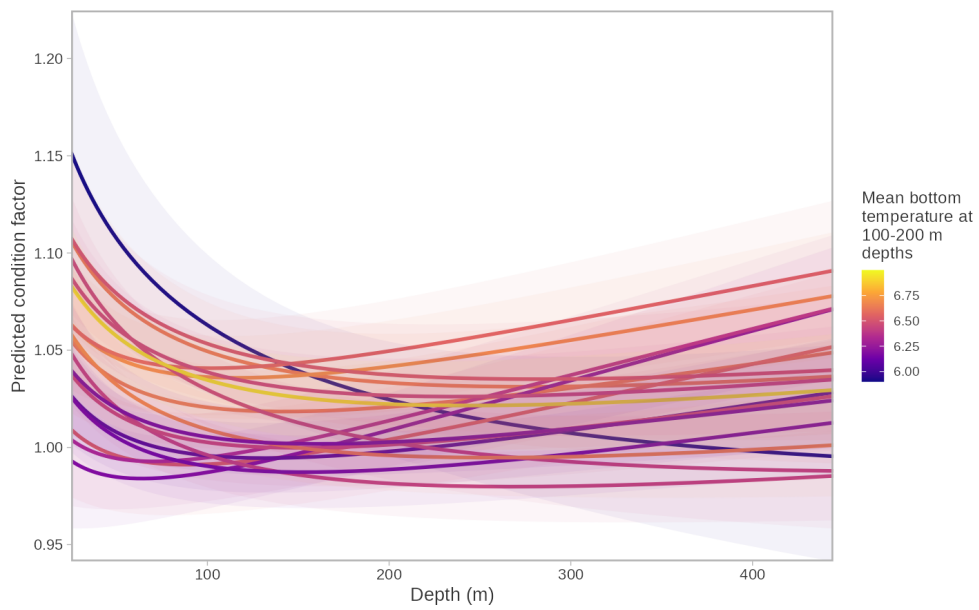


Figure E.5. Time-varying third order polynomial effect of depth on condition. Line represents mean and the ribbon 95% confidence intervals and both are coloured by the mean bottom temperatures (degrees C) recorded on all trawl tows at depths between 100 and 200 m in each year.

APPENDIX F. ECOSYSTEM CONSIDERATIONS

Arrowtooth Flounder are habitat and prey generalists (Fargo et al. 1981; Yang 1993; Doyle et al. 2018). However, we report diet composition from Alaska, because no diet data are collected on any of the surveys used in this assessment. Based on almost 2,000 stomachs collected in the early 1990s in the GOA, Arrowtooth Flounder consumed a diet dominated by zooplankton, fish, and benthic invertebrates (Yang 1993; Spies et al. 2019). For juveniles (≤ 20 cm TL), euphausiids made up nearly 60% of their diet, followed by capelin at 24%. Adults consumed mostly capelin (*Mallotus villosus*), euphausiids, adult and juvenile Walleye Pollock (*Gadus chalcogrammus*), Pandalid shrimp, herring, and other forage fish, none of which account for more than 22% of the overall diet. In the same region and time period, predation by Pacific Cod (*Gadus macrocephalus*), Pacific Halibut (*Hippoglossus stenolepis*), and Steller sea lions (*Eumetopias jubatus*) together explained about 10% of adult arrowtooth mortality and the flatfish trawl fishery accounted for 2% (Spies et al. 2019). Juvenile Arrowtooth Flounder mortality was caused by adult Arrowtooth Flounder, and both adult and juvenile pollock, but the total of these mortality sources is less than 7% of juvenile Arrowtooth Flounder production (Spies et al. 2019).

Migration patterns are not well known for Arrowtooth Flounder, but there is some indication that larger fish may migrate to deeper water in winter and shallower water in summer (Rickey 1995; Fargo and Starr 2001). Spawning and hatching occur in these deeper waters (> 350 m) along the continental shelf break in fall and winter (Rickey 1995; Blood et al. 2007). At these depths, predation risk is relatively low, and cold temperatures along with intrinsically low metabolic rates ensure extended availability of yolk reserves, lowering the risk of larval starvation (Doyle et al. 2018). Larval duration and drift is protracted, contributing to widespread delivery of larvae to coastal, continental shelf and slope waters and resulting in low connectivity between spawning and settlement areas (Doyle et al. 2018). In the GOA, the smallest fish (< 10 cm) were typically found shallower than 200 m with all immature fish (< 30 cm) concentrating at < 400 m. In colder years, these size classes tended to be found deeper. In contrast, mature fish (30–60 cm) tended to be found deepest (> 800 m) in warmer years (Doyle et al. 2018). A preliminary climate-related vulnerability assessment for GOA indicated low risk, high resilience overall; however, there exists some potential stage-specific sensitivity to temporal mis-match between larvae and zooplankton prey with increased temperatures (Doyle et al. 2018).

Within Canadian Pacific waters, a lack of correlation between change in abundance and changes in condition suggests that bottom-up ecosystem effects are unlikely to be driving overall stock status for Arrowtooth Flounder. Coastwide within Canada, the condition index dropped steadily between 2004 and 2012 (Fig. E.1), while the survey biomass index for the same area increased by over 50% (Fig. D.7). Likewise, a sharp increase in condition index in 2015 has not been associated with any positive trajectories in biomass in the following 7 years.

The evidence that condition tends to be higher in deeper, and therefore cooler, waters is consistent with findings of some potential sensitivity to temperature (English et al. 2021). Local warming (positive temperature velocity) was associated with declines in biomass only in already warmer areas, and associated with increases biomass of immatures (~ 38 cm for females, ~ 31 cm for males) in cooler areas. However, when the shape of depth effect on condition was allowed to vary between year, there was not an obvious difference between warmer and cooler years (Fig. E.5). If there is any weak association, it might be that condition is higher in shallower waters in the warmer year, which is consistent with the coastwide condition index also climbing steeply between 2013 and 2015, the period that includes the 2014–2016 marine heat wave and spikes in the abundances of some more southern species of euphausiid (Boldt et al. 2021). In contrast, mean body condition in the GOA was low during the marine heat wave (2015) and even lower in 2017 (Spies et al. 2019). This was hypothesized to be due to both increased energetic demands with warm temperatures and lack of forage

fish prey. Marine heat wave conditions occurred again in the Northeast Pacific in 2018, and 2019–2020, although they were not as extreme as in 2014–2016 (Boldt et al. 2021).

Of what are presumed to be the dominant natural predators (based on data from Alaska (Spies et al. 2019)) few appear likely to cause the declines in Arrowtooth Flounder spawning biomass since 2011 (Figure 7). Walleye Pollock, predators of juvenile Arrowtooth Flounder, have experienced an overall increase in survey biomass punctuated by a shortterm declines that either coincided with (southern stock) or preceded (northern stock) the downturn in Arrowtooth Flounder. Abundances of both Pacific Cod (Forrest et al. 2020) and Pacific Halibut (DFO 2022) appear to have been relatively stable at the decadal scale, despite considerable interannual variability. Only Steller's Sea Lion have experienced a steady population growth rate of around 4.3% per year during the past two decades (DFO 2021), but without any obvious changes in trajectory that could be associated with the changes in Arrowtooth Flounder spawning biomass.

APPENDIX G. MODEL DESCRIPTION

G.1. INTRODUCTION

Stock Assessment modelling was done using the Integrated Statistical Catch Age Model (ISCAM), developed by S. Martell (Martell et al. 2011). ISCAM was written using the AD Model Builder framework. ISCAM is a statistical catch-at-age model with many modelling options implemented in a Bayesian estimation framework. The authors have modified ISCAM substantially over the years, and further extensive modifications were made for this assessment. The package `gfiscam`, on the `WSL2` branch, contains all code and Makefiles necessary to compile ISCAM to run the models presented in this assessment. The `gfiscam` repository can be found on GitHub, in the `pbs-assess` organization's repository list.

The execution of all ISCAM models was performed in Linux using Bourne again shell (Bash) scripts. Compilation of results, and generation of tables and figures was done in R using the `gfiscamutils` package developed by the authors. The `gfiscamutils` repository can be found on GitHub, in the `pbs-assess` organization's repository list.

G.2. MODEL DESCRIPTION

This section contains the documentation and equations for the ISCAM age-structured model, its steady-state version that is used to calculate reference points, the observation models used in predicting observations, and the components of the objective function that formulate the statistical criterion used to estimate model parameters. A documented list of symbols used in model equations is given in Table G.1. The documentation presented here is essentially a revised version of the ISCAM user guide (Martell 2011).

Note that all the model equations are presented for a sex structured model with S sexes. Models can therefore be constructed with data and estimates for two sexes, female only, or both male and female combined into a single sex bin.

The following list describes modifications specific to the Arrowtooth Flounder assessment:

1. Split sex, $S = 2$.
2. Two-fleet commercial fishery.
3. Total mortality is constant across ages, $Z_{t,a} = Z_t$. Age- and Sex- specific mortality was tried but the model would not converge with the extra parameters required.
4. Sex-specific selectivity.
5. Optional time-varying selectivity for the Queen Charlotte Sound Synoptic Survey.
6. Age-composition observations were assumed to come from a Dirichlet-multinomial distribution.
7. Fecundity and maturity are synonymous and used interchangeably.
8. Unfished spawning biomass is represented as SB_0 or B_0 , and includes biomass from both sexes.

G.3. ANALYTIC METHODS: EQUILIBRIUM CONSIDERATIONS

G.3.1. A Steady-State Age-Structured Model

For the steady-state conditions represented in Section G.5.6, we assume the parameter vector Θ in Eq. G.15 is unknown and would be estimated by fitting ISCAM to data.

For a given set of growth parameters and maturity-at-age parameters defined by Eq. G.16, growth is assumed to follow von Bertalanffy (Eq. G.17). Mean weight-at-age is given by the allometric relationship in Eq. G.18, and the age-specific vulnerability and fecundity are given by age-based logistic functions (Eqns. G.19 and G.20). The terms vulnerability and selectivity are used interchangeably throughout this document, although, technically, selectivity refers to the fishing gear, while vulnerability refers to all processes affecting the availability of fish to the fishery. Selectivity parameters can be fixed or estimated.

Survivorship for unfished and fished populations is defined by Eqns. G.21 and G.22, respectively. It is assumed that all individuals ages A and older (i.e., the plus group) have the same total mortality rate. The incidence functions refer to the life-time or per-recruit quantities such as spawning biomass per recruit (ϕ_E and ϕ_e , Eq. G.23) or vulnerable biomass per recruit (ϕ_B and ϕ_b , Eq. G.24). Note that upper and lower case subscripts denote unfished and fished conditions, respectively. Unfished spawning biomass is given by Eq. G.26 and the recruitment compensation ratio (Myers and Mertz 1998) is given by Eq. G.27. The steady-state equilibrium recruitment R_e is given by Eq. G.29. It is assumed that recruitment follows a Beverton-Holt stock recruitment model of the form shown in Eq. G.29, where the maximum juvenile survival rate s_o is given by:

$$s_o = \frac{\kappa}{\phi_E}$$

and the density-dependent term is given by:

$$\beta = \frac{\kappa - 1}{R_o \phi_E}$$

which simplifies to Eq. G.29. The equilibrium yield C_e for a given fishing mortality rate is given by Eq. G.30. These steady-state conditions are critical for determining various reference points such as F_{MSY} and B_{MSY} .

G.3.2. MSY-Based Reference Points

When defining reference points for this assessment, the two commercial trawl fleets were used to calculate MSY quantities. ISCAM calculates F_{MSY} by finding the value of F_e that results in the zero derivative of Eq. G.30. This is accomplished numerically using a Newton-Raphson method where an initial guess for F_{MSY} is set equal to $1.5M$ (Martell 2011; Grandin and Forrest 2017).

G.4. ANALYTIC METHODS: STATE DYNAMICS

The estimated parameter vector in ISCAM is defined in Eq. G.31 in Section G.5.7. The estimated parameters R_0 , h , and M , are the leading population parameters that define the overall scale and productivity of the population.

Variance components of the model were partitioned using an errors in variables approach. The key variance parameter is the inverse of the total variance ϑ^2 (i.e., total variance). This parameter can be fixed or estimated, and was estimated for this model. The total variance is partitioned into observation and process error components by the model parameter ρ , which represents the proportion of the total variance that is due to observation error (Eq. G.32) (Punt and Butterworth 1999; Deriso et al. 2007).

The unobserved state variables in Eq. G.33 include the numbers-at-age of sex s in year t ($N_{t,a,s}$), the spawning stock biomass in year t (SB_t) and the total age-specific total mortality

rate ($Z_{t,a,s}$). The initial numbers-at-age in the first year (Eq. G.34) and the annual recruits (Eq. G.35) are treated as estimated parameters and used to initialize the numbers-at-age array. Vulnerability-at-age is here assumed time-invariant and is modeled using a two-parameter logistic function (Eq. G.36). The annual fishing mortality for each gear k in year t is the exponent of the estimated vector $\Gamma_{k,t}$ (Eq. G.37). The vector of log fishing mortality rate parameters $\Gamma_{k,t}$ is a bounded vector with a minimum value of -30.0 and an upper bound of 3.0 . In arithmetic space this corresponds to a minimum value of $9.36e^{-14}$ and a maximum value of 20.01 for annual fishing mortality rates. In years where there are zero reported catches for a given fleet, no corresponding fishing mortality rate parameter is estimated and the implicit assumption is there was no fishery in that year.

State variables in each year are updated using Eqns. G.38–G.41, where the spawning biomass is the product of the numbers-at-age and the mature biomass-at-age (Eq. G.38). The total mortality rate is given by Eq. G.39, and the total catch (in weight) for each gear is given by Eq. G.40, assuming that both natural and fishing mortality occur simultaneously throughout the year.

Numbers-at-age are propagated over time using Eq. G.41, where members of the plus group (age A) are all assumed to have the same total mortality rate.

Recruitment to age k is assumed to follow a Beverton-Holt model for Arrowtooth Flounder (Eq. G.42) where the maximum juvenile survival rate (s_0) is defined by $s_0 = \kappa/\phi_E$. For the Beverton-Holt model, β is derived by solving Eq. G.42 for β conditional on estimates of h and R_0 .

G.5. RESIDUALS, LIKELIHOODS, AND OBJECTIVE FUNCTION VALUE COMPONENTS

The objective function contains five major components:

1. The negative log-likelihood for the catch data
2. The negative log-likelihood for the relative abundance data
3. The negative log-likelihood for the age composition data
4. The prior distributions for model parameters
5. Three penalty functions that are invoked to regularize the solution during intermediate phases of the non-linear parameter estimation. The penalty functions:
 - a. constrain the estimates of annual recruitment to conform to a Beverton-Holt stock-recruit function
 - b. weakly constrain the log recruitment deviations to a normal distribution
 - c. weakly constrain estimates of log fishing mortality to a normal distribution ($\sim N(\ln(0.2), 4.0)$) to prevent estimates of catch from exceeding estimated biomass..

Tests showed the model was insensitive to changes in the penalty function parameters, indicating that the other likelihood components and prior probability distributions were the most important contributors to the objective function.

The objective function components are discussed in more detail in the following sections.

G.5.1. Catch Data

It is assumed that the measurement errors in the catch observations are log-normally distributed, and the residuals given by:

$$\eta_{k,t} = \ln(C_{k,t} + o) - \ln(\hat{C}_{k,t} + o) \quad (\text{G.1})$$

where o is a small constant (e^{-10}) to ensure the residual is defined in the case of a zero catch observation. The residuals are assumed to be normally distributed with a user-specified standard deviation σ_C . At present, it is assumed that observed catches for each gear k have the same standard deviation. The negative log-likelihood (ignoring the scaling constant) for the catch data is given by:

$$\ell_C = \sum_k [T_k \ln(\sigma_C) + \frac{\sum_t (\eta_{k,t})^2}{2\sigma_C^2}] \quad (\text{G.2})$$

where T_k is the total number of catch observations for gear type k .

G.5.2. Relative Abundance Data

The relative abundance data are assumed to be proportional to spawning biomass that is vulnerable to the sampling gear:

$$V_{k,t} = \sum_a S N_{t,a} e^{-\lambda_{k,t} Z_{t,a}} v_{k,a} w_a \quad (\text{G.3})$$

where $v_{k,a}$ is the age-specific selectivity of gear k , and w_a is the mean-weight-at-age. A user specified fraction of the total mortality $\lambda_{k,t}$ adjusts the numbers-at-age to correct for survey timing. The residuals between the observed and predicted relative abundance index is given by:

$$\epsilon_{k,t} = \ln(I_{k,t}) - \ln(q_k) + \ln(V_{k,t}) \quad (\text{G.4})$$

where $I_{k,t}$ is the observed relative abundance index, q_k is the catchability coefficient for index k , and $V_{k,t}$ is the predicted vulnerable biomass at the time of sampling. The catchability coefficient q_k is evaluated at its conditional maximum likelihood estimate:

$$q_k = \frac{1}{N_k} \sum_{t \in I_{k,t}} \ln(I_{k,t}) - \ln(V_{k,t})$$

where N_k is the number of relative abundance observations for index k (Walters and Ludwig 1994). The negative log-likelihood for relative abundance data is given by:

$$\ell_I = \sum_k \sum_{t \in I_{k,t}} \ln(\sigma_{k,t}) + \frac{\epsilon_{k,t}^2}{2\sigma_{k,t}^2} \quad (\text{G.5})$$

where:

$$\sigma_{k,t} = \frac{\rho\varphi^2}{\omega_{k,t}}$$

where $\rho\varphi^2$ is the proportion of the total error that is associated with observation errors, and $\omega_{k,t}$ is a user specified relative weight for observation t from gear k .

The $\omega_{k,t}$ terms allow each observation to be weighted relative to the total error $\rho\varphi^2$. Note that if $\omega_{k,t} = 0$ then Eq. G.5 is undefined; therefore, ISCAM adds a small constant to $\omega_{k,t}$ (e^{-10} , which is equivalent to assuming an extremely large variance) to ensure the likelihood can be evaluated. In this assessment, values for $\omega_{k,t}$ were set to the inverse of the annual CVs from the survey or Discard CPUE index (Table 4).

G.5.3. Age Composition Data

Multivariate Distribution

Sampling theory suggests that age composition data are derived from a multinomial distribution (Fournier and Archibald 1982). However, applications of ISCAM have typically assumed that age-proportions are obtained from a multivariate logistic (also called logistic normal) distribution (Schnute and Richards 1995; Richards et al. 1997). ISCAM departs from the traditional multinomial model due to choices regarding weighting of the age-composition data in the objective function. First, the multinomial distribution requires the specification of an effective sample size. This weighting may be done arbitrarily or through iterative re-weighting Gavaris and Ianelli (2002), and in the case of multiple and potentially conflicting age-proportions, this procedure may fail to converge. The assumed effective sample size can have a large impact on the overall model results.

A feature of the multivariate logistic distribution is that the age-proportion data can be weighted based on the conditional maximum likelihood estimate of the variance in the age-proportions. Therefore, the contribution of the age-composition data to the overall objective function is 'self-weighting' and is conditional on other components in the model. Ignoring the subscript for gear type for clarity, the observed and predicted proportions-at-age must satisfy the constraint:

$$\sum_{a=1}^A p_{t,a} = 1$$

for each year. The residuals between the observed ($p_{t,a}$) and predicted proportions ($\hat{p}_{t,a}$) is given by:

$$\eta_{t,a} = \ln(p_{t,a}) - \ln(\hat{p}_{t,a}) - \frac{1}{A} \sum_{a=1}^A [\ln(p_{t,a}) - \ln(\hat{p}_{t,a})] \quad (\text{G.6})$$

The conditional maximum likelihood estimate of the variance is given by

$$\hat{\tau}^2 = \frac{1}{(A-1)T} \sum_{t=1}^T \sum_{a=1}^A \eta_{t,a}^2$$

and the negative log-likelihood evaluated at the conditional maximum likelihood estimate of the variance is given by:

$$\ell_A = (A-1)T \ln(\hat{\tau}^2). \quad (\text{G.7})$$

In short, the multivariate logistic likelihood for age-composition data is just the log of the residual variance weighted by the number observations over years and ages. The multivariate logistic was used in the 2015 assessment and bridge models in this assessment prior to the 1 bridge model (Section 2.4.1).

Dirichlet Multinomial Distribution

The Dirichlet Multinomial (DM) was implemented in ISCAM for this assessment as a replacement for iterative reweighting of age data and instead of the multivariate logistic likelihood, which had convergence issues with several of the more complex model configurations. The DM avoids estimates effective sample sizes from within the model. The distribution incorporates one additional parameter per fleet compared to the multinomial. This method has been tested against the iterative reweighting approach introduced in McAllister and Ianelli (1997), with similar results (Thorson et al. 2016).

The likelihood for the DM is similar to the multinomial likelihood, with two extra terms (Eq. G.8). The first term of the DM likelihood $\frac{\Gamma(n+1)}{\prod_{a=1}^{a_{max}} \Gamma(n\tilde{\pi}_a+1)}$ is the multinomial likelihood. This term does not depend on parameters and guarantees a multinomial likelihood when $\beta \gg n$.

$$L(\pi, \beta | \tilde{\pi}, n) = \frac{\Gamma(n+1)}{\prod_{a=1}^{a_{max}} \Gamma(n\tilde{\pi}_a+1)} \frac{\Gamma(\beta)}{\Gamma(n+\beta)} \prod_{a=1}^{a_{max}} \frac{\Gamma(n\tilde{\pi}_a + \beta\pi_a)}{\Gamma(\beta\pi_a)} \quad (\text{G.8})$$

The effective sample size n_{eff} is:

$$n_{\text{eff}} = \frac{n + n\beta}{n + \beta} \quad (\text{G.9})$$

The ‘saturating’ parameterization of the DM was implemented in ISCAM for this assessment. This parameterization will revert to the multinomial distribution with sufficiently large β (Eq. G.9) i.e. $n_{\text{eff}} \simeq n$ when $\beta \gg n$. It provides an upper bound on low values of $\hat{\beta}$, i.e. $n_{\text{eff}} \simeq 1 + \beta$ when $n \gg \beta$.

G.5.4. Stock Recruitment

This stock assessment assumes Beverton-Holt recruitment. Annual recruitment and the initial age-composition are treated as latent variables in ISCAM, and residuals between estimated recruits and the deterministic stock-recruitment models are used to estimate unfished spawning stock biomass and recruitment compensation. The residuals between the estimated and predicted recruits is given by:

$$\delta_t = \ln(\bar{R}e^{w_t}) - \ln(R_t) \quad (\text{G.10})$$

where R_t is given by Eq. G.42. In that equation, k is the age at recruitment. A bias correction term for the lognormal process errors is included in Eq. G.42. The negative log likelihood for the recruitment deviations is given by the normal density (ignoring the scaling constant):

$$\ell_\delta = n \ln(\tau) + \frac{\sum_{t=1+k}^T \delta_t^2}{2\tau^2} \quad (\text{G.11})$$

Eqs. G.10 and G.11 are key for estimating unfished spawning stock biomass and recruitment compensation via the recruitment models. The relationship between (s_o, β) and (B_o, κ) is given by:

$$s_o = \frac{\kappa}{\phi_E} \quad (\text{G.12})$$

$$\beta = \frac{\kappa - 1}{B_o} \quad (\text{Beverton - Holt}) \quad (\text{G.13})$$

where s_o is the maximum juvenile survival rate, and β is the density effect on recruitment, and B_o is the unfished spawning stock biomass. Unfished steady-state spawning stock biomass per recruit is given by ϕ_E , which is the sum of products between age-specific survivorship and relative fecundity.

G.5.5. Parameter Estimation and Uncertainty

Parameter estimation and quantifying uncertainty was carried out using the tools available in AD Model Builder. AD Model Builder (ADMB) is software for creating executable code to

estimate the parameters and associated probability distributions for nonlinear statistical models. The software is available online from the ADMB project, on the ADMB organization's GitHub webpage. The ADMB software was used to develop `gfiscam`, which was created using the original ISCAM code, written by Steve J. Martell.

There are five distinct components that make up the objective function that ADMB is minimizing:

$$f = \text{negative loglikelihoods} + \text{constraints} + \text{priors for parameters} \\ + \text{survey priors} + \text{convergence penalties.}$$

The purpose of this section is to document all of the components that make up the objective function.

Negative log-likelihoods

The negative log-likelihoods pertain specifically elements that deal with the data and variance partitioning and have already been described in detail in earlier portions of Section G.5. There are four specific elements that make up the vector of the objective function:

$$\vec{\ell} = \ell_C, \ell_I, \ell_A, \ell_\delta. \quad (\text{G.14})$$

To reiterate, these are the likelihood of the catch data ℓ_C , likelihood of the survey data ℓ_I , the likelihood of the age-composition data ℓ_A and the likelihood of the stock-recruitment residuals ℓ_δ . Each of these elements are expressed in negative log-space, and ADMB attempts to estimate model parameters by minimizing the sum of these elements.

Constraints

There are two specific constraints that are described here: (1) parameter bounds and (2) constraints to ensure that a parameter vector sums to 0.

In ISCAM the user must specify the lower and upper bounds for the leading parameters defined in the control file ($\ln(R_o)$, h , $\ln(M_s)$, $\ln(\bar{R})$, $\ln(R_{\text{init}})$, ρ , ϑ). All estimated selectivity parameters $\vec{\gamma}_k$ are estimated in log space and have a minimum and maximum values of -5.0 and 5.0, respectively. These values are hard-wired into the code, but should be sufficiently large/small enough to capture a wide range of selectivities.

Estimated fishing mortality rates are also constrained (in log space) to have a minimum value of -30, and a maximum value of 3.0, also hard-wired. Log annual recruitment deviations are also constrained to have minimum and maximum values of -15.0 and 15.0 and there is an additional constraint to ensure the vector of deviations sums to 0. This is necessary in order to be able to estimate the average recruitment \bar{R} .

Priors for parameters

Each of the seven leading parameters (eight if there are two sexes) specified in the control file ($\ln(R_o)$, h , $\ln(M_s)$, $\ln(\bar{R})$, $\ln(R_{\text{init}})$, ρ , ϑ) are declared as bounded parameters and in addition the user can also specify an informative prior distribution for each of these parameters. Five distinct prior distributions can be implemented: uniform, normal, lognormal, beta and a gamma distribution. See Table 5 for initial values and prior types and values used for this Arrowtooth Flounder assessment.

Table G.1. Descriptions of the symbols used in ISCAM.

Symbol	Description
Indices	
s	Index for sex
a	Index for age
t	Index for year
k	Index for gear
b	Index for year block in time-varying selectivity
Model dimensions	
S	Number of sexes
\acute{a}, A	Youngest and oldest age group (A is a plus group)
\acute{t}, T	First and last year of catch data
K	Number of gears, including survey gears
Observations (data)	
$C_{k,t}$	catches in weight by gear k in year t
$I_{k,t}$	relative abundance index for gear k in year t
Estimated parameters	
R_0	recruits in unfished conditions
h	Steepness of the stock-recruitment relationship
\bar{R}	Average age- \acute{a} recruitment from year \acute{t} to T
\bar{R}_{init}	Average age- $\acute{a} - 1$ to A recruitment for initialization
M_s	Instantaneous natural mortality rate for sex s
$\hat{a}_{k,s,b}, \hat{\gamma}_{k,s,b}$	Selectivity parameters for gear k , sex s , year block b
$\Gamma_{k,s,t}$	Logarithm of the instantaneous fishing mortality for gear k , sex s , year t
ω_t	Age- \acute{a} deviates from \bar{R} for years \acute{t} to T
$\omega_{\text{init},t}$	Age- \acute{a} deviates from \bar{R}_{init} for year \acute{t}
q_k	Catchability parameter for survey k
ρ	Fraction of the total variance associated with observation error
ϑ^2	Total precision (inverse of variance) of the total error
Standard deviations	
σ	Standard deviation for observation errors in survey index
τ	Standard deviation in process errors (recruitment deviations)
σ_C	Standard deviation in observed catch by gear
Residuals	
δ_t	Annual recruitment residual
η_t	Residual error in predicted catch
Fixed growth & maturity parameters	
$l_{\infty s}$	Asymptotic length for sex s
\acute{k}_s	Brody growth coefficient for sex s
t_{0s}	Theoretical age at zero length for sex s
\acute{a}_s	Scalar in length-weight allometry for sex s
\acute{b}_s	Power parameter in length-weight allometry for sex s
\acute{a}_s	Age at 50% maturity for sex s
$\acute{\gamma}_s$	Standard deviation at 50% maturity for sex s

G.5.6. Steady-State Age-Structured Model

Assumptions in this steady-state model include:

- Unequal vulnerability-at-age
- Age-specific fecundity
- Beverton-Holt type recruitment

Parameters

The model includes steady-state parameters:

$$\Theta = (B_0, h, \kappa, M_s, \hat{a}_{k,s,b}, \hat{\gamma}_{k,s,b}); \quad B_0 > 0; \quad 0.2 \leq h < 1; \quad \kappa > 1; \quad M_s > 0 \quad (\text{G.15})$$

and fixed growth and maturity parameters:

$$\Phi = (l_{\infty,s}, \hat{k}_s, t_{o,s}, \hat{a}_s, \hat{b}_s, \hat{a}_s, \hat{\gamma}_s) \quad (\text{G.16})$$

Age-schedule information

Length-at-age is defined as:

$$l_{a,s} = l \left(1 - e^{(-k_s(a-t_{o,s}))} \right) \quad (\text{G.17})$$

and weight-at-age by sex as:

$$w_{a,s} = \hat{a}_s (l_{a,s})^{\hat{b}_s}. \quad (\text{G.18})$$

Vulnerability at age is defined as:

$$v_{a,s} = \left(1 + e^{\left(\frac{-(\hat{a}_s - a)}{\hat{\gamma}_s} \right)} \right)^{-1} \quad (\text{G.19})$$

and fecundity at age as:

$$f_{a,s} = w_{a,s} \left(1 + e^{\left(\frac{-(\hat{a}_s - a_s)}{\hat{\gamma}_s} \right)} \right)^{-1} \quad (\text{G.20})$$

Survivorship

Survivorship for unfished populations is defined as:

$$l_{a,s} = \begin{cases} \frac{1}{S}, & a = 1 \\ l_{a-1,s} e^{-M_s}, & 1 < a < A \\ \frac{l_{a-1,s}}{(1 - e^{-M_s})}, & a = A \end{cases} \quad (\text{G.21})$$

and for fished populations:

$$\hat{l}_{a,s} = \begin{cases} \frac{1}{S}, & a = 1 \\ \hat{l}_{a-1,s} e^{-M_s - F_e v_{a-1,s}}, & 1 < a < A \\ \frac{\hat{l}_{a-1,s} e^{-M_s - F_e v_{a-1,s}}}{(1 - e^{-M_s - F_e v_{a,s}})}, & a = A \end{cases} \quad (\text{G.22})$$

Incidence functions

The incidence functions refer to the lifetime or per-recruit quantities. Spawning biomass per recruit for unfished or fished populations is defined as:

$$\phi_E = \sum_{s=1}^S \sum_{a=1}^{\infty} l_{a,s} f_{a,s} \qquad \phi_e = \sum_{s=1}^S \sum_{a=1}^{\infty} \hat{l}_{a,s} f_{a,s} \qquad (\text{G.23})$$

Vulnerable biomass per recruit for unfished or fished populations is defined as:

$$\phi_B = \sum_{s=1}^S \sum_{a=1}^{\infty} l_{a,s} w_{a,s} v_{a,s} \qquad \phi_b = \sum_{s=1}^S \sum_{a=1}^{\infty} \hat{l}_{a,s} w_{a,s} v_{a,s} \qquad (\text{G.24})$$

Per recruit yield to the fishery is given by:

$$\phi_q = \sum_{s=1}^S \sum_{a=1}^{\infty} \frac{\hat{l}_{a,s} w_{a,s} v_{a,s}}{M_s + F_e v_{a,s}} \left(1 - e^{-(M_s - F_e v_{a,s})} \right) \qquad (\text{G.25})$$

Steady-state conditions

Biomass in unfished conditions is defined as:

$$B_0 = R_0 \phi_E \qquad (\text{G.26})$$

Equilibrium recruitment is given by:

$$\kappa = \frac{4h}{1-h} \qquad (\text{G.27})$$

$$R_0 = \frac{B_0}{\phi_E} \qquad (\text{G.28})$$

$$R_e = R_0 \frac{\kappa - \frac{\phi_E}{\phi_e}}{\kappa - 1}; \quad (\text{Beverton - Holt}) \qquad (\text{G.29})$$

Equilibrium yield is given by:

$$C_e = F_e R_e \phi_q \qquad (\text{G.30})$$

G.5.7. Statistical Catch-Age Model

This model uses the Baranov catch equation and C^* and F^* as leading parameters.

Estimated or fixed parameters

$$\Theta = (R_0, M_s, \bar{R}, \bar{R}_{\text{init}}, \vartheta^2, \rho, F_{k,t}, \{\omega_t\}_{t=1-A}^{\ell=T}, \{\omega_{\text{init},t}\}_{t=\ell+1}^{\ell-1}) \qquad (\text{G.31})$$

$$\sigma = \frac{\sqrt{\rho}}{\vartheta}; \quad \tau = \frac{\sqrt{(1-\rho)}}{\vartheta} \qquad (\text{G.32})$$

Unobserved states

The numbers-at-age, spawning stock biomass, and total mortality rates:

$$N_{t,a,s}; \quad B_{t,s}; \quad Z_{t,a,s} \quad (G.33)$$

Initial states

The initial numbers-at-age in the first year and the annual recruits are treated as estimated parameters and used to initialize the numbers-at-age matrix:

$$N_{t,a,s} = \frac{1}{S} \bar{R}_{\text{init}} e^{\omega_{\text{init},t}} e^{-M_s(a-1)}; \quad (t-A) < t < 1; \quad 2 \leq a \leq A \quad (G.34)$$

$$N_{t,a,s} = \frac{1}{S} \bar{R} e^{\omega t}; \quad 1 \leq t \leq T; \quad a = 1 \quad (G.35)$$

Age-specific selectivity for gear type k is a function of the selectivity parameters and the annual fishing mortality for each gear k in year t :

$$v_{k,a} = \frac{1}{1 + e^{-\frac{(a-\hat{a}_k)}{\hat{\gamma}_k}}} \quad (G.36)$$

The fishing mortality for each gear k in year t is the exponent of the estimated log fishing mortality $F_{k,t}$:

$$F_{k,t} = e^{F_{k,t}} \quad (G.37)$$

State dynamics ($t > 1$)

State variables in each year are updated using the following equations, where the spawning biomass is the product of the numbers-at-age and the mature biomass-at-age.

$$B_{t,s} = \sum_a N_{t,a,s} f_{a,s} \quad (G.38)$$

The total mortality rate is given by:

$$Z_{t,a,s} = M_s + \sum_k F_{k,t} v_{k,t,a,s} \quad (G.39)$$

and the total catch (in weight) for each gear is given by:

$$\hat{C}_{k,t} = \sum_s \sum_a \frac{N_{t,a,s} w_{a,s} F_{k,t} v_{k,t,a,s} (1 - e^{-Z_{t,a,s}})^{\eta t}}{Z_{t,a,s}} \quad (G.40)$$

assuming that both natural and fishing mortality occur simultaneously throughout the year. The numbers-at-age are propagated over time as:

$$N_{t,a,s} = \begin{cases} \frac{s_o E_{t-1}}{1 + \beta E_{t-1}} e^{(\omega_t - 0.5\tau^2)} & a = 1 \\ N_{t-1,a-1,s} e^{(-Z_{t-1,a-1,s})} & a > 1 \\ N_{t-1,a,s} e^{(-Z_{t-1,a,s})} & a = A \end{cases} \quad (\text{G.41})$$

where members of the plus group (age A) are all assumed to have the same total mortality rate.

Recruitment model

Recruitment for this model is a Beverton-Holt formulation with the lognormal bias correction term $-0.5\tau^2$:

$$R_t = \frac{s_o B_{t-k}}{1 + \beta B_{t-k}} e^{\delta_t - 0.5\tau^2}; \quad (\text{Beverton - Holt}) \quad (\text{G.42})$$

APPENDIX H. COMPUTATIONAL ENVIRONMENT

The source code for this assessment can be found on GitHub, in several packages in the pbs-assess organization's repository list (Table H.1).

This version of the document was generated on Tue Jun 24, 2025 with R version 4.5.1 (2025-06-13) (R Core Team 2022).

Table H.1. The packages, their associated GitHub organizations and package versions used for this assessment. All are R packages except for `gfiscam` which is an ADMB/C++ package containing the ISCAM implementation used in this assessment. The 'Package Version' given for `gfiscam` is the commit SHA on GitHub. The 'Package Version' for the R packages are what is returned when running the `session_info()`\$packages command in R.

Package/Repository	GitHub User/Organization	Package Version
arrowtooth	pbs-assess	0.0.0.9000
bookdown	rstudio	0.41
csasdown	pbs-assess	0.2.0
devtools	r-lib	2.4.5.9000
dplyr	tidyverse	1.1.4
gfdata	pbs-assess	0.1.4
gfiscamutils	pbs-assess	0.0.0.9000
gfplot	pbs-assess	0.2.1
ggplot2	tidyverse	3.5.1
glmmTMB	glmmTMB	1.1.9
gridExtra	baptiste	2.3
here	r-lib	1.0.1
kableExtra	cgrandin (forked from haozhu233)	1.4.0.4
knitr	yihui	1.50
purrr	tidyverse	1.0.4
rmarkdown	rstudio	2.29
rosettafish	pbs-assess	0.0.0.9000
sdmTMB	pbs-assess	0.6.0.9004
tidylog	elbersb	1.0.2
TMB	kaskr/adcomp	1.9.14
gfiscam	pbs-assess	24277c